

A PALAEOMAGNETIC INVESTIGATION OF THE
LAYERED MAFIC SEQUENCE OF THE BUSHVELD COMPLEX

by

PIERRE JOHANNES HATTINGH

Submitted in partial fulfilment of the requirements
for the degree of
DOCTOR OF SCIENCE
in the Faculty of Science,
University of Pretoria, Pretoria.

September, 1983



1241582

ABSTRACT

Orientated samples were collected from 88 sites in the marginal, lower, critical, main and upper zones of the layered sequence of the Bushveld Complex. Apart from measuring the remanent magnetization of these samples, the magnetization of the samples was subjected to detailed analyses, using alternating field and thermal demagnetization techniques. This was supplemented by various heating experiments and tests to establish the stability and origin of the observed magnetization.

The critical zone yielded six sites with stable and consistent magnetization directions, forming a group with a corresponding palaeomagnetic pole at 37°S , 135°W . With the igneous layering in a horizontal position, the group statistics improve, but not significantly at the 95 per cent confidence limit. However, the mixed polarity of this group, which becomes significantly more antipodal after correction for the dip of the layering, is considered to be an indicator that the critical zone could have acquired its remanent magnetization with the igneous layering in a horizontal position. The pole position corresponding to this corrected group is situated at $39,5^{\circ}\text{S}$, 133°W .

Heating experiments and mineralogical evidence suggest the possibility that the magnetic polarity of the critical zone could be due to a self-reversal of magnetization. This is further supported by the position and polarity of the palaeomagnetic pole of the critical zone on the apparent polar wander (APW) path for Africa.

Magnetization directions from the main zone in the eastern Bushveld Complex form two groups, approximately antipodal to each other. The majority of sites are situated in subzone B, forming a group with a reversed magnetization which improves significantly with the igneous layering in a horizontal position. The palaeomagnetic pole of this group is situated at $17,3^{\circ}\text{N}$, $35,7^{\circ}\text{E}$. The second group represents sites from the top of the main zone (subzone C) which again yield greatly improved results when a fold test is applied. The group is magnetized in a normal direction with the corresponding palaeomagnetic pole at

28°S, 161,7°W. The polarity difference between the two groups is considered to be due to a geomagnetic field reversal towards the end of formation of the main zone.

With the exception of two sites, the magnetization directions from all the sites in the main zone in the western Bushveld Complex group together and are reversely magnetized. Rotation of the layering to a horizontal position improves the grouping, which indicates that the main zone could have acquired its remanent magnetization with the igneous layering in a horizontal position. The corresponding pole position is at 9,2°N, 27,3°E. The two sites situated in the lower part of the main zone have normal magnetization directions similar to those of the critical zone.

Consistent normal magnetization directions from sites in the upper zone were obtained after alternating field and thermal demagnetization of specimens. Structural folding failed to improve group statistics, suggesting that the upper zone acquired its remanent magnetization with the igneous layering in its present attitude. The palaeomagnetic pole representing the upper zone is situated at 16,1°S, 148,5°W.

The layered sequence exhibits a magnetic polarity pattern, which allows the subdivision of the sequence into three magnetic polarity zones. The lower- and uppermost zones have normal magnetization directions with respect to the present-day geomagnetic field. The third, situated between the former two, is reversely magnetized.

SAMEVATTING

Georiënteerde monsters is versamel by 88 lokaliteite in die rand-, laer-, kritieke-, hoof- en bosones van die gelaagde opeenvolging van die Bosveldkompleks. Behalwe die meting van die remanente magnetisasie van die monsters, is die magnetisasie van hierdie monsters volledig geanaliseer deur gebruik te maak van wisselveld en termale demagnetisasie-tegnieke. Dit is verder aangevul met verskeie verhittingseksperimente en -toetse om die stabiliteit en oorsprong van die waargenome magnetisasie te bepaal.

Ses lokaliteite in die kritieke sone het stabiele en bestendige magnetisasierigtings gelewer, wat 'n groep vorm met 'n ooreenstemmende paleomagnetiese pool by 37°S , 135°W . Met die stollingsgelaagdheid in 'n horisontale posisie verbeter die groepstatistiek, maar nie betekenisvol by 'n 95 persent betroubaarheidsvlak nie. Die gemengde polariteit van die groep, wat betekenisvol antipodies word na die korreksie vir die helling van die gelaagdheid, word beskou 'n aanduiding te wees dat die kritieke sone sy remanente magnetisasie verkry het met die stollingsgelaagdheid in 'n horisontale posisie. Die poolposisie van hierdie gekorrigeerde groep is geleë by $39,5^{\circ}\text{S}$, 133°W .

Verhittingseksperimente en mineralogiese getuienis dui op die moontlikheid dat die magnetiese polariteit van die kritieke sone moontlik te wyte kan wees aan 'n self-omkering van magnetisasie. Dit word verder ondersteun deur die posisie en polariteit van die paleomagnetiese poolposisie van die kritieke sone op die skynbare poolswerfkerwe (SPS) vir Afrika.

Magnetisasierigtings van die hoofsones in die oostelike Bosveldkompleks vorm twee groepe, wat ongeveer antipodies ten opsigte van mekaar is. Die meerderheid lokaliteite is in subsone B geleë, en vorm 'n groep met 'n omgekeerde magnetisasie, wat betekenisvol verbeter met die stollingsgelaagdheid in 'n horisontale posisie. Die paleomagnetiese pool is geleë by $17,3^{\circ}\text{N}$, $35,7^{\circ}\text{O}$. Die tweede groep verteenwoordig lokaliteite aan die bokant van die hoofsones (subsone C) wat weer verbeterde resultate lewer wanneer 'n plooi-toets uitgevoer word. Hierdie groep is normaal gemagnetiseer met 'n paleomagnetiese pool by 28°S , $161,7^{\circ}\text{W}$. Die

polariteitsverskil tussen die twee groepe, word beskou as die resultaat van 'n geomagnetiese veldomkering te wees.

Met die uitsondering van twee lokaliteite, groepeer die magnetisasierigtings van al die lokaliteite in die hoofsonne van die westelike Bosveldkompleks saam en is omgekeerd gemagnetiseerd. Rotasie van die gelaagdheid na 'n horisontale posisie verbeter die groepering, wat aandui dat die hoofsonne moontlik sy magnetisasie verkry het met die stollingsgelaagdheid in 'n horisontale posisie. Die ooreenstemmende poolposisie is by $9,2^{\circ}\text{N}$, $27,3^{\circ}\text{O}$. Die twee lokaliteite wat geleë is in die onderste gedeelte van die hoofsonne het normale magnetisasierigtings, gelyksoortig aan die van die kritieke sone.

Bestendige magnetisasierigtings van lokaliteite in die bosone is verkry na wisselveld- en termale demagnetisasie van monsters. Strukturele rotasie lei nie tot 'n verbetering van groepstatistiek nie, wat oënskynlik daarop dui dat die bosone sy remanente magnetisasie verkry het met die stollingsgelaagdheid in die huidige stand. Die paleomagnetiese pool wat die bosone verteenwoordig is geleë by $16,1^{\circ}\text{S}$ en $148,5^{\circ}\text{W}$.

Die gelaagde opeenvolging vertoon 'n magnetiese polariteitspatroon wat die onderverdeling van die opeenvolging in drie polariteitssones toelaat. Die onderste en boonste sones het normale magnetisasierigtings met betrekking tot die huidige geomagnetiese veld. Die derde sone, wat tussen die vorige twee geleë is, is omgekeerd gemagnetiseerd.

CONTENTS

I	INTRODUCTION	1
II	THE LAYERED SEQUENCE	2
III	COLLECTION AND PREPARATION OF ROCK SAMPLES	6
	A. The distribution of sampling sites	6
	B. Sampling techniques	7
	C. Sample preparation	8
	D. Measurement of dip and dip directions of the igneous layering	8
IV	LABORATORY MEASUREMENTS AND PROCEDURES	9
	A. Laboratory instruments	9
	B. Laboratory procedures	11
	C. Statistical analysis of results	12
V	THE PALAEOMAGNETISM OF THE CRITICAL ZONE	14
	A. Introduction	14
	B. Natural remanent magnetization	14
	C. Bulk alternating field demagnetization	18
	D. Stepwise alternating field demagnetization of pilot specimens	26
	E. Thermal demagnetization	33
	F. Mineralogy of opaque minerals	37
	G. Mixed polarity	38
	H. Summary of results	43
VI	THE PALAEOMAGNETISM OF THE MAIN ZONE IN THE EASTERN BUSHVELD COMPLEX	46
	A. Introduction	46
	B. Natural remanent magnetization	46
	C. Bulk and stepwise alternating field demagnetization	52
	D. Thermal demagnetization	61
	E. Mineralogy of opaque minerals	67
	F. The mixed polarity of site 11	75
	G. The polarity difference of magnetization between subzones B and C	88
	H. Summary of results	88

VII	THE PALAEOMAGNETISM OF THE MAIN ZONE IN THE WESTERN BUSHVELD COMPLEX	90
	A. Introduction	90
	B. Natural remanent magnetization	90
	C. Bulk alternating field demagnetization	95
	D. Stepwise alternating field demagnetization of pilot specimens	102
	E. Thermal demagnetization	111
	F. Mineralogy of opaque minerals	117
	G. Haematite as carrier of the more stable secondary magnetization	120
	H. Summary of results	123
VIII	THE PALAEOMAGNETISM OF THE UPPER ZONE	126
	A. Introduction	126
	B. Natural remanent magnetization	126
	C. Bulk alternating field demagnetization	129
	D. Stepwise alternating field demagnetization of pilot specimens	132
	E. Results of Lowrie-Fuller tests	135
	F. Thermal demagnetization	142
	G. Mineralogy of opaque minerals	147
	H. Geomagnetic field reversal or self-reversal?	151
	I. Summary of results	153
IX	DISCUSSION OF PALAEOMAGNETIC RESULTS	154
	A. Palaeomagnetic subdivision of the layered sequence	154
	B. Palaeomagnetic pole positions of the layered sequence	158
X	TECTONIC IMPLICATIONS	165
	ACKNOWLEDGEMENTS	167
	REFERENCES	168

LIST OF TABLES AND FIGURES IN THE TEXT

Table I	Natural remanent magnetization directions of sites in the critical zone	16
Table II	Natural remanent magnetization directions of sites in the critical zone with the igneous layering in a horizontal position	18
Table III	Magnetization directions of sites in the critical zone after alternating field demagnetization	20
Table IV	Magnetization directions of sites in the critical zone after alternating field demagnetization, with the igneous layering in a horizontal position	22
Table V	Natural remanent magnetization directions of sites in the main zone, eastern Bushveld Complex	48
Table VI	Natural remanent magnetization directions of sites in the main zone, eastern Bushveld Complex with the igneous layering in a horizontal position	50
Table VII	Magnetization directions of sites in the main zone, eastern Bushveld Complex after bulk alternating field demagnetization	52
Table VIII	Magnetization directions of sites in the main zone, eastern Bushveld Complex after alternating field demagnetization, with the igneous layering in a horizontal position	58
Table IX	Semi-quantitative analyses of chromite grains from the main zone, eastern Bushveld Complex	74
Table X	Natural remanent magnetization directions of sites in the main zone, western Bushveld Complex	90
Table XI	Natural remanent magnetization directions of sites in the main zone, western Bushveld Complex with the igneous layering in a horizontal position	94

Table XII	Magnetization directions of sites in the main zone, western Bushveld Complex, after bulk alternating field demagnetization	97
Table XIII	Magnetization directions of sites in the main zone, western Bushveld Complex, after bulk alternating field demagnetization, with the igneous layering in a horizontal position	98
Table XIV	Measured and calculated dip and dip directions of the igneous layering at four sites in the main zone, western Bushveld Complex	121
Table XV	Natural remanent magnetization directions of sites in the upper zone	129
Table XVI	Magnetization directions of sites in the upper zone, after bulk alternating field demagnetization	129
Table XVII	Magnetization directions of sites in the upper zone, after bulk alternating field demagnetization, with the igneous layering in a horizontal position	130
Table XVIII	End point magnetization vectors obtained with thermal demagnetization of specimens from the upper zone, with the igneous layering in a horizontal position	144
Figure 1	Geological map of the Bushveld Complex showing sample site positions	Back folder
Figure 2	Simplified lithostratigraphic column of the mafic layered sequence in the eastern Bushveld Complex indicating the stratigraphic positions of the sampling sites	3
Figure 3	Lithostratigraphic column of the mafic layered sequence in the western Bushveld Complex. Stratigraphic positions of the sampling sites are indicated	4
Figure 4	Histogram plot of NRM intensities of specimens from the critical zone	15

Figure 5	Stereographic projection of NRM directions of sites 24, 79, 80, 81, 83, 84, 85, 86 and 87	17
Figure 6	NRM directions of sites in the critical zone, with the igneous layering in a horizontal position	19
Figure 7	Magnetization directions of sites in the critical zone after AF demagnetization	21
Figure 8	Magnetization directions of sites in the critical zone after AF demagnetization, with the igneous layering in a horizontal position	23
Figure 9	The same data as in Fig. 7 with the magnetization directions of sites 85 and 87 inverted	25
Figure 10	Stepwise AF demagnetization of specimens from sites 79, 83 and 84	27
Figure 11	Stepwise AF demagnetization of specimens from site 83 ...	29
Figure 12	Repeated stepwise AF demagnetization of a single specimen from site 83	30
Figure 13	Normalized AF demagnetization curve of the intensity response of specimen 83/5D during repeated AF demagnetization at each step	31
Figure 14	Normalized thermal demagnetization response curves for specimens 83/5F and 86/4E	34
Figure 15	The change of magnetization directions of specimens 83/5F and 86/4E during continuous thermal demagnetization.	35
Figure 16	Normalized thermal demagnetization curve of a specimen which was given a TRM	36
Figure 17	Normalized AF demagnetization response curve of a specimen which was given a TRM	40
Figure 18	Normalized thermal demagnetization curve of specimen 86/1B over a temperature range from -67°C to 452°C	41

Figure 19	Thermal demagnetization of a specimen from -36°C to 598°C , the specimen was first given an IRM	42
Figure 20	Circles of 95 per cent confidence for group Bcz3AFR (inverted, layering horizontal) and that given by Gough and Van Niekerk (1959) for the main zone of the layered sequence	45
Figure 21	Histogram plot of the NRM intensities of specimens from the main zone in the eastern Bushveld Complex	47
Figure 22	NRM directions of sites in the main zone of the layered sequence in the eastern Bushveld Complex	49
Figure 23	NRM directions of sites in the main zone, eastern Bushveld Complex, with the igneous layering in a horizontal position	51
Figure 24	Magnetization directions of sites in the main zone, eastern Bushveld Complex, after bulk AF demagnetization .	53
Figure 25	Stepwise AF demagnetization results of specimen 36/4C ...	55
Figure 26	Normalized intensity response curve of specimen 36/4C during AF demagnetization	56
Figure 27	Stepwise AF demagnetization of specimens from sites 11B, 19 and 22	57
Figure 28	Magnetization directions of sites in the main zone, eastern Bushveld Complex, after bulk AF demagnetization, with the igneous layering in a horizontal position	60
Figure 29	The change in magnetization directions of two specimens from group Bmz3AF, subzone B, main zone, eastern Bushveld Complex, during continuous thermal demagnetization.....	62
Figure 30	Typical normalized intensity response curves during continuous thermal demagnetization of two specimens from subzone B, main zone, eastern Bushveld Complex	63

Figure 31	The change in magnetization directions of specimens from sites 11A, 13 and 14 during continuous thermal demagnetization	65
Figure 32	Thermal demagnetization response of specimens from sites 19, 20, 21 and 22	66
Figure 33	Normalized intensity response curves of two specimens from sites 20 and 21, during continuous thermal demagnetization	68
Figure 34	Normalized intensity response curve of a specimen from subzone B, main zone, eastern Bushveld Complex during AF demagnetization. The curve illustrates the "hardness" of magnetization which is typical of most of the specimens from subzone B	69
Figure 35	Magnetite lamellae in a pyroxene crystal, main zone, eastern Bushveld Complex. Transmitted light, magnification 870X	71
Figure 36	Magnetite lamellae in a plagioclase crystal, main zone, eastern Bushveld Complex. Transmitted light, magnification 870X	71
Figure 37	Normalized intensity response curve of specimen 20/1C of subzone C, main zone, eastern Bushveld Complex, during AF demagnetization	73
Figure 38	AF demagnetization response of specimen 11/3B (site 11A). Resultant and difference magnetization vectors shown	76
Figure 39	Normalized intensity response curve of specimen 11/3B (site 11A) during AF demagnetization	78
Figure 40	AF response of specimen 11/4C (site 11B). Resultant and difference vectors shown	79
Figure 41	Normalized intensity response curve of specimen 11/4C (site 11B) during AF demagnetization	80

Figure 42	Thermal demagnetization response of specimen 11/3C (site 11A). Resultant and difference vectors shown	82
Figure 43	Thermal demagnetization response of specimen 11/1B (site 11A). Resultant and difference vectors shown	83
Figure 44	AF demagnetization response of specimen 11/5E (site 11B), after the specimen had been given an artificial TRM	84
Figure 45	Normalized intensity response curve of specimen 11/5E (site 11B) during AF demagnetization, after the specimen had been given an artificial TRM	85
Figure 46	Thermal demagnetization of specimen 11/3A (site 11A), after the specimen had been given an artificial TRM	87
Figure 47	Histogram plot of NRM intensities of all the specimens from the main zone in the western Bushveld Complex	92
Figure 48	NRM directions from sites in the main zone, western Bushveld Complex	93
Figure 49	NRM directions from sites in the main zone, western Bushveld Complex, with the igneous layering in a horizontal position	96
Figure 50	Magnetized directions from sites in the main zone, western Bushveld Complex, after bulk AF demagnetization .	100
Figure 51	Magnetization directions from sites in the main zone, western Bushveld Complex, after bulk AF demagnetization, with the igneous layering in a horizontal position	101
Figure 52	The directional response of two specimens from sites 56 and 62, to stepwise AF demagnetization	103
Figure 53	The directional response of four specimens from sites 56, 57, 65 and 67 to stepwise AF demagnetization. Solid lines represent circles of remagnetization fitted to the respective data sets	105

Figure 54	Circles of remagnetization fitted to the stepwise AF demagnetization data (corrected for the dip of the igneous layering) from one specimen of each site in group A. Remagnetization circles are shown only on the lower hemisphere of the stereographic projection	106
Figure 55	Difference vectors, removed between successive AF demagnetization steps, are shown for sites 56, 57, 67 and 70	108
Figure 56	Difference vectors removed between successive AF demagnetization steps, from specimens of sites where the NRM was recognized to consist of more than two magnetization components	110
Figure 57	Normalized intensity response curve to stepwise AF demagnetization of specimen 57/4B	112
Figure 58	Directional response of magnetization vectors from specimens 76/3A and 75/1C to stepwise AF demagnetization	113
Figure 59	Directional response of magnetization vectors from specimens 56/3C, 66/1A, 63/4B and 62/1A, to continuous thermal demagnetization	114
Figure 60	Normalized intensity response curve of specimen 56/3D during continuous thermal demagnetization	116
Figure 61	Magnetite lamellae in a pyroxene crystal, main zone, western Bushveld Complex. Transmitted light, magnification 870x	118
Figure 62	Magnetite lamellae in a plagioclase crystal, main zone, western Bushveld Complex. Transmitted light, magnification 870X	118
Figure 63	Ilmenite grains with haematite exsolution lamellae, main zone, western Bushveld Complex. Reflected light, magnification 1800x	119

Figure 64	The directional response of magnetization vectors to AF demagnetization, of four specimens, before and after correction for the dip of the igneous layering. A remagnetization circle on the lower hemisphere, fitted to all the corrected vectors, is also shown	122
Figure 65	Magnetization directions of sites 75 and 76 after bulk AF demagnetization. The same circle of remagnetization as in Fig. 64 is shown, but the circle is shown here on both hemispheres of the stereographic projection	124
Figure 66	Histogram plot of NRM intensities of all the specimens from the upper zone of the Bushveld Complex	127
Figure 67	NRM directions of sites in the upper zone of the layered sequence	128
Figure 68	Magnetization directions of sites in the upper zone after bulk AF demagnetization	131
Figure 69	Magnetization directions of sites in the upper zone after bulk AF demagnetization with the igneous layering in a horizontal position	133
Figure 70	Directional response of magnetization directions from sites in the upper zone, to stepwise AF demagnetization.	134
Figure 71	Typical normalized intensity response curve to AF demagnetization by a specimen from site 17 in the upper zone.	136
Figure 72	Normalized intensity response curves of specimens with a NRM, a TRM, an IRM and an ARM respectively, to AF demagnetization	137
Figure 73	Normalized intensity response curves of specimens with an ARM, and IRM respectively, to AF demagnetization ...	139
Figure 74	Normalized average intensity response curve to AF demagnetization	141

Figure 75	Directional response of magnetization vectors of specimens from sites in the upper zone to continuous thermal demagnetization	143
Figure 76	End point vectors after continuous thermal demagnetization of specimens from the upper zone	145
Figure 77	End point vectors shown, corrected for the dip of the igneous layering at each site	146
Figure 78	Remagnetization circles on the upper hemisphere obtained by fitting circles to thermal demagnetization data presented in Fig. 75. The calculated intersection point of the remagnetization circles is also shown	148
Figure 79	Normalized intensity response curve to continuous thermal demagnetization of a specimen from site 16	149
Figure 80	Mean magnetization directions and circles of 95 per cent confidence for groups Bmz3AF, Bmz7AF and Buz1AF	152
Figure 81	The zonal subdivision of the mafic layered sequence showing the magnetic polarity pattern observed in the western and eastern Bushveld Complex	155
Figure 82	A simplified lithostratigraphic column of the layered sequence in the western Bushveld Complex, showing the magnetic polarity zones	156
Figure 83	A simplified lithostratigraphic column of the layered sequence in the eastern Bushveld Complex, showing the magnetic polarity zones	157
Figure 84	Apparent polar wander path for African cratons, 2300 - 1900 m.y.....	159
Figure 85	APW path for Africa, with selected pole positions shown for southern Africa, ca. 2070 - 1700 m.y.....	160

Figure 86	APW path for Africa, with pole positions from this study	161
Figure 87	APW path for Africa with pole positions corresponding to the magnetic polarity zones of the layered sequence .	164

I INTRODUCTION

Recent palaeomagnetic investigations on certain layered intrusions such as Sudbury (Morris, 1980, 1981) and Skaergaard (Schwarz, *et al.*, 1979) have shown that palaeomagnetic data can be an important indicator of the tectono-intrusive history of layered intrusions.

One of the first palaeomagnetic investigations in South Africa was undertaken by Gough and Van Niekerk (1959) on the mafic layered sequence of the Bushveld Complex. With data from five sites in the main zone these authors calculated a pole position for the Bushveld Complex and provided strong evidence that the magnetization of the main zone was acquired with the igneous layering in a horizontal position. Although their study was highly significant, it was not exhaustive. Firstly no alternating field (AF) or thermal demagnetization techniques were employed and, secondly, the study was restricted to only a few sites in the main zone of the layered sequence.

This investigation was initiated in order to extend the study of Gough and Van Niekerk (1959) and to relate the new palaeomagnetic results from the layered sequence to more modern concepts on the genesis and structure of the Complex (Hunter, 1975a; Hunter and Hamilton, 1978; Sharpe and Snyman, 1978; Von Gruenewaldt, 1979; Sharpe, 1980; Sharpe and Bahat, 1981).

For the purpose of this investigation 88 sites of all zones of the layered sequence of both the eastern and western Complex, including the marginal zone were sampled. Several samples were found to be extensively altered and yielded inconsistent palaeomagnetic data at site and sample levels. Magnetization directions were, however, recovered from 69 sites.

II THE LAYERED SEQUENCE

The mafic and ultramafic rocks of the layered sequence or Rustenburg Layered Suite (South African Committee for Stratigraphy (SACS), 1980) crop out in three separate large lobate areas, referred to as the western, eastern and northern parts of the Bushveld Complex (Fig. 1, see Folder). Near Nietverdiend in the western Transvaal, a fourth occurrence is exposed, which may represent a discrete intrusive that was emplaced simultaneously with the Bushveld Complex. The exposed parts of the layered sequence cover an area of 12 000 km² and attain a thickness of 9000 m in the eastern Bushveld and 7750 m in the western Bushveld (SACS, 1980). The sequence comprises a variety of rock types ranging from dunites, pyroxenites, harzburgites, anorthosites, gabbros, norites to magnetite gabbros and diorites.

Subdivision of the layered sequence into zones was first proposed by Hall (1932) and subsequently altered by Lombaard (1934), Wager and Brown (1967), Willemse (1969) and Cameron (1970). Schweltnus *et al.*, (1962) and Coertze (1974) departed from this and used a lithostratigraphic subdivision. In 1980 the South African Committee for Stratigraphy (SACS) abandoned the zonal subdivision in favour of a lithostratigraphic one. The well-entrenched zonal subdivision, which is based largely on petrogenetic considerations, was retained as an informal subdivision. For ease of correlation between the eastern and the western Bushveld, as well as clarification, the informal, zonal nomenclature has been adopted for this study. Both subdivisions are shown on the lithostratigraphic columns of the layered sequence in the eastern and western Transvaal in Figures 2 and 3 respectively.

Early radiometric age determinations on the granite and mafic rocks of the Bushveld Complex (Schreiner, 1958; Nicolaysen *et al.*, 1958, and Davies *et al.*, 1970) indicated an age between 2100 m.y. and 1830 m.y. Hamilton (1977) studied the Sr isotope ratios of the layered sequence and arrived at a weighted mean age of 2095 ± 24 m.y. for the mafic rocks. He also found the ⁸⁷Sr/⁸⁶Sr ratios to increase in a step-wise manner upwards in the sequence and from this he concluded that the layered sequence was emplaced as a succession of magma influxes, each of which had a higher ⁸⁷Sr/⁸⁶Sr ratio than its predecessor.

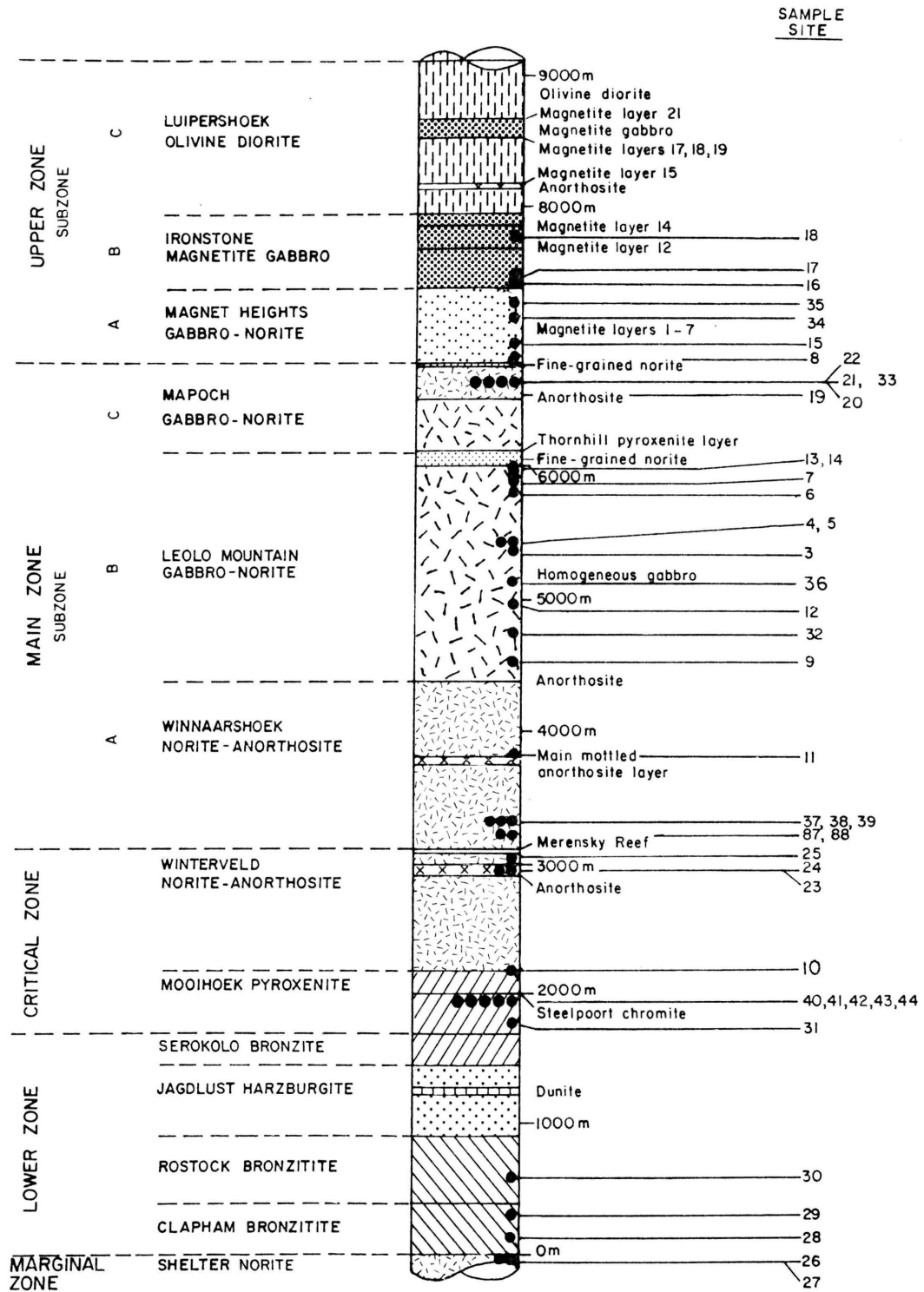


Fig. 2 Simplified lithostratigraphic column of the mafic layered sequence in the eastern Bushveld Complex indicating the stratigraphic positions of the sampling sites.

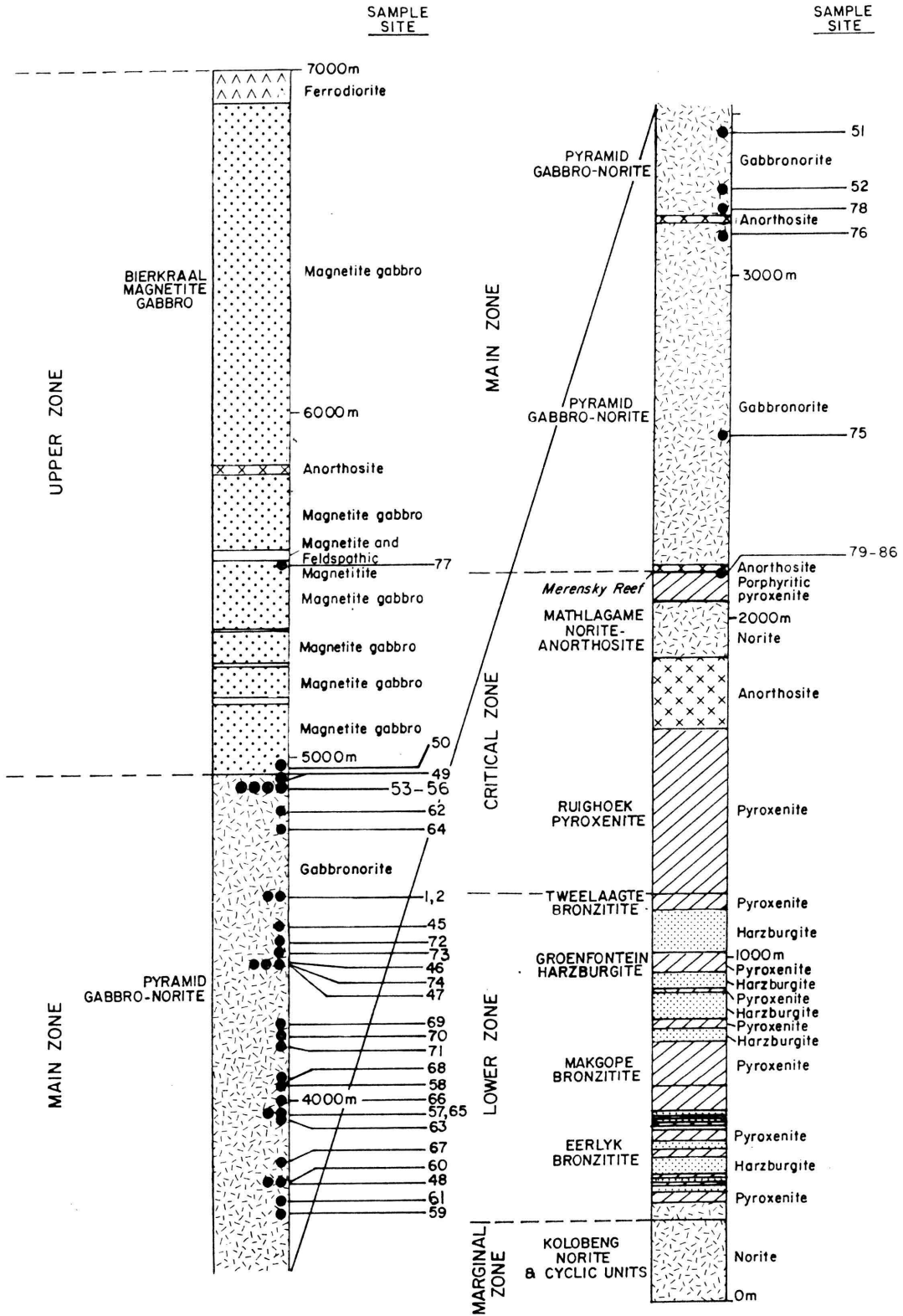


Fig. 3 Lithostratigraphic column of the mafic layered sequence in the western Bushveld Complex. Stratigraphic positions of the sampling sites are indicated.

Geological events leading to the emplacement, present structure and siting of the layered sequence have been debated in detail by numerous authors (Daly, 1929; Hall, 1932; Van Biljon, 1949; Truter, 1955; Cousins, 1959; Willemse, 1964, 1969; Hamilton, 1970; Hunter, 1975; Sharpe and Snyman, 1978; Von Gruenewaldt, 1979; Sharpe and Bahat, 1981, and Sharpe, 1982) to name but a few. Modern theories on the emplacement of the Bushveld Complex all consider tectonic events in the Kaapvaal craton, coupled with the deposition of the Transvaal Sequence into which the Bushveld magmas intruded, as major parameters in the evolution of the Complex.

The interpretation of gravity and magnetic data (Cousins, 1959; Smit *et al.*, 1962 and Hattingh, 1980) does not support the earlier view of Daly (1929) and Hall (1932) that the Bushveld Complex is a lopolith, with mafic material present underneath the centre of the Complex. The more modern concept, according to which the Bushveld Complex consists of a number of separate, overlapping intrusions (Hunter, 1975a, 1976; Sharpe and Snyman, 1978) is generally accepted.

The dip of the igneous layering in the western and eastern lobes is generally towards the centre of the Complex at fairly low angles (Hunter, 1975a). To the east of the Dennilton dome (Fig. 1) dip directions are away from the central area. This feature was interpreted by Hunter (1975) to be the result of tectonic processes which also led to the emplacement of the layered sequence. Von Gruenewaldt (1979) extended the above theory by postulating the existence of the Pretoria-Zebediela anticline, part of which is manifested by the Dennilton dome. He further suggested that this anticline was active before, during and after the emplacement of the Bushveld Complex.

The origin of the igneous layering has been attributed mainly to two possible processes: differentiation in depth with subsequent intrusion of different fractions with or without further differentiation in place or emplacement of essentially one batch of magma followed by differentiation *in situ* (Hunter and Hamilton, 1978). More recent research has clearly indicated that multiple magma injections have given rise to the layered sequence (Hamilton, 1977; Von Gruenewaldt, 1979; and Sharpe, 1980, 1982).

III COLLECTION AND PREPARATION OF ROCK SAMPLES

A. The distribution of sampling sites

The dominant cause of variation of direction of remanent magnetization in surface exposures in igneous rocks in southern Africa is due to a variable isothermal remanent magnetization (IRM) caused by magnetic fields associated with lightning discharges to the ground (Gough, 1967). This, coupled with the absence of Pleistocene glaciation and prevailing climatic conditions favourable for chemical weathering (Brink, 1979) generally render surface exposures in southern Africa unsuitable for palaeomagnetic sampling (Gough, 1956, 1967; Graham and Hales, 1957; Gough and Van Niekerk, 1959).

Sampling sites for this study were therefore confined to quarries, road cuttings, mines and, where no such sampling sites were available, streambeds. Unfortunately this procedure led to an uneven distribution of sampling sites over the layered sequence, in that the position and number of sites were dictated by their availability.

The distribution of sampling sites in the layered sequence is shown in Figure 1, and the position of the sampling sites in the stratigraphic columns of the layered sequence of the eastern and western Bushveld Complex is shown in Figures 2 and 3. Two sites are in the marginal zone, three in the lower zone, twenty in the critical zone, fifty-four in the main zone and nine in the upper zone.

Samples collected initially from the marginal and lower zones in the eastern Bushveld Complex yielded inconsistent magnetization directions at specimen, sample and site levels and were subsequently

proven to be magnetically unstable. Consequently no samples were collected from the equivalent marginal and lower zones in the western Bushveld and the palaeomagnetism of these two zones is not discussed further in the text.

B. Sampling techniques

Sampling was done with a commercially available, petrol driven, portable core drill. This drill produced core samples 25 mm in diameter and up to 200 mm in length. Thirteen sampling sites were underground where this drill was unsuitable due to the emission of exhaust gases from the petrol motor. Initially, the block method of sampling (Gough, 1967) was employed at four of these sites, but this proved to be unsatisfactory, especially when sampling hard, unjointed rock. Consequently, a core drill, driven by an Atlas Copco air motor, was designed by the author and built by the Technical Services Division of the University of Pretoria. This drill performed excellently at underground sites in mines where compressed air was readily available.

Orientation of core samples in the field was done with a sun compass (Creer and Sanver, 1967). At underground sites orientation was done relative to the mine survey networks with an open sight alidade. The precision of orientation was higher for cores orientated by means of the sun compass than for alidade orientated cores. The former can be orientated reliably with a precision of 1° (Gough, 1967), but orientations relative to mine survey networks were found by repeated orientations, to be reproducible within 2° and 3° . Block samples usually had only a rough plane surface and the uncertainty of orientation is probably more than 3° .

The number of samples taken at each sampling site, varied between four and six, with four core samples being the average.

C. Sample preparation

Core samples usually consisted of a number of separate pieces, which were carefully matched for a given core and glued together with a non-magnetic glue. Block samples were first set in concrete with fiducial marks in a horizontal position. A Seco diamond drill in the laboratory was then used to drill vertical 25 mm diameter cores

D. Measurement of dip and dip directions of the igneous layering

With the exception of sites at mines where the dip and dip directions of the igneous layering are accurately known, an attempt was made to measure dip and dip directions at each sampling site. This was done with a clinometer and magnetic compass.

However, at many sites no visible layering is present, and in these instances the orientation of natural fracture planes in the rock was measured, with the assumption that these planes follow the pseudo-stratification. A number of these directions were later found to be incompatible with the regional dip and dip directions of the layered sequence. For these sites the measured values were rejected and replaced with regional dip and dip direction values given for their respective areas by Hunter (1975b); Von Gruenewaldt (1973), Molyneux (1970) and Coertze (1974), as well as the dip indicated on the 1:50 000 mapsheets of the area northwest of Pretoria (Geological Survey of South Africa, 1975). However, at sites where the measured dip and dip directions were compatible with the regional values, the former were considered to be more accurate.

The estimated accuracy of the dip values and dip directions used in this study for structural fold tests (Graham, 1949) can only be considered accurate to the nearest five degrees.

IV LABORATORY MEASUREMENTS AND PROCEDURES

A. Laboratory instruments

The remanent magnetization of specimens was measured using a Digico "Complete Results" fluxgate spinner magnetometer. This instrument spins a core specimen at 7 Hz to produce an output signal, the amplitude of which is proportional to the intensity of magnetization of the specimen. The phase of this signal relative to a fiducial on the rotating shaft, indicates the angle of the vector of magnetization in a plane perpendicular to the axis of rotation. Six successive measurements were made with the specimen in different orthogonal positions in the sample holder; this allowed the three orthogonal components of the remanent magnetization vector to be determined. The manufacturers of this instrument claim a sensitivity of $0,01 \times 10^{-3} \text{ Am}^{-1}$. In practice, however, it was found that to measure a reliable direction of magnetization to within one degree a minimum intensity of magnetization of $0,5 \times 10^{-3} \text{ Am}^{-1}$ was required.

Continuous thermal demagnetization was done with a slightly modified form of this instrument. It was possible to measure remanence at high temperatures, without the need for cooling the specimen in a field free space. Operating the instrument in this mode led to a decreased sensitivity as a result of the positioning of a heater element as well as a water jacket between the specimen and sensor coils of the magnetometer. With repeated measurements the minimum intensity of magnetization that could be measured reliably was found to be in the region of $4 \times 10^{-3} \text{ Am}^{-1}$. The temperature of the specimen was continuously monitored with a chromal-alumal thermocouple positioned 2 mm from the core specimen. The temperature difference between the specimen and the thermocouple could never be established accurately, but according to the manufacturers of the instrument, this difference does not exceed 10°C in the temperature range $200\text{--}600^\circ\text{C}$. No correction for this difference was applied to the thermal data.

Alternating-field (AF) demagnetization of specimens was done with an apparatus built at the Geological Survey of South Africa following a description by McElhinny (1964a). The specimens were tumbled with a three axis tumbler situated in the centre of a coil, through which a

decaying 50 Hz current flowed which demagnetized all magnetic domains with coercivities below the maximum field produced by the peak current. The whole apparatus is contained in Helmholtz coils which annul the earth's magnetic field at the tumbler and thus prevent specimens from acquiring an anhysteretic remanent magnetization (ARM) (Patton and Fitch, 1962). At later stages of this study it was, however, found that a residual magnetic field of approximately 500 nT exists in the centre of the Helmholtz coils. Subsequent adjustments to the coils failed to cancel this field completely. It is therefore possible that certain specimens did, in fact, acquire a weak ARM during AF demagnetization. The magnitude of the ARM is, however, so small that its effect can be considered to be negligible on the magnetization directions presented in this study. This demagnetization apparatus is capable of creating a peak alternating demagnetization field of 100 mT, but due to heat generation in the demagnetization coil and overloading of the tuning capacitors in the circuit, 80 mT was considered to be the safe peak field. Higher AF values were only used occasionally when it was absolutely necessary to glean more information from specimens.

For a number of specimens self-reversing properties were examined. Thermoremanent magnetization (TRM) was imparted to specimens by heating them to 700°C in a quartz tube through which nitrogen was circulated. A positive nitrogen pressure was at all times maintained in the tube. The specimens, still in the quartz tube were then cooled in the Earth's magnetic field. In this way it was hoped to minimize chemical changes in the specimens which occur when heating in a normal atmosphere.

An isothermal remanent magnetization (IRM) was imparted to the specimens by placing them in a magnetic field of 500 mT for 15 minutes.

Lowrie-Fuller tests (Lowrie and Fuller, 1971) as modified by Dunlop, *et al.* (1973) were conducted to investigate magnetic domain characteristics of specimens from the upper zone. To do this, specimens were given an ARM by placing them in the coil of the AF demagnetization apparatus, with the current flow in the Helmholtz coils reversed. In this way an alternating magnetic field of 80 mT with a static field of 0,05 mT superimposed on it, was produced at the centre of the coil.

The possibility of self-reversals of magnetization, or, of specimens acquiring a transitional thermoremanence (TTRM) at low temperatures,

was investigated by placing a specimen in liquid nitrogen for 20 minutes. The specimen was then quickly transferred to the high temperature spinner magnetometer and the magnetization of the specimen measured as it warmed up to room temperature.

Initially a polished thin section from two specimens from each sampling site was made. The opaque mineralogy was then investigated with the aid of an ore-microscope. Whenever the grain size was too small to allow for positive identification optically the minerals were identified with the aid of an electron scanning microscope equipped with an energy dispersive spectrometer (EDS) for semi quantitative element analysis of minerals. Microprobe analysis and X-ray diffraction (XRD) identification of separated minerals were made where necessary.

B. Laboratory procedures

The natural remanent magnetization (NRM) of each specimen was first measured, followed by statistical analysis of the NRM directions. Subsequently AF demagnetization of at least two pilot specimens from each site in steps at 10, 20, 40, 60 and 80 mT was done and the remanent magnetization determined after each step. To find the optimum alternating demagnetization field to optimize grouping of stable remanent magnetization directions, the Briden stability index (SI) (Briden, 1972) was then calculated for each demagnetization step, for each pilot specimen. Bulk AF cleaning was then carried out on two specimens from each core sample at an AF value indicated by the Briden SI as being the optimum for a given site. Although the measured remanent magnetizations yielded satisfactory results for a number of sites, it was found that when dealing with multicomponent remanent magnetization it was essential to do more detailed stepwise AF demagnetization on randomly selected specimens. The remanent magnetization results were then subjected to vector analysis or least squares methods (Halls, 1976, 1978, 1979), as well as a modification of the latter method by Hoffman and Day (1978) to recover primary and secondary magnetization directions.

At least one specimen per site was retained for thermal demagnetization. The specimens were demagnetized thermally in steps of 100°C, and as the Curie point was approached, this was reduced to intervals of 20° and

10°C. After each step the remanent magnetization was measured.

C. Statistical analysis of results

The directions of magnetization of specimens were first averaged to give a sample mean. Sample means were then, in turn, combined to yield site mean directions, which were then combined to give the group overall mean directions.

The best estimate of the mean direction of magnetization is the vector sum of the unit vectors, having the directions of the several observations (McElhinny, 1973). The declination (D) and the inclination (I) of each observed direction can be expressed in cartesian coordinates by its direction cosines (Tarling, 1971):

$$\begin{aligned}x &= \cos D \sin I \\y &= \sin D \cos I \\z &= \sin I\end{aligned}$$

with the z axis vertical and positive in an upward direction and D measured clockwise from north. These direction cosines can then be summed for a number of vectors to obtain the length of the resultant vector (R) and its direction (\bar{D} , \bar{I}):

$$R^2 = (\Sigma x)^2 + (\Sigma y)^2 + (\Sigma z)^2$$

$$\bar{x} = \frac{\Sigma x}{R} ; \bar{y} = \frac{\Sigma y}{R} ; \bar{z} = \frac{\Sigma z}{R}$$

$$\text{and } D = \tan^{-1} \frac{\bar{y}}{\bar{x}} ; I = \sin^{-1} \bar{z}$$

Watson's (1956) test for randomness of directions was then applied at sample and site levels. Sample or site mean directions, which were not significant at 95% probability, were rejected.

The distribution of points (or directions) on a sphere can be described in terms of a probability density (ρ) given by

$$\rho = \frac{K}{4\pi \sinh K} \exp (K \cos \theta)$$

where θ is the angle between the observed individual directions and the true mean direction and K is the precision parameter- varying from

0 for a perfect random distribution to infinity for identical directions (Fisher, 1953). The best estimate k of the precision K is

$$k = \frac{N-1}{N-R}$$

with N the number of observations (Fisher, 1953).

The reliability of the mean direction can be defined by measuring the radius (α) of a circle on the surface of the sphere, centred on the observed mean direction, within which there is a particular probability (ρ) of the true mean direction lying in this cone of confidence. The radius can, according to Irving (1964, p62) be expressed as:

$$\alpha = \cos^{-1} \left[1 - \frac{N-R}{R} \left[\rho - \frac{1}{(N-1)} - 1 \right] \right]$$

ρ was taken as, in most palaeomagnetic studies (Tarling, 1971), to be 0,05, so that there is a 20 to 1 chance of the true mean lying within α_{95} degrees of the observed mean.

The estimate k of the precision parameter K and the radius (α_{95}) of the circle of confidence were calculated for each site, as well as for the different groups of site directions.

For any Fisherian group of points on a sphere defined by K , a circle of radius Δ about the mean can be drawn which encloses a selected percentage of points (Tarling, 1971). The radius of this circle will be a measure of the scatter or dispersion of directions about their mean. The radius of the circle enclosing sixty-three per cent of the points is generally known as the circular standard deviation and was calculated for groups as follows (Irving, 1964, p60):

$$\Delta_{63} = 81 K^{\frac{1}{2}}$$

In practice k and not K must be used in the calculation and the upper and lower confidence limits of k were calculated using the method of Cox (1969a).

The palaeomagnetic pole positions corresponding to group mean magnetization directions were calculated using the conventional premise that the Earth's field is that of a geocentric dipole (McElhinny, 1973). The polar error (dp , dm) is termed the oval of ninety five per cent confidence about the pole position. This was calculated from an equation given by McElhinny (1973, p83).

V THE PALAEOMAGNETISM OF THE CRITICAL ZONE

A. Introduction

Twenty sampling sites are situated in the critical zone. The rock types sampled consist of pyroxenites, anorthositic norites, norites and pegmatitic feldspathic pyroxenite of the Merensky Reef. The NRM's of samples of pyroxenites are characterized by a low intensity of magnetization (generally below $10 \times 10^{-3} \text{ Am}^{-1}$) with inconsistent and unstable magnetization directions at sample and site levels. As a result, data from 12 sampling sites had to be rejected.

With the exception of site 24, which is situated in a shallow road cutting, the remainder of the sites, are all situated in platinum mines in the western and eastern Bushveld Complex. The eight sites which yielded consistent palaeomagnetic directions are positioned below the Merensky Reef, but generally above the footwall marker which is usually not more than 10 m below the Merensky Reef.

Two sampling sites, numbers 82 and 88, are situated on the Merensky Reef. The rock material, a coarse-grained feldspathic pyroxenite, proved to be unsuitable for palaeomagnetic sampling, because of its tendency to crumble during and after the drilling of a core sample. Even samples which were recovered in this case, proved to be inconsistently magnetized and data from these two sites also had to be rejected.

B. Natural remanent magnetization

The mean intensity of the natural remanent magnetization of all the specimens from the critical zone is $27 \times 10^{-3} \text{ Am}^{-1}$. A histogram plot of these intensities are shown in Figure 4.

The magnetization directions, with α_{95} values and the estimate k of the precisions for each site, where the in-site grouping of magnetization directions is significant at the 95 per cent confidence limit (Watson, 1965) are given in Table I.

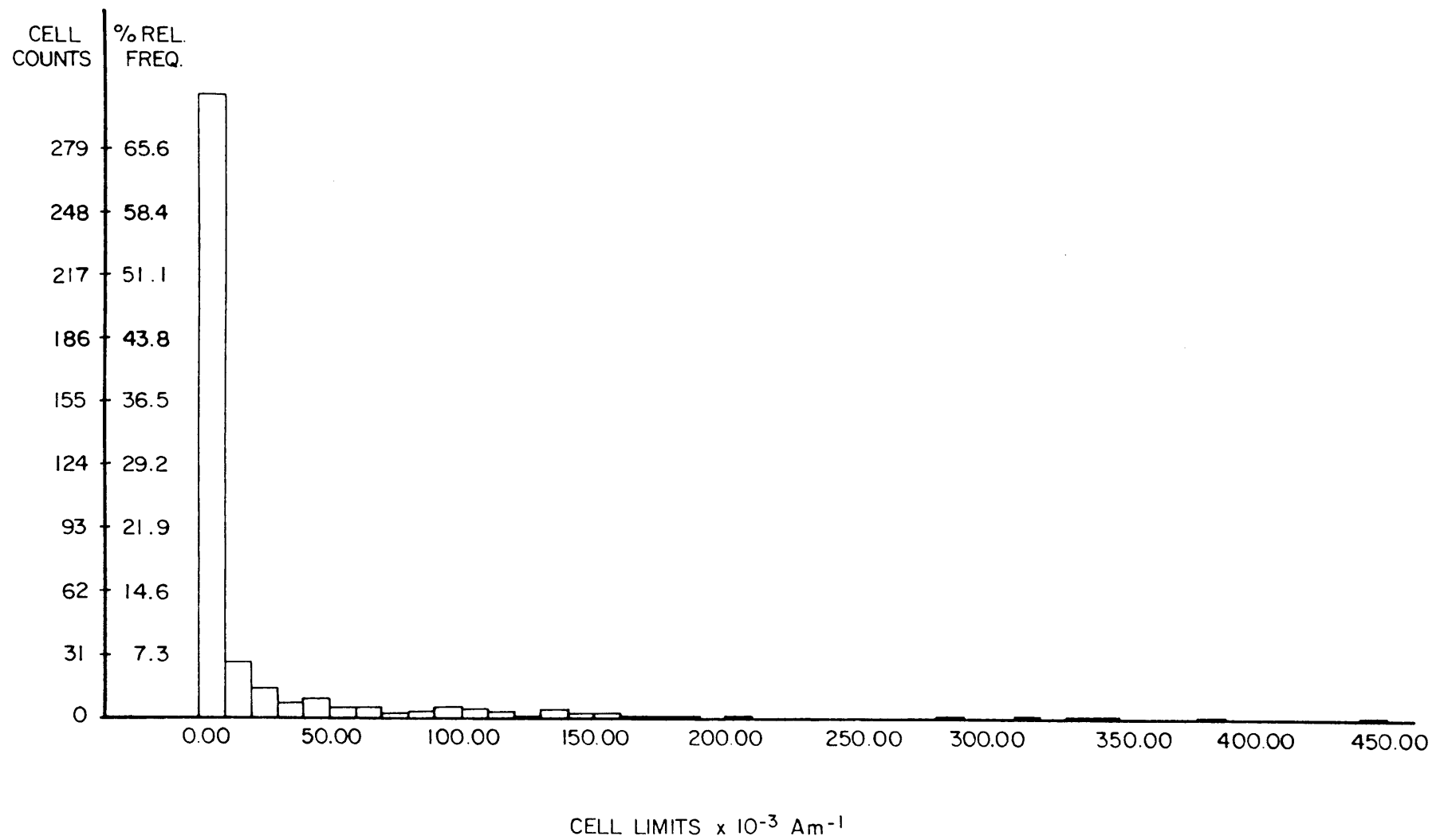


Fig. 4 Histogram plot of NRM intensities of specimens from the critical zone.

Table I. Natural remanent magnetization directions of sites in the in the critical zone.

Site	N*	D**	I***	α_{95}	k
24	3	28,3°	21,2°	20,0°	39
79	4	200,0°	-52,4°	20,6°	21
80	4	199,0°	-60,9°	16,8°	31
81	5	201,0°	-61,4°	15,5°	25
83	5	155,0°	-62,0°	10,8°	51
84	5	226,3°	-62,8°		39
85	5	1,1°	68,2°	10,7°	52
86	5	312,7°	-74,8°	18,1°	18
87	5	3,0°	9,8°	9,9°	60

*N is the number of core samples

**D is the declination of the magnetization direction, measured from north in a clockwise direction

***I is the inclination of the magnetization direction; downward is positive, upwards negative.

The site magnetization directions are shown in Figure 5. With the exception of sites 24, 85 and 87 all the sites in Table I are normally magnetized and form group Bcz1 with the following group statistics:

Group: Bcz1 ; N = 6 ; D = 202,9° ; I = -67,2° ; α_{95} = 16,0° ; k = 18

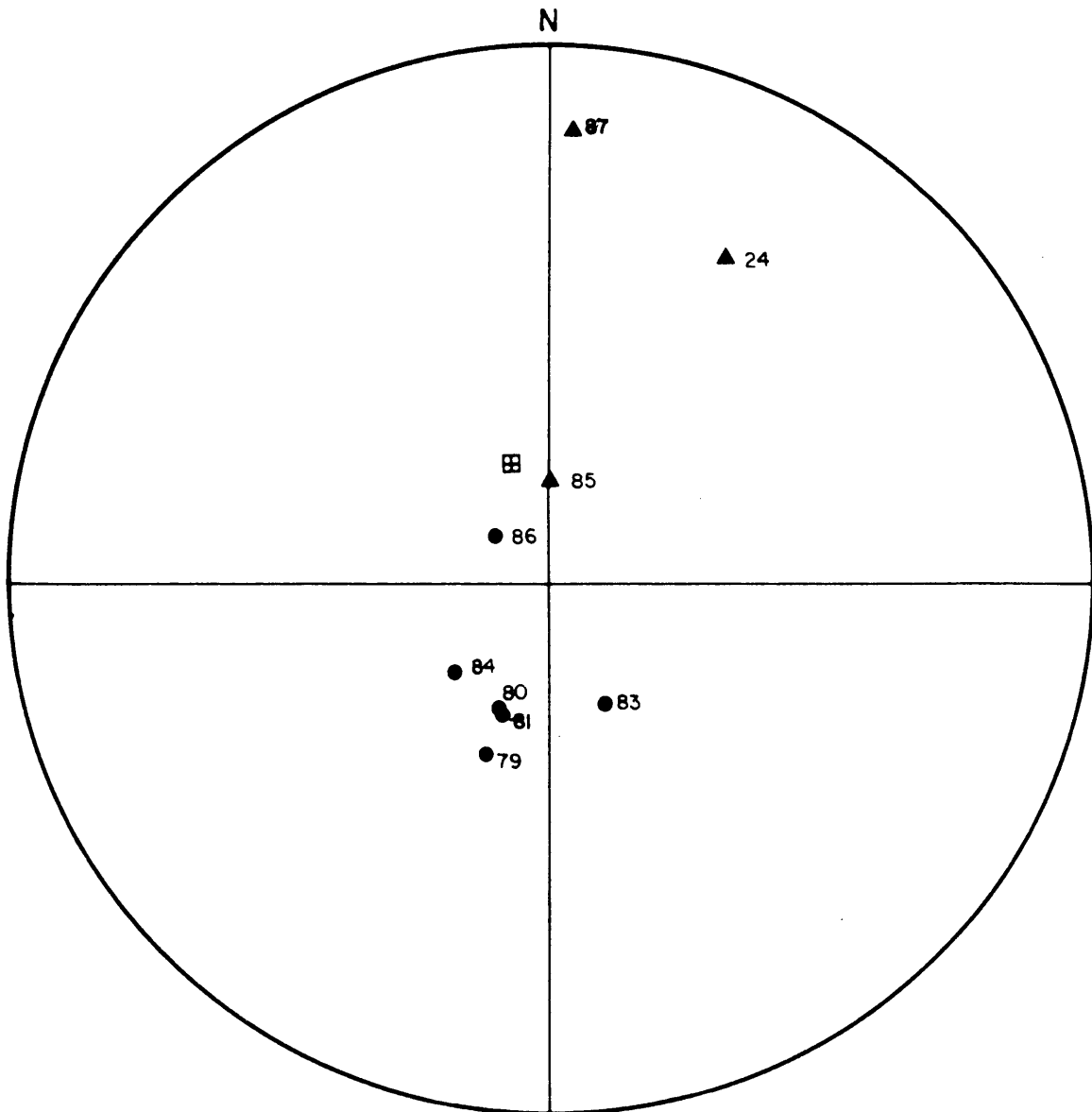


Fig. 5 Stereographic (equal angle) projection of NRM directions of sites 24, 79, 80, 81, 83, 84, 85, 86 and 87. ▲ = lower hemisphere, ● = upper hemisphere. Present day magnetic field direction upwards indicated by ⊠.

The dip and dip direction of the layered sequence at each site, as well as the declination and inclination of the magnetization vectors, after rotating the layering to horizontal, are given in Table II. The magnetization directions thus corrected for dip are shown in Figure 6.

Table II. Natural remanent magnetization directions of sites in the critical zone, with the igneous layering in a horizontal position.

Site	Dip	Dip direction*	D**	I**
24	11°	N300°	24,1°	20,5°
79	8°	N 50°	204,3°	-45,3°
80	9°	N 39°	203,2°	-52,3°
81	9°	N 23,5°	201,5°	-52,4°
83	8°	N 6,5°	161,2°	-54,9°
84	10°	N 20°	219,9°	-53,6°
85	38°	N135°	99,0°	62,0°
86	20,5°	N134°	313,5°	-54,3°
87	22°	N202°	0,1°	30,5°

*Dip direction measured from north in a clockwise direction

**After rotation of the layering to horizontal

If the sites from group Bcz1 are combined after structural folding a deterioration of the group statistics results:

Group: Bcz1R ; N = 6 ; D = 210,1° ; I = -59,9° ; $\alpha_{95} = 23,1$; k = 9

C. Bulk alternating field demagnetization

Alternating field demagnetization of two pilot specimens from each site in the critical zone of the layered sequence was done to calculate the Briden stability index (SI), (Briden, 1972), from which the optimum demagnetization field for each site was determined. The twelve sites where the NRM was inconsistent, all proved to be unstable

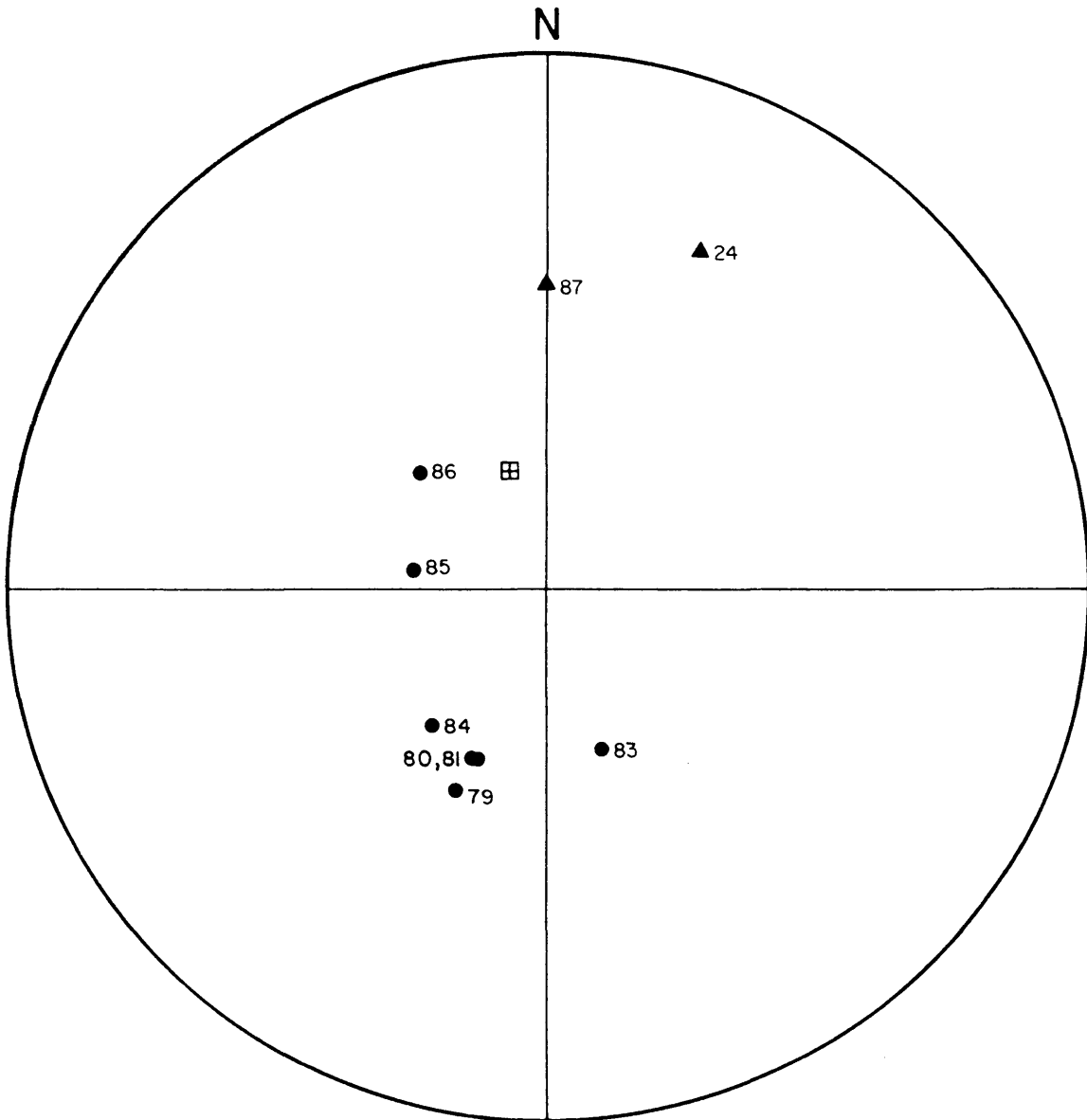


Fig. 6 NRM directions of sites in the critical zone with igneous layering in a horizontal position. Plotting convention as in Fig. 5.

during AF demagnetization, with magnetization directions changing randomly during each AF demagnetization step. Site 24 yielded a consistent NRM direction but immediately on AF demagnetization this became unstable and the site was rejected.

The results of the bulk AF demagnetization of sites are given in Table III and the magnetization directions are plotted in Figure 7.

Table III. Magnetization directions of sites in the critical zone after alternating field demagnetization.

Site	Alternating field (mT)	D	I	α_{95}	k
79	30	190,7°	-44,5°	12,1°	56
80	30	184,5°	-50,3°	12,6°	54
81	30	203,2°	-47,6°	24,4°	10
83	30	182,9°	-49,0°	20,6°	14
84	30	229,5°	-48,4°	13,5°	33
85	50	9,5°	80,3°	10,2°	57
86	20	355,5°	-84,0°	11,5°	43
87	30	2,7°	14,0°	7,5°	107

After bulk AF demagnetization, group Bcz1 changes to

Group: Bcz1AF ; N = 6 ; D = 198,7° ; I = -56,6° ; α_{95} = 18,7 ; k = 14

which is not much different from group Bcz1, but the grouping has become weaker instead of improving. Despite this, it is clear from Figure 7, that the magnetization direction of site 83 has moved towards the group mean direction and that the directions of sites 85 and 86 tend to group together away from Bcz1AF. The magnetization directions of sites 85 and 87 have remained reversed with respect to the magnetization directions of all the other sites. With site 86 excluded from group Bcz1AF, group Bcz2AF forms:

Group: Bcz2AF ; N = 5 ; D = 198,0° ; I = -49,2° ; α_{95} = 12,2° ; k = 40

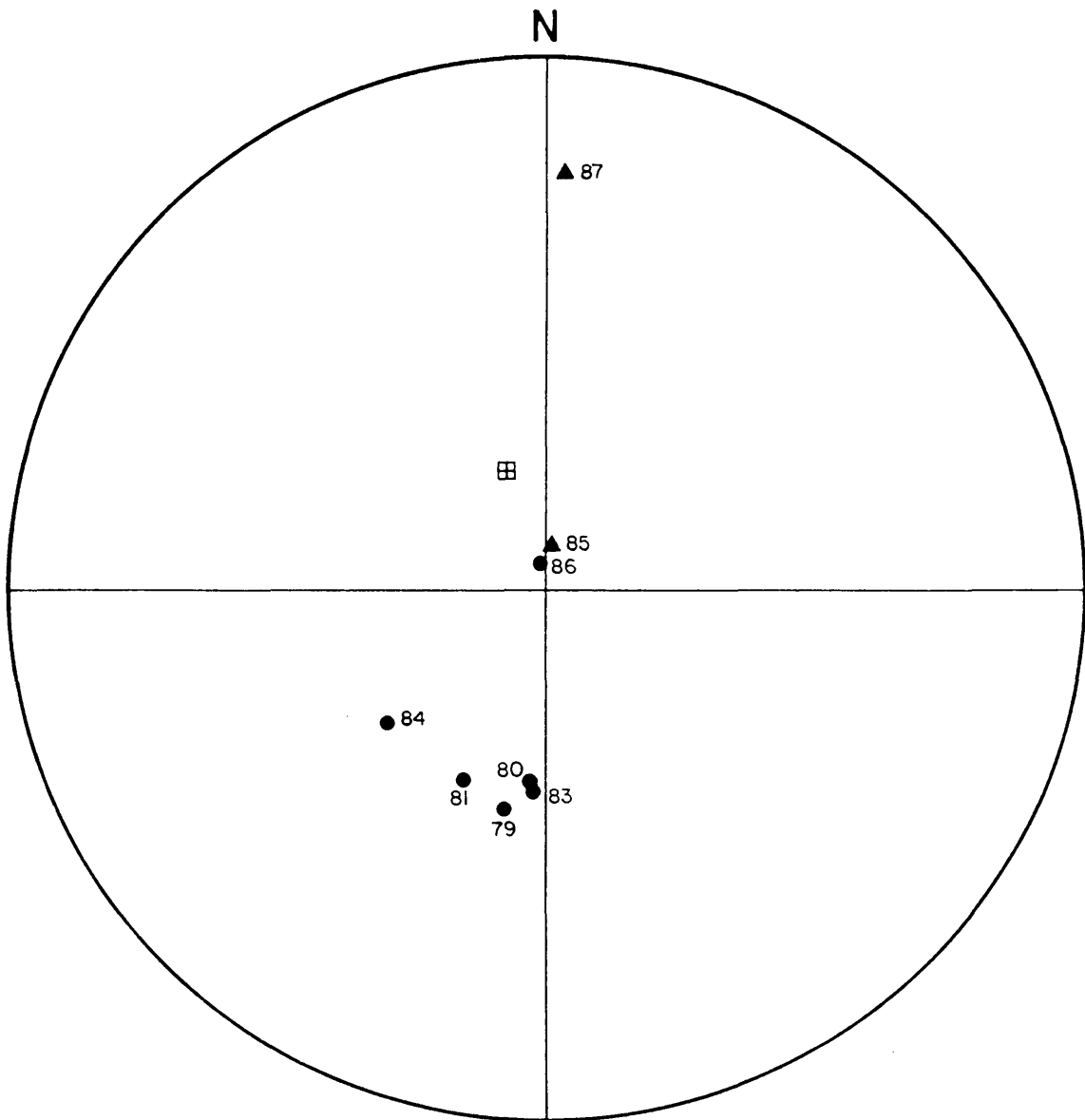


Fig. 7 Magnetization directions of sites in the critical zone, after AF demagnetization. Plotting convention as in Fig. 5.

Although group Bcz2AF is an improvement on both groups Bcz1 and Bcz1AF, it is only in the case of site 83 where the Briden SI (Briden, 1972) located a magnetization component which resulted in an improved grouping.

To evaluate the results of the bulk AF demagnetization fully, a structural fold test (Graham, 1949) was done on the magnetization directions yielded by the AF demagnetization. The results after rotation of the layering to the horizontal position are listed in Table IV, whereas the magnetization directions are plotted in Figure 8. In Figure 9 the same directions are shown but with the directions of site 85 and 87 inverted.

Table IV. Magnetization directions of sites in the critical zone after alternating field demagnetization, with the igneous layering in a horizontal position.

Site	D*	I*
79	194,9°	-38,1°
80	189,5°	-42,7°
81	203,2°	-38,6°
83	183,4°	-41,0°
84	225,0°	-39,5°
85	120,5°	56,8°
86	323,3°	-64,7°
87	359,0°	34,5°

*Declination and inclination after rotation of the layering to horizontal.

This gives rise to group Bcz2AFR, which is the corrected equivalent of group Bcz2AF, and has the following statistics:

Group: Bcz2AFR ; N = 5 ; D = 199,2° ; I = -40,9° ; $\alpha_{95} = 11,8$; k = 42

which are not significantly better at 95 per cent confidence limit according to the criteria of McElhinny (1964b). This lack of significant improvement, however, could be because the dip and dip directions at

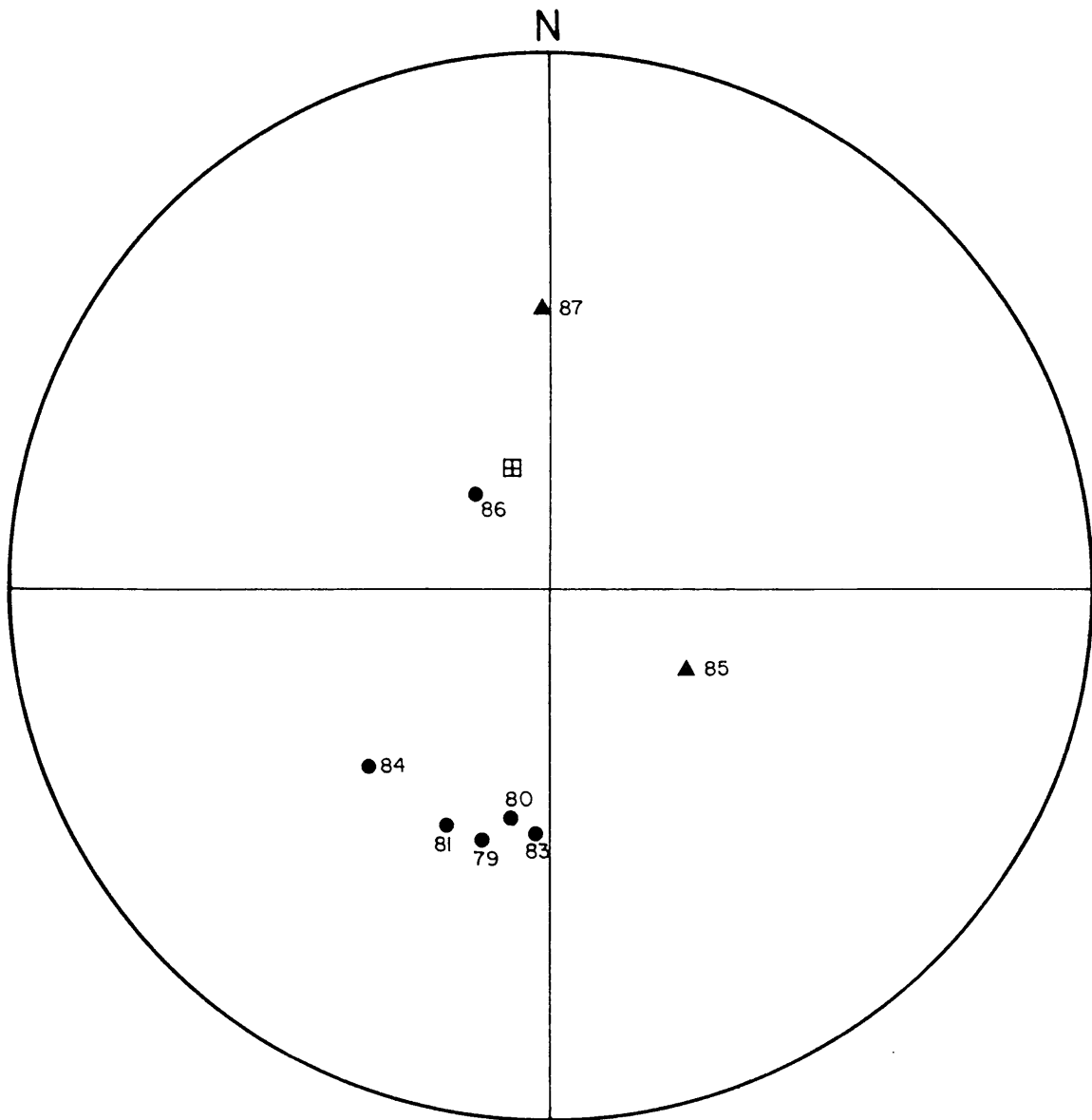


Fig. 8 Magnetization directions of sites in the critical zone, after AF demagnetization, with the igneous layering in a horizontal position. Plotting convention as in Fig. 5.

the sites included in group Bcz2AFR are very similar.

After rotation, the magnetization direction of site 87 is approximately antipodal to the mean direction of group Bcz2AFR. If one includes the inverted magnetization direction of site 87 in group Bcz2AF, the following two groups can be established:

Before rotation:

Group: Bcz3AF ; N = 6 ; D = 194,4° ; I = -43,6° ; $\alpha_{95} = 16,0^\circ$; k = 18

After rotation:

Group: Bcz3AFR ; N = 6 ; D = 195,6° ; I = -40,0° ; $\alpha_{95} = 10,9^\circ$; k = 38

The improvement after rotation is, however, still not significant at 95 per cent confidence limit according to the criteria of McElhinny (1964b). Because site 87 is the only site where the dip and dip direction is much different from the other five sites in the group Bcz3AFR, one cannot conclude that the result of this fold test is totally insignificant. The result is inconclusive due to the lack of evenly distributed sampling sites in the critical zone.

The mixed polarity of group Bcz3AFR, irrespective of whether it is the result of a geomagnetic field reversal or a self-reversal of magnetization, can be regarded as an indication of the consistency of magnetization (McElhinny, 1973). This further implies that the mean direction of magnetization of group Bcz3AFR, represents the mean direction of the primary magnetization of the rock units immediately below the Merensky Reef.

The magnetization directions of sites 85 and 86 after correction for dip are, however, incompatible with the mean direction of group Bcz3AFR. Furthermore, the two directions are approximately antipodal after rotation of the layering to the horizontal position (Figs. 8 and 9). This suggests that the magnetization direction of either site

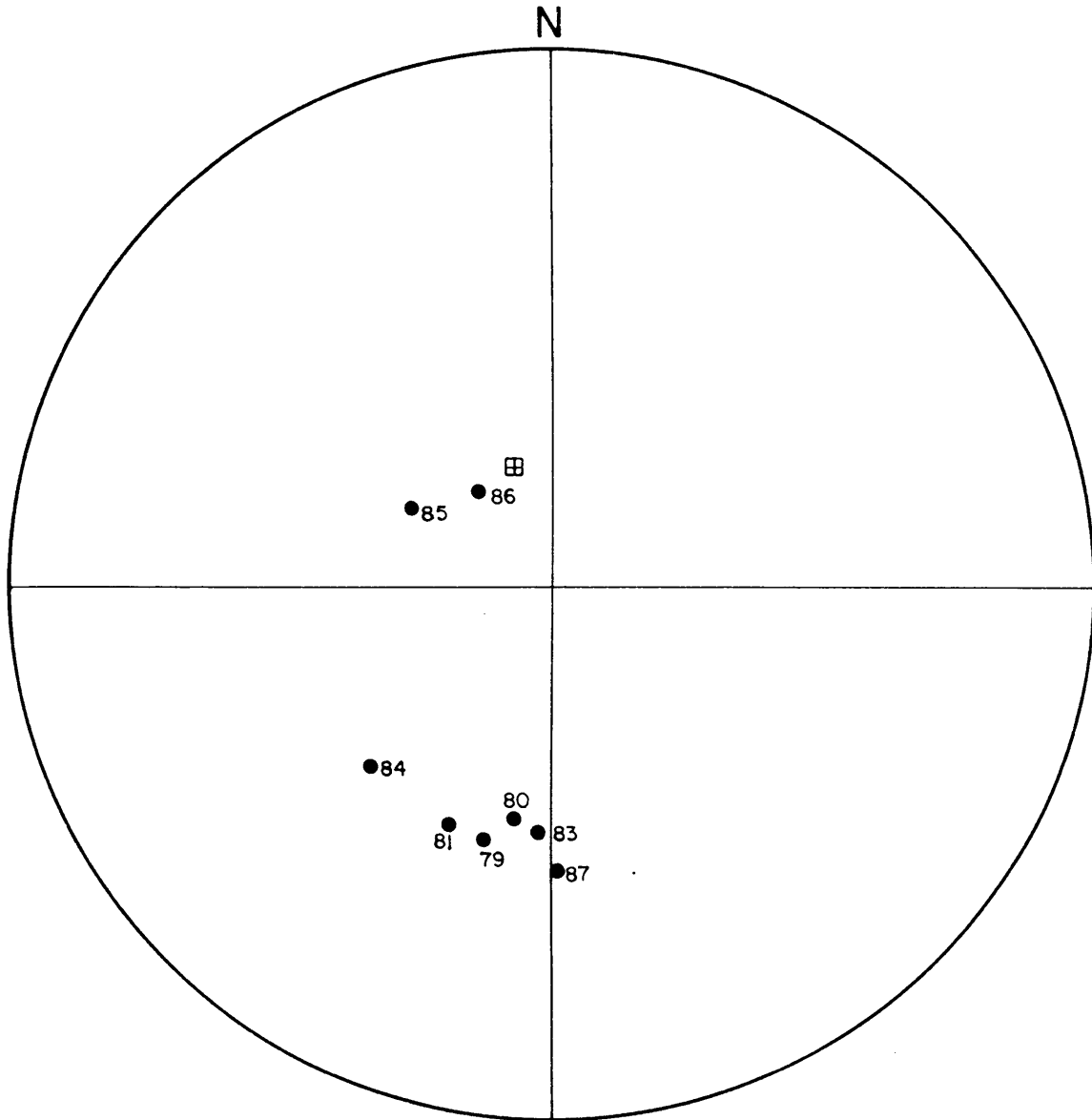


Fig. 9 The same data as Fig. 7 with the magnetization directions of sites 85 and 87 inverted. Plotting convention as in Fig. 5.

85 or site 86 (or both) is a stable primary magnetization direction of the rock unit below the Merensky Reef in the western lobe of the layered sequence to the north of the Pilanesberg Complex. Although this conclusion is based on data from only two sampling sites and should be treated with caution, the question why this magnetization direction is different from that of group Bcz3AFR, is still relevant. The difference in direction of magnetization can have the following possible causes:

- (i) The igneous layering of the critical zone in the southern and northern parts of the western lobe had different orientations in space when the rock units acquired their primary NRM.
- (ii) The primary NRM's were acquired at different geological times.
- (iii) The difference in magnetization directions is due to experimental errors in the determination of the magnetization directions of both sites 85 and 86.

Possibility (iii) can only be proved with more palaeomagnetic data from the area north of the Pilanesberg Complex, but seems unlikely in view of the consistency of magnetization of sites 85 and 86 after correction for dip of the layered sequence. The complex geological structure of this area with transgressions of the upper zone on to the critical zone is an indicator of a tectonic history which favours the first possibility. If remagnetization occurred during the emplacement of the upper zone, one can expect the magnetization directions of sites 85 and 86 to be strung out between the mean magnetization direction of the critical zone and that of the upper zone.

D. Stepwise alternating field demagnetization of pilot specimens.

The magnetization directions of all the specimens subjected to stepwise AF demagnetization at progressively higher AF values, changed after each successive demagnetization step. Although the patterns generally did not follow great circles (called remagnetization circles by some authors; Halls, 1976), it is clear that the changes are not random, which would indicate a totally unstable NRM (Figure 10).

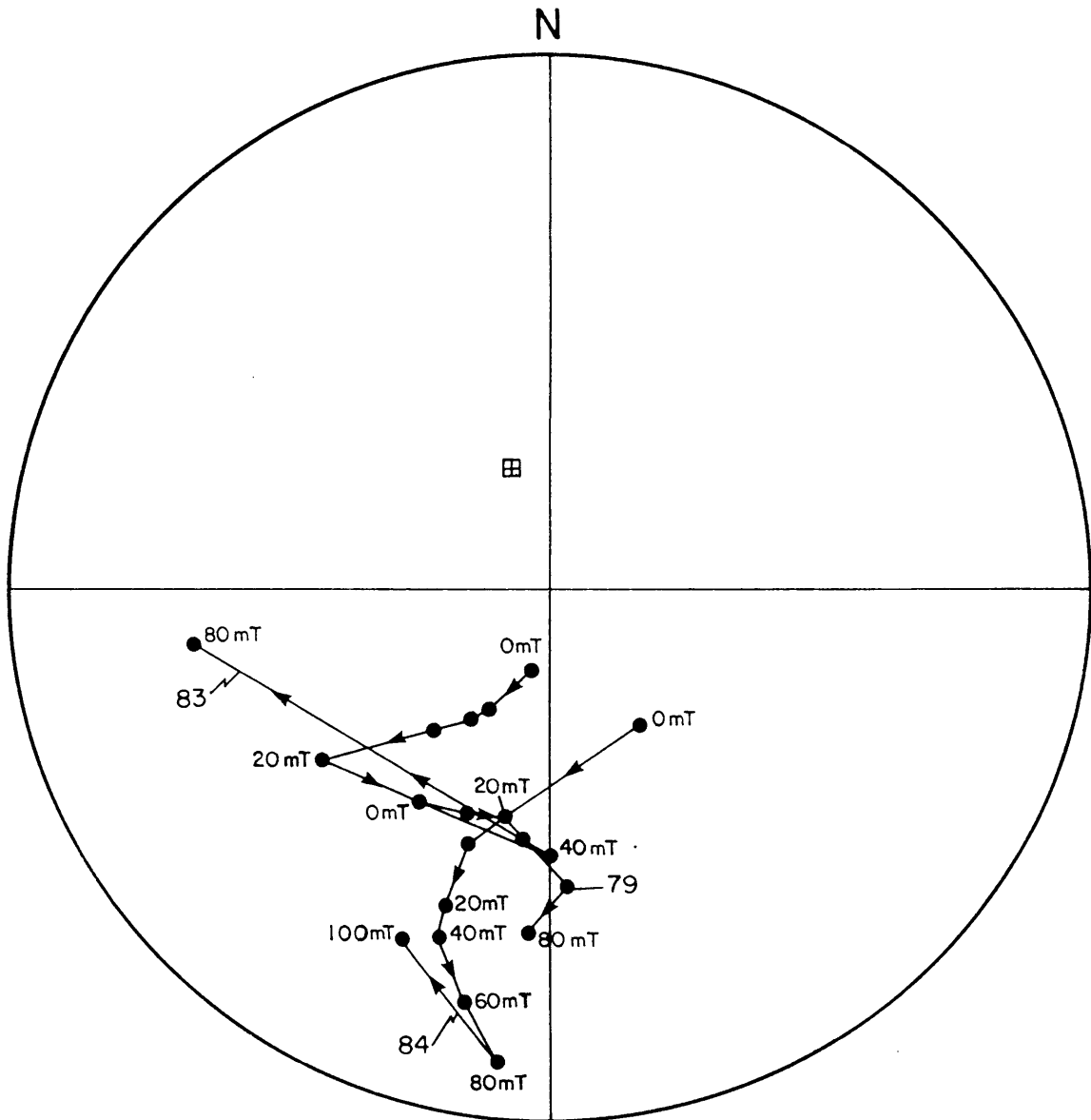


Fig. 10 Stepwise AF demagnetization of specimens from sites 79, 83 and 84. Plotting convention as in Fig. 5.

When the changes in magnetization directions during AF demagnetization of different specimens from the same site are compared (Figure 11), one finds that the initial response to low AF values is a convergence of directions, but at high AF values the directions tend to diverge. This behaviour led to the investigation of the repeatability of a given AF demagnetization step for the same specimen. Specimen 83/5d was demagnetized three times at each AF step value, with measurements of the remanent magnetization following each demagnetization run. In this way, three separate directional and intensity of magnetization response curves were obtained for this single specimen (Figs. 12 and 13). The different sets of magnetization directions for this specimen behaved much the same as directions of magnetization from different specimens from a site and, to a somewhat lesser degree, similar to behaviour of specimens from different sites. In all these cases an initial convergence of directions was observed followed by a divergence of directions at high AF values. A further conclusion from Figure 12 is that AF demagnetization data obtained at high AF values (for specimen 85/5d anything higher than 30 mT) are unreliable and cannot be used in any attempt to delineate a primary or secondary magnetization component.

The mean normalized intensity response curve during stepwise AF demagnetization of specimen 83/5d is shown in Figure 13. The error bars at each demagnetization step represent the standard deviation of the mean normalized intensity of magnetization calculated from the three sets of data. From this it can be seen that the repeatability of this curve is not good and any attempt to draw conclusions from this curve regarding the magnetic characteristics of the specimens would be futile. Because of similar behaviour during stepwise AF demagnetization specimen 83/5d can be taken as representative of all specimens from site 79 to site 87, and on this basis any attempt to recover magnetization directions with the aid of vector analyses, was abandoned.

There are three possible causes for the non-repeatability of the AF demagnetization data at high AF values:

- i) After demagnetization with an AF value of 30 mT the intensity of magnetization of specimens is in the general order of $0,5 \times 10^{-3} \text{ Am}^{-1}$

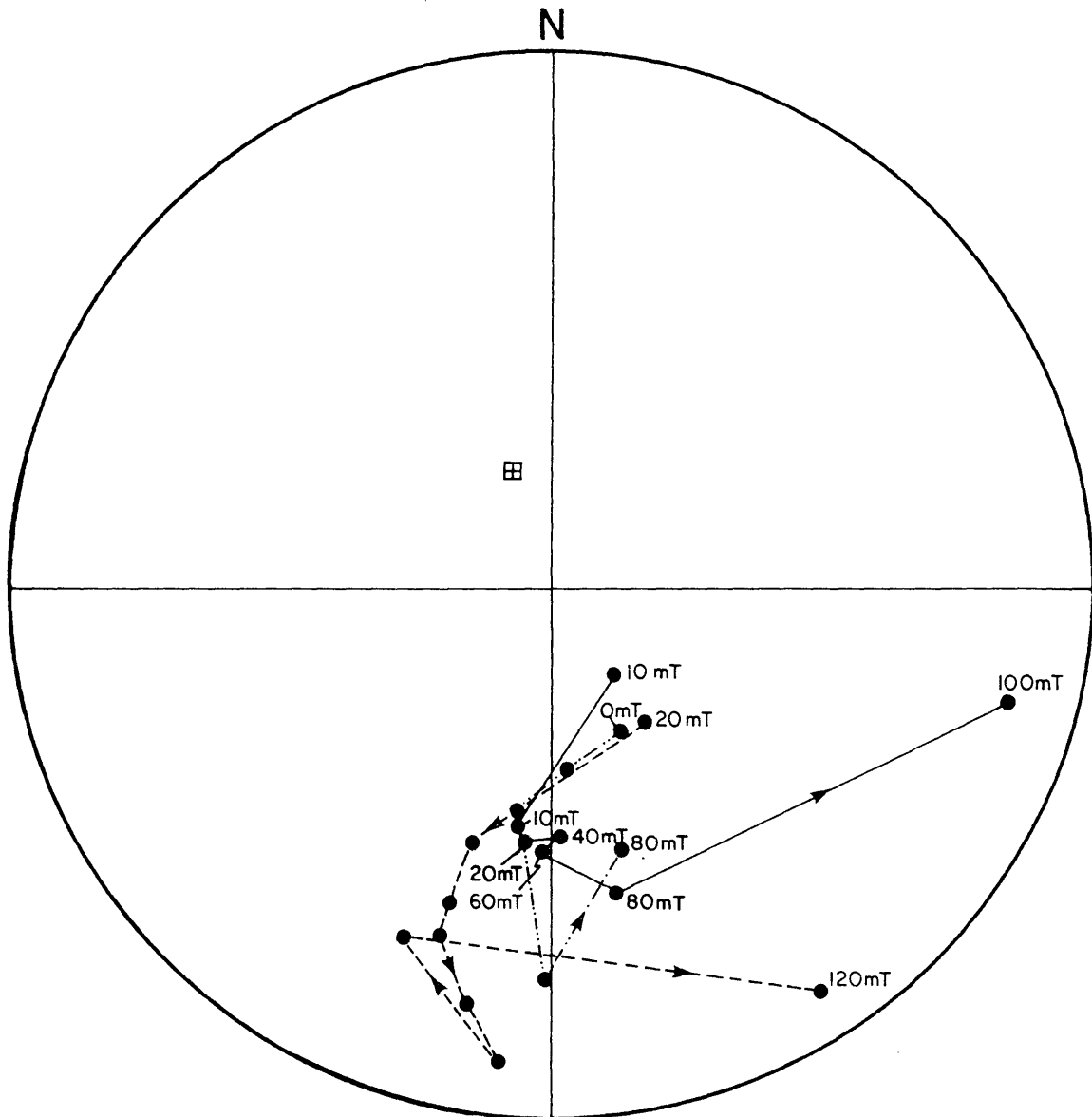


Fig. 11 Stepwise AF demagnetization of three specimens from site 83. Plotting convention as in Fig. 5.

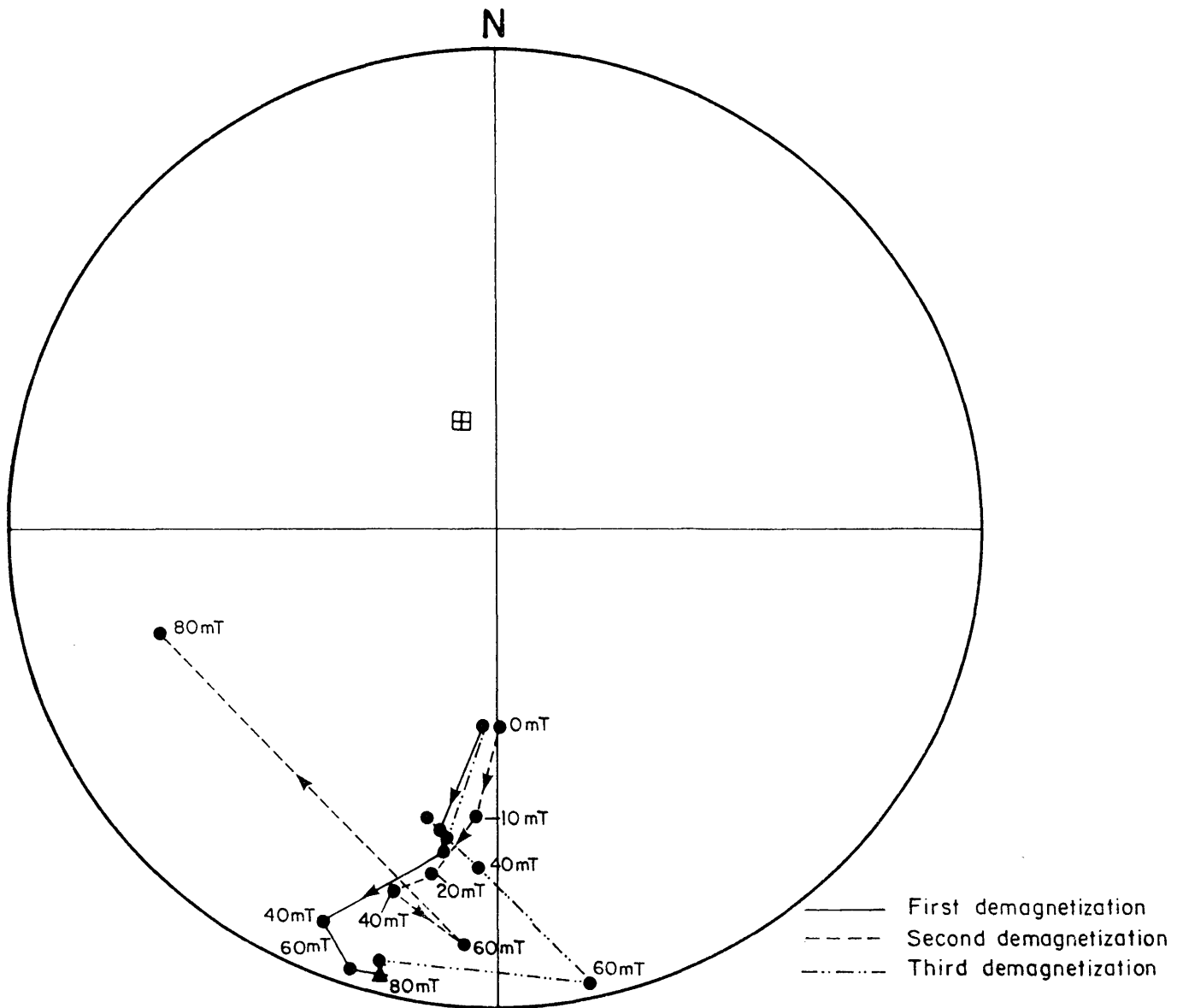


Fig. 12 Repeated stepwise AF demagnetization of a single specimen from site 33. Plotting convention as in Fig. 5.

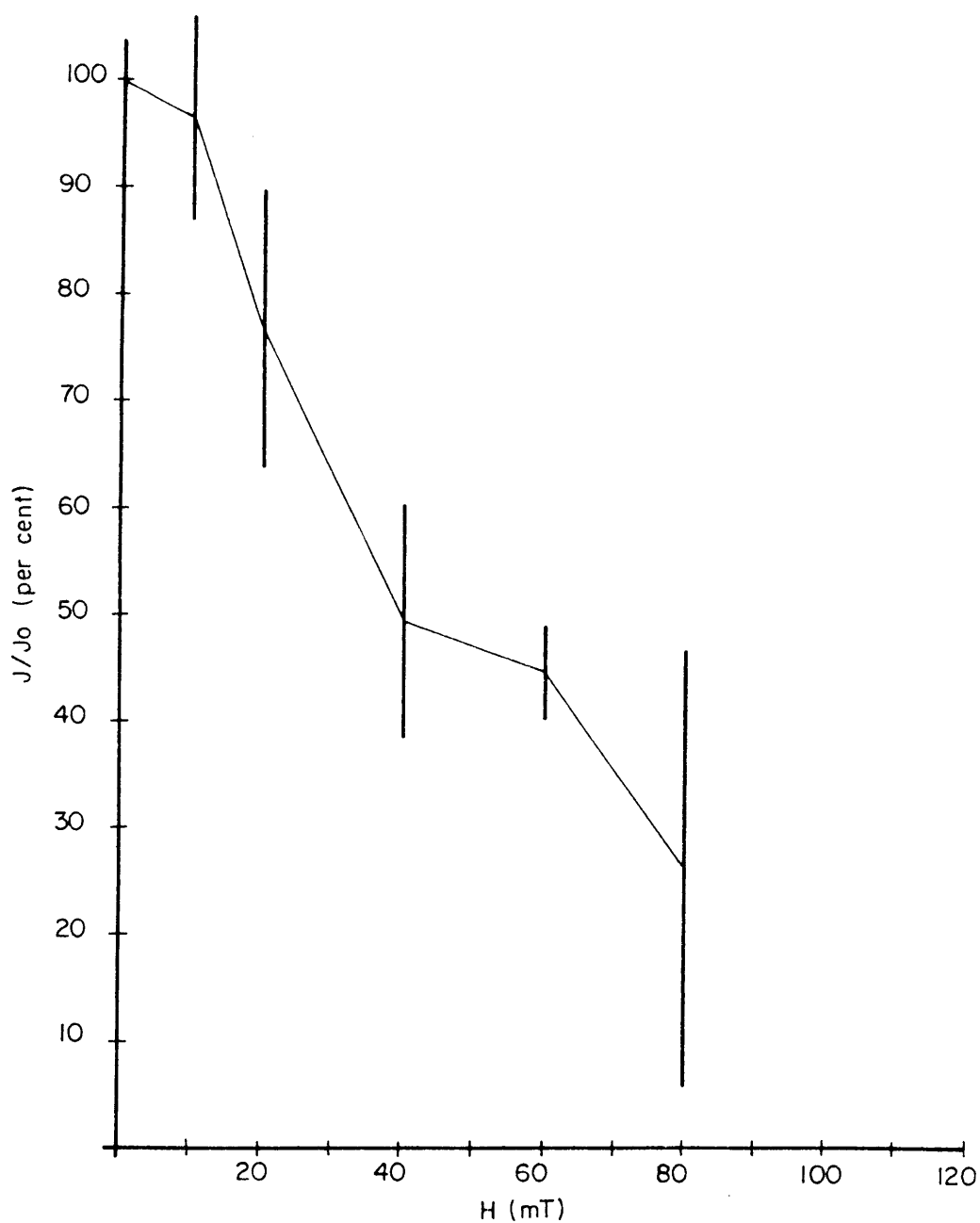


Fig. 13 Normalized AF demagnetization curve of the intensity response of specimen 83/5D during repeated AF demagnetization at each step. Vertical bars at each step indicate the standard deviation of the mean normalized intensity.

(with the exception of specimens from site 85, which have a slightly higher intensity), which approaches the maximum sensitivity of the spinner magnetometer. At higher AF demagnetization values with a smaller intensity of magnetization could lead to faulty data

- ii) It is possible that the AF demagnetization apparatus imparted an ARM (Patton and Fitch, 1962; Doell and Cox, 1967) on the specimens, which can cause the apparent divergence of magnetization directions at high AF values.
- iii) Specimens could have acquired a viscous remanent magnetization (VRM) after removing them from the field free space at the AF demagnetization apparatus to place them in the spinner magnetometer.

The last possibility was thoroughly investigated with repeated measurements on specimens after moving them from the AF demagnetization apparatus to the spinner magnetometer. Measurements were also repeated at different time intervals, the longest interval being eighteen months. These measurements of magnetization were always repeatable with no indication of the acquisition of a VRM by the specimens. Bearing in mind the limitations of the instruments, it is possible that both possibilities (i) and (ii) together contributed to the non-repeatability of magnetization directions at high AF demagnetization values.

The Briden SI (Briden, 1972) is based on both the change in magnetization direction and intensity of magnetization between successive AF demagnetization steps. To some extent the calculation of the Briden SI is in fact a form of vector analysis. Any inaccuracies in the AF demagnetization data will be reflected in the Briden SI value and will make it a less reliable parameter to determine the optimum AF value at which bulk AF demagnetization of specimens should be carried out. It is interesting to note that the AF value indicated by the Briden SI for bulk demagnetization of specimens from each site, was generally around 30 mT (Table III) with the exception of site 85, where 50 mT was indicated. At approximately this AF value one finds that magnetization directions of specimens from a site tend to converge (Figure 10). However, from the relatively

unchanged mean magnetization directions of sites after bulk AF demagnetization, one must conclude that the application of the Briden SI, with the possible exception of sites 83, 85 and 87, was not successful due to the unreliability of the AF demagnetization data at high AF values.

E. Thermal demagnetization

Because of the low intensity of magnetization of specimens, thermal demagnetization of only a few selected specimens with slightly higher intensities of magnetization, was attempted. In Figure 14 the intensity responses of the demagnetization at progressively higher temperatures for two specimens are shown. The two curves differ substantially. However, this difference does not necessarily indicate widely different blocking temperature spectra, but rather the effect of using the high temperature spinner magnetometer with a weaker sensitivity than the normal spinner magnetometer. This again gave rise to data which may not be exactly repeatable. In broad terms one can, however, draw two conclusions from the shape of the intensity response curves:

- i) It appears as if both specimens have thermally distributed blocking temperatures;
- ii) The final Curie point of the specimens is in excess of 500°C.

The change of magnetization directions of one of the specimens 83/5F (Figure 15) at progressively higher temperatures is a movement towards the mean magnetization direction of group Bcz1, but at temperatures above 520°C the change in direction becomes random, indicating that the Curie point has been reached, or simply that the remaining intensity of magnetization is too low to measure accurately. The direction of magnetization of the other specimen 86/4E changes very little up to 500°C; thereafter it exhibits the same tendency as specimen 83/5F and the magnetization directions at temperatures higher than 500°C cannot be considered reliable.

One specimen was given a TRM in the Earth's magnetic field in a nitrogen atmosphere and was subsequently thermally demagnetized. The intensity response curve (Fig. 16) is in broad agreement with the curves from the thermal

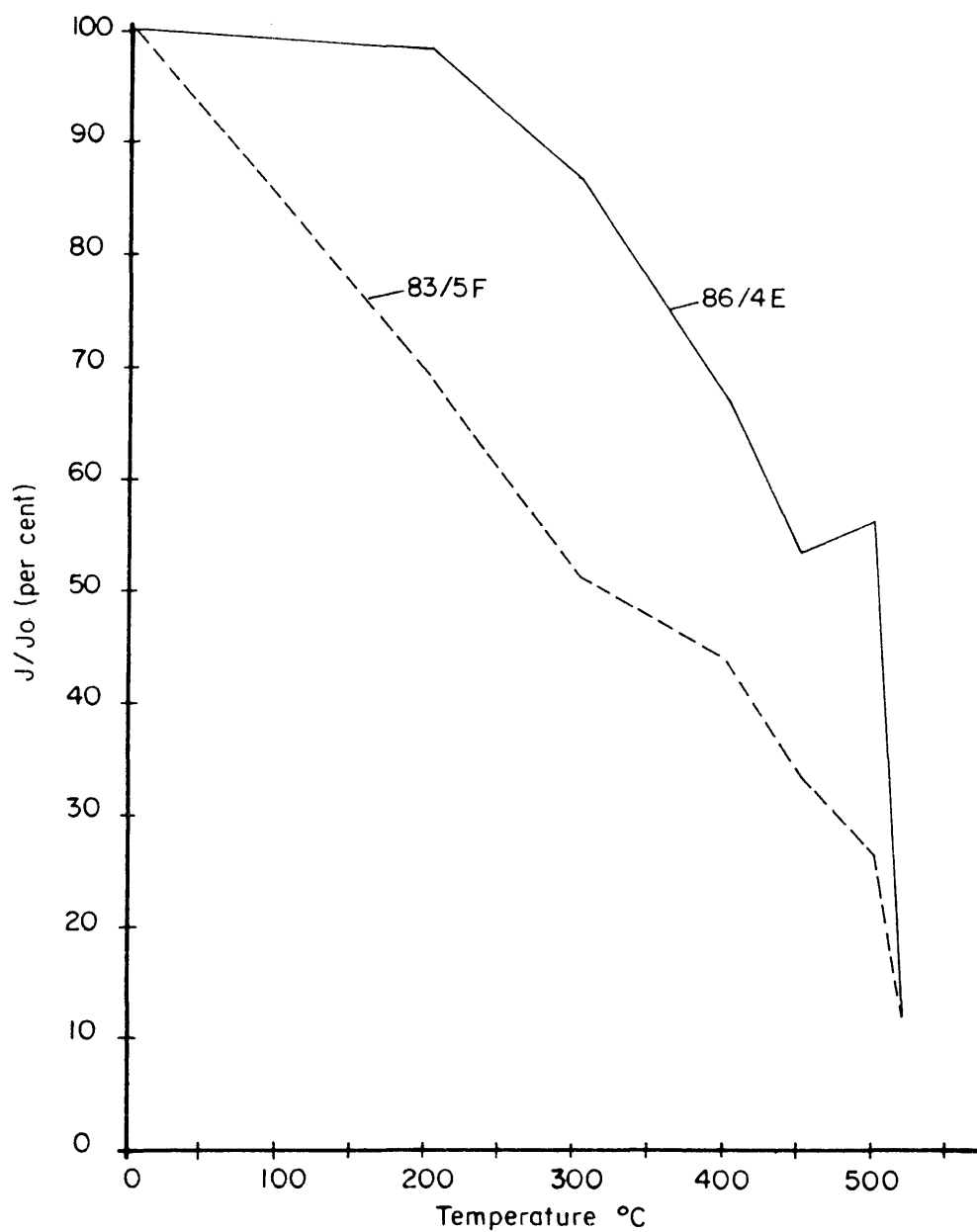


Fig. 14 Normalized thermal demagnetization response curves for specimens 83/5F and 36/4E.

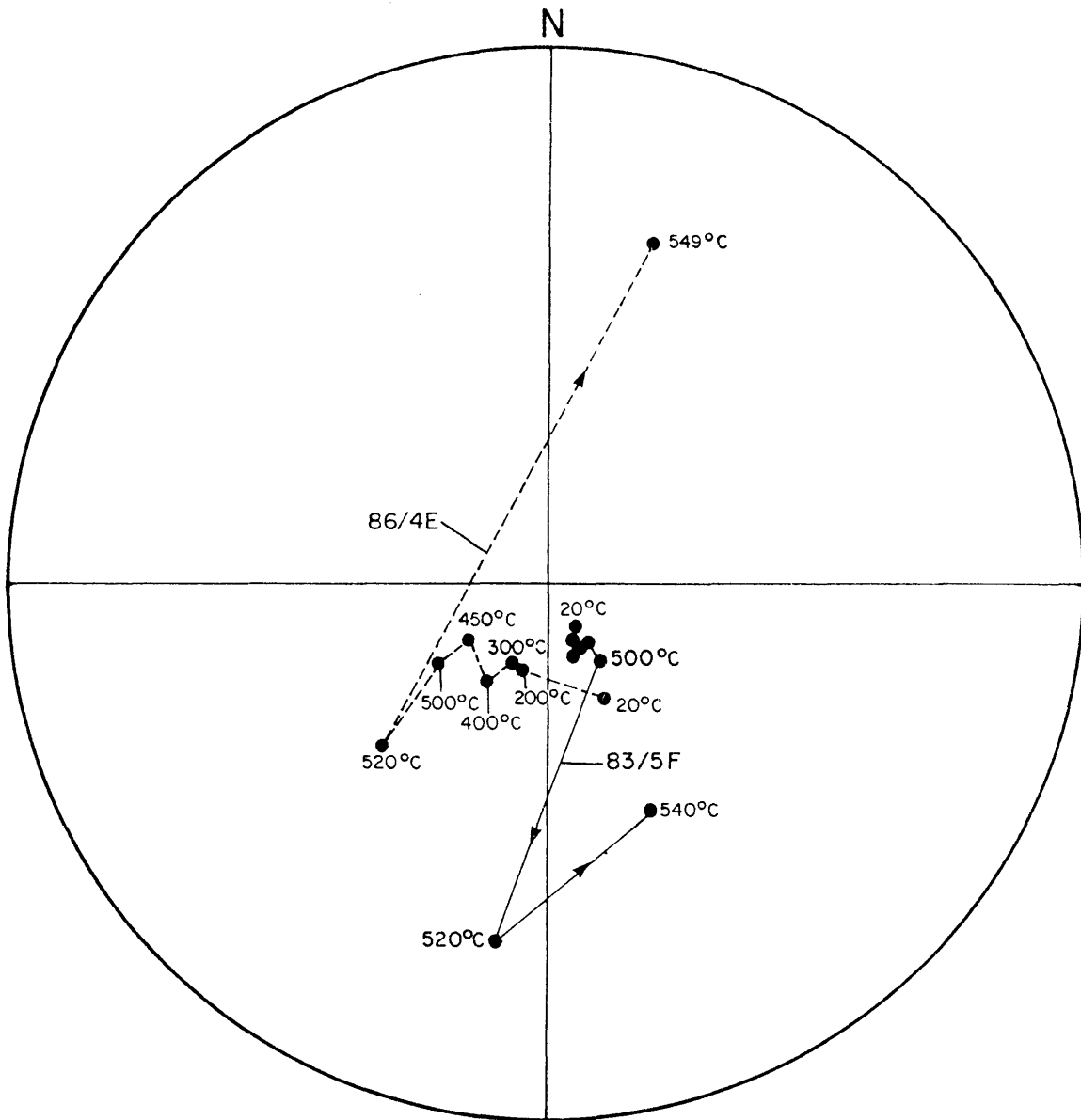


Fig. 15 The change of magnetization directions of specimens 33/5F and 36/4E during continuous thermal demagnetization. Plotting convention as in Fig. 5.

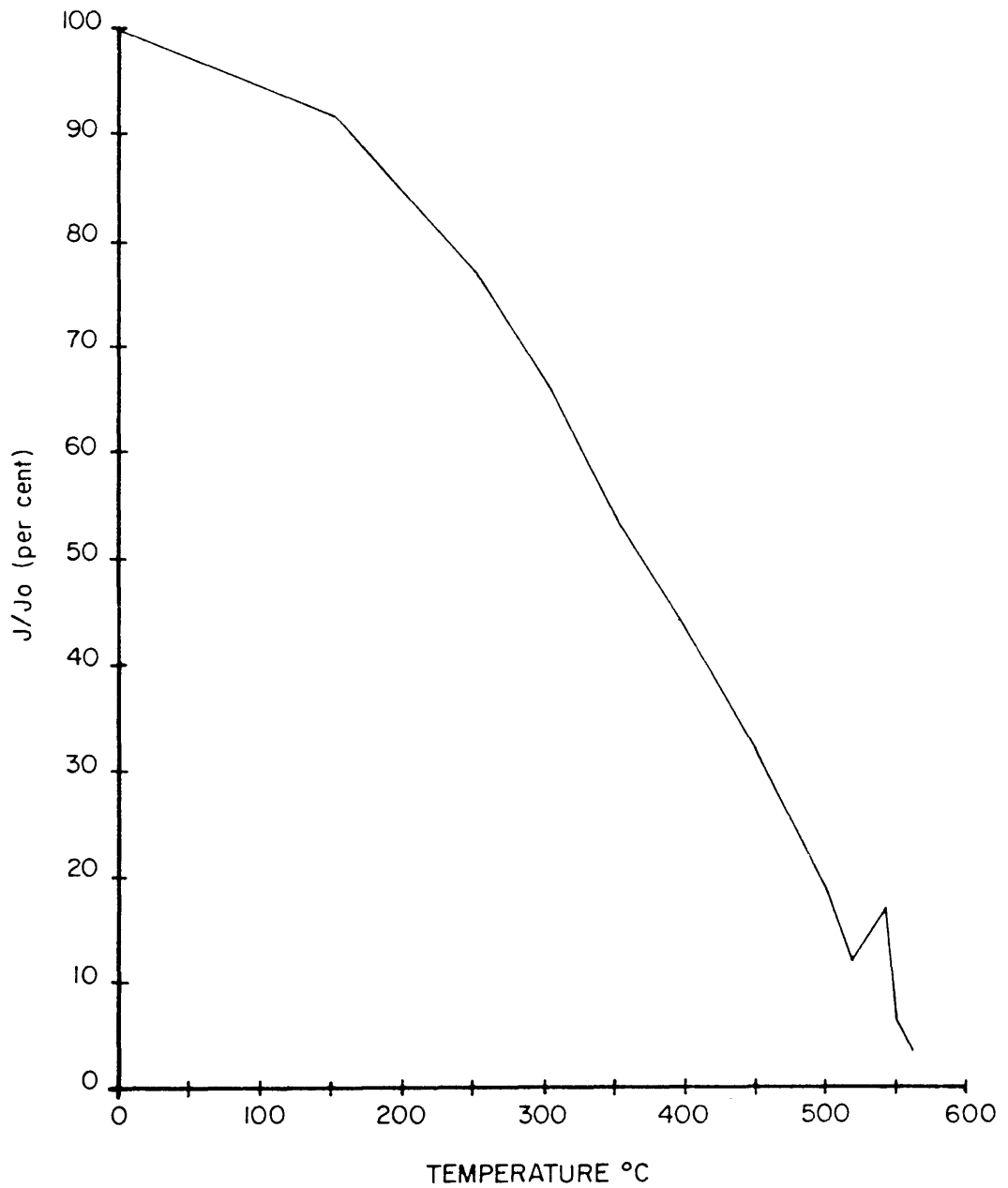


Fig. 16 Normalized thermal demagnetization of specimen 87/4B which was given a TRM in the earth's magnetic field.

demagnetization of the NRM of specimens. Because the intensity of the artificial TRM was 300 per cent higher than the intensity of the NRM in the specimens, the intensity response curve is better defined, and a Curie point between 550° and 580°C is indicated (Fig. 16). A Curie point between 550°C and 578°C suggests that the source of magnetization is magnetite (McElhinny, 1973). The increase in intensity between 520° and 540°C is attributed to the low intensity of magnetization, which at that temperature was $5 \times 10^{-3} \text{ Am}^{-1}$, and the apparent increase is regarded as a spurious effect.

F. Mineralogy of opaque minerals

The investigation of polished thin sections with an ore-microscope revealed the presence of several different sulphides and chromite in the specimens.

A large percentage of the sulphide grains consists of pyrrhotite. Pyrrhotite has a Curie point between 300°C and 325°C (Nagata, 1953) and although the thermal demagnetization intensity curves (Figs. 14 and 16) indicate a thermally distributed spectrum of blocking temperatures, it is clear that the pyrrhotite cannot be the main source of remanent magnetization.

Pure chromite is normally antiferromagnetic, but when small amounts of Ti^{4+} and/or Al^{3+} are substituted for chrome atoms in the crystal lattice, chromite becomes a ferrimagnetic mineral (Banerjee, 1972). Qualitative analyses with a scanning electron microscope, confirmed the microscopic identification of the chromite and further indicated the presence of Al and small amounts of Ti in the chromite. Vermaak and Hendriks (1976) found that the chromites of the Merensky Reef contained as much as 2% TiO_2 . According to Schmidtbauer (1971) the Curie point of chromite decreases with an increase in Ti content, with a maximum Curie temperature in the region of 400°C. From this again one can conclude that the chromite in the specimens possibly contributes to the remanent magnetization, but it is definitely not the major carrier of remanent magnetization, because it cannot explain a Curie temperature above 500°C.

A thorough search with a scanning electron microscope, revealed the presence of magnetite grains in the polished thin sections, but this could never be confirmed with an ore-microscope, due to the small grain size and scarcity of the magnetite grains. The presence of magnetite would, however, be compatible with a Curie temperature of between 550°C and 580°C and magnetite must be regarded as a major carrier of remanent magnetization in the specimens.

G. Mixed polarity

The fact that sites 85 and 87 have magnetic polarities which are inverted with respect to magnetization directions from all the other sites, can be attributed to one of the following causes:

- i) The geomagnetic field was reversed and during the cooling of that part of the critical zone from which the sites originate.
- ii) The observed mixed polarity is the result of a self-reversal of magnetization of the samples.

Possibility (i) is difficult to support, because this would imply that the Merensky Reef at sites 85 (Union Section of Rustenburg Platinum Mines and 86 (Amandelbult Section of Rustenburg Platinum Mine) was not formed simultaneously. Furthermore it would suggest that the magnetization at sites 85 and 87 (Atok mine) were acquired during one polarity event, while the magnetization at sites 79, 80, 81, 83 (Rustenburg area) and site 86 were acquired during a different polarity event. With reference to the geological and geographical distribution of the sites (Figs. 1, 2 and 3), this seems highly unlikely.

The second possibility is supported by the presence of pyrrhotite in the specimens. Self-reversals of magnetization attributed to the presence of pyrrhotite with another magnetic phase in specimens, have been reported by a number of authors (Almond *et al.*, 1956; Everitt, 1962; Robertson, 1963; Bhimasankaram, 1964). In these cases the specimens had Curie points at approximately 310°C and at a higher temperature, which indicated the existence of more than one magnetic phase in the specimens. Everitt (1962) found that he could reproduce the self-reversals in the laboratory by thermal demagnetization of specimens with pyrrhotite present.

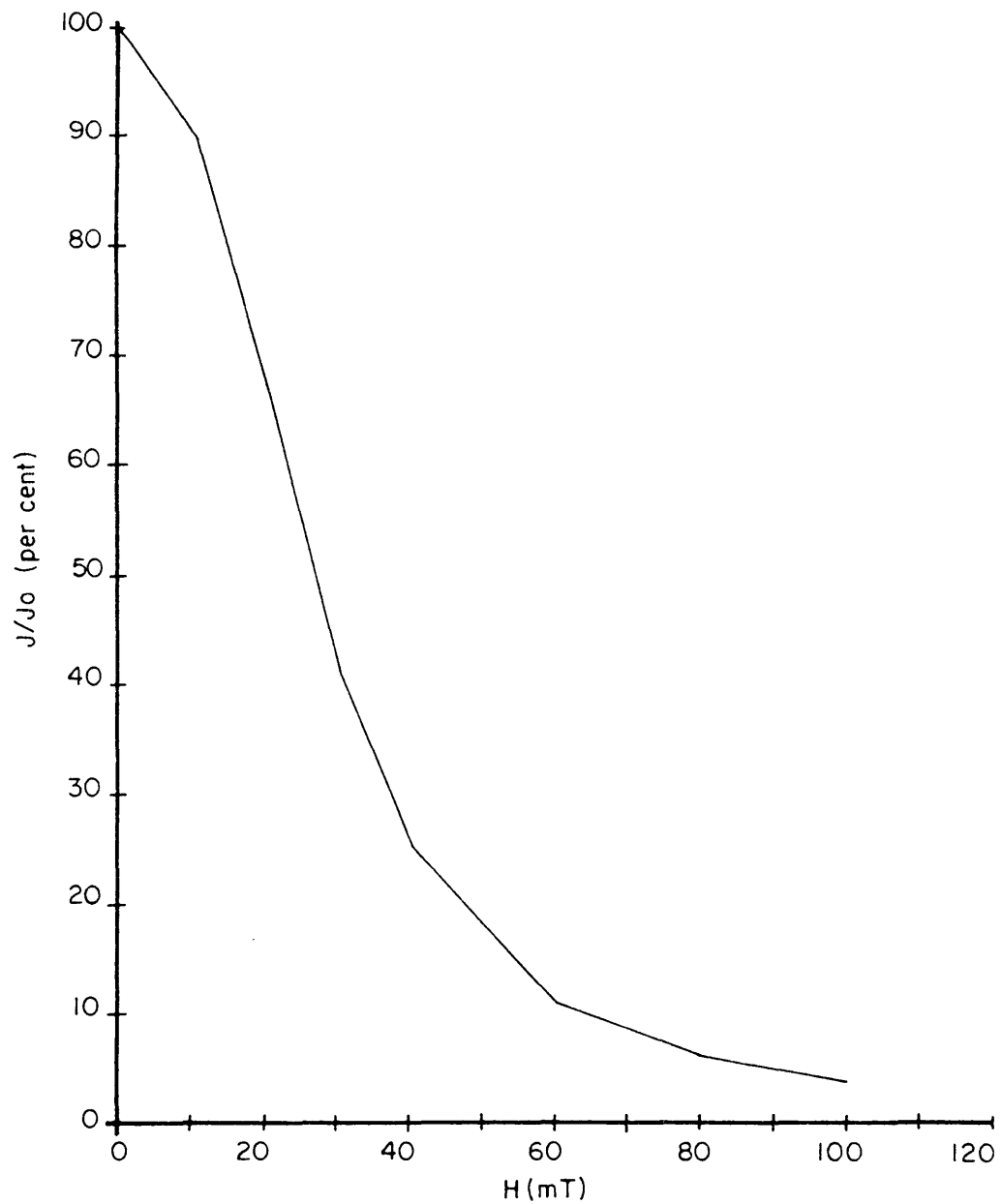


Fig. 17 Normalized AF demagnetization response curve of a specimen which was given a TRM in the earth's magnetic field.

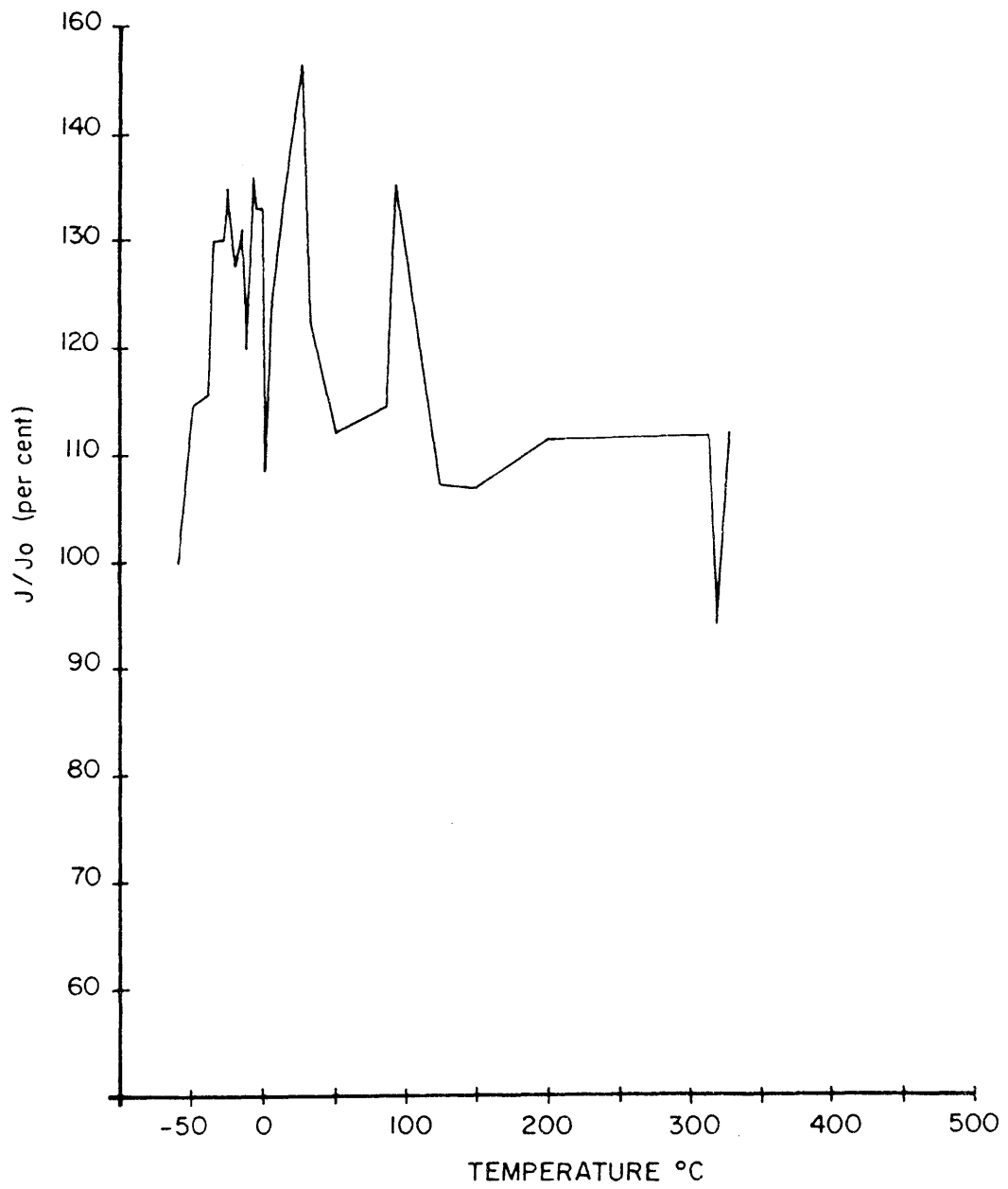


Fig. 18 Normalized thermal response curve of specimen 86/1B over a temperature range from -67°C to 452°C .

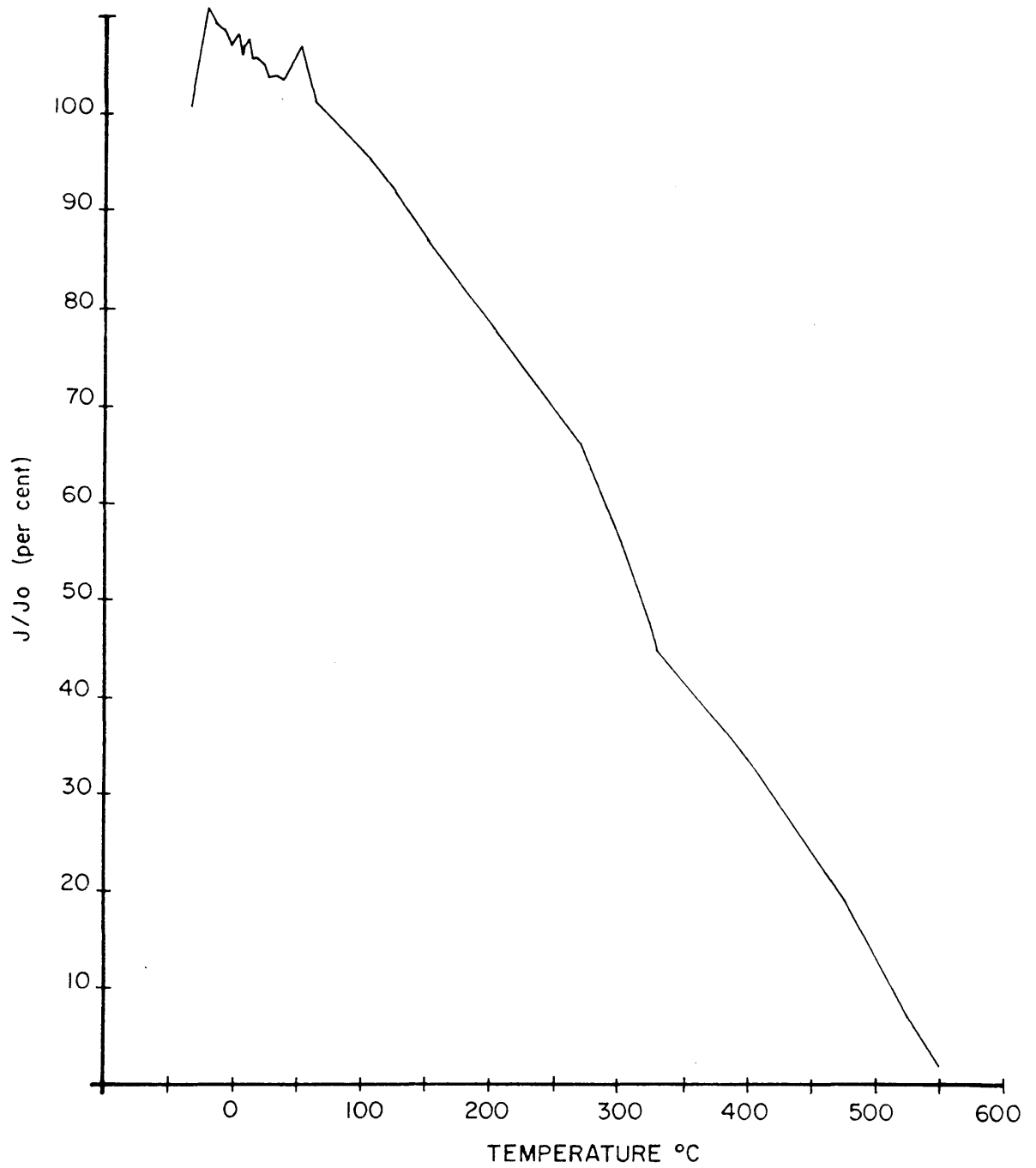


Fig. 19 Thermal demagnetization of specimen 85/5D from -36°C to 598°C , the specimen was first given an IRM in a 500 mT field.

acquired by the chromite during the thermal cycle to which it was subjected to in the laboratory or, alternatively, it can represent a minor partial self-reversal of magnetization.

However, not in one of the experiments could a total self-reversal of magnetization be produced. If the specimens are, in fact, capable of self-reversal it must be classified at this stage as a non-reproducible self-reversal (Merril, 1975), thus the possibility of a self-reversal of magnetization cannot be totally excluded.

In spite of the inconclusive evidence from experimental work the following facts do favour a self-reversal of magnetization to explain the observed mixed polarity:

- i) A field reversal cannot readily be explained in terms of the geology.
- ii) Pyrrhotite is a mineral which in other investigations was identified as the cause of self-reversal.
- iii) Chromite cannot be excluded as a possible factor relating to a self-reversal of magnetization.
- iv) The presence of at least three magnetic phases in the specimens, create circumstances which are conducive for a self-reversal to take place.
- v) The position and polarity of the pole of the critical zone on the apparent APW path for Africa (as described later, Chapter IX, Section B).

From this it must be concluded that there is a possibility that the observed reversed polarity of sites 85 and 87 is the result of a self-reversal of magnetization.

H. Summary of results

Although all specimens were characterized by a low intensity NRM, a stable and consistent magnetization direction has been established for that part of the critical zone immediately below the Merensky Reef. The best estimate of this mean direction is given by group Bcz3AF:

$$N = 6 \quad ; \quad D = 194,4^{\circ} \quad ; \quad I = -43,6^{\circ} \quad ; \quad \alpha_{95} = 16,0^{\circ} \quad ; \quad k = 18$$

with the corresponding palaeomagnetic north pole position:

latitude 37°S ; longitude 135°W
with polar error (dp, dm) : $12,5^{\circ}$, $19,9^{\circ}$ respectively

The same group with the igneous layering in a horizontal position (group Bcz3AFR) gives the direction:

$N = 6$; $D = 195,6^{\circ}$; $I = -40,0^{\circ}$; $\alpha_{95} = 10,9^{\circ}$; $k = 38$

and the palaeomagnetic north pole position:

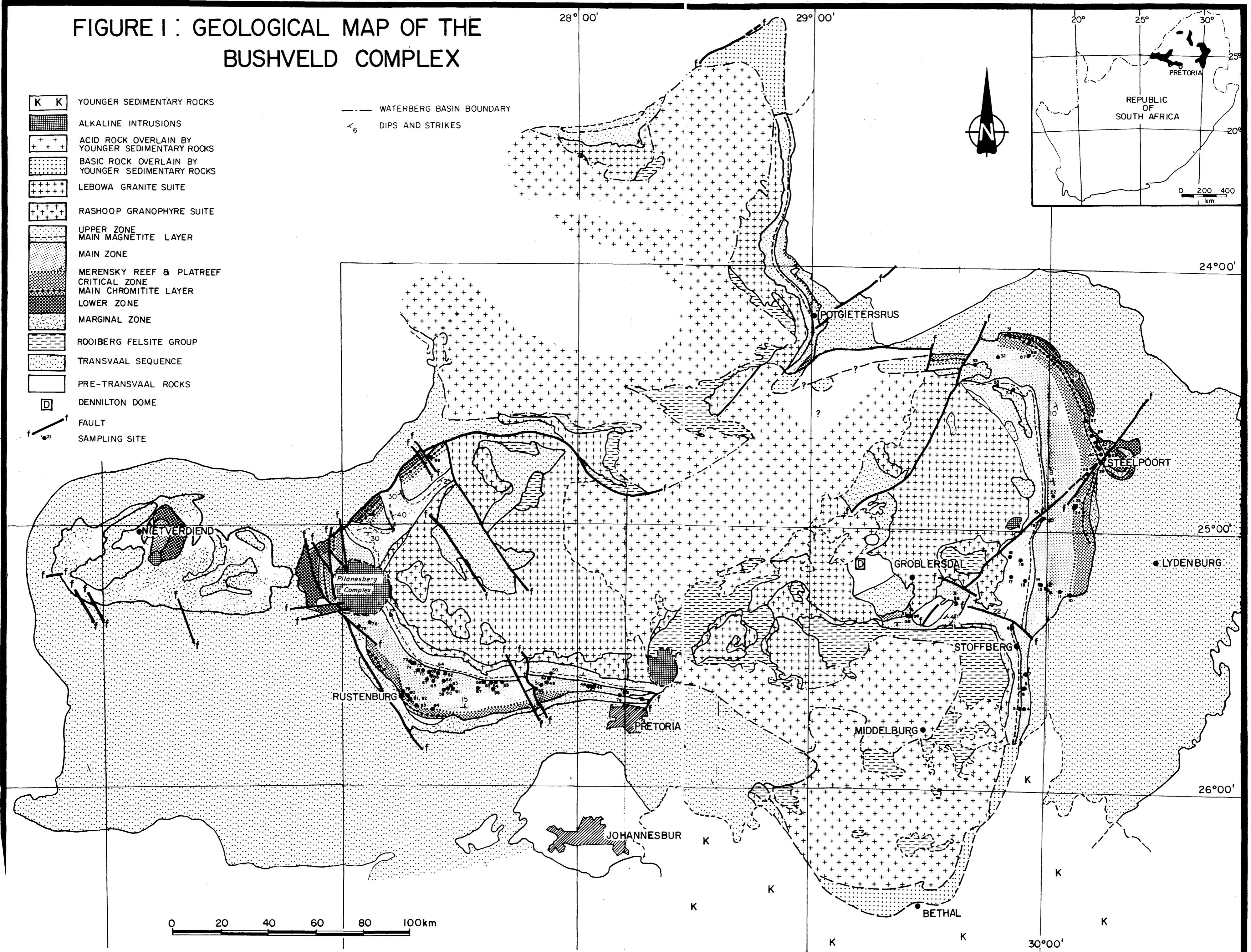
latitude $39,5^{\circ}\text{S}$; longitude 133°W
with polar error (dp, dm) $7,8^{\circ}$; $13,1^{\circ}$ respectively

with the result of the fold test (Graham, 1949) regarded as inconclusive.

The mixed polarity of these two groups is provisionally accepted to be the result of a self-reversal of magnetization, with the mean direction quoted for each group corresponding to the polarity exhibited by the majority of sites in the respective group. The mean directions both differ in polarity with respect to the magnetization direction given by Gough and Van Niekerk (1959) for the main zone of the layered sequence. However, if the mean direction of group Bcz3AFR is inverted, the direction not only lies close to the direction given by Gough and Van Niekerk (layering horizontal), but also there is an overlap of the circles of 95 per cent confidence of the groups (Fig. 20). This shows that the two groups are approximately antipodal.

Two sites in the critical zone to the north of the Pilanesberg Complex, yield magnetization directions incompatible with groups Bcz3AF and Bcz3AFR. These two sites are the only sampling sites situated in that particular area, and one cannot calculate a reliable mean direction for that portion of the critical zone. It is, however, possible that tectonic events which took place in this area, are responsible for these observed magnetization directions.

FIGURE 1: GEOLOGICAL MAP OF THE BUSHVELD COMPLEX



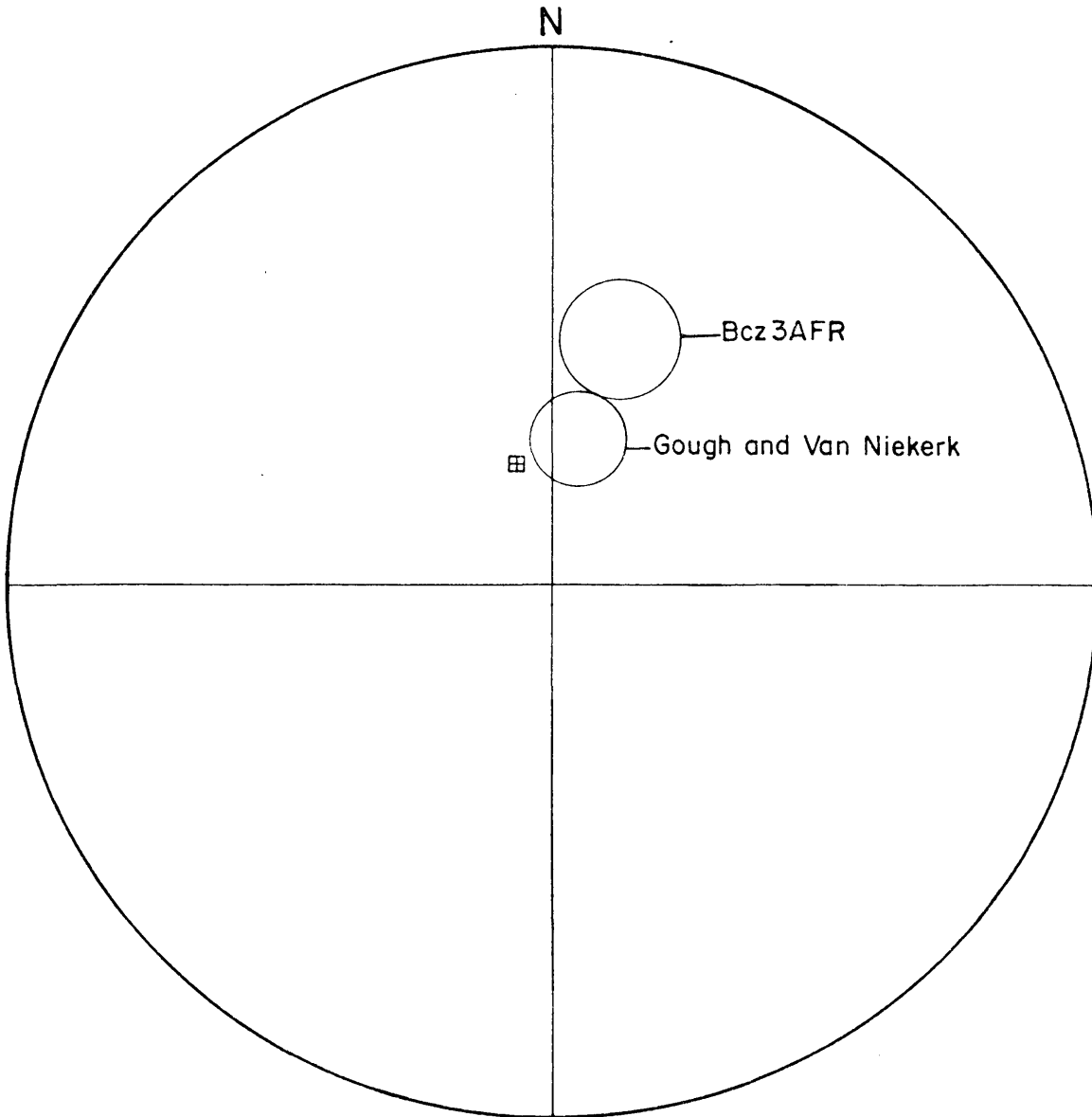


Fig. 20 Circles of 95 per cent confidence for group Bcz3AFR (inverted, layering horizontal) and that given by Gough and Van Niekerk (1959) for the main zone of the layered sequence.

VI THE PALAEOMAGNETISM OF THE MAIN ZONE IN THE EASTERN BUSHVELD COMPLEX

A. Introduction

Gough and Van Niekerk (1959) presented palaeomagnetic data from one sampling site in the main zone of the layered sequence in the eastern Transvaal. From this site, situated near Roossenekal, 23 core samples were obtained, which yielded a mean palaeomagnetic magnetization direction with a declination (D) of $36,8^\circ$ and an inclination (I) of $55,3^\circ$ (Gough and Van Niekerk, 1959, p.131). The rock unit which was sampled is now formally known as the Leolo Mountain Gabbro-Norite (S.A.C.S., 1980) or informally, as subzone B of the main zone (Fig. 2).

The sampling pattern of the present study yielded twenty sampling sites, covering subzones A, B and C of the main zone in the eastern Transvaal. Gabbro, norite and anorthosite, exhibiting very little, if any, alteration, are the main rock types. The relative freshness of the samples is due to siting all sampling sites in quarries or road cuttings.

With the aid of AF and thermal demagnetization techniques, magnetization directions from eighteen of the twenty sampled sites were recovered. Data from only two sites had to be rejected because of inconsistency in the magnetization directions.

B. Natural remanent magnetization

The mean intensity of the NRM of all specimens from the main zone in the eastern Bushveld Complex is $3395 \times 10^{-3} \text{ Am}^{-1}$. A histogram plot of the intensities of these specimens is presented in Figure 21.

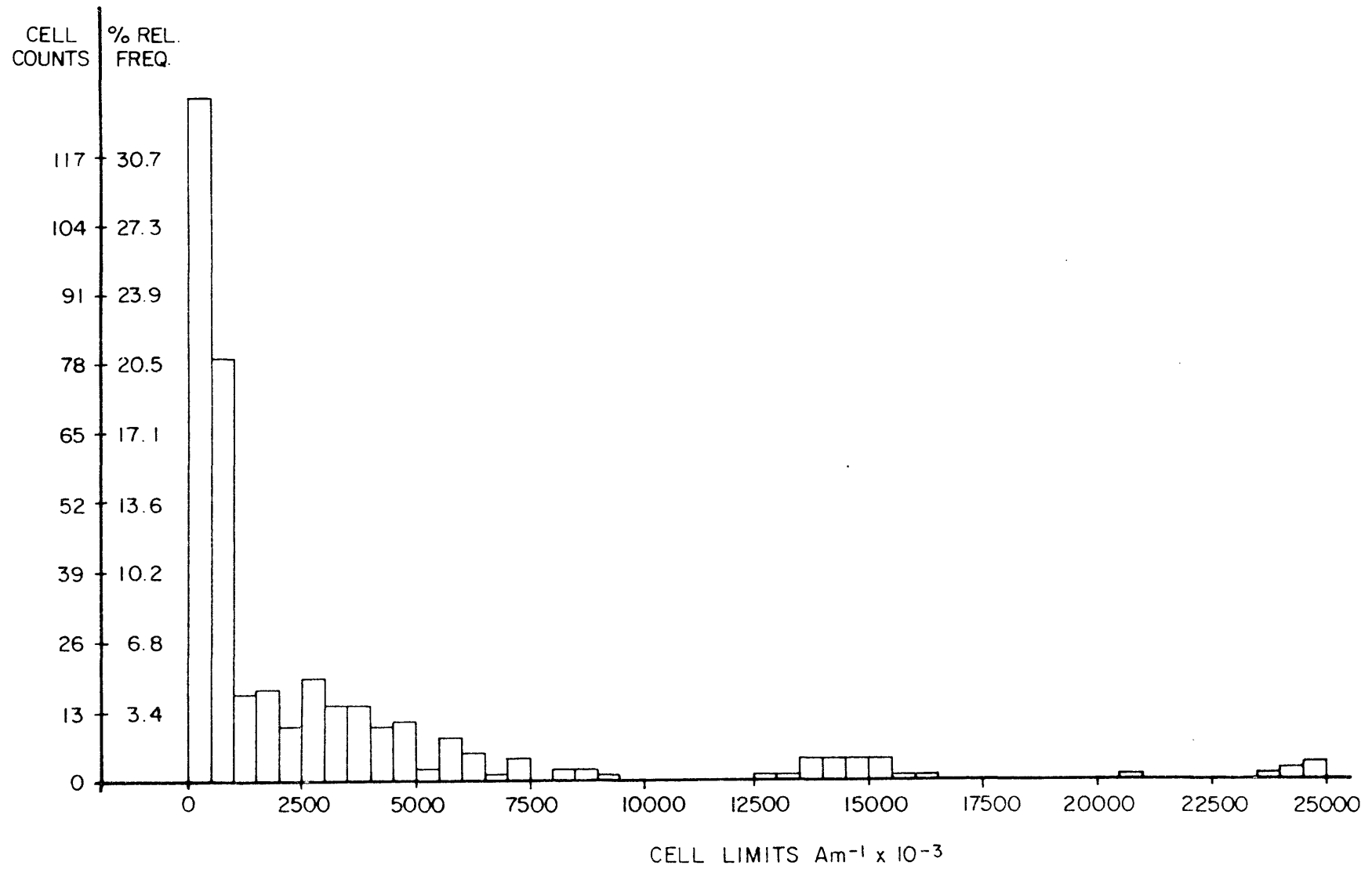


Fig. 21 Histogram plot of the NRM intensities of specimens from the main zone in the eastern Bushveld Complex.

Five sites had random NRM directions at sample level according to the criterion of Watson (1956) at 95 per cent confidence limit. The NRM data of the remaining sites are listed in Table V and the NRM directions of these sites are shown in Figure 22.

Table V. Natural remanent magnetization directions of sites in the main zone, eastern Bushveld Complex.

Site	N	Declination(D)	Inclination(I)	α_{95}	k
3	4	34,5°	58,1°	1,9°	2330
4	4	29,9°	59,6°	4,3°	461
5	3	30,0°	60,0°	6,5°	351
6	4	29,5°	59,7°	5,5°	281
7	3	28,5°	65,2°	11,3°	120
9	4	33,2°	60,7°	8,2°	127
12	4	30,6°	59,7°	4,0°	537
19	4	195,0°	-58,8°	21,5°	34
20	4	16,7°	-41,2°	8,9°	195
21	4	353,7°	-14,0°	7,0°	171
22	4	220,0°	-80,0°	9,7°	90
32	4	21,0°	43,0°	4,4°	432
36	4	354,0°	61,9°	4,2°	496
37	4	8,7°	39,5°	6,9°	177
38	4	358,7°	41,7°	8,6°	114

Sites 3, 4, 5, 6, 7, 9 and 12 group well together in the first quadrant (Fig. 22) with the following group statistics:

Group: Bmz1 ; N = 7 ; D = 31,0° ; I = 60,4° ; α_{95} = 1,8° ; k = 1065

There is however, no reason to exclude other sites with positive inclination of magnetization directions from this group (sites 32, 36, 37 and 38) and with these sites included:

Group: Bmz2 ; N = 11 ; D = 20,4° ; I = 56,2° ; α_{95} = 7° ; k = 44

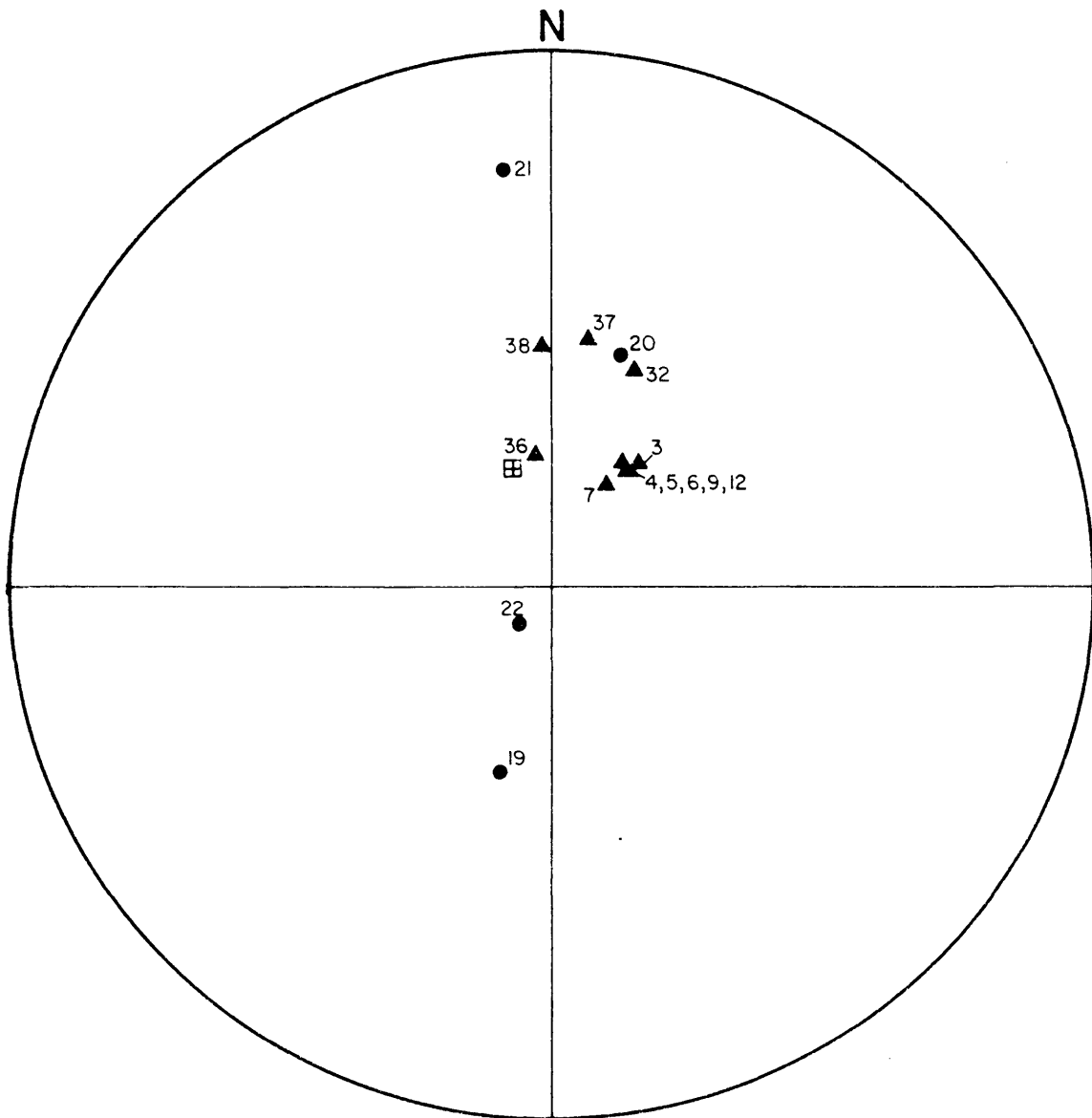


Fig. 22 NRM directions of sites in the main zone of the layered sequence in the eastern Bushveld Complex. Plotting convention as in Fig. 5.

To evaluate the effect of the dip of the igneous layering, a fold test (Graham, 1949) was applied to the data in Table V. In Table VI, the NRM directions of all the sites listed in Table V are presented, with the igneous layering rotated to the horizontal.

Table VI. Natural remanent magnetization directions of sites in the main zone, eastern Bushveld Complex with the igneous layering in a horizontal position.

Site	Dip	Dip direction*	D**	I**
3	8°	N282°	21,5°	60,3°
4	8°	N280°	16,0°	61,4°
5	10°	N275°	12,3°	62,8°
6	12°	N274°	8,1°	62,8°
7	8°	N270°	11,0°	67,9°
9	12°	N278°	10,9°	63,7°
12	12°	N278°	9,3°	62,3°
19	26°	N285°	166,7°	-44,2°
20	24°	N295°	37,8°	-40,2°
21	22°	N301°	0,5°	-26,4°
22	26°	N310°	151,9°	-62,3°
32	11°	N245°	12,3°	50,4°
36	18°	N120°	29,0°	67,5°
37	30°	N175°	23,9°	67,7°
38	30°	N175°	3,8°	71,0°

*Measured from north in a clockwise direction

**Declinations and inclinations corrected for dip

In Figure 23 the magnetization directions corrected for the dip of the igneous layering are shown and group Bmz2 now becomes group Bmz2R with the following statistics:

Group: Bmz2R ; N = 11 ; D = 14,3° ; I = 63,6° ; $\alpha_{95} = 3,5^\circ$; k = 165

The increase of k (the estimate of the precision K) from 44 to 165 is

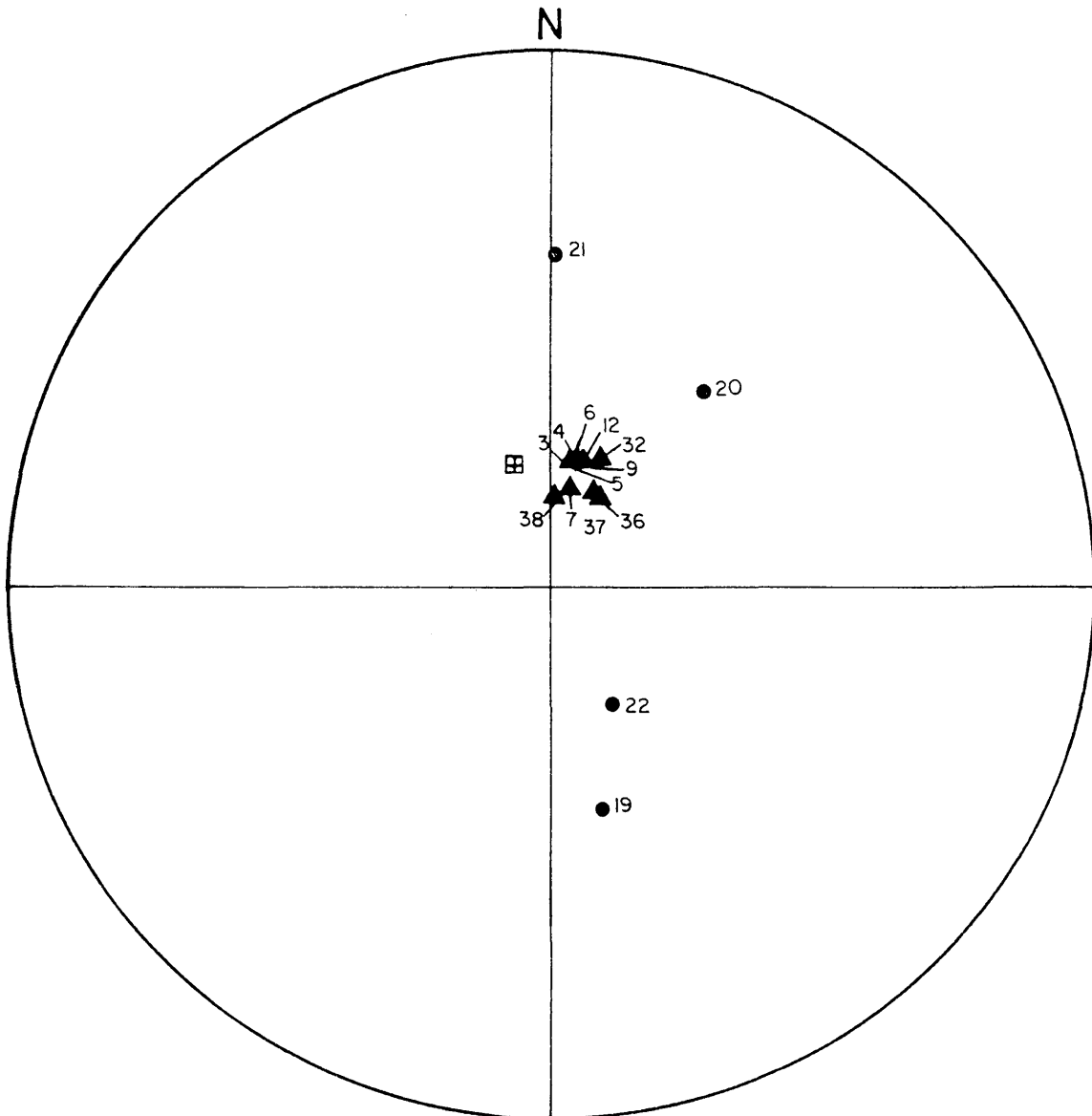


Fig. 23 NRM directions of sites in the main zone, eastern Bushveld Complex, with the igneous layering in a horizontal position. Plotting convention as in Fig. 5.

significant at even the 99 per cent confidence limit, using the method of McElhinny (1964b). This implies that at least that part of the main zone represented by the sites in group Bm2 acquired its observed NRM with the igneous layering in a horizontal position.

C. Bulk and stepwise alternating field demagnetization

Bulk AF demagnetization of specimens was done at optimum AF demagnetization values indicated by the Briden SI (Briden, 1972) for each site. The results are listed in Table VII and the magnetization directions are shown in Figure 24.

Table VII. Magnetization directions of sites in the main zone, eastern Bushveld Complex after bulk alternating field demagnetization.

Site	Alternating Field (mT)	D	I	α_{95}	k
3	10	36,2°	57,6°	2,2°	1775
4	20	29,6°	59,3°	4,4°	444
5*	20	27,5°	58,2°	-	-
6	10	26,4°	60,6°	6,2°	219
7*	20	32,6°	60,8°	-	-
9	20	35,7°	64,4°	8,7°	111
11A*	40	1,4°	65,0°	-	-
11B*	40	182,4°	-58,4°	-	-
12	60	38,4°	64,2°	4,8°	695
14	60	35,8°	71,5°	19,4°	23
19	20	198,6°	-62,9°	17,0°	53
20	40	13,8°	-37,2°	7,6°	258
21	20	348,7°	-19,3°	11,0°	70
22	20	211,5°	-77,5°	9,9°	86
32	10	13,8°	41,9°	8,4°	120
33	20	202,7°	-14,7°	26,0°	23
36	0	354,0°	61,9°	4,2°	496
37	10	6,7°	39,5°	7,8°	140
38	20	352,5°	40,8°	10,5°	76

*N = 2

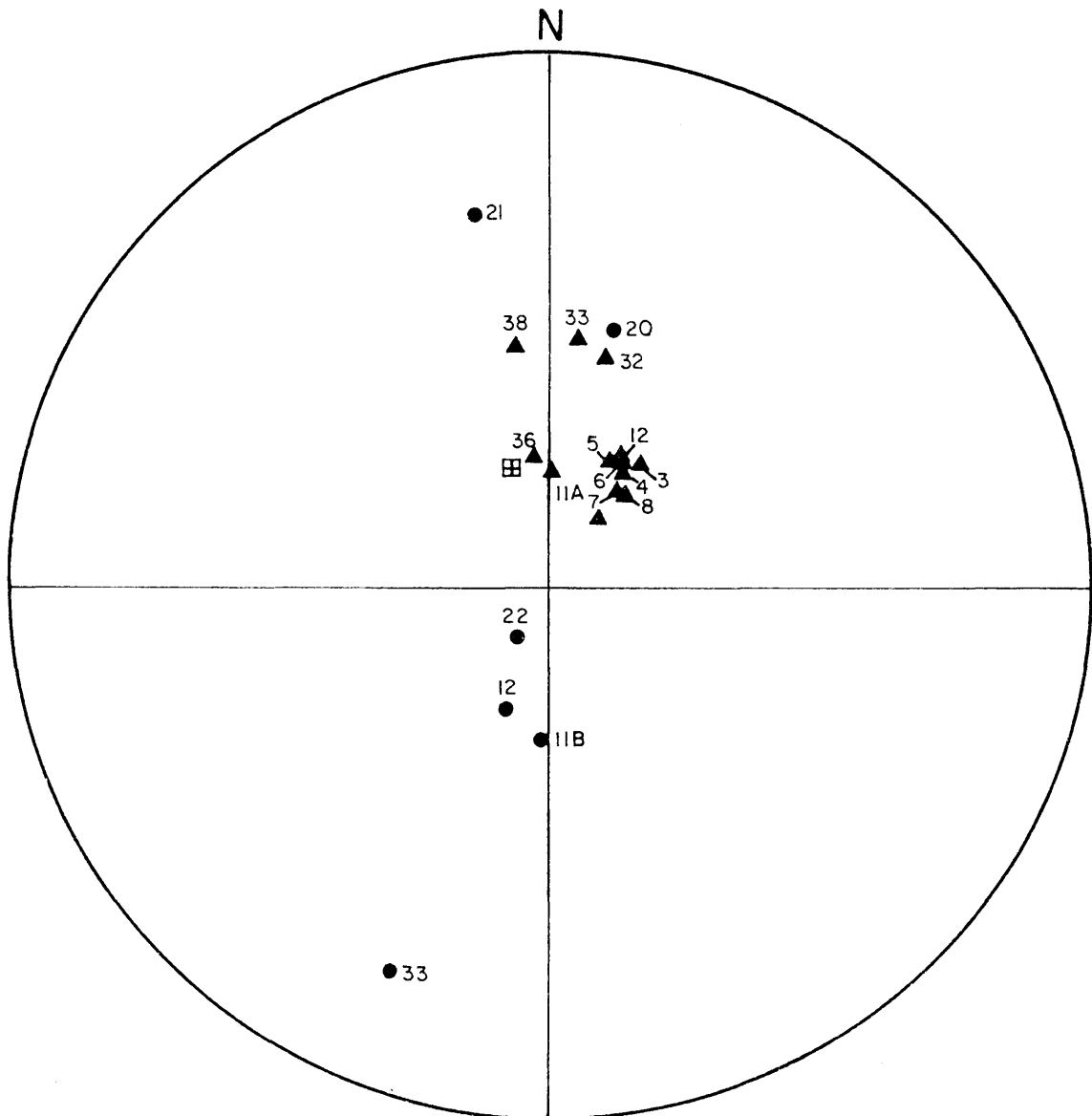


Fig. 24 Magnetization direction of sites in the main zone, eastern Bushveld Complex, after bulk AF demagnetization. Plotting convention as in Fig. 5.

Three sites 11, 14 and 33, which had inconsistent NRM directions at sample level, grouped significantly after AF demagnetization of specimens. The directions from site 11 are bipolar and the site has correspondingly been split into two sub-sites, 11A and 11B.

Thirteen sites are reversely magnetized (positive inclinations). These sites form group Bmz3AF:

Group: Bmz3AF ; N = 13 ; D = 18,8° ; I = 58,5° ; $\alpha_{95} = 7,0^\circ$; k = 36

The mean magnetization direction of this group does not differ much from that of group Bmz2. Apart from two new sites (11A and 14) included in Bmz3AF, it is evident that the bulk AF demagnetization failed to improve the grouping of the majority of the magnetization directions from the different sites. The stepwise demagnetization of specimens from this group produced very little or no change in the magnetization directions with the behaviour of specimen 36/4C, shown in Figure 25 as a typical example.

The intensity response curve of the same specimen (Fig. 26) during stepwise AF demagnetization, revealed a stable and very "hard" magnetization, with more than 40 per cent of the magnetization remaining after demagnetization in a field of 80 mT. This type of "hard" stable magnetization has been found by other authors e.g. in the Modipe Gabbro (Evans, McElhinny and Gifford, 1968) and in the Lambertville diabase (Hargraves and Young, 1969). The source of this stable "hard" magnetization was in both cases shown to be single domain magnetite grains, showing extensive shape anisotropy.

It is interesting to note further that all the sites in group Bmz3AF, with the exception of site 11A, are situated in subzone B of the main zone, i.e. the Leolo Mountain Gabbro-Morite. Site 11 is situated at the base of the main zone within subzone A i.e. the Winnaarshoek Norite-Anorthosite.

At three sites (11B, 19 and 22) where the magnetization directions are normal (negative inclinations) the magnetization directions converge during step-wise AF demagnetization (Fig. 27) and a fourth site (33)

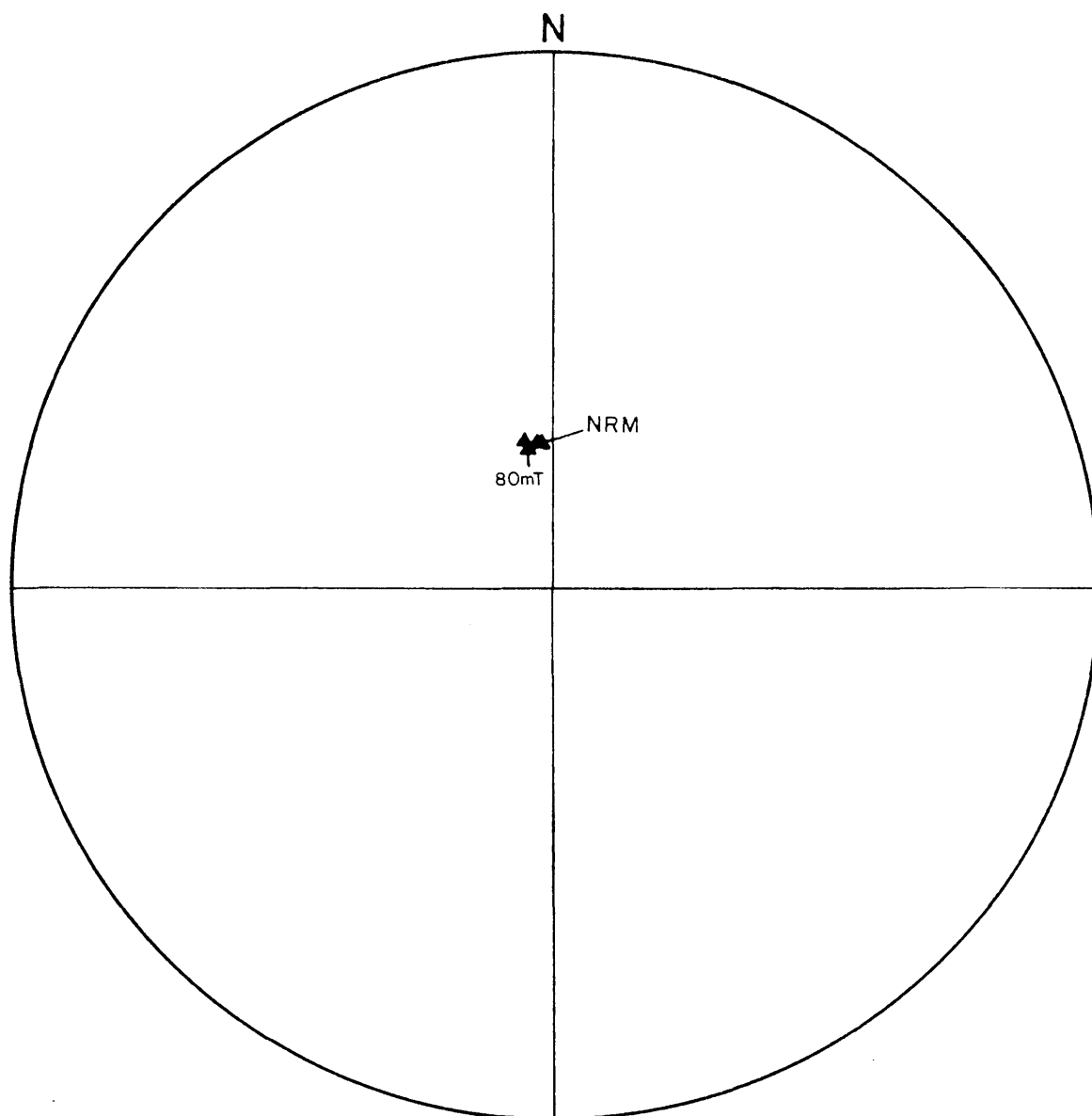


Fig. 25 Stepwise AF demagnetization results of specimen 36/4C. Maximum AF value 80 mT. Plotting convention as in Fig. 5.

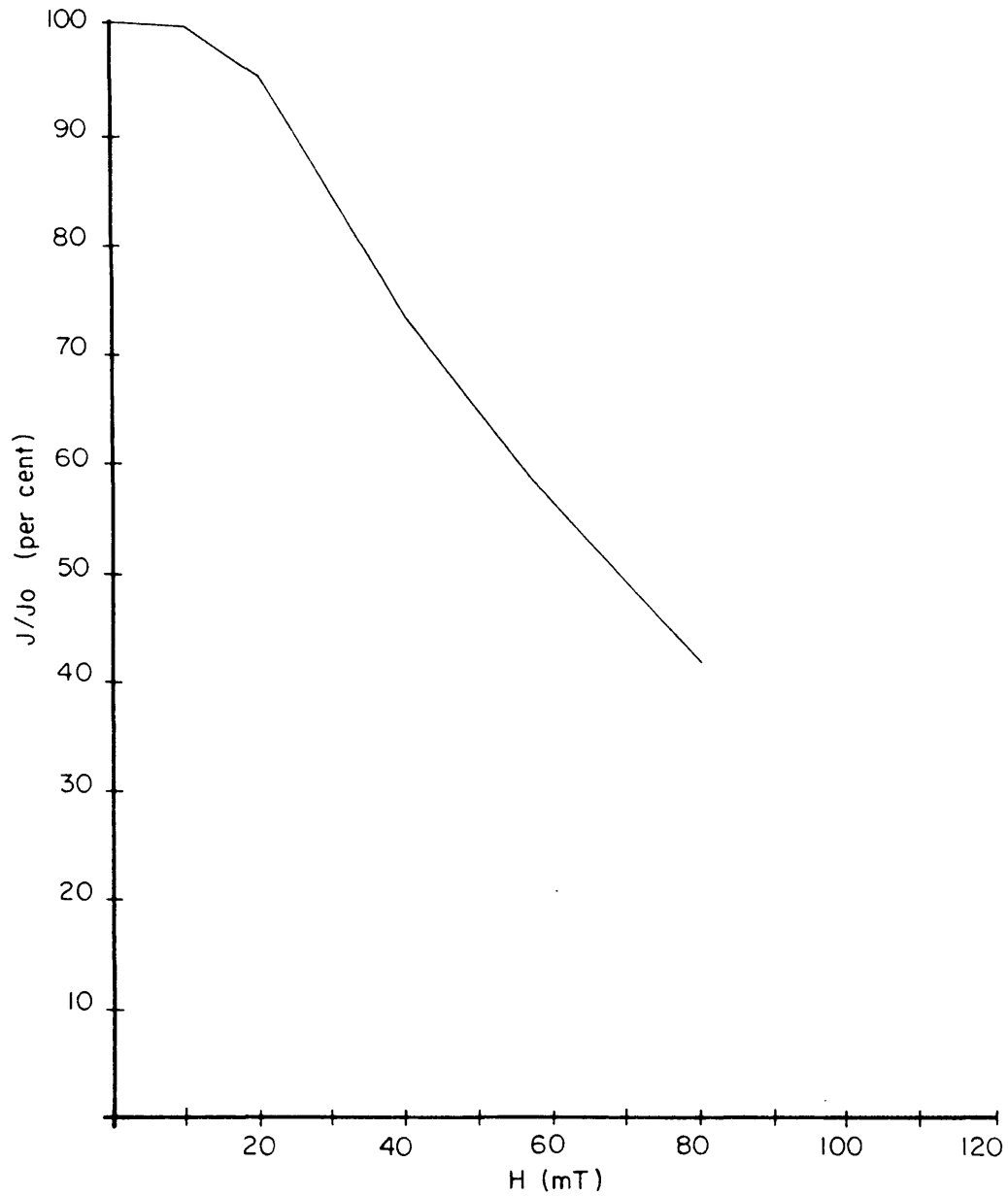


Fig. 26 Normalized intensity response curve of specimen 36/4C during AF demagnetization.

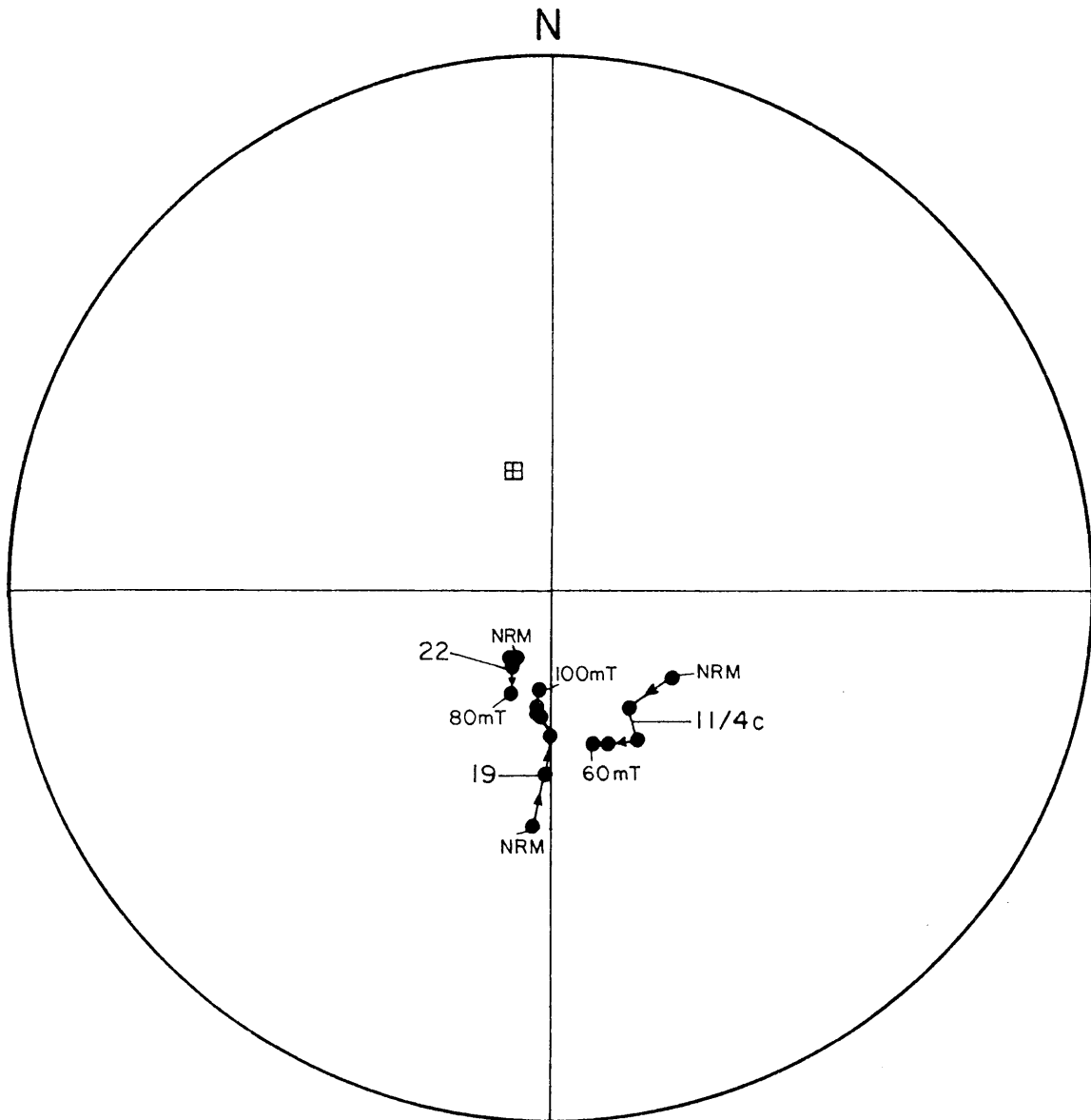


Fig. 27 Stepwise AF demagnetization of specimens from sites 11B, 19 and 22. Plotting convention as in Fig. 5.

shows a significant sample grouping of magnetization directions (negative inclination) after bulk AF demagnetization.

These four sites form group Bmz4AF:

Group: Bmz4AF ; N = 4 ; D = 197,8° ; I = -54,3° ; $\alpha_{95} = 32,8^\circ$; k = 9

With the radius of the circle of 95 per cent confidence of this group being 32,8° and an estimate of the precision of 9, the grouping is very weak, but this may be due to the effect of the dip and dip directions of the layered sequence at the sites.

Two other sites, 20 and 21, also show magnetization directions with negative inclinations. These directions changed very little during stepwise AF demagnetization, and after bulk AF demagnetization failed to group with the sites in group Bmz4AF. The reason for this is not apparent, especially because with the exception of site 11B, all the sites normally magnetized are situated in subzone C of the main zone.

The magnetization directions obtained with bulk AF demagnetization and then corrected for the dip at each sampling site, are listed in Table VIII.

Table VIII Magnetization directions of sites in the main zone, eastern Bushveld Complex after alternating field demagnetization, with the igneous layering in a horizontal position.

Site	Declination(D)*	Inclination(I)*
3	23,6°	60,0°
4	15,9°	61,1°
5	11,0°	60,7°
6	4,2°	63,0°
7	18,6°	64,3°
9	9,3°	67,5°
11A	339,2°	63,7°

11B	172,6°	-58,2°
12	12,3°	67,8°
14	0,3°	75,0°
19	156,4°	-54,0°
20	32,6°	-37,9°
21	41,8°	-16,5°
22	155,0°	-59,7°
32	4,6°	48,2°
33	191,2°	-48,7°
36	29,0°	67,5°
37	19,9°	68,2°
38	349,3°	70,0°

*Declinations and inclinations of magnetization directions after the igneous layering has been rotated to horizontal.

These directions are plotted in Figure 28 and group Bmz3AFR with the following statistics forms:

Group: Bmz3AFR ; N = 13 ; D = 10° ; I = 64,7° ; $\alpha_{95} = 4,2^\circ$; k = 100

The equivalent of group Bmz3AFR, uncorrected for dip, is group Bmz3AF, and from a comparison of the group statistics it is clear that the fold test has resulted in a much better grouping of magnetization directions in group Bmz3AFR. The increase in the value of k from 36 to 100 is significant at even the 99 per cent confidence limit according to the test of McElhinny (1964b). This confirms the previous results of fold tests carried out on NRM data.

The circular standard deviation of group Bmz3AFR is 8,1° with upper and lower limits of 11,3° and 6,3° at the 95 per cent confidence limit (Cox, 1969), against an expected value of 11,7° for a palaeolatitude of 46,6° (Brock, 1971). According to Opdyke (1972) 27 000 years are needed in relative recent geological times to average out

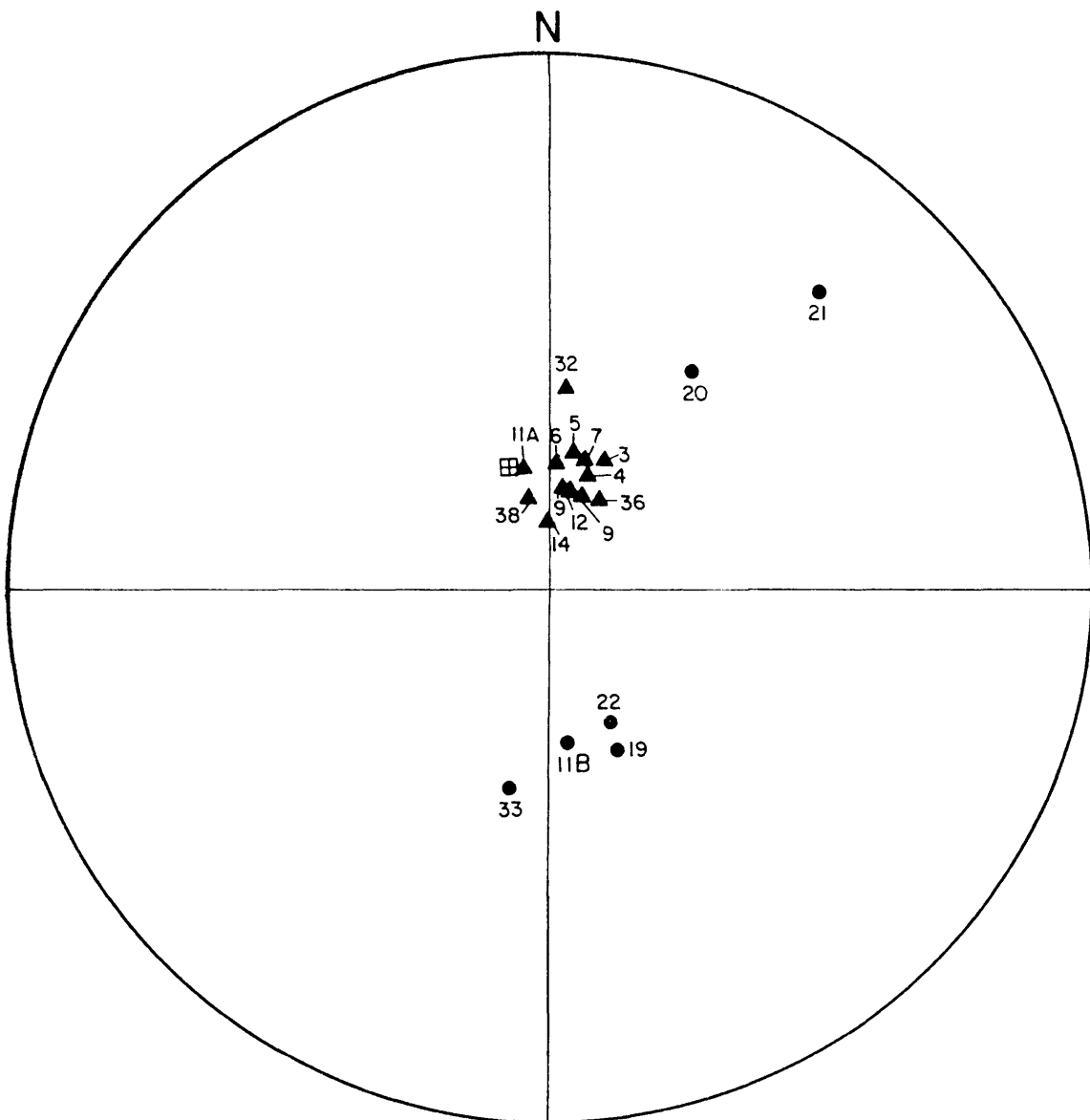


Fig. 28 Magnetization directions of sites in the main zone, eastern Bushveld Complex after AF demagnetization, with the igneous layering in a horizontal position. Plotting convention as in Fig. 5.

palaeosecular variation. If one assumes a similar time span for the Precambrian, it follows that the Curie isotherm must have moved through that part of the main zone represented by the sites in group Bmz3AFR over a period of less than 27 000 years.

After rotation, group Bmz4AF has the following statistics:

Group: Bmz4AFR ; N = 4 ; D = 169,8°; I = -56,0° ; α_{95} ; 12,6° ; k = 54

The improvement in k from 9 to 54 is significant at the 95 per cent confidence limit (McElhinny, 1964b) and this fold test (Graham, 1949) confirms the results from previous fold tests on data predominantly from subzone B of the main zone. There can be little doubt now, that the main zone of the layered sequence in the eastern Bushveld Complex, acquired its present dip and dip direction only after cooling, to a temperature below its Curie point.

D. Thermal demagnetization

The stable behaviour exhibited by specimens belonging to group Bmz3AF during AF demagnetization was manifested by different specimens from the same group during continuous thermal demagnetization (Fig. 29). The intensity response curves of two specimens (Fig. 30), which can be regarded as typical of all these specimens display distributed blocking temperature spectra but show a well defined Curie point at 575°C. This Curie point indicates magnetite as the primary source of remanent magnetization in these specimens (McElhinny, 1973).

The magnetization direction of two sites, (11A and 14), from group Bmz3AF, which became consistent with directions from other sites in this group only after AF demagnetization, as well as the magnetization directions from site 13, which up to this stage of the

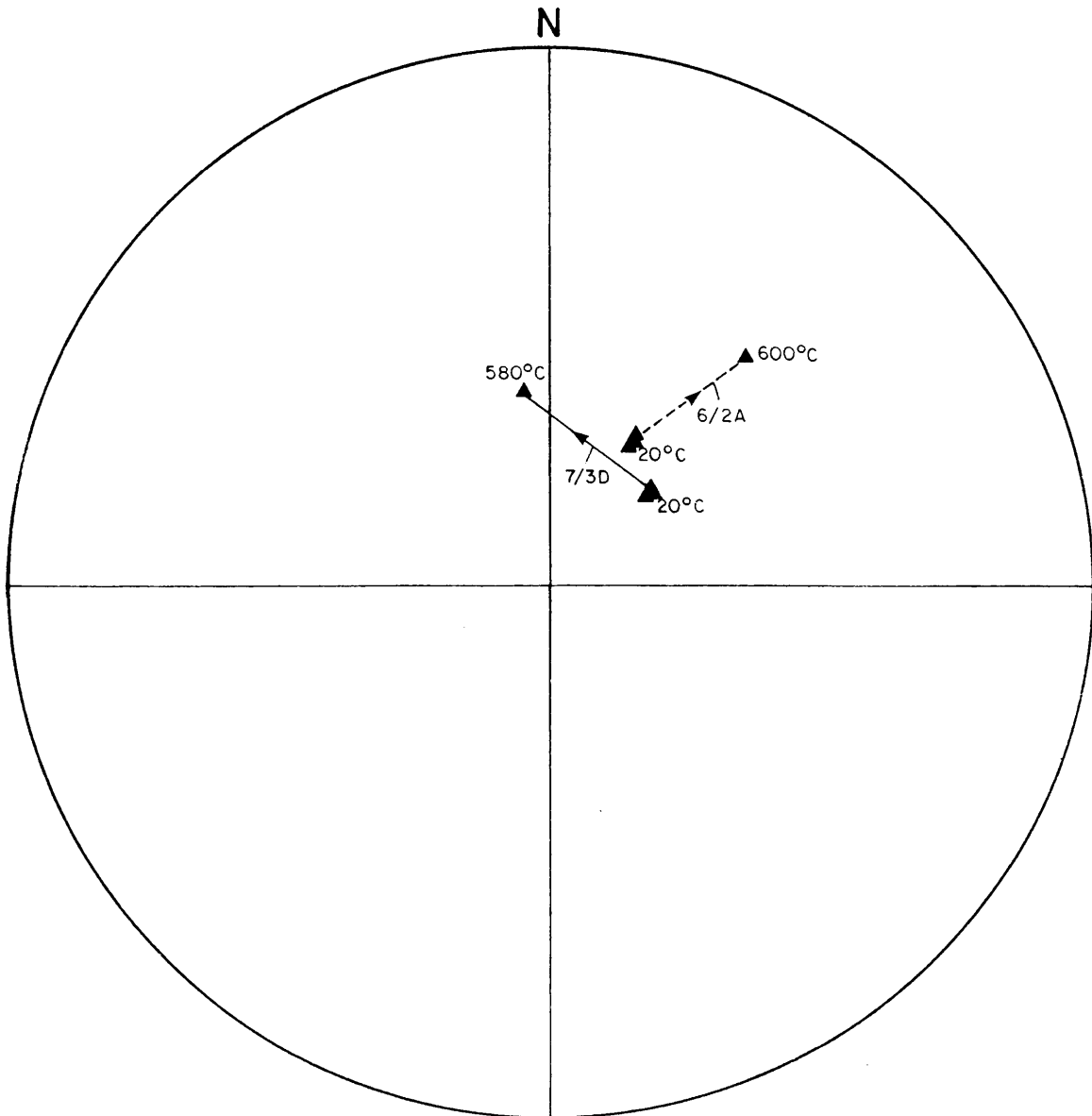


Fig. 29 The change in magnetization directions of two specimens from group Bmz3AF, subzone B, main zone, eastern Bushveld Complex, during continuous thermal demagnetization. Plotting convention as in Fig. 5.

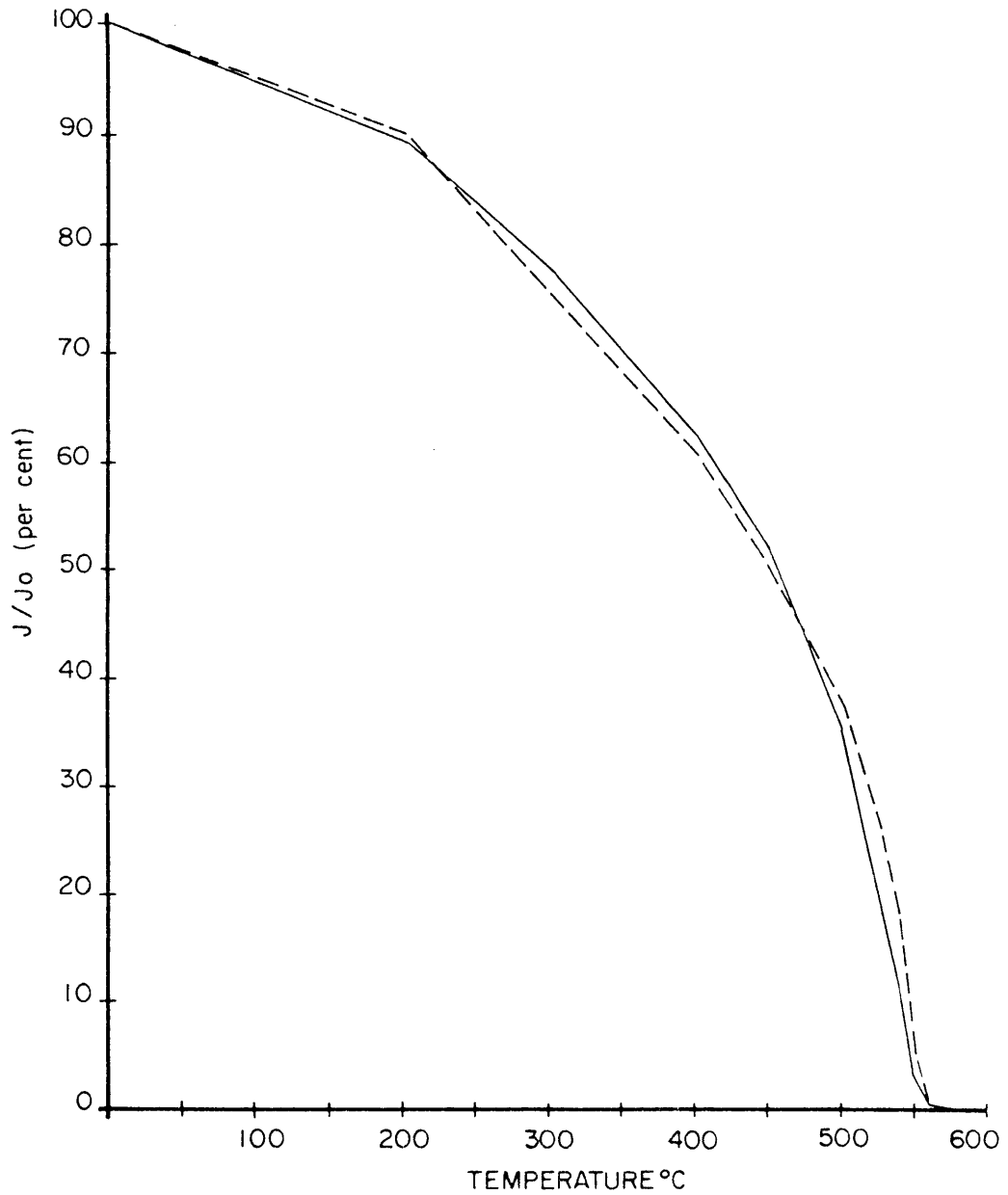


Fig. 30 Typical normalized intensity response curves during continuous thermal demagnetization of two specimens from group Bmz3AF which are situated in subzone B, main zone, eastern Bushveld Complex.

investigation had been rejected due to inconsistency of sample directions, converged during continuous thermal demagnetization towards the mean direction of group Bmz3AF (Fig. 31). This is additional evidence that, although uncorrected for dip of the layered sequence, the mean magnetization direction of group Bmz3AF represents a primary magnetization direction.

The intensity of magnetization of specimens from sites 11B and 33 are too low to allow thermal demagnetization of the specimens with the present equipment. In Figure 32, however, the directional response to thermal demagnetization of specimens from sites 19, 20, 21 and 22 are shown. The remanent remagnetization direction of sites 19 and 22, which grouped well with group Bmz4AF, display a tendency to move closer together during thermal demagnetization (Fig. 32). The movement is not much and does not follow circles of remagnetization. From this it would seem that the thermal demagnetization succeeds in removing numerous very small viscous remanent magnetizations (VRM's) resulting in a closer grouping of magnetization directions at high temperatures.

The remanent magnetization directions of two sites (20 and 21), which proved to be stable during AF demagnetization, but incompatible with either group Bmz3AF or group Bmz4AF, change rapidly at high temperatures (Fig. 32). Although the change of the vector directions does not describe circles of remagnetization, it is clear that the directions move towards the mean direction of magnetization of group Bmz4AF. This behaviour during demagnetization (thermal and AF) can only be explained by the presence of magnetization components with high coercivities and low blocking temperatures, which mask the primary magnetization direction at low temperatures and during AF demagnetization.

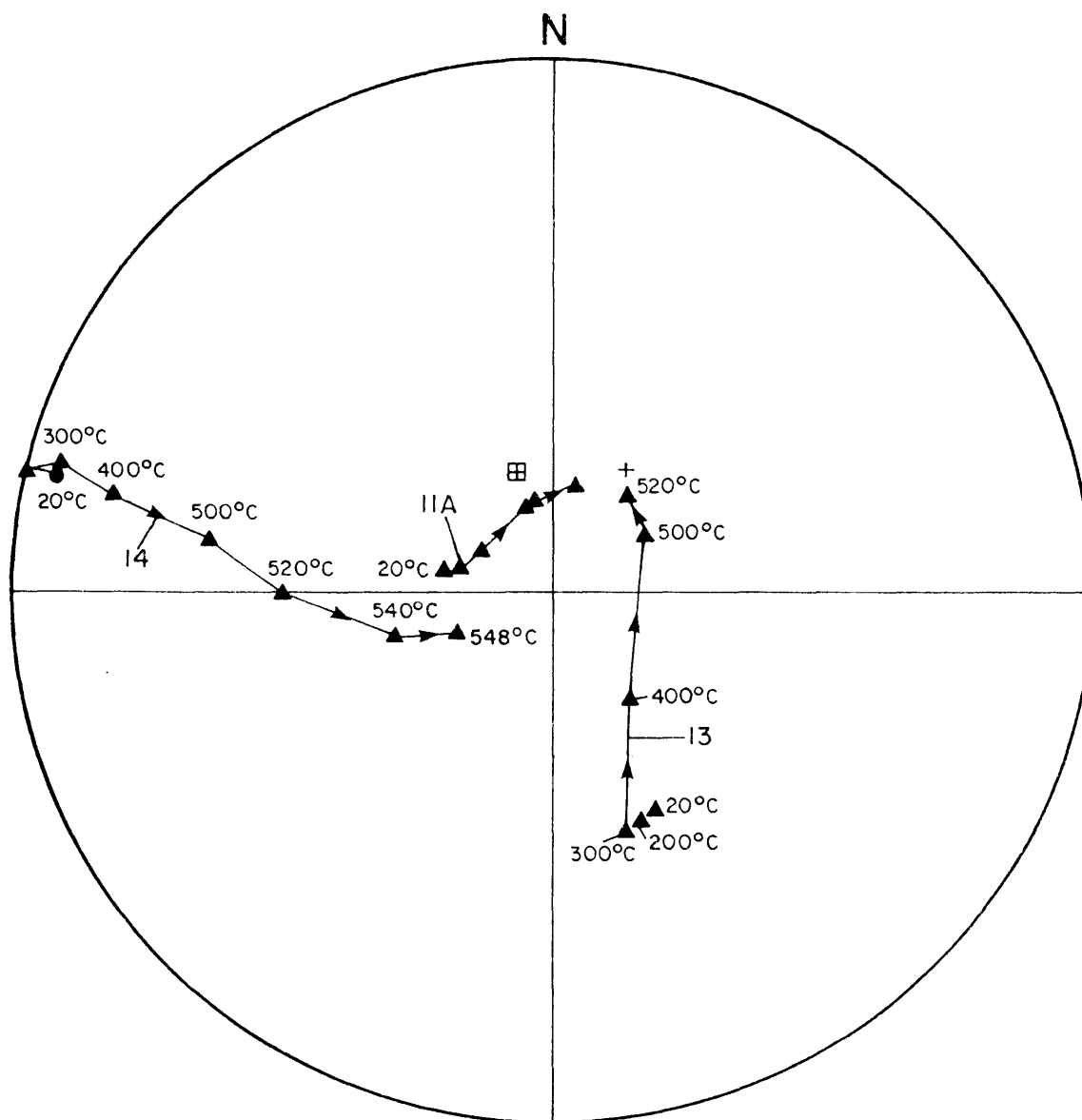


Fig. 31 The change in magnetization directions of specimens from sites 11A, 13 and 14, during continuous thermal demagnetization. Plotting convention as in Fig. 5.

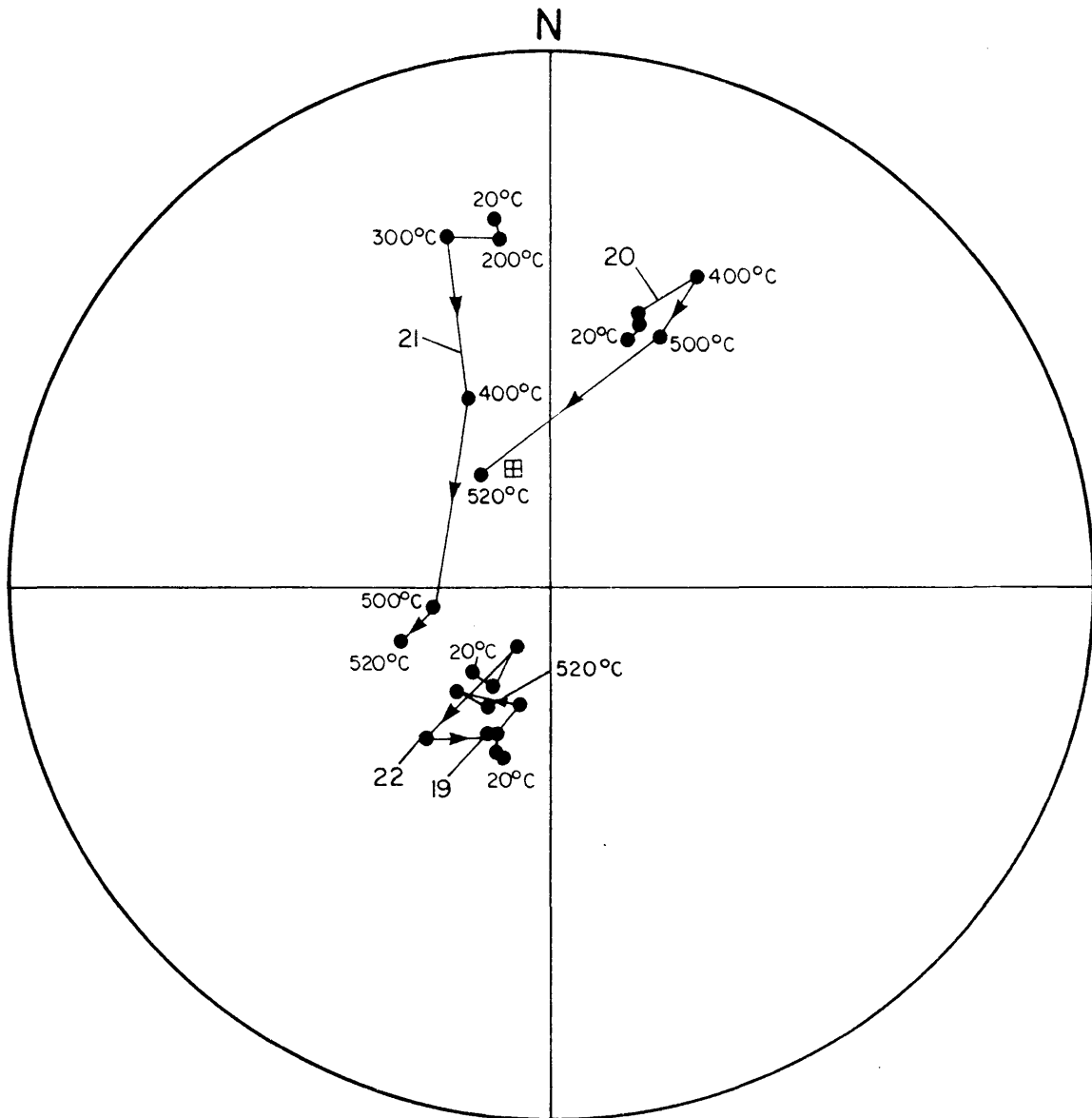


Fig. 32 Thermal demagnetization response of specimens from sites 19, 20, 21 and 22. Plotting convention as in Fig. 5.

Sites 19, 20, 21, 22 and 33 are situated in subzone C of the main zone. The mean magnetization direction is obtained by grouping directions from sites 19, 22 and 33 together (obtained by AF demagnetization) which represents the mean magnetization direction of subzone C, or the Mapoch Gabbro-Norite as it is formally known. Uncorrected for dip, this group of three sites yields the following rather poor, statistical data:

Group: Bmz5AF ; N = 3 ; D = 202,7° ; I = -52,3° ; $\alpha_{95} = 54^\circ$; k = 6

However, with the layering restored to horizontal, the statistics improve considerably to:

Group: Bmz5AFR ; N = 3 ; D = 168,9° ; I = -55,0° ; $\alpha_{95} = 20^\circ$; k = 37

For this last group the fold test (Graham, 1949) is significant at the 90% confidence limit. It is further clear that these two groups can only be accepted on the basis of the additional evidence supplied by the thermal demagnetization of specimens from sites 20 and 21.

The thermal intensity response curves of two specimens, 20/3D and 21/3B (Fig. 33) are fairly typical of a multicomponent remanent magnetization. The curve of specimen 20/3D suggests the existence of two Curie points, one at 525° and the other at 550°C. This feature is, however, absent on the curve of specimen 21/3B, which indicates a Curie point at approximately 570°C.

E. Mineralogy of opaque minerals

Specimens from subzone B of the main zone are characterized by the presence of magnetite, ilmenite and various sulphide minerals. A preliminary investigation of polished thin sections with an ore microscope, however, failed to identify any opaque grains as magnetite. If magnetite were not present it would be very difficult to explain the observed Curie point of 575°C of these specimens. This combined with the previously described "hard" (Fig. 34)

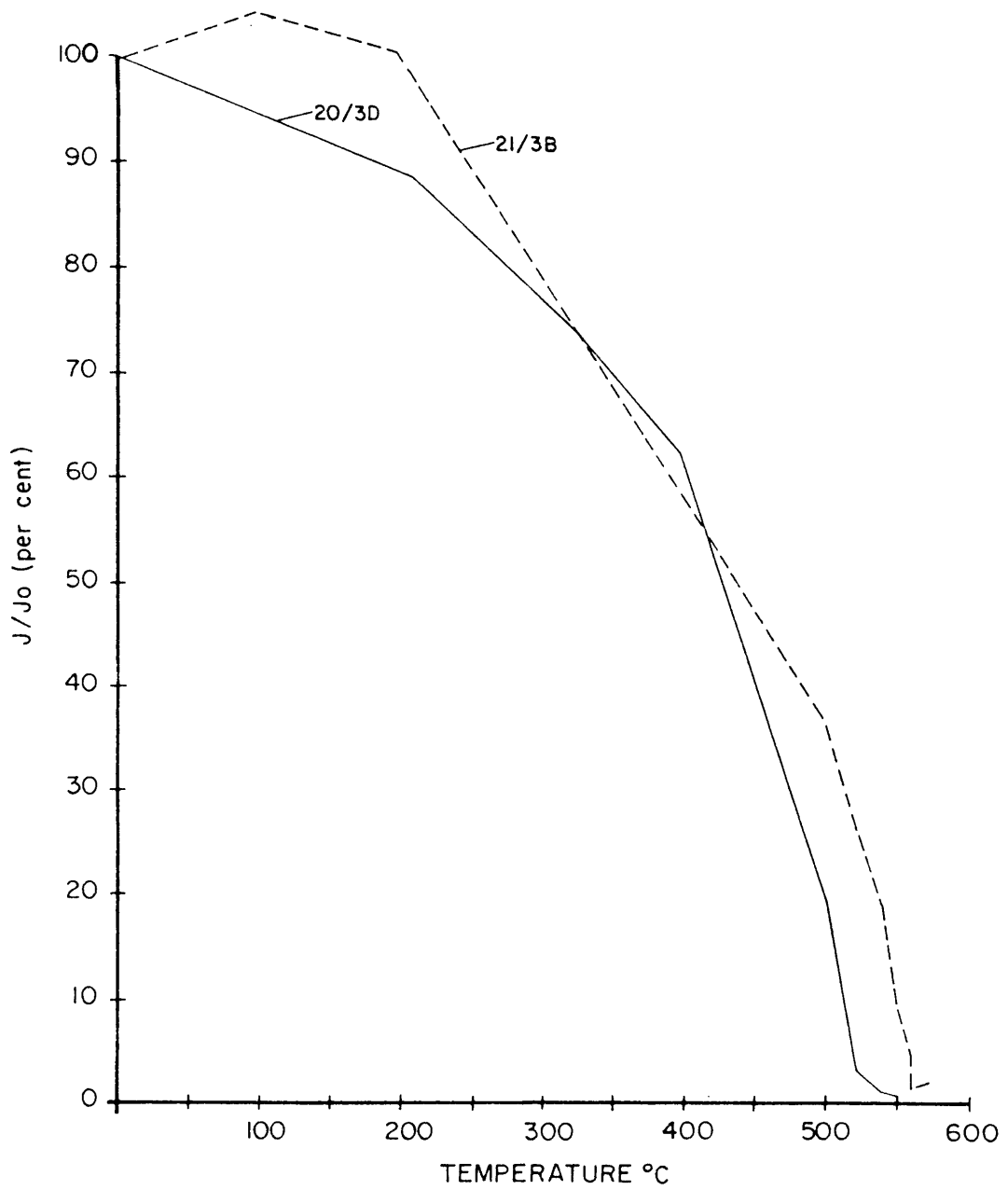


Fig. 33. Normalized intensity response curves of two specimens from sites 20 and 21 during continuous thermal demagnetization.

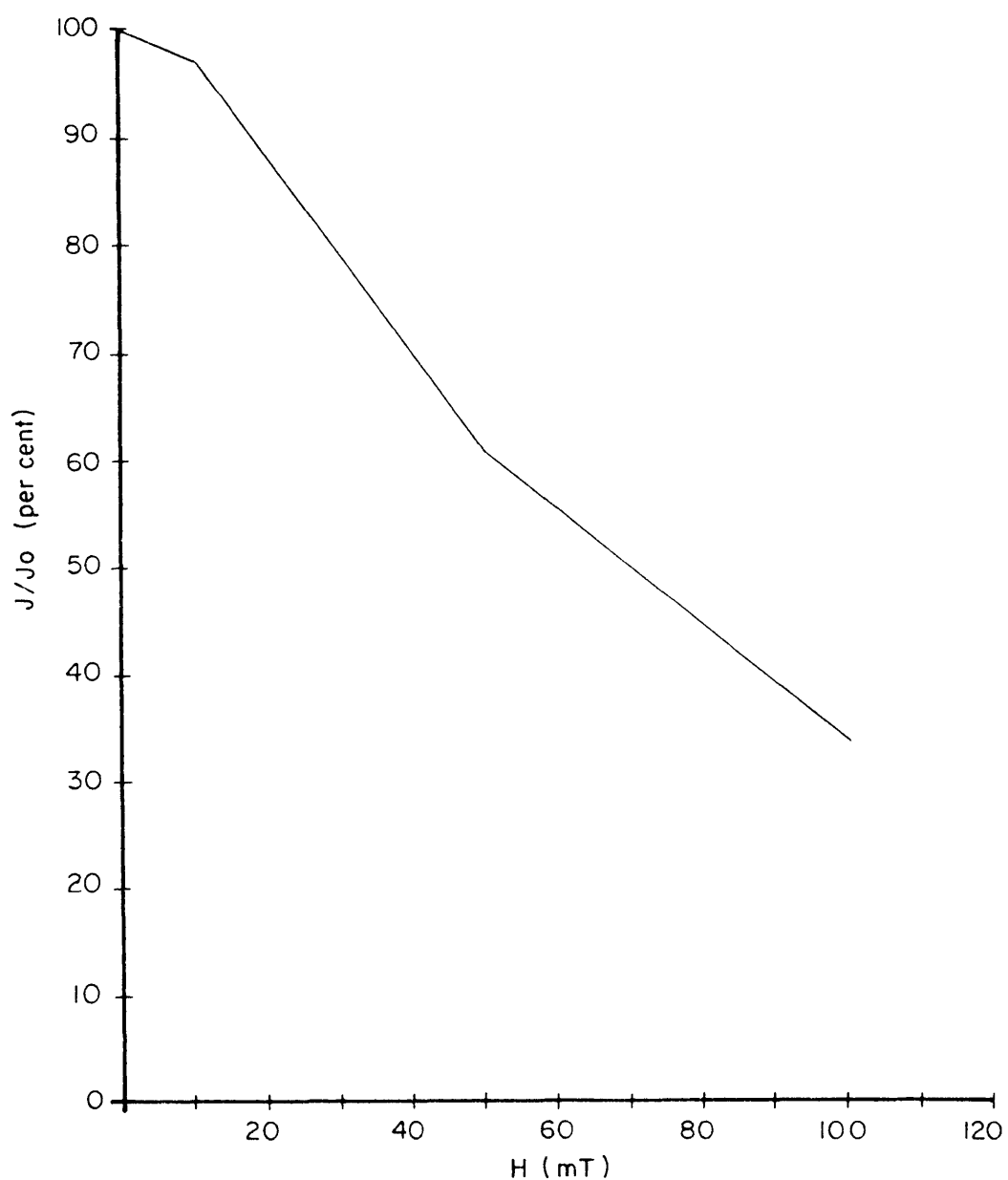


Fig. 34 Normalized intensity response curve of specimen 7/3B from subzone B, main zone eastern Bushveld Complex during AF demagnetization. This curve illustrates the "hardness" of magnetization which is typical of most of the specimens from subzone B.

magnetization, which in other studies was found to be due to the existence of fine magnetite needles in either pyroxenes (Evans *et al.*, 1968) or in plagioclase grains (Hargraves and Young, 1969), led to a more detailed examination of the pyroxene and plagioclase grains under maximum magnification with reflected and transmitted light microscopy. The result of this was, that opaque, needle-like grains were indeed found in both the pyroxene and plagioclase crystals (Figs. 35 and 36). The opaque grains in the pyroxene crystals are typically needle-like with an average width of approximately 1,5 μm , and a length to width ratio of 3:1, but occasionally larger lamellae are present. What appear to be long thin needles in some cases, can also be thin plates being looked at edge-on. The opaque grains observed in the plagioclase crystals are very similar, apart from being a little smaller with an average width of approximately 1 μm , and more elongated with a length to width ratio of up to 10:1.

The identification of these lamellae proved to be very difficult because of their small size, and only some of the larger opaque grains in the pyroxene crystals enabled their positive identification as magnetite with the aid of a scanning electron microscope. The presence of magnetite as needles in plagioclase crystals of the gabbros from the main zone of the layered sequence in the eastern Bushveld Complex was amongst others recognized by Groeneveld (1970) and Scharlau (1972), although earlier workers argued that these opaque grains could possibly also be needles of rutile and ilmenite (Brandt, 1946; Willemse and Viljoen, 1970). It was further observed, that the more abundant these needles appeared in a thin section, the higher the intensity of remanent magnetization of the specimen. Dunlop (1981), pointed out that this type of very "hard" remanent magnetization can only be explained by the presence of single domain grains (grain size $\approx 1 \mu\text{m}$; Soffel, 1971), which are characterized by a high degree of shape anisotropy. From this evidence it is concluded that the main carrier of remanent magnetization in these specimens, is the observed magnetite lamellae in the pyroxene and plagioclase crystals.

The genesis of magnetite needles in pyroxene crystals from the Grenville province is described by Fleet *et al.*, (1980), who argue that the needles exsolved from the parent pyroxene crystal at high temperatures.



Fig. 35 Magnetite lamellae in a pyroxene crystal, main zone, eastern Bushveld Complex. Transmitted light, magnification 870X.

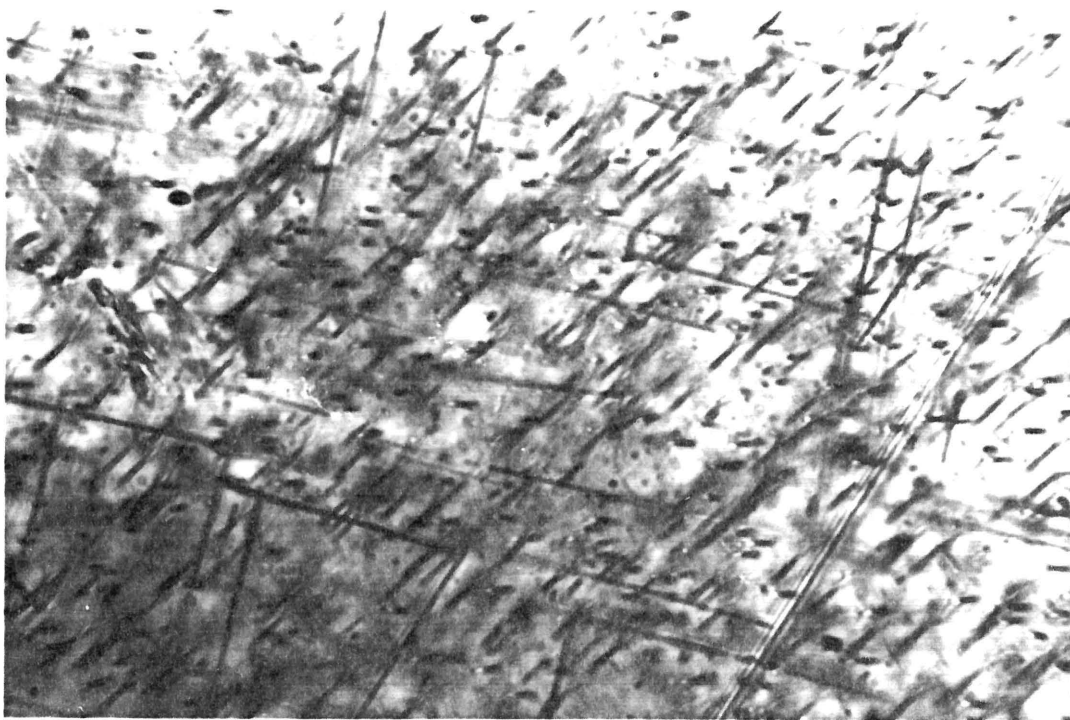


Fig. 36 Magnetite lamellae in a plagioclase crystal, main zone, eastern Bushveld Complex. Transmitted light, magnification 870X.

Similarly, for the opaque grains in the plagioclase crystals from the Bushveld Complex, Scharlau (1972) describes an exsolution process at high temperatures which took place shortly after crystallization of the plagioclase from the magma. This indicates that the remanent magnetization of these exsolution lamellae is a primary magnetization, associated with the crystallization and subsequent cooling of subzone B of the main zone.

Ilmenite occurs as discrete grains up to 0,5 mm in diameter. The ilmenite is generally unaltered, and the presence of haematite exsolution lamellae in ilmenite is very rare. The total ilmenite content is estimated to be less than one volume per cent. Electron microprobe analyses of ilmenite grains indicated a composition of approximately 85 per cent FeTiO_3 and 15 per cent Fe_2O_3 . In the composition range 45 to 95 per cent ilmenite the haemo-ilmenites are ferromagnetic (McElhinny, 1973) but with Curie temperatures generally below room temperature.

Several types of sulphides are present in the specimens, some of which have been identified as pyrrhotite. These grains are smaller and less abundant than the ilmenite grains. Pyrrhotite is a ferromagnetic mineral with a Curie point between 300°C and 325°C (Nagata, 1953), and will contribute to the remanent magnetization of specimens.

The three sites (19, 22 and 33) in group Bmz5AFR as well as sites 20 and 21, which are compatible with this group on the basis of results from the thermal demagnetization, are characterized by a very similar opaque mineralogy and to a certain extent the same "hard" NRM (Fig. 37) as sites in group Bmz3AFR. Magnetite exsolution lamellae are present in both pyroxene and plagioclase crystals, although less abundant, whereas discrete grains of magnetite are very rare. Ilmenite, as well as pyrrhotite are present as smaller grains. In the case of subzone C, however, more ilmenite grains with hematite exsolution lamellae are present.

Although the magnetization direction of site 11B can be grouped with group Bmz5AF, it has a marked different opaque mineralogy to both the sites in groups Bmz5AF and Bmz3AF including site 11A. The specimens

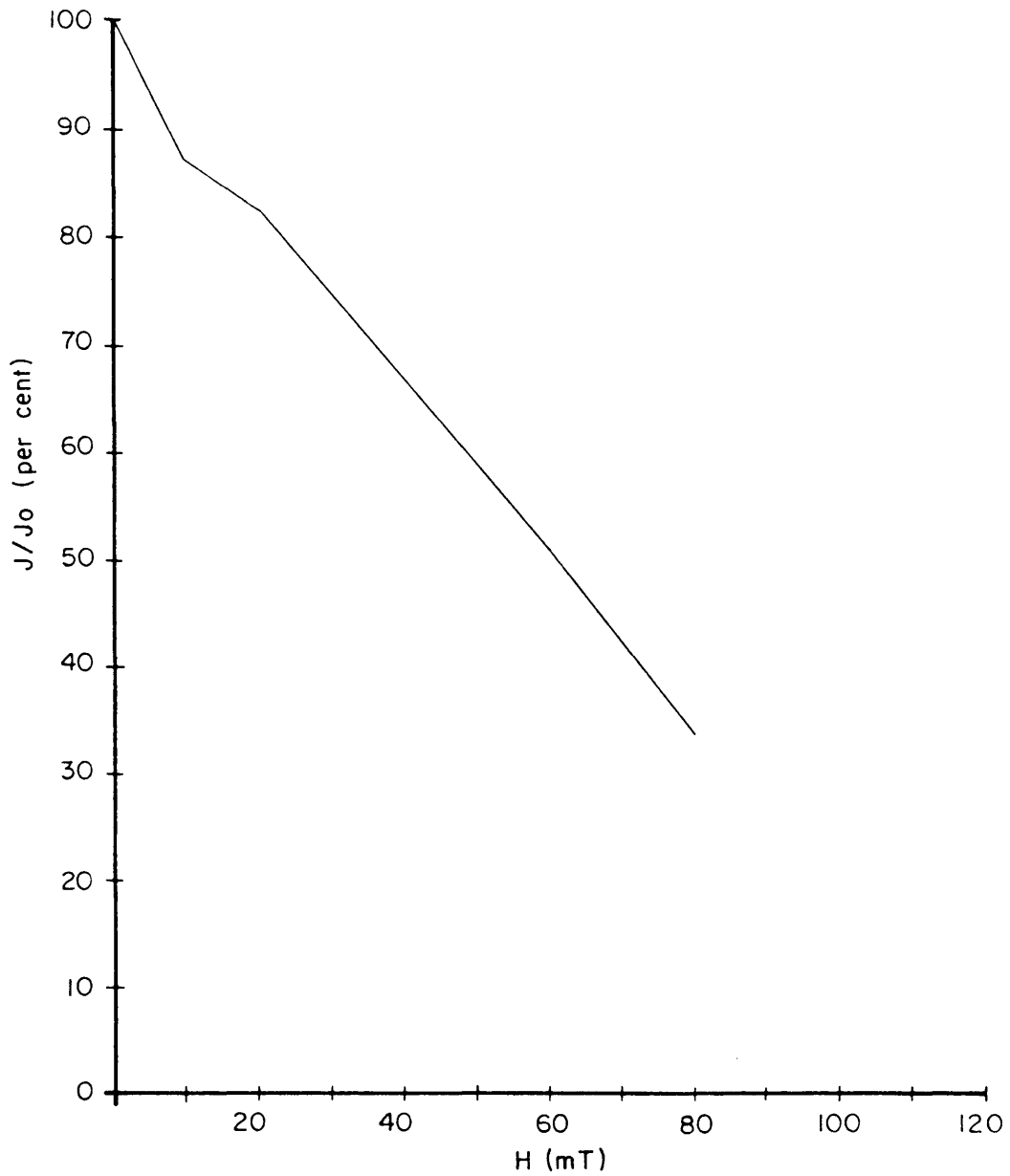


Fig. 37 Normalized intensity response curve of specimen 20/1C of subzone C, main zone, eastern Bushveld Complex during AF demagnetization.

are characterized by a lack of opaque minerals and neither tiny magnetite rods nor discrete magnetite grains could be found in the polished thin sections with an ore microscope. The absence of magnetite correlates well with the observed low NRM intensity. Pyrrhotite grains are present in small quantities; however, more striking is the presence of chromite grains. Chromite could actually be identified in a hand specimen.

The chromite grains are generally very small and semi-quantitative analyses with an energy dispersive X-ray spectrometer attached to a scanning electron microscope revealed these to be very iron-rich, with an iron-chrome ratio larger than 1.

Table IX. Semi-quantitative analyses of chromite grains from the main zone, eastern Bushveld Complex.

Oxides	Specimen 11B/5C	Specimen 11B/5D
Σ Fe as FeO	60	63
Cr_2O_4	33	28
TiO_4	<0,3	<2
Al_2O_3	1	<0,5
MnO	<u>5</u>	<u>6</u>
Total	\approx 99,3	99,5

Although very little Ti and Al are present in the chromite, these elements, can again be relevant to the magnetization of the specimens for the same reasons stated previously in the section dealing with chromite in specimens from the critical zone. Furthermore, the high Fe content may have a pronounced influence on the remanent magnetization of the specimens, as virtually no information is available on the remanent magnetization of iron-rich chromites in the literature. A thorough magnetic investigation of chromite, which is beyond the scope of this study, is required to determine the magnetic behaviour of this type of chromite.

Magnetite was never identified optically in the polished thin sections, but in search of suitable chromite grains to analyse, opaque grains were found which contain no Cr but a fairly high percentage of Ti,

which indicates that the grains are either magnetite or ilmenite.

The presence of chromite is further a possible indicator that the geological location of this site (subzone A of the main zone) has been wrongly identified, and that the site could be situated in the critical zone. Both Prof G von Gruenewaldt and Dr M R Sharpe (personal communication), confirmed the site position as being near the base of the main zone and definitely not in the critical zone.

F. The mixed polarity of site 11

Specimens from site 11 (sub-sites 11A and 11B) exhibited a complex change in magnetization directions during stepwise AF and continuous thermal demagnetization. With the aid of the Briden SI (Briden, 1972) alternating demagnetization fields were found for the bulk AF demagnetization of specimens from the site. The bulk AF demagnetization successfully located two magnetization directions. The first direction in core samples 11/1 and 11/3 is in agreement with the mean magnetization direction of group Bmz3AF, and is now referred to as the A magnetization direction. The second magnetization direction, which can be called the B direction, was isolated in core samples 11/4 and 11/5, and this magnetization direction is in agreement with the mean direction of group Bmz5AF. For grouping purposes site 11 was then split into two sites, 11A and 11B, representing the A (reversed) and B (normal) field magnetization directions respectively.

In an attempt to decide whether the approximately antipodal A and B magnetization directions represent a geomagnetic field-reversal or a self-reversal of magnetization, extensive analyses of thermal and AF demagnetization data, as well as various experiments were undertaken, the results of which will be presented and analysed in the following paragraphs.

The change in magnetization directions of specimen 11/3B during stepwise AF demagnetization and the difference vector removed after each step, are shown in Figure 38. In the initial AF demagnetization steps, a magnetization component is removed with a direction approximately parallel to the NRM directions of the specimen (say the C direction). This, however, changes rapidly as the AF values increase, and at the

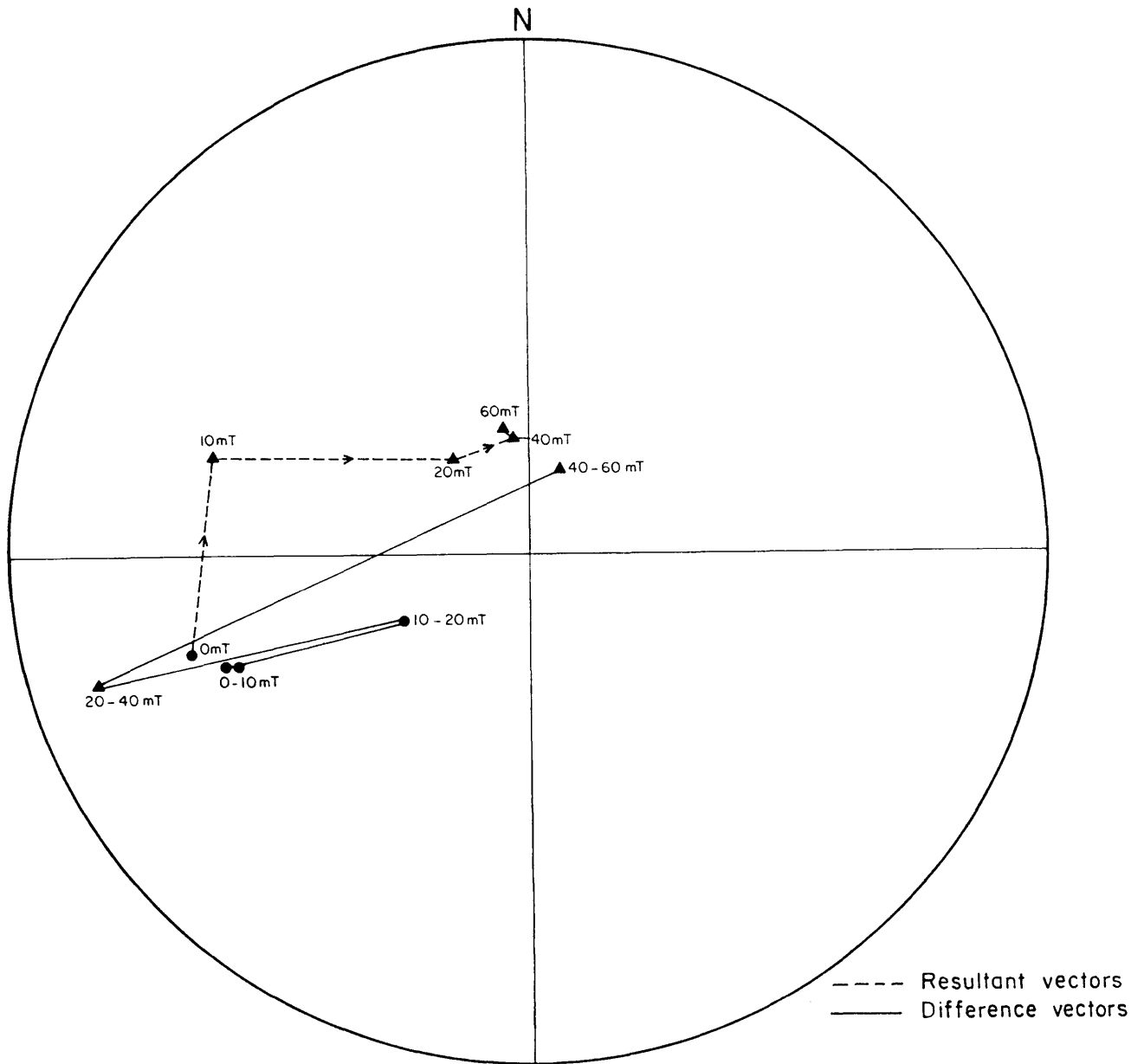


Fig. 38 AF demagnetization response of specimen 11/3B (site 11A). Resultant and difference vectors are shown. Difference vectors represent the magnetization vector destroyed between each AF step. Plotting convention as in Fig. 5.

40 mT to 60 mT step a direction broadly corresponding to the A direction is removed. At this stage the resultant and the difference vectors converge, indicating that only one component is removed. The AF demagnetization intensity curve of this specimen is shown in Figure 39, from which it is clear that two more or less opposing vectors are removed during AF cleaning. The first vector is destroyed at low AF values, manifested by a sharp decrease in the intensity of magnetization, but from 10 mT the intensity actually increases, reaches a maximum at 20 mT, from where, at higher AF values, the second component is destroyed. These data clearly indicate that two magnetization directions C and A reside in the specimens from site 11A, the C direction being the lower coercivity component.

The directional response of specimen 11/4C (site 11B) with the difference vector removed during stepwise AF demagnetization is shown in Figure 40. Again, at low AF values a magnetization direction is removed, which broadly corresponds to the NRM direction of the specimen and which is similar to the C direction removed in specimen 11/3B. At higher AF values the resultant vector changes rapidly, whereafter it follows a circle of remagnetization converging to the B magnetization direction. The difference vector indicates that at intermediate AF values a direction corresponding to the A magnetization direction is removed, and only at 60 mT do the difference and resultant vectors converge, indicating the removal of the B magnetization direction. Present in this specimen there are three magnetization components, C, A and B in order of their relative stability. The AF demagnetization intensity curve is shown in Figure 41, and this curve also indicates the removal of opposed magnetization directions.

The C direction of magnetization can be regarded as either an IRM or a VRM, because it is easily removed at relatively low AF values, but the A and B directions must, at this stage, be regarded as primary magnetization components of sites 11A and 11B respectively. This indicates then that the bipolarity of site 11 is due to primary magnetization directions.

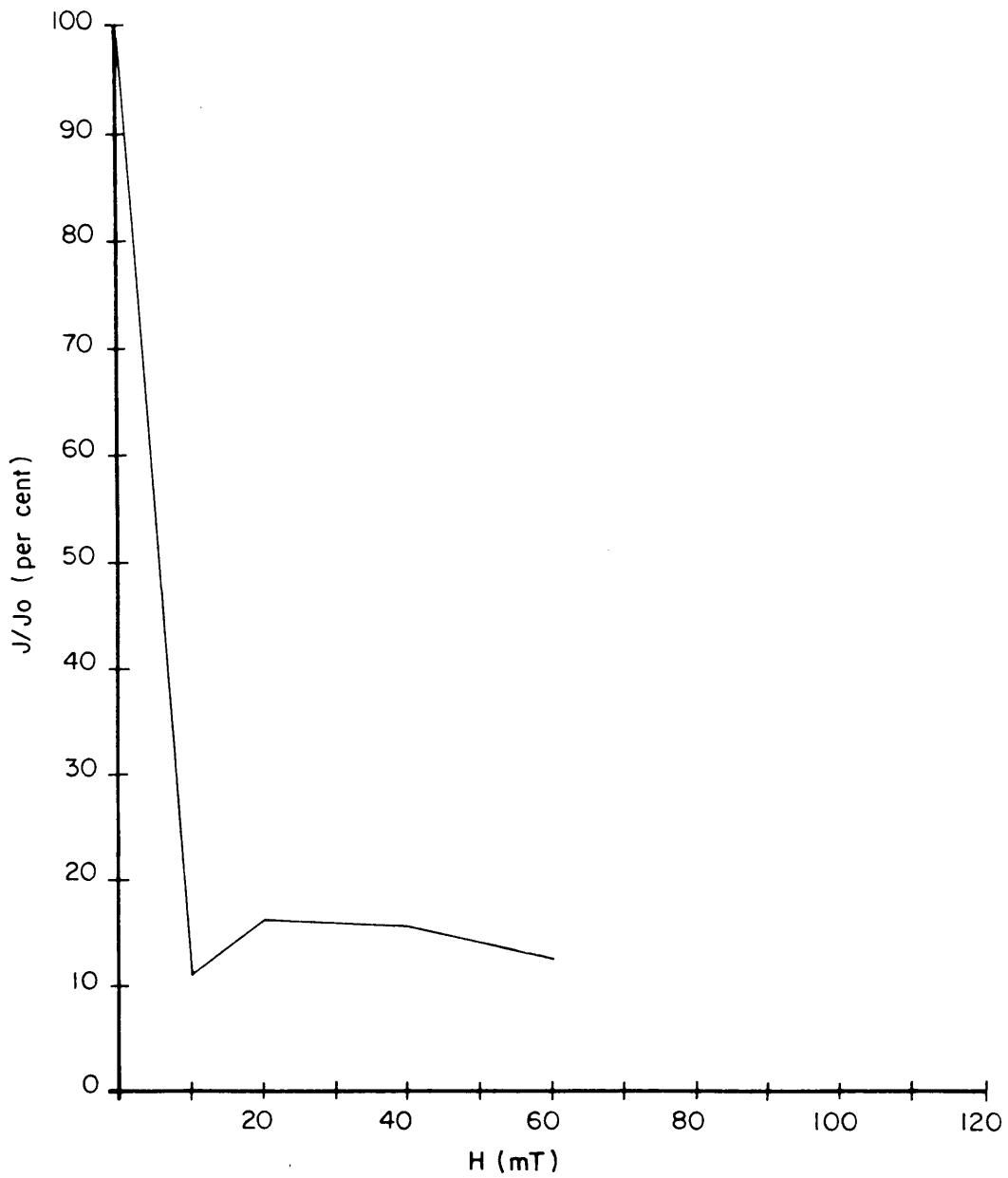


Fig. 39 Normalized intensity response curve of specimen 11/3B (site 11A) during AF demagnetization.

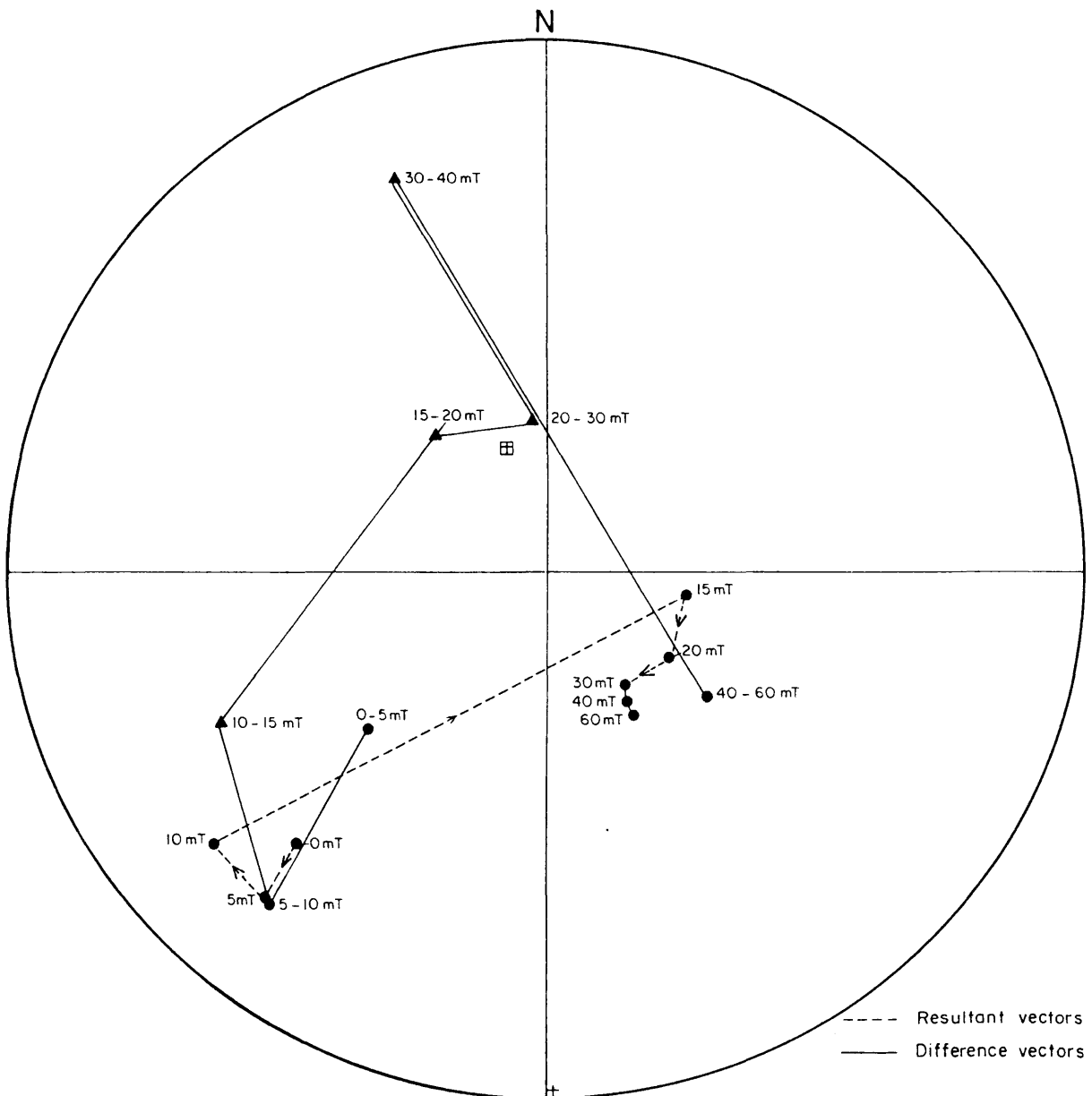


Fig. 40 AF response of specimen 11/4C (site 11B). Resultant and difference vectors shown. Plotting convention as in Fig. 5.

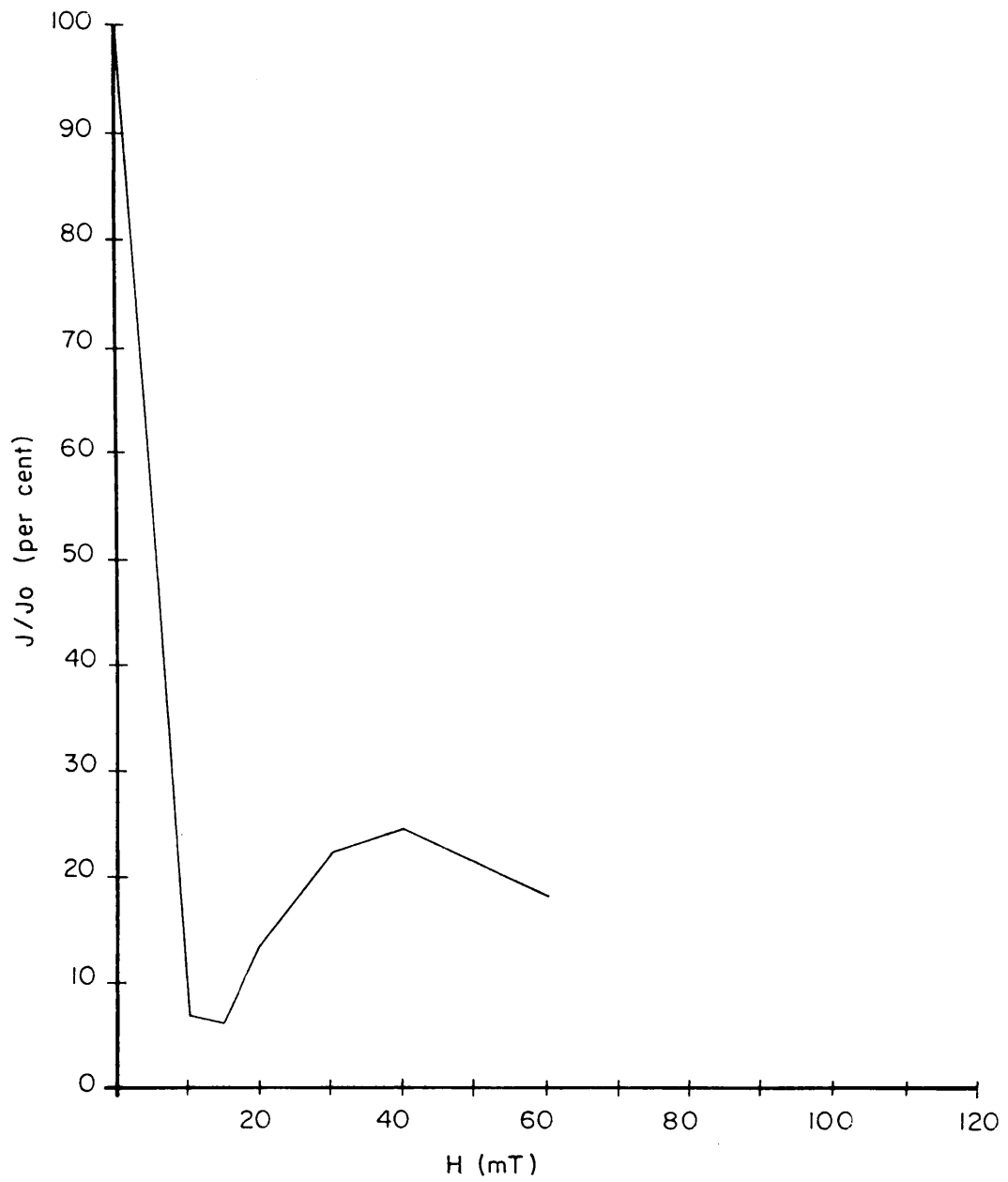


Fig. 41 Normalized intensity response curve of specimen 11/4C (site 11B) during AF demagnetization.

The directional response of specimen 11/3C to thermal demagnetization is shown in Figure 42. The difference vector here again indicates the presence of two magnetization directions C and A, similar to that indicated by the AF demagnetization. The C direction is a low temperature component, while the A direction emerges just before the Curie point of the specimen is reached. The same data for specimen 11/1B (Fig. 43) again show two magnetization components, an A direction, and a direction corresponding to the C direction, but with the inclination changed from negative to positive. Either this illustrates the capability of specimens from sample 11/1 to undergo a partial self-reversal of magnetization, or it is possibly due to an IRM, caused by lightning which affected samples 11/1 and 11/3 differently.

The intensity of the NRM of specimens from site 11B (samples 11/4 and 11/5), is too low to allow thermal demagnetization of the specimens, and consequently no further information on the blocking temperature spectra is available.

One specimen from each sample at site 11 was heated in the presence of nitrogen to 650°C and allowed to cool in the earth's magnetic field. All the specimens, with the exception of 11/5E, acquired a magnetization parallel to the magnetic field in which they cooled. Specimen 11/5E acquired a magnetization direction of which the declination differed by 180° to the field in which it cooled, but the inclination was in the same direction as that of the magnetic field in which it cooled.

The AF demagnetization response of the artificial TRM given to this specimen is shown in Figures 44 and 45. The change in vector direction during stepwise AF demagnetization of the specimen, shows that the TRM was acquired in such a way that it represents a multicomponent magnetization. The intensity response curve (Fig. 45) has a shape broadly similar to the intensity response curves obtained by AF demagnetization of the NRM of specimens from site 11B (Fig. 41). A possible conclusion here is that a partial self-reversal of magnetization had been reproduced in the specimen. It was later found that this specimen contains macroscopically visible chromite grains.

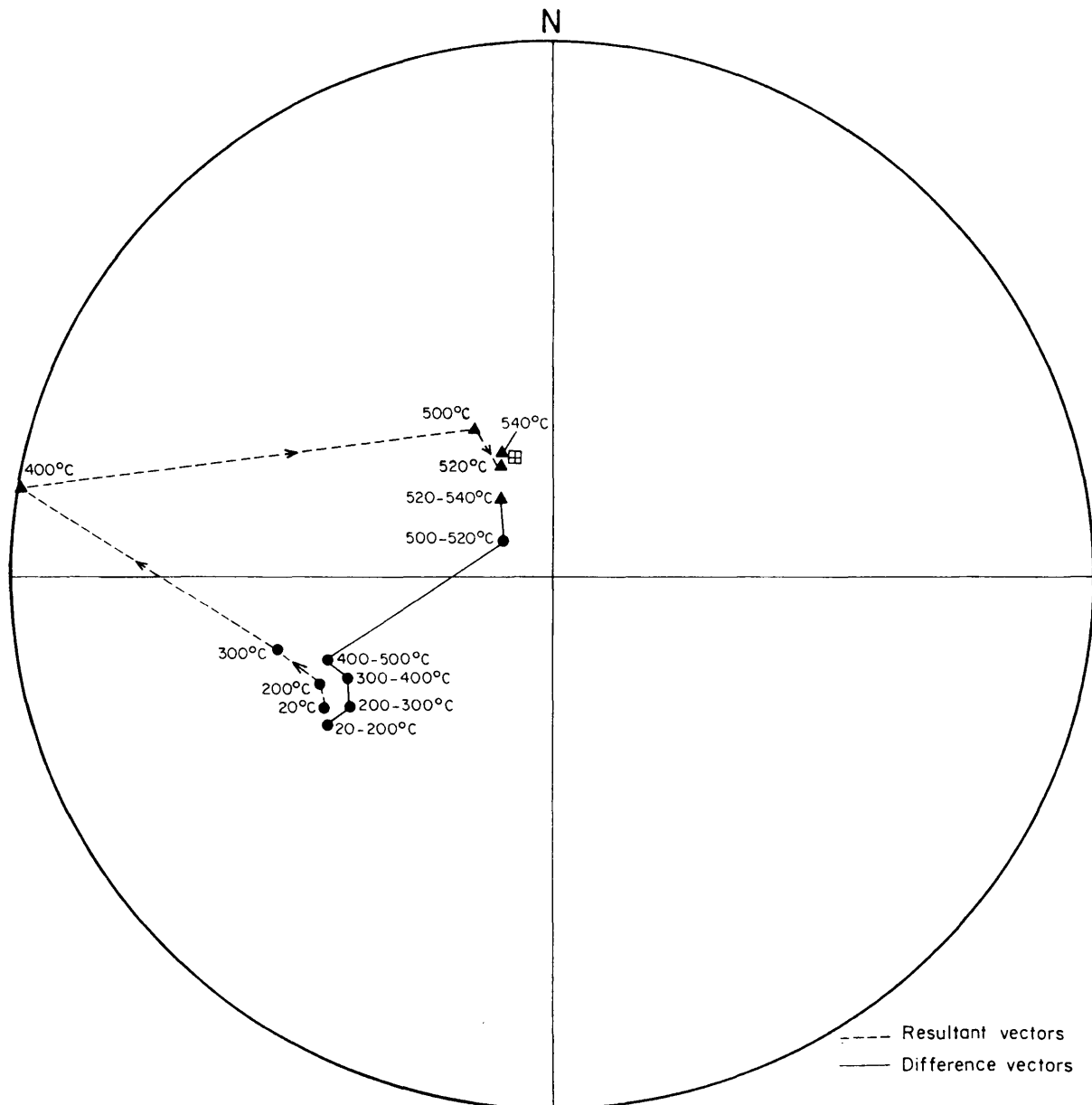


Fig. 42 Thermal demagnetization response of specimen 11/3C (site 11A). Resultant and difference vectors shown. Plotting convention as in Fig. 5.

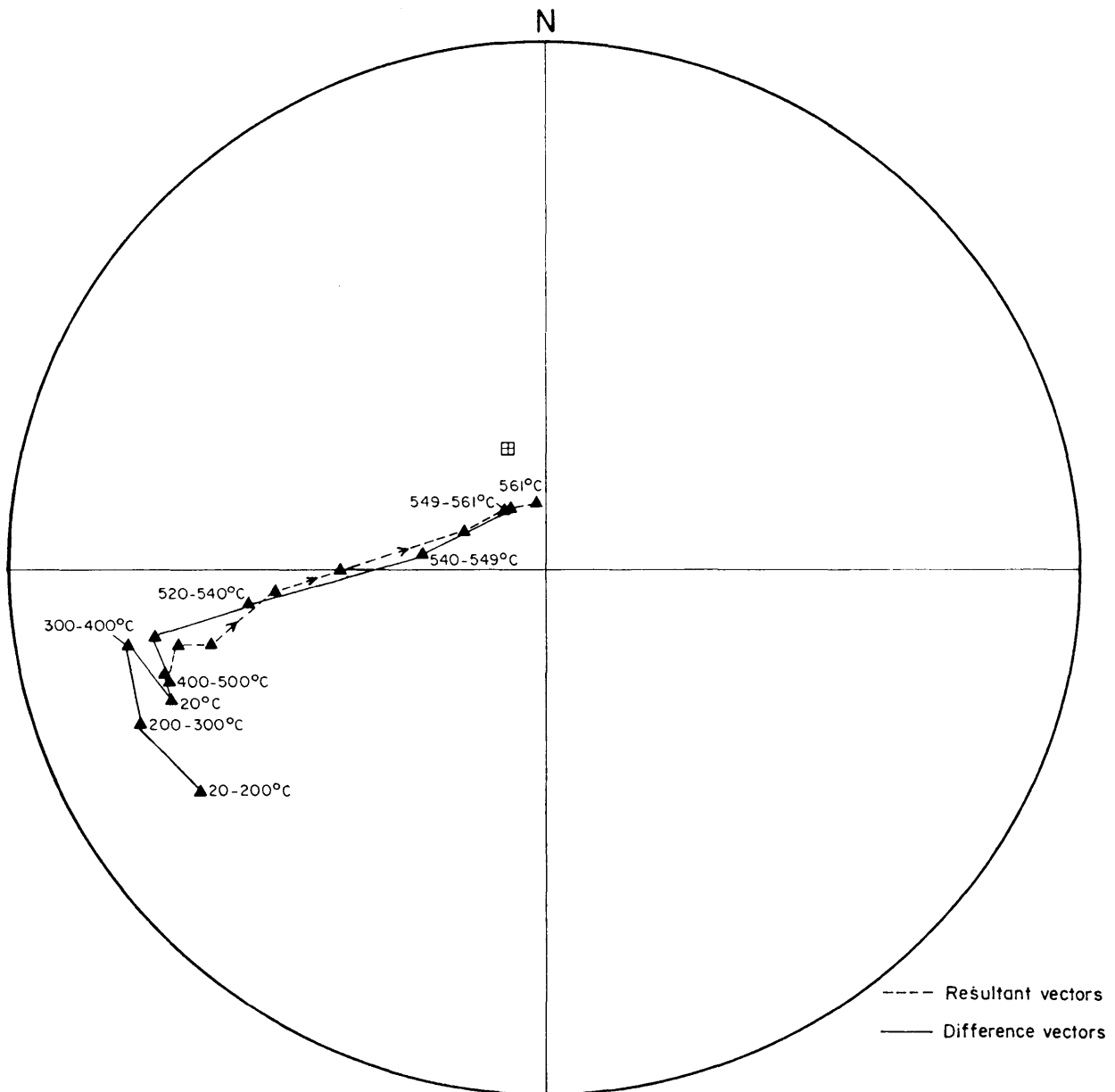


Fig. 43 Thermal demagnetization response of specimen 11/1B (site 11A). Resultant and difference vectors shown. Plotting convention as in Fig. 5.

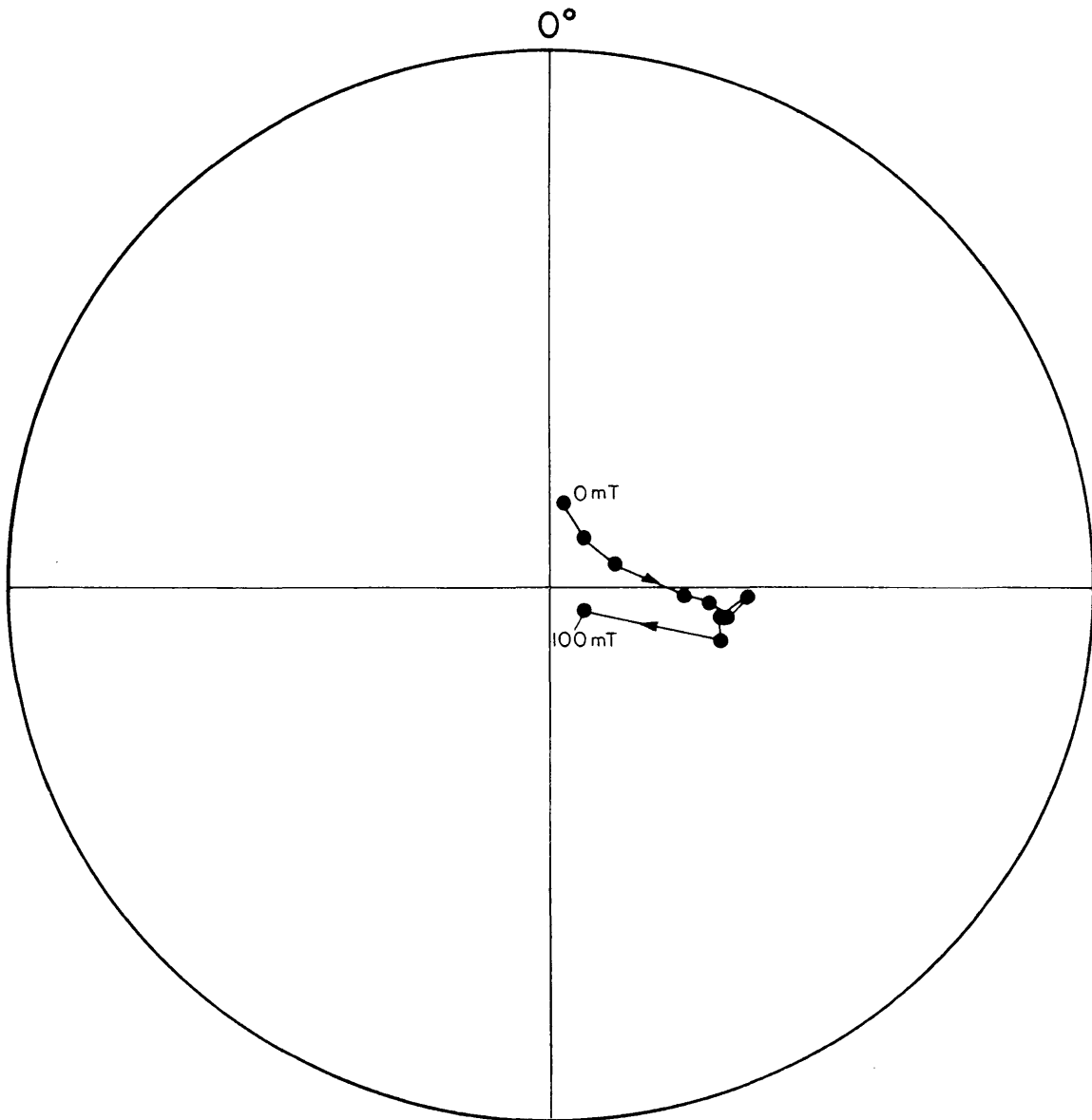


Fig. 44 AF demagnetization response of specimen 11/5E (site 11B), after the specimen had been given an artificial TRM in the earth's magnetic field. Plotting convention as in Fig. 5.

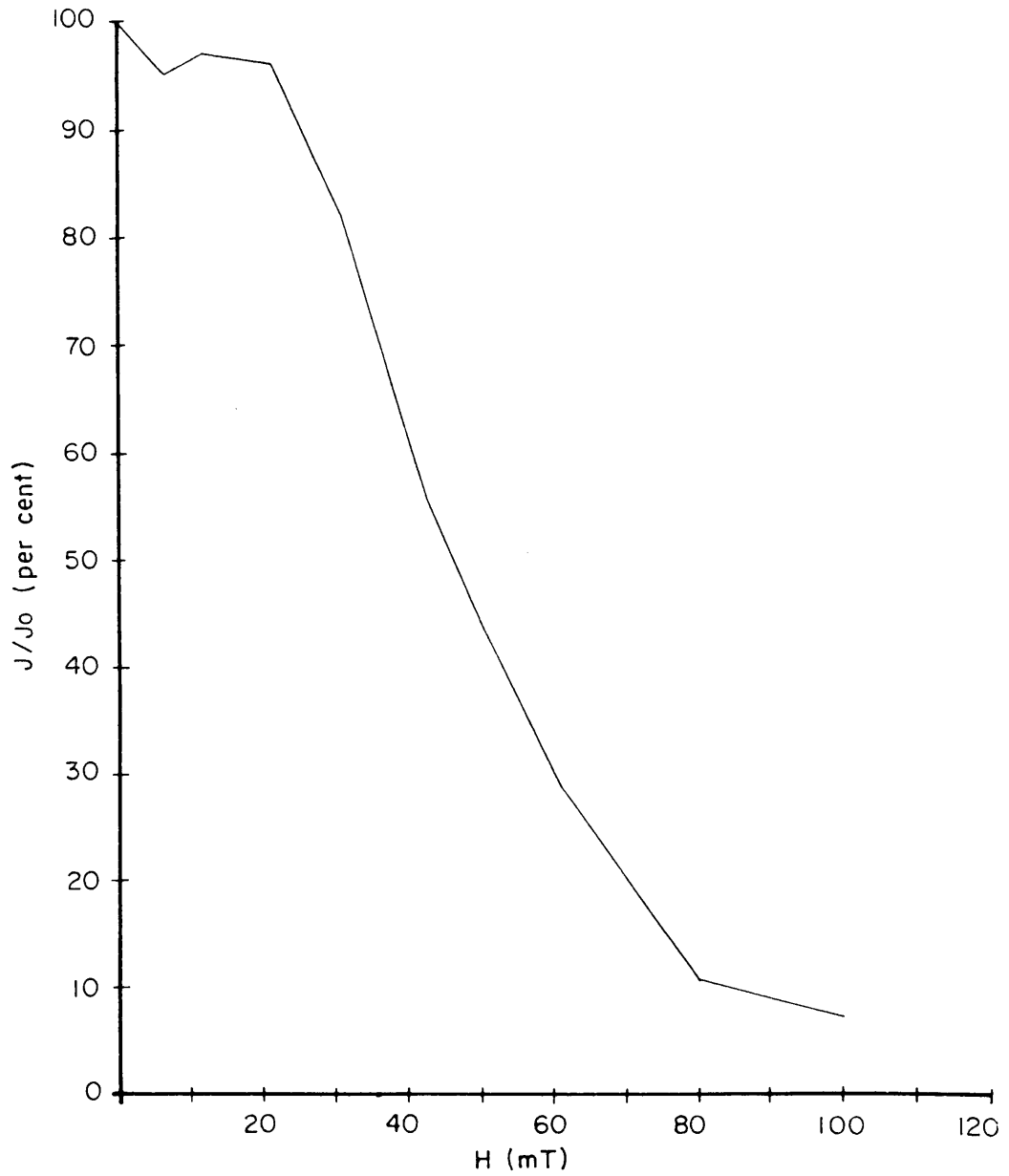


Fig. 45 Normalized intensity response curve of specimen 11/5E (site 11B) during AF demagnetization, after the specimen had been given an artificial TRM in the earth's magnetic field.

Another specimen from site 11A with an artificial TRM, was thermally demagnetized. Because this specimen had acquired a magnetization parallel to the field in which it cooled down it was thought that the magnetization direction should change very little during thermal demagnetization. This was not the case, and during continuous thermal demagnetization the magnetization direction exhibited a swinging behaviour (Fig. 46). The reason for this observed behaviour is not clear, but it is possibly an indication of the ability of specimens from site 11, to acquire magnetization components which are not parallel to the field in which they acquire a TRM.

To test the stability of magnetization of site 11 further, the measurement of the NRM of a number of specimens was repeated after 12 months. All the magnetization directions remained the same, except for one specimen from site 11B. In this case the inclination of the magnetization relative to a fiducial mark on the specimen, changed from -45° to $+45^\circ$. Although it is possible that the specimen had acquired a VRM in the laboratory during the twelve months, no indication of it could be found, because the intensity of magnetization remained exactly the same.

Despite the previous slight evidence in favour of a self-reversal of magnetization, the fact that all the measured specimens from site 11B also contain the A magnetization direction of site 11A, can be used to argue in favour of a geomagnetic field-reversal. If a field reversal had taken place immediately after the Curie isotherm had passed through site 11B, it is conceivable that the samples from site 11B, at that stage at a relatively high temperature, could have acquired at least a component of magnetization parallel to the new (reversed) ambient magnetic field. A similar argument to explain mixed polarities at one site in the Limpopo belt, is used by Morgan and Briden (1981) in support of a geomagnetic field-reversal. However, these authors give no details on the mineralogy of the specimens, which in the case of sites 11A and 11B do differ.

It can therefore be concluded that evidence supporting both a geomagnetic field-reversal and a self-reversal of magnetization exist, and that neither possibility can be completely discarded.

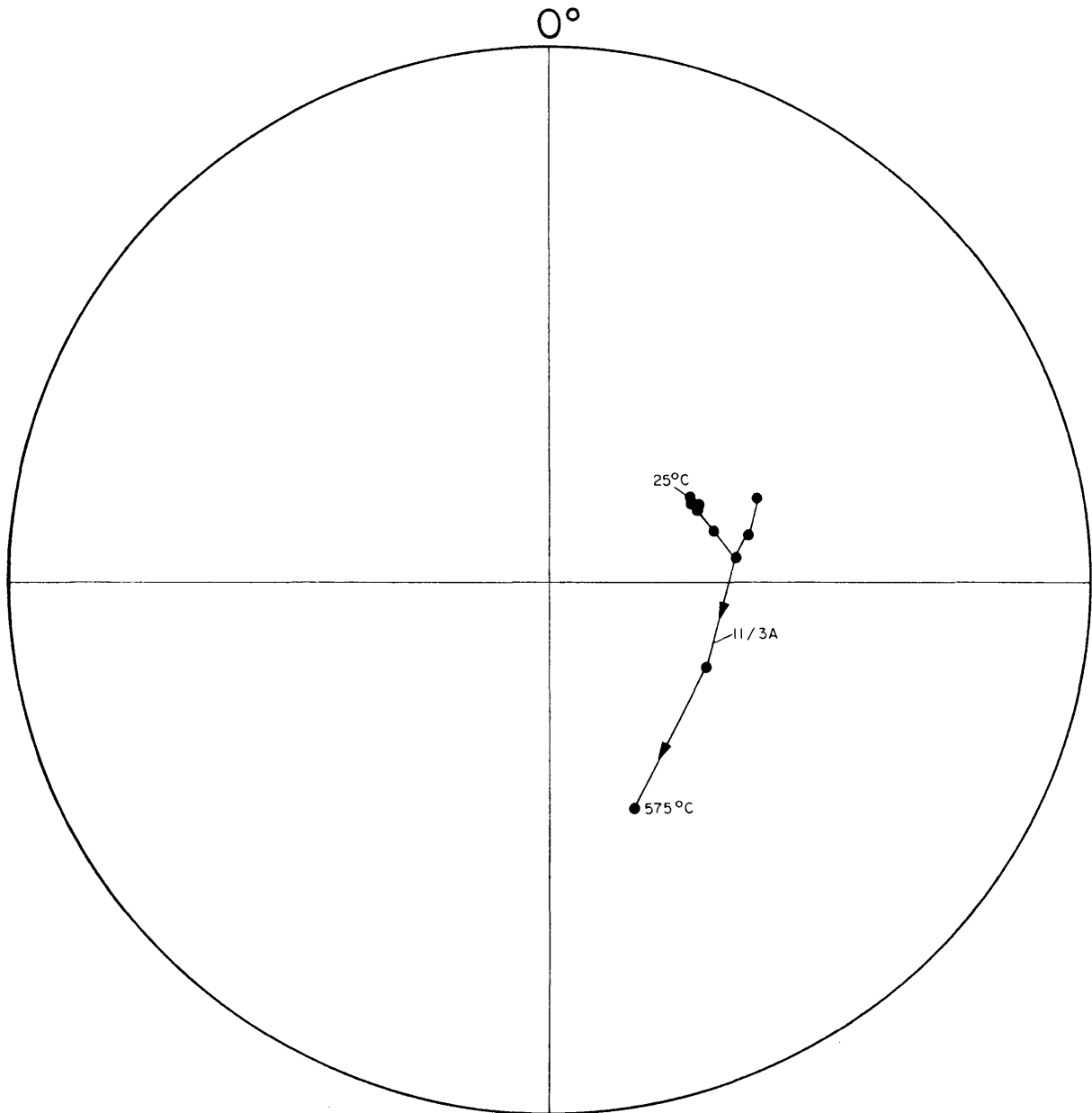


Fig. 46 Thermal demagnetization of specimen 11/3A (site 11A), after the specimen had been given an artificial TRM in the earth's magnetic field. Plotting convention as in Fig. 5.

G. The polarity difference of magnetization between subzones B and C

The mean magnetization direction of subzone B of the main zone in the eastern Bushveld Complex is reversed as given by group Bmz3AFR, and that of subzone C is normal as given by group Bmz5AFR. These different polarities can be regarded as approximately antipodal. This immediately gives rise to the question whether this feature is due to a self-reversal of magnetization or to a geomagnetic field-reversal.

The opaque mineralogy of specimens from the two groups is similar the only difference being the amounts and relative proportions of the minerals present in the specimens. For this reason, the opaque mineralogy of the specimens does not support the possibility of a self-reversal of magnetization.

Heating and cooling experiments on specimens from both groups always resulted in the specimens acquiring an artificial TRM parallel to the magnetic field in which they cooled. The same results were obtained by imparting an IRM to the specimens and at no time was any evidence whatsoever found to support a self-reversal or even partial self-reversal of magnetization.

With lack of evidence to the contrary, it must be concluded that the polarity difference between subzones B and C is due to a reversal of the earth's magnetic field which took place approximately 2000 m.y. ago.

H. Summary of results

All the fold tests carried out on palaeomagnetic data from the main zone in the eastern Bushveld Complex, improved group statistics. This implies that the main zone acquired its present dip and dip direction after cooling to below its Curie temperature.

The investigation succeeded in establishing magnetization directions for subzones B and C of the main zone, which are as follows:

subzone B:

Group: Bmz3AFR ; N = 13 ; D = 10° ; I = 64,7° ; $\alpha_{95} = 4,2^\circ$; k = 100

with pole position: latitude : 17,3°N
 longitude : 35,7°E
 and polar error (dp, dm) : 5,4° and 6,4° respectively

subzone C:

Group: Bmz5AFR ; N = 3 ; D = 168,9°; I = -55,0° ; $\alpha_{95} = 20^\circ$; k = 37

with pole position: latitude : 28°S
 longitude : 161,7°W
 and polar error (dp, dm) : 20,1° and 28,6° respectively

The polarity difference between groups Bmz3AFR and Bmz5AFR strongly suggests a reversal of the earth's magnetic field.

Subzone A at the base of the main zone, is represented by only one site, which contains mixed polarities of magnetization. One direction is approximately parallel to the mean of group Bmz5AFR, and the other direction parallel to the mean direction of group Bmz3AFR. Experimental evidence exists which supports both a geomagnetic field reversal and a self-reversal of magnetization as cause for the observed mixed polarity.

VII THE PALAEOMAGNETISM OF THE MAIN ZONE IN THE WESTERN BUSHVELD COMPLEX

A. Introduction

The part of the main zone under discussion in this chapter, extends from north of Pretoria westwards, towards Rustenburg and the Pilanesberg Complex (Fig. 1). Although the main zone exists in the area to the north of the Pilanesberg Complex (Fig. 1), no suitable sampling sites could be located in that area.

Sampling was done at thirty-four sites, the majority of which are situated in quarries. The resultant relatively unweathered samples enabled the extraction of consistent and stable magnetization directions from all sampling sites and it was unnecessary to reject any data.

Gough and Van Niekerk (1959) had four sampling sites in this area, which yielded a mean NRM direction with $D = 4,5^\circ$ and $I = 73,5^\circ$ (calculated from the data presented by Gough and Van Niekerk, 1959, p131) uncorrected for the dip of the layered sequence. If the site directions are corrected for the dip, using dip and dip directions given by Gough and Van Niekerk (1959, p129) the mean magnetization direction of the four sites changes to $D = 8,6^\circ$; $I = 58,9^\circ$. The estimate k of the precision parameter K (Fisher, 1953), increases from 32 to 54, but this is not significant at the 95 per cent confidence limit, according to the criterion of McElhinny (1964b).

B. Natural remanent magnetization

With the exception of specimens from sites 75 and 76, specimens from all the sites have a fairly high intensity of NRM. The average intensity of the NRM is $2078 \times 10^{-3} \text{ Am}^{-1}$, (Fig. 47), which is slightly lower than the average intensity of the NRM of the main zone in the eastern Bushveld Complex.

The NRM directions of thirtytwo sites, together with the site statistics, are listed in Table X, while the magnetization directions are shown in Figure 48. Magnetization directions of specimens from sites 48 and 51 were random at 95 per cent confidence limits, using the test by Watson (1956); accordingly, these two sites were rejected from the analysis of NRM data.

Table X. Natural remanent magnetization directions of sites in the main zone, western Bushveld Complex.

Site	N*	Declination(D)	Inclination(I)	α_{95}	k
1	4	215,3°	64,8°	9,6°	167
2	4	319,9°	81,8°	2,6°	1259
45	4	270,6°	87,6°	3,7°	612

46	4	274,2°	87,2°	5,7°	180
47	4	143,5°	86,9°	3,0°	893
49	4	313,6°	89,0°	9,7°	161
52	4	12,9°	66,8°	10,9°	72
53	4	326,6°	85,0°	5,1°	582
54	4	342,8°	82,3°	3,6°	663
55	4	321,0°	85,6°	3,9°	554
56	4	43,4°	77,0°	3,0°	956
57	4	348,5°	82,5°	4,7°	381
58	4	0,5°	72,3°	5,5°	280
59	4	1,4°	69,6°	4,0°	526
60	4	46,6°	66,6°	6,8°	183
61	4	346,9°	67,7°	6,3°	216
62	4	346,1°	67,2°	3,8°	582
63	4	358,9°	73,8°	7,7°	142
64	4	299,8°	82,4°	4,6°	402
65	4	336,2°	72,0°	6,4°	204
66	4	342,2°	68,3°	0,6°	9839
67	4	332,3°	68,0°	6,0°	233
68	4	326,5°	75,4°	3,4°	743
69	4	356,7°	73,5°	3,0°	953
70	4	325,7°	80,5°	2,7°	1201
71	4	314,8°	79,0°	2,0°	2094
72	4	336,4°	75,7°	4,8°	366
73	4	329,5°	77,7°	4,5°	343
74	4	345,7°	69,9°	3,3°	772
75	4	153,4°	-54,0°	5,9°	257
76	4	182,3°	-49,8°	5,7°	257
78	4	75,4°	83,8°	13,9°	79

*N is the number of core samples taken at each site.

There are thirty sites with NRM directions reversed (positive inclination).

These sites form group Bmz6:

Group: Bmz6 ; N = 30 ; D = 345,8° ; I = 79,5° ; α_{95} = 3,7° ; k = 52

Group Bmz6 exhibits a smeared distribution in a mainly north-north-westerly direction, but a number of magnetization directions lie along a north-northeast trend (Fig. 48). This may be due to the dip and dip direction of the igneous layering at each site, or due to a multi-

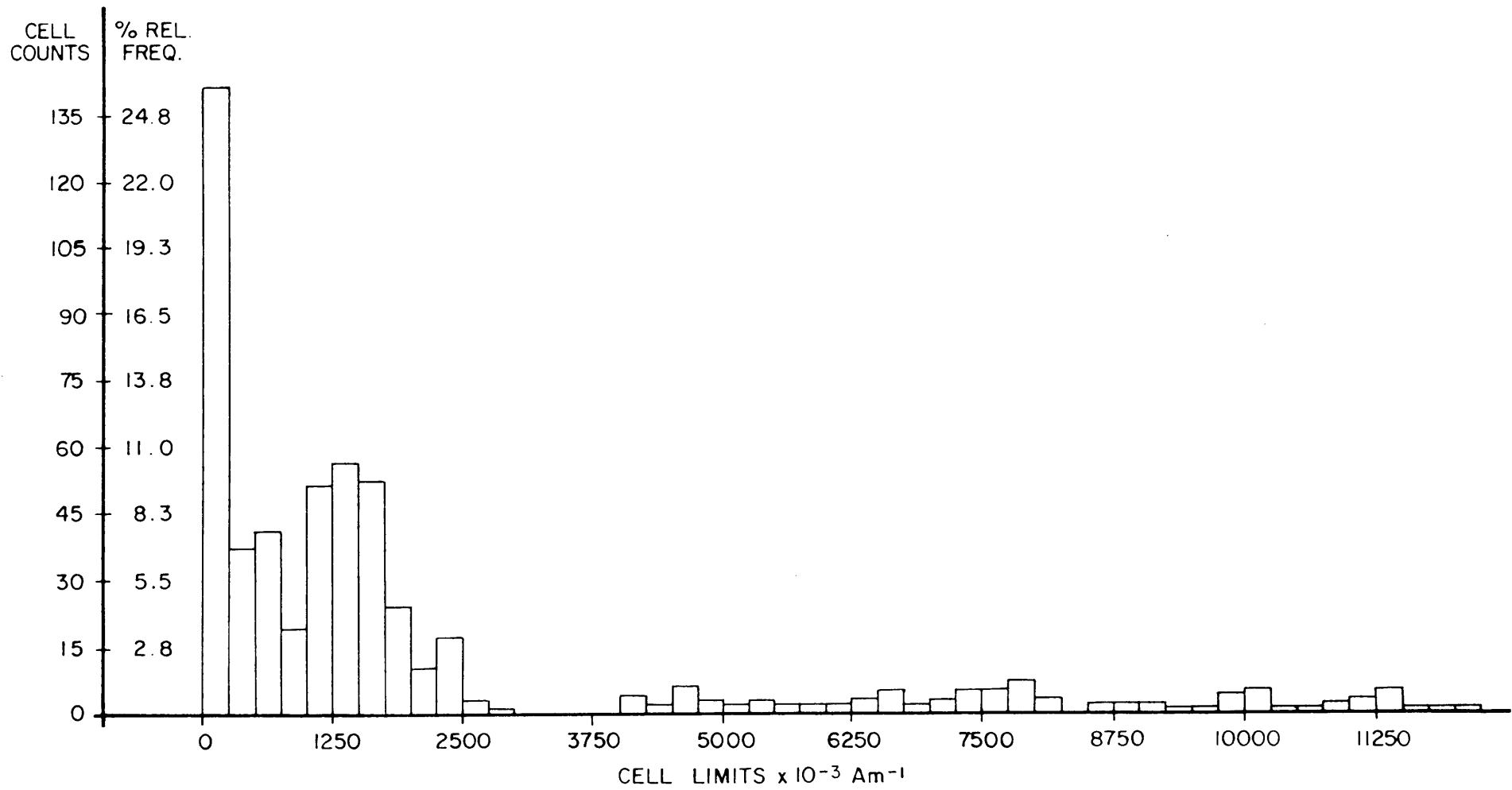


Fig. 47 Histogram plot of NRM intensities of all the specimens from the main zone in the western Bushveld Complex.

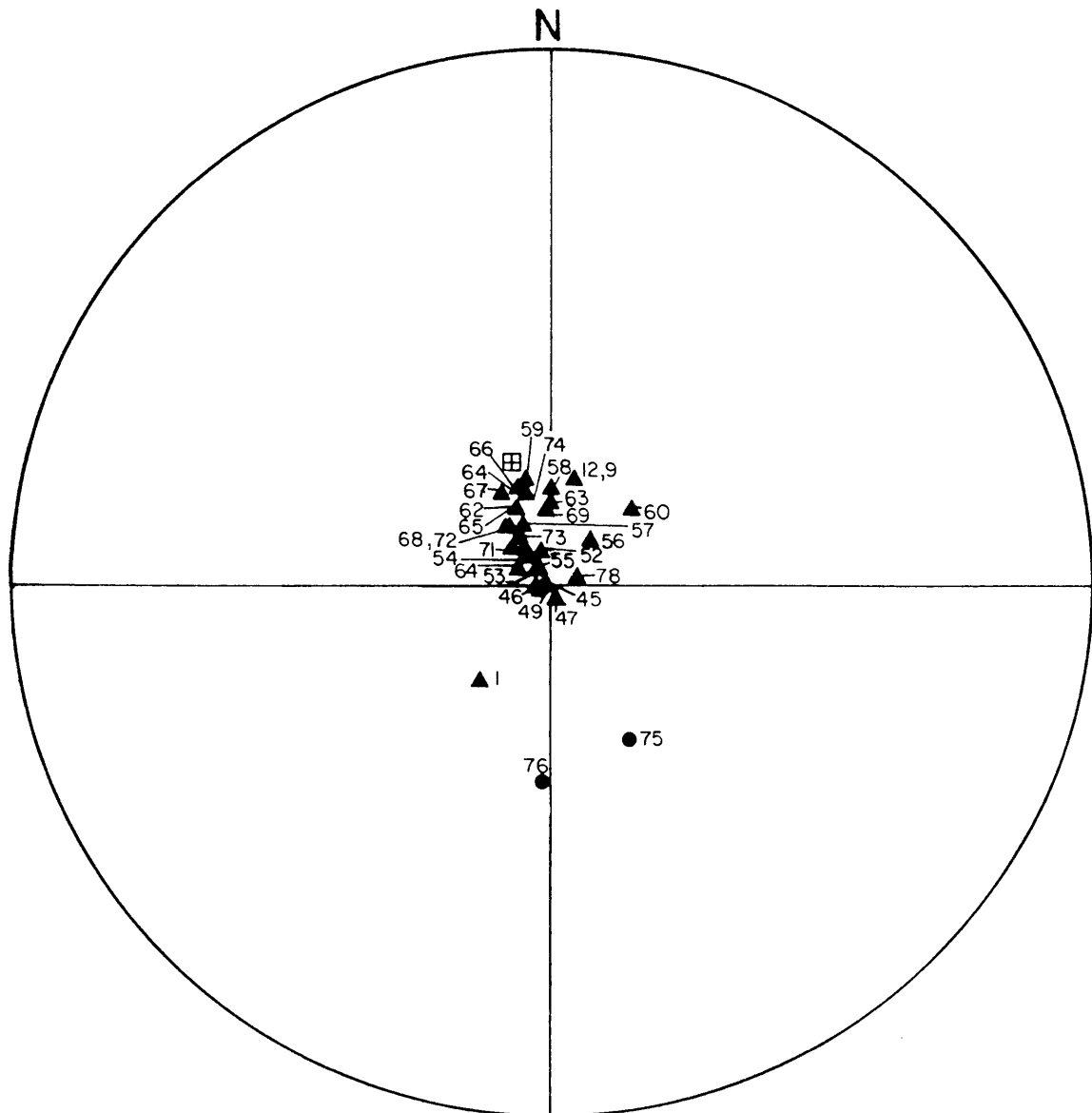


Fig. 48 NRM directions from sites in the main zone, western Bushveld Complex. Plotting convention as in Fig. 5.

component NRM.

The magnetization directions of two sites have negative inclinations (sites 75 and 76, Table X and Fig. 48) and lie in a roughly antipodal position to group Bmz6. There is no obvious explanation for this, especially because both sampling sites are situated, like many of the other sites, in the Pyramid Gabbro-norite unit of the layered sequence.

The NRM directions of the sites, with the igneous layering rotated to a horizontal position, as well as the dip and dip direction of the layering at each site, are listed in Table XI.

Table XI. Natural remanent magnetization directions of sites in the main zone, western Bushveld Complex with the igneous layering in a horizontal position.

Site	Dip	Dip direction*	D	I
1	20°	N10°	264,0°	79,0°
2	20°	N10°	355,5°	64,0°
45	25°	N10°	4,3°	65,3°
46	25°	N10°	4,3°	65,1°
47	25°	N10°	15,7°	67,0°
49	14°	N10°	6,7°	75,0°
52	15°	N355°	6,4°	53,0°
53	10°	N350°	342,2°	75,3°
54	10°	N350°	346,8°	72,3°
55	10°	N350°	341,1°	76,0°
56	25°	N355°	12,0°	55,1°
57	25°	N05°	1,0°	57,8°
58	10°	N03°	2,0°	62,3°
59	8°	N20°	6,3°	61,9°
60	5°	N20°	42,0°	62,0°
61	5°	N20°	352,2°	62,4°
62	6,5°	N22°	353,4°	61,7°
63	10°	N25°	8,5°	64,5°
64	15°	N20°	354,9°	72,0°
65	5°	N25°	8,5°	64,5°
66	5°	N25°	345,8°	68,4°

67	7°	N30°	344,5°	63,6°
68	8°	N30°	347,4°	70,5°
69	8°	N30°	7,1°	66,4°
70	7,5°	N35°	355,4°	75,9°
71	10°	N40°	354,4°	74,5°
72	15°	N40°	8,2°	65,2°
73	10°	N40°	0,1°	71,7°
74	10°	N40°	2,3°	62,9°
75	20°	N70°	180,0°	-51,6°
76	20°	N70°	199,0°	-39,5°
78	20°	N05°	20,2°	67,2°

*Measured from north in a clockwise direction.

The magnetization directions listed in Table XI are shown in Figure 49. After correction for dip, group Bmz6 now becomes group Bmz6R with the following statistics:

Group: Bmz6R ; N = 30 ; D = 0,5° ; I = 67,6° ; $\alpha_{95} = 3,0^\circ$; k = 78

The ratio of the estimates of the two precision parameters of groups Bmz6 and Bmz6R, k_1/k_2 , is 1,5 and this improvement in k after application of the fold test (Graham, 1949), is not significant at the 95 per cent confidence limit according to the criterion of McElhinny (1964b). However, if the improvement is tested at the 90 per cent confidence limit, the improvement in k is significant. Because the dip values and dip directions used in this test are only accurate to within a few degrees, it is reasonable to accept the result of the fold test as an improvement, which implies that the igneous layering acquired its present orientation after the main zone in the western Bushveld had cooled to a temperature below its Curie point.

C. Bulk alternating field demagnetization

As in previous cases, bulk AF demagnetization of specimens of each site was done at an optimum AF value indicated by the Briden SI (Briden, 1972) for each site. The results of the bulk AF demagnetization are presented

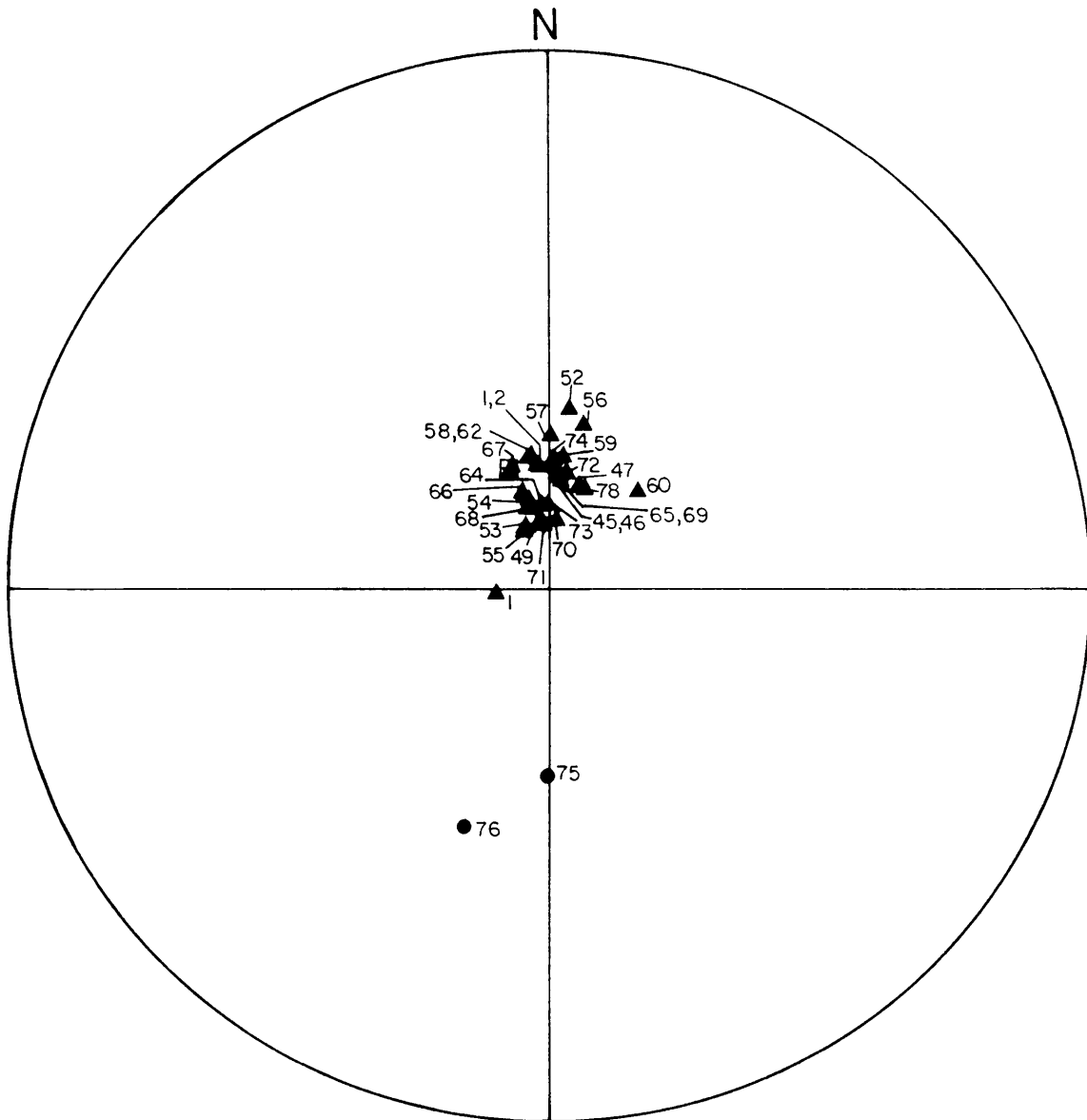


Fig. 49 NRM directions from sites in the main zone, western Bushveld, with the igneous layering in a horizontal position. Plotting convention as in Fig. 5.

in Table XII and the magnetization directions of the sites are shown in Figure 50.

Table XII. Magnetization directions of sites in the main zone, western Bushveld Complex, after bulk AF demagnetization.

Site	Demagnetization field (mT)	D	I	α_{95}	k
1	20	214,8°	77,8°	8,0°	236
2	40	193,1°	86,4°	4,7°	386
45	60	209,9°	79,6°	4,2°	483
46	40	182,7°	83,9°	4,7°	256
47	50	141,3°	84,1°	3,9°	555
48	60	352,5°	71,8°	13,1°	50
49	30	87,2°	85,8°	1,6°	2970
51	30	11,1°	73,5°	20,6°	20
52	30	27,0°	68,8°	5,6°	268
53	10	303,0°	86,6°	4,9°	358
54	20	320,0°	82,7°	3,9°	532
55	20	185,5°	89,6°	3,7°	605
56	30	61,0°	76,6°	3,6°	640
57	20	334,0°	84,0°	2,9°	973
58	40	353,6°	78,7°	4,7°	388
59	20	5,0°	69,5°	3,4°	731
60	60	25,2°	80,4°	2,6°	1226
61	70	330,2°	74,6°	6,3°	213
62	30	336,0°	72,7°	1,8°	2650
63	50	354,6°	80,6°	6,6°	197
64	20	270,0°	85,9°	2,2°	1778
65	30	328,6°	75,0°	6,0°	231
66	30	342,2°	72,1°	1,3°	5304
67	30	323,2°	70,6°	2,4°	1425
68	30	319,5°	77,8°	2,9°	950
69	30	332,4°	79,4°	3,0°	892
70	30	323,4°	79,2°	2,2°	1676
71	30	312,3°	76,4°	2,4°	1503
72	30	317,2°	74,2°	3,3°	775
73	30	317,8°	76,7°	4,9°	346
74	30	325,9°	70,1°	5,1°	314

75	30	153,5°	-52,1°	14,0°	43
76	30	165,8°	-56,3°	4,5°	414
78	30	243,0°	84,9°	12,0°	57

After AF demagnetization, the magnetization directions of sites 48 and 51 are consistent at sample and site levels. Group Bmz7AF now forms, which includes directions from sites 48 and 51.

Group: Bmz7AF ; N = 32 ; D = 336,1° ; I = 82,0° ; $\alpha_{95} = 3,4^\circ$; k = 58

Although two additional sites are included in this group, it is not a significant improvement on group Bmz6. This is further reflected by the tendency of some sites to show weaker in-site grouping of magnetization directions after bulk AF demagnetization, which is apparent from smaller k values in Table XII. It is therefore uncertain at this stage whether the Briden SI (Briden, 1972) succeeded in locating primary magnetization components at the majority of sites.

Before such a statement can be accepted, however, the effect of the dip of the igneous layering on the obtained magnetization directions has to be evaluated. The magnetization directions corrected for the dip at each site are listed in Table XIII and plotted in Figure 51.

Table XIII. Magnetization directions of sites in the main zone, western Bushveld Complex, after bulk alternating field demagnetization, with the igneous layering in a horizontal position.

Site	Declination(D)	Inclination(I)
1	304,0°	81,7°
2	9,3°	73,6°
45	356,8°	74,4°
46	12,4°	71,0°
47	22,1°	68,5°
48	357,1°	46,9°
49	25,5°	74,5°
51	9,9°	75,5°
52	14,6°	55,2°

53	338,5°	77,4°
54	337,3°	73,3°
55	349,2°	80,4°
56	18,0°	57,3°
57	358,9°	59,7°
58	358,8°	68,8°
59	9,0°	61,7°
60	23,5°	75,4°
61	341,5°	71,0°
62	347,7°	67,7°
63	354,6°	80,6°
64	4,0°	75,9°
65	341,5°	71,7°
66	350,8°	68,2°
67	338,7°	67,0°
68	345,9°	73,4°
69	356,5°	73,7°
70	351,4°	75,0°
71	347,2°	72,9°
72	356,3°	67,0°
73	351,2°	72,4°
74	347,9°	65,5°
75	178,5°	-49,9°
76	191,4°	-49,7°
78	359,7°	72,2°

If all the magnetization directions with positive inclinations are grouped together, group Bmz7AFR is formed:

Group: Bmz7AFR ; N = 32 ; D = 357,8° ; I = 70,9° ; $\alpha_{95} = 2,8^\circ$; k = 80

which is the equivalent of group Bmz7AF corrected for the dip of igneous layering. Although the value of k has increased from 58 (before correction for dip) to 80 (after correction for dip), the improvement is not significant at confidence limits as low as 90 per cent, using the criterion of McElhinny (1964b). This result then supports the conclusion that the Briden SI (Briden, 1972) failed in the

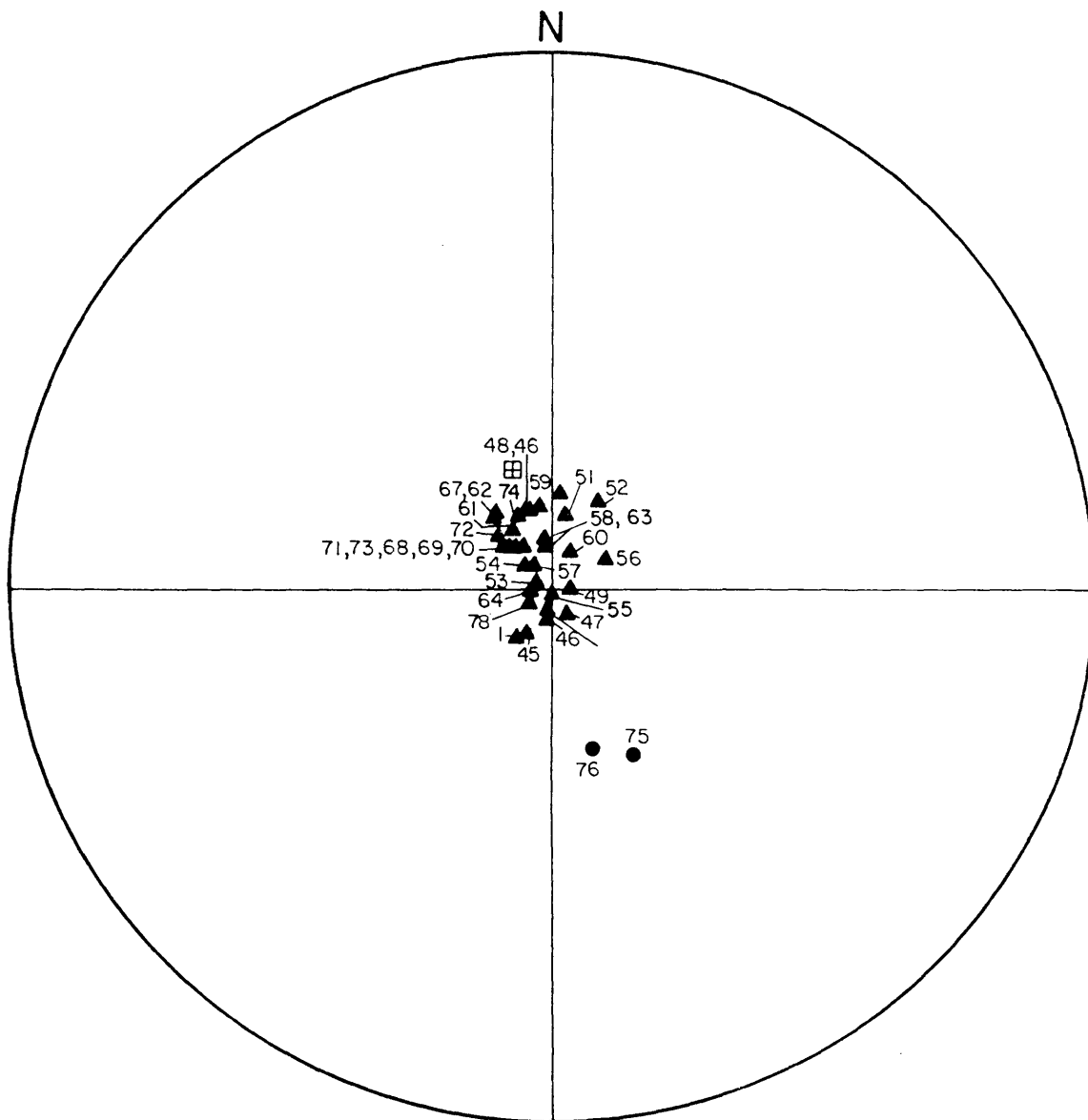


Fig. 50 Magnetization directions from sites in the main zone, western Bushveld Complex, after bulk AF demagnetization. Plotting convention as in Fig. 5.

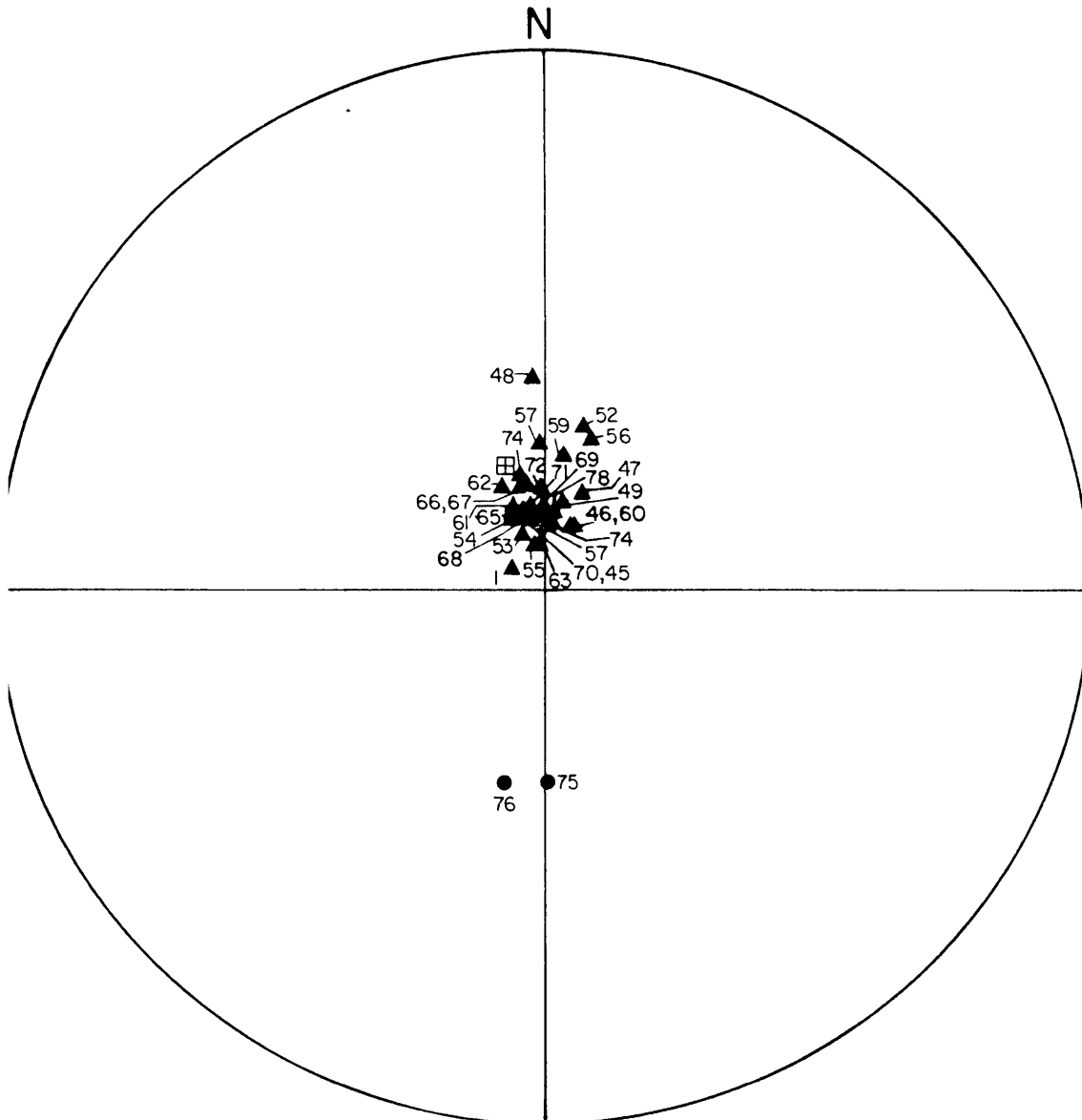


Fig. 51 Magnetization directions from sites in the main zone of the western Bushveld Complex after bulk AF demagnetization, with the igneous layering in a horizontal position. Plotting convention as in Fig. 5.

majority of cases to locate a primary magnetization direction.

The above conclusion does not hold true for sites 75 and 76, the only two sites where the magnetization directions are normal. Figures 48 to 51 show that these two directions grouped closer together after bulk AF demagnetization, but it is not certain whether the rotation of the igneous layering to the horizontal, has resulted in a significantly improved grouping of these two directions.

D. Stepwise alternating field demagnetization of pilot specimens.

During stepwise AF demagnetization of specimens at progressively higher AF values, magnetization directions from virtually all the sites in group Bmz7AF exhibited a slow change in direction. At low AF values the magnetization vectors remain stable with very little movement, but at AF values higher than approximately 40 mT the directions start to change, with the directional change becoming larger as the AF values increase. This type of response is illustrated in Figure 52 with the aid of specimens from sites 56 and 62.

From Figure 52 it is further evident that the magnetization direction of specimen 56/1B describes a circle of remagnetization during stepwise AF demagnetization, which indicates that two magnetization components are removed. Specimen 62/3C, however, exhibits a much more complex response, from which it can be concluded that the NRM of this specimen consists of more than two components. Perhaps more important is the fact that the magnetization directions in Figure 52 diverge from each other during progressive stepwise AF demagnetization. From this, and from Figures 53 and 54 it must be concluded that the magnetization directions in groups Bmz6 and Bmz7AFR are not primary magnetization directions, but rather resultant magnetization directions due to primary and secondary magnetization.

On the basis of the behaviour of specimens during stepwise AF demagnetization, the sites from group Bmz7AF have divided into two groups. Group A contains sites where the NRM consists essentially of two components, viz. a medium to high coercivity component and a more stable high coercivity component. There are seventeen sites in this group.

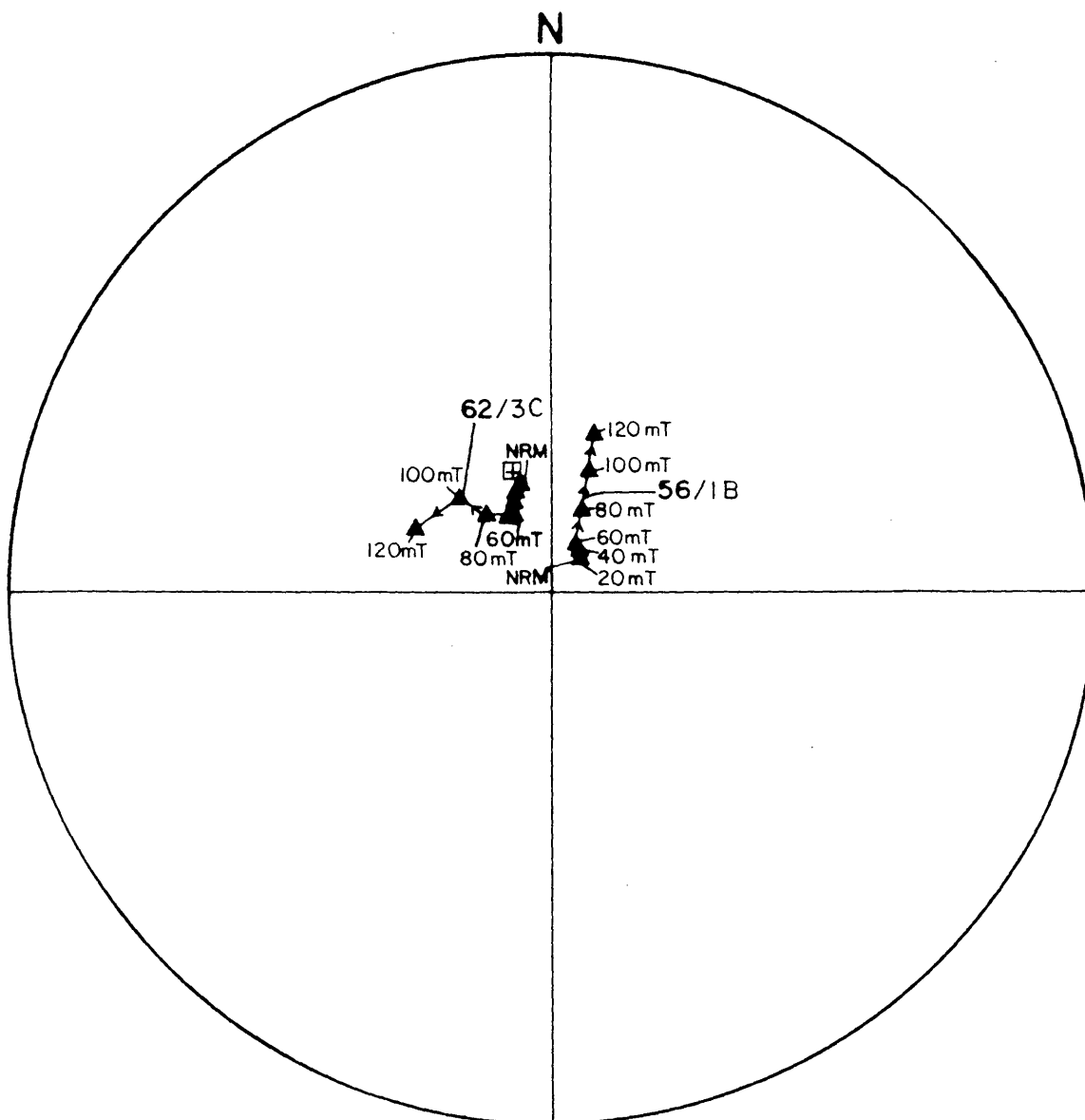


Fig. 52 The directional response of two specimens from sites 56 and 62 to stepwise AF demagnetization. Plotting convention as in Fig. 5.

The second group, group B, consists of fifteen sites, exhibiting a response to stepwise AF demagnetization, which indicates that the NRM of the specimens consists of more than two components.

The magnetization of group A can now be studied further. If the primary and secondary magnetization components of the sites in group A were acquired at different time intervals, but all the elements of the primary component simultaneously, and all the elements of the secondary component simultaneously, with the dip of the igneous layering in its present orientation, one would expect the circles of remagnetization of all the sites in group A to coincide. In Figure 53 the remagnetization circles of 4 sites in group A are shown. These results indicate that the circles intersect and are not coincidental. Similarly, if both magnetization components had been acquired with the igneous layering in a horizontal position, one would expect the circles of remagnetization, corrected for the dip of the layering, to be roughly coincidental. This is not the case (Fig. 54).

The last possibility, that one component was acquired with the igneous layering in a horizontal position and the other with the layering in its present attitude, would require, that wherever the dip and dip directions at two sites are similar, the respective circles of remagnetization should be coincidental. In Figure 53 the remagnetization circles of sites 56 and 57, clearly intersect and have very different orientations, despite the fact that at these two sites, the igneous layering has the same dip value, with the dip directions differing by only 10° . Conversely, the remagnetization circles for sites 57 and 67, have very similar orientations (Fig. 53), although the dip of the igneous layering at the two sites differs by 18° and the dip direction by 25° . These examples indicate that there is no obvious relation between the positions of the circles of remagnetization and the dip and dip directions of the igneous layering at each site.

The magnetization component responsible for the grouping of the magnetization vectors into group Bmz7AFR, dominates the magnetic characteristics of the specimens and this primary magnetization component almost certainly was acquired by all the specimens at more or less the same time. With this and the previous arguments on the effect of the dip of the igneous layering in mind, only one plausible explanation for the diverging circles of remagnetization can be

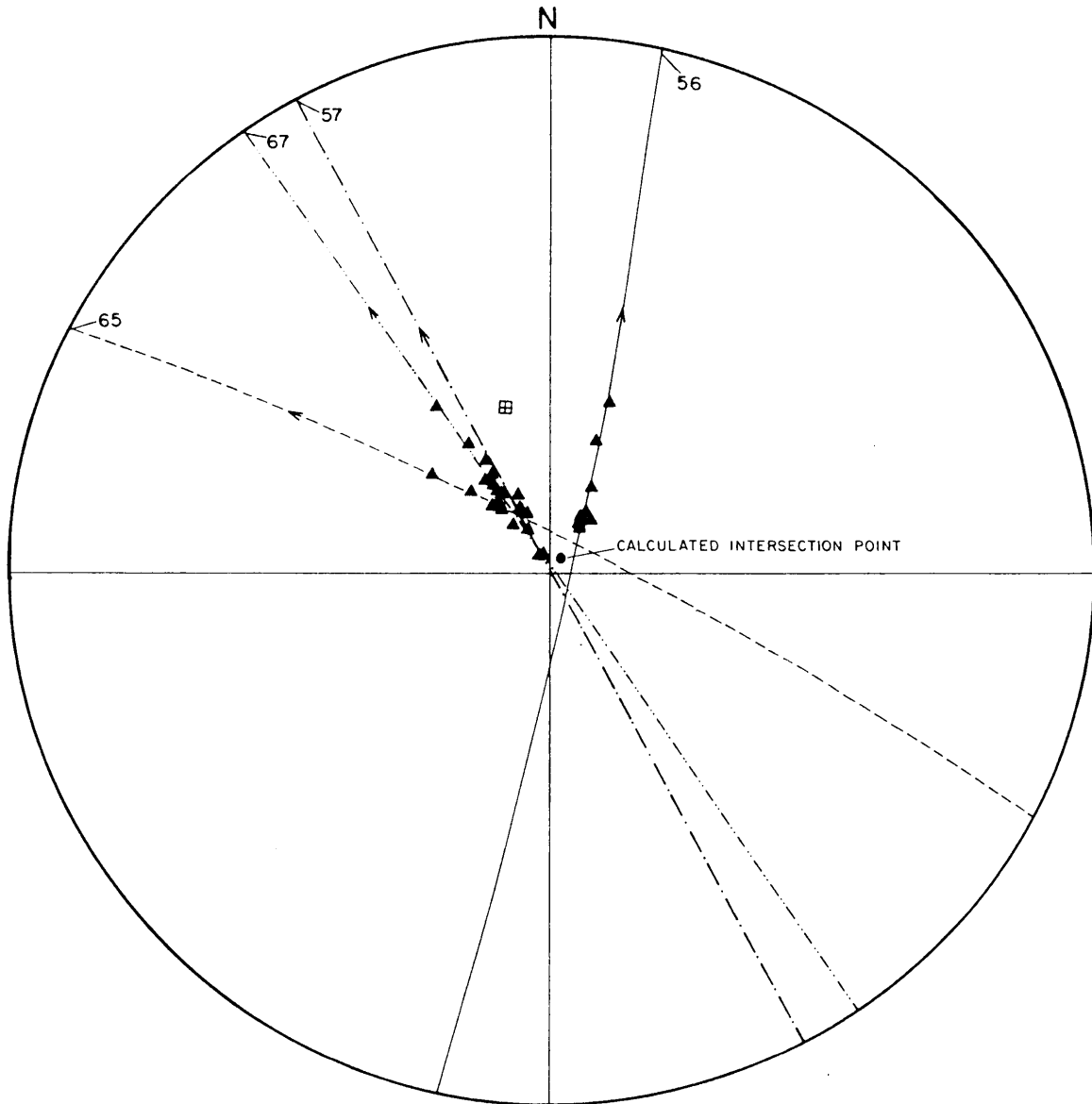


Fig. 53 The directional response of four specimens from sites 56, 57, 65 and 67 to stepwise AF demagnetization. Solid lines represent circles of remagnetization fitted to the respective data sets. Plotting convention as in Fig. 5.

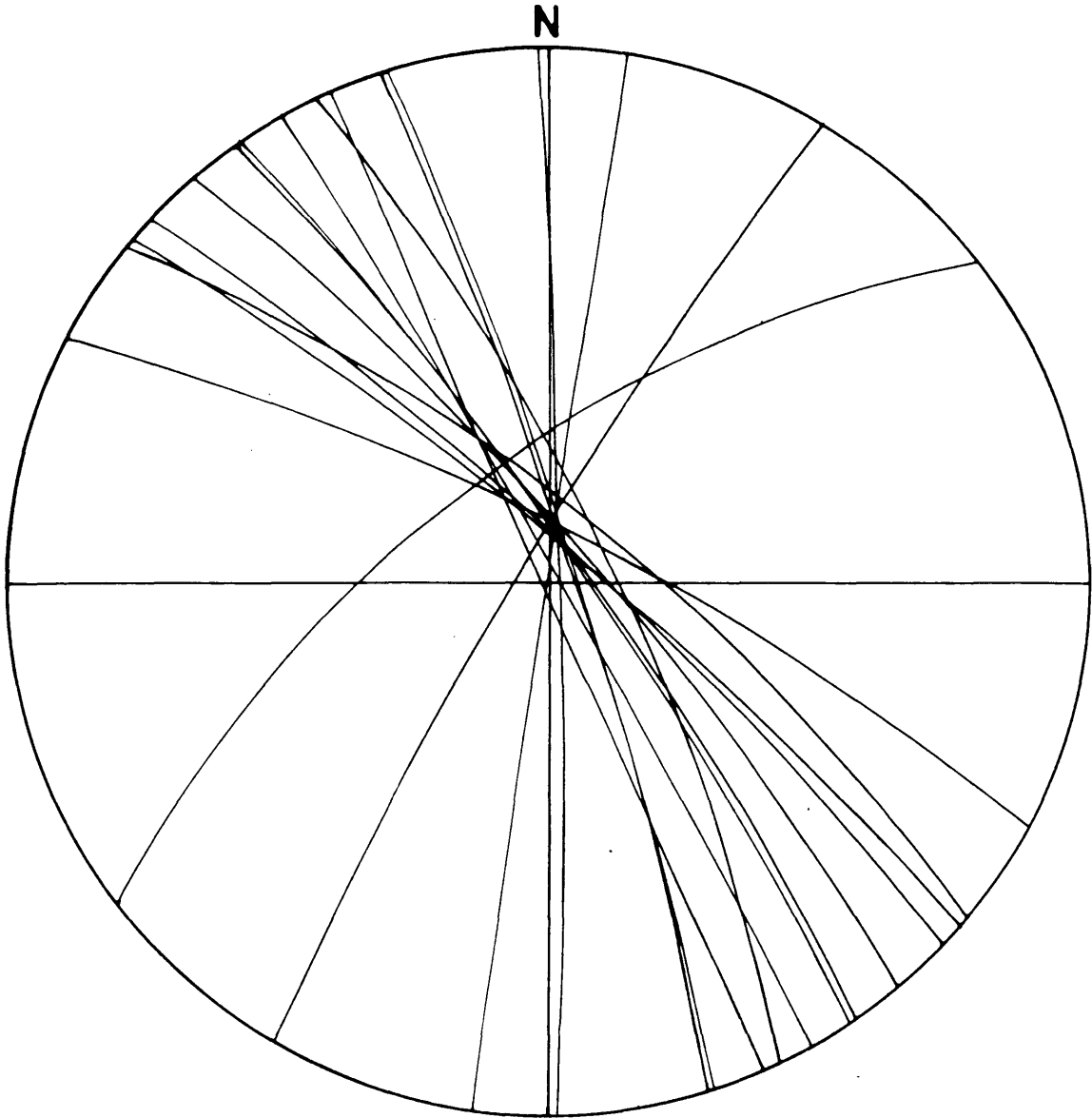


Fig. 54 Circles of remagnetization fitted to the stepwise AF demagnetization data (corrected for the dip of the igneous layering) from one specimen of each site in group A. Remagnetization circles are shown only on the lower hemisphere of the stereographic projection.

postulated, namely that the secondary, more stable magnetization component was acquired at a different time at each site, resulting in a different direction of secondary magnetization for each site. It must, however, be emphasized that this explanation is heavily dependent on the accuracy of the dip and dip direction values used to rotate the igneous layering to a horizontal position.

The direction of the primary magnetization vector can possibly be recovered by the use of intersecting remagnetization circles, following the technique of Halls (1978). To do this, a number of assumptions are made:

- i) The primary magnetization component was acquired with the igneous layering in a horizontal position.
- ii) The primary magnetization component has a lower coercivity than the secondary magnetization components.
- iii) Sets of remagnetization circles will always define more than one intersection point on a sphere, but in this particular case, the correct intersection point yielding the direction of the primary magnetization component, will be the point from which the magnetization vectors diverge during stepwise AF demagnetization.

Circles of remagnetization (great circles) were fitted with a least squares technique (Halls, 1976) to data corrected for dip, obtained from one specimen from each site in group A during stepwise AF demagnetization. The remagnetization circles are shown in Figure 54 and the calculated intersection point yields the direction of the primary magnetization vector with $D = 354,7^\circ$ and $I = +72,0^\circ$. This direction does not differ much from the mean direction of group Bmz7AFR, but it is corrected for the effect of the secondary magnetization components.

Difference vectors, corrected for the dip of the igneous layering, representing the removed vector between each successive AF demagnetization step, are plotted in Figure 55 for four sites from group A. From this it appears that the assumption that there are only two magnetization components present in the specimens, is not correct. At very low

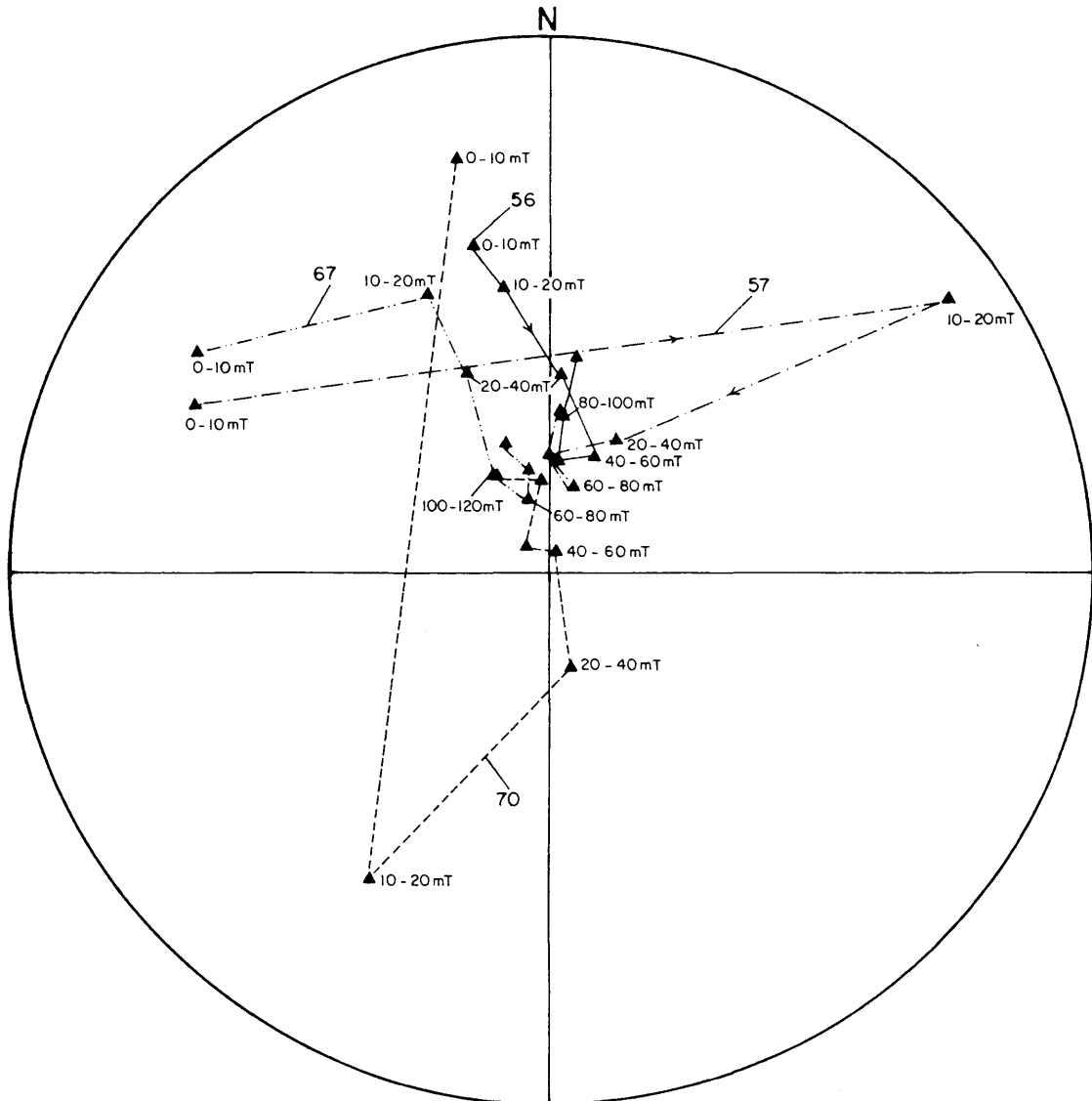


Fig. 55 Difference vectors, removed between successive AF demagnetization steps, are shown for sites 56, 57, 67 and 70. Plotting convention as in Fig. 5.

AF values the vectors removed are different for each site; thereafter, at progressively higher AF values, the difference vectors converge rapidly to a direction which agrees with the mean magnetization direction given by group Bmz7AFR. At still higher AF values, the difference vectors then move very rapidly away from this position, each in its own direction, along circles of remagnetization. This pattern of change in direction by the difference vectors at the intersection point, is similar to examples presented by Hoffman and Day (1978). According to them, this pattern indicates the existence of three magnetization components in the specimens, with marginal overlapping of the respective coercivity spectra. Furthermore, at the position where the difference vectors converge and sharply change direction, only one magnetization component has been removed. These positions in Figure 55 were grouped together and yield the following group statistics:

Group: Bmz8AFR ; N = 4 ; D = 357,1° ; I = 69° ; $\alpha_{95} = 5,8^\circ$; k = 248

and again this mean direction differs very little from that of group Bmz7AFR.

The existence of a third magnetization component in these specimens does not invalidate the previous results obtained with intersecting circles of remagnetization. This is because the third component is very small at the low end of the coercivity spectrum, removed with an AF value of only 10 to 20 mT. In all possibility, as can be seen in Figure 55, this component can be regarded as a VRM acquired by the specimens at various stages during their geological past.

Difference vectors of specimens from sites belonging to group B which were initially recognized as having more than two magnetization components, are shown (uncorrected for dip) in Figure 56. The patterns these vectors display are more complex than the previous set and do not exhibit the tendency to describe parts of remagnetization circles. This indicates the truly multicomponent nature of the NRM and that the coercivity spectra of these components overlap. One aspect in common with the difference vectors of group A, is the convergence of the vectors at intermediate

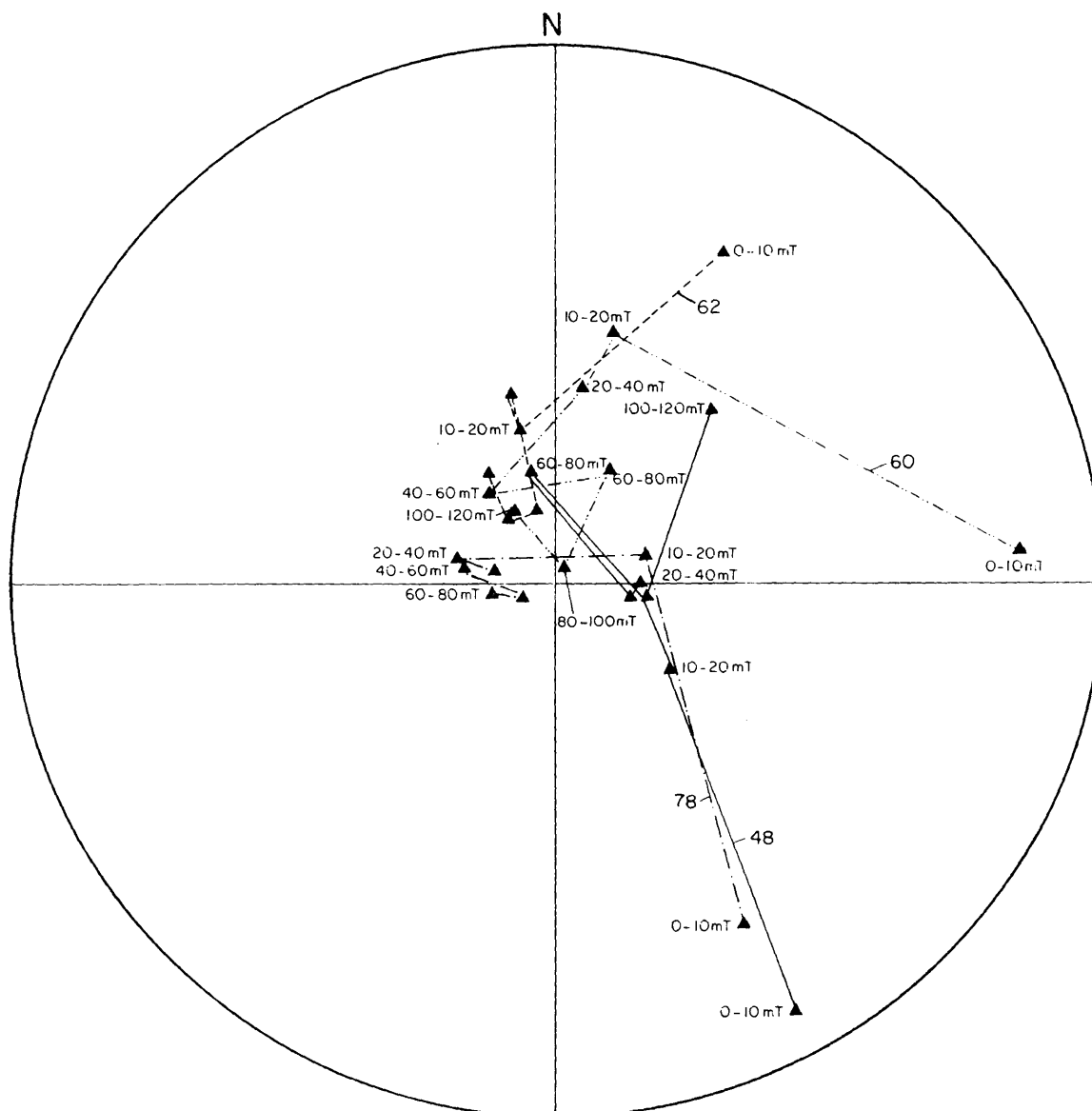


Fig. 56 Difference vectors, removed between successive AF de-magnetization steps, from specimens of sites where the NRM was recognized to consist of more than two magnetization components. Plotting convention as in Fig. 5.

AF values, although this is not readily seen in Figure 56, because the difference vectors have not been corrected for the dip of the igneous layering at each site. This convergence point is expected to be similar to the mean direction of group Bmz7AF, but due to the complex nature of the change pattern making the determination of primary directions even less reliable, no attempt was made to calculate the mean position of these convergence points.

From these analyses it is clear that the NRM directions of sites are in effect resultant magnetization directions, but that the resultant directions differ very little from the primary magnetization direction, because all the secondary components are small compared to the primary magnetization component. Furthermore, all directions obtained for the primary magnetization component with the previous methods, fall within the circle of 95 per cent confidence of group Bmz7AFR; consequently, the mean direction of this group is acceptable as that of the primary magnetization vector.

A characteristic of all the specimens from sites in group Bmz7AFR, is the "hardness" of the magnetization, manifested by the fact that after demagnetization in an AF of 120 mT, 10 to 20 per cent of the magnetization remains (Fig. 57). This is similar to the behaviour of specimens from certain parts of the main zone in the eastern Bushveld Complex (Chapter VI).

Specimens from sites 75 and 76, which are normally magnetized, have a mean NRM intensity of $4,5 \times 10^{-3} \text{ Am}^{-1}$. This made the results from stepwise AF demagnetization less reliable, but in Figure 58 the directional response of two specimens from these sites, displays a tendency to converge during AF demagnetization. The approximate convergence zone in Figure 58 is roughly antipodal to the mean magnetization direction of group Bmz7AF. There is little doubt that the two magnetization directions from sites 75 and 76, obtained by bulk AF demagnetization, do represent a stable and consistent magnetization component.

E. Thermal demagnetization

The directional response of the NRM vector of specimens from group Bmz6 to continuous thermal demagnetization (Fig. 59) is similar to the

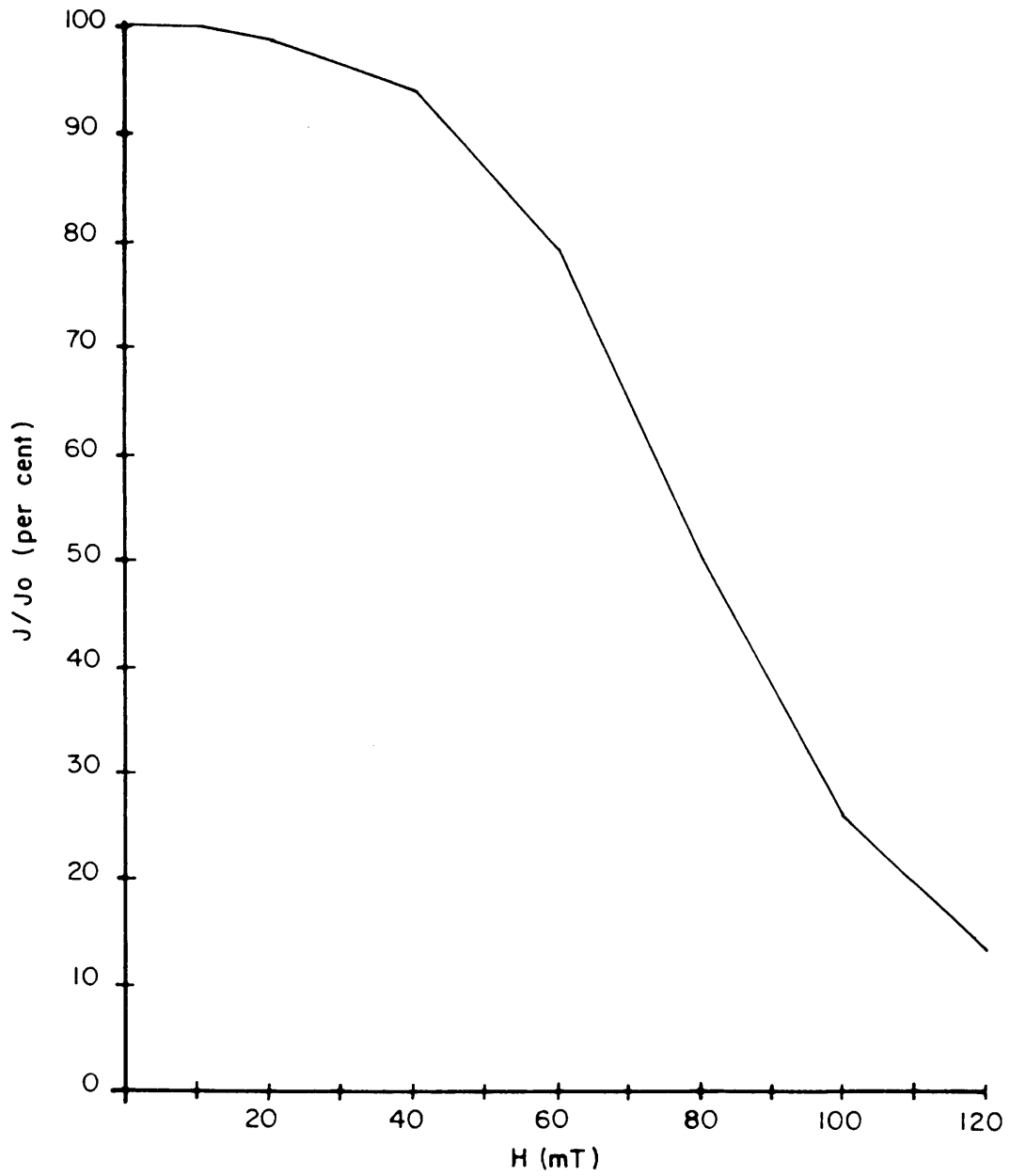


Fig. 57 Normalized intensity response curve to stepwise AF demagnetization of specimen 57/4B.

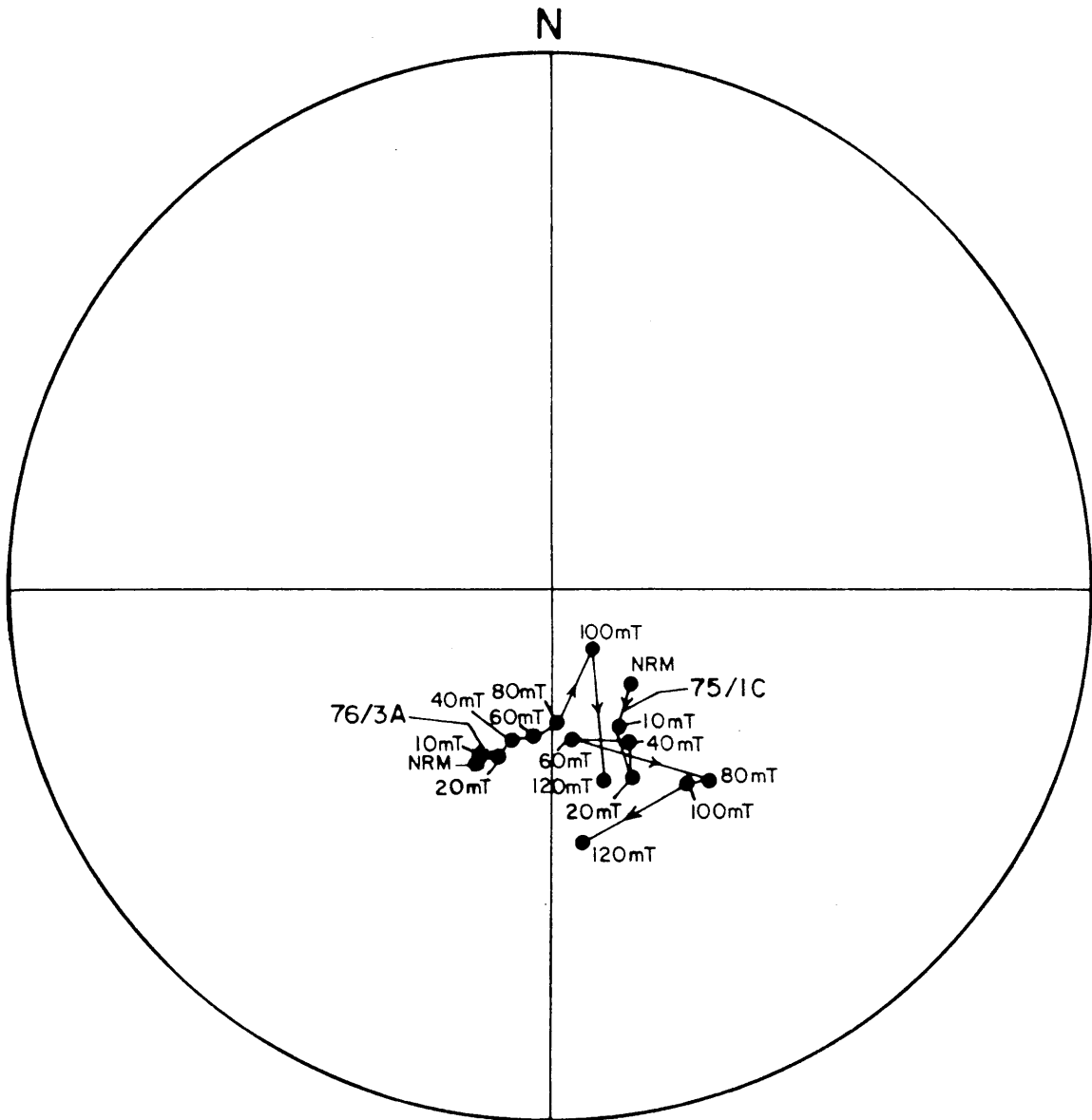


Fig. 58 Directional response of magnetization vectors from specimens 76/3A and 75/1C to stepwise AF demagnetization. Plotting convention as in Fig. 5.

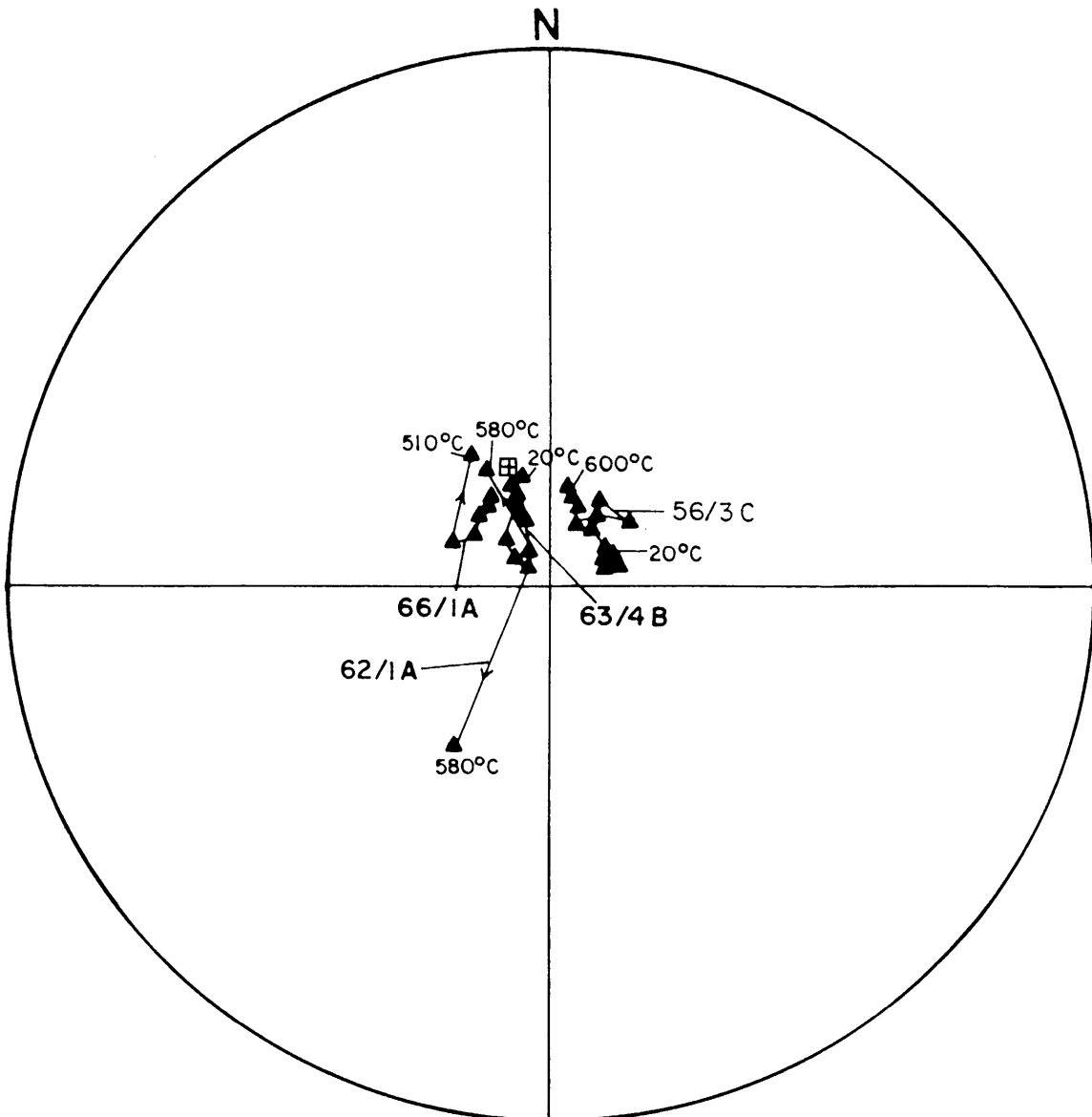


Fig. 59 Directional response of magnetization vectors from specimens 56/3C, 66/1A, 63/4B and 62/1A, to continuous thermal demagnetization.

response to AF demagnetization. At low temperatures the magnetization directions remain virtually constant, but at higher temperatures the magnetization directions start to change, with the change becoming larger at high temperatures. The vectors do not describe remagnetization circles as in some instances during AF demagnetization but, as during AF demagnetization, the directions diverge more and more as the demagnetization process proceeds. From this it appears as if, again, there are mainly only two magnetization components. The dominant primary magnetization is removed at slightly lower temperatures than the smaller secondary component, which is possibly different for each site.

A typical normalized thermal intensity response curve of a specimen from group Bmz6, is shown in Figure 60. The curve shows a thermally distributed blocking temperature spectrum, but at temperatures higher than 500°C, two separate Curie points are evident. The lower of these, at approximately 575°C, indicates magnetite as the source of remanent magnetization, while the higher Curie point in the region of 600°C, possibly indicates haematite (McElhinny, 1973) as the source of the magnetization. Apart from the low coercivity VRM's this site was one regarded, on the basis of AF demagnetization, as having only a primary and a secondary magnetization component. Evidence from the intensity response curve (Fig. 60) suggests that the sources of these magnetization components are two separate mineralogical phases.

The main secondary magnetization component(s) is apparently more stable than the primary magnetization in terms of coercivity and blocking temperatures. If it is accepted that the secondary component at each site differed and was acquired at different time intervals, chemical remanent magnetization (CRM) must be considered as a possible cause. This is in accordance with the view of Merrill (1975), that CRM can often be more stable than a TRM. He further states that where the CRM is the more stable component, the demagnetization will change the directions from the primary to the secondary rather than the reverse as is often assumed.

Thermal demagnetization of specimens from sites 75 and 76 (negative inclinations), could not be carried out due to the low intensity of the magnetization of these specimens.

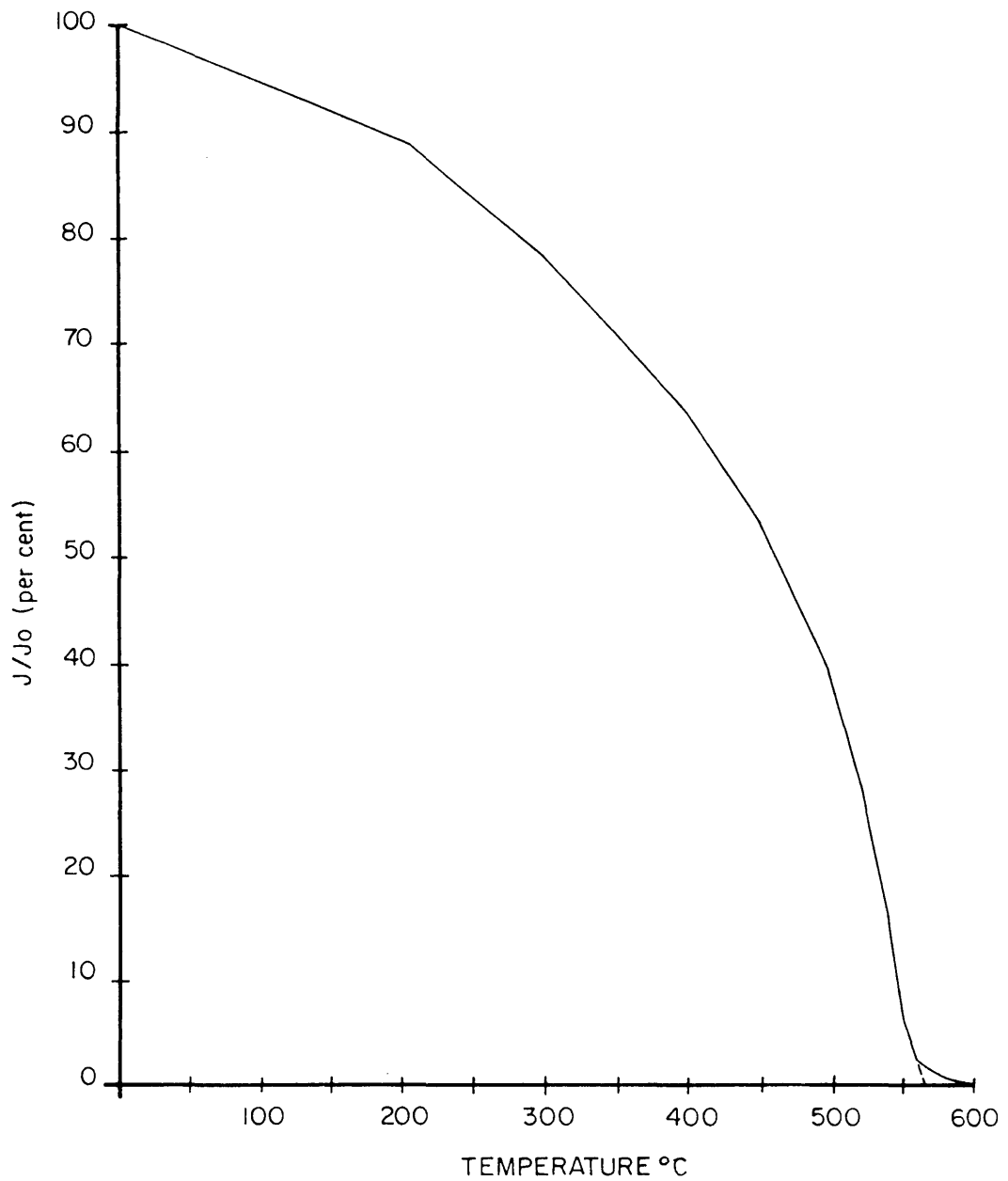


Fig. 60 Normalized intensity response curve of specimen 56/3D during continuous thermal demagnetization.

F. Mineralogy of opaque minerals

All the specimens from sites with reversed magnetization directions (positive inclinations, group Bmz7AF) contain similar opaque minerals. Magnetite occurs as lamellae in both the pyroxene and plagioclase crystals (Figs. 61 and 62) similar to the magnetite in specimens from the main zone in the eastern Bushveld Complex (see discussion Chapter VI, Section E). Magnetite lamellae seem to be less abundant in specimens from the western Bushveld Complex. It must be concluded that the lower Curie point of 575°C, observed for these specimens, can be attributed to these magnetite lamellae. Discrete magnetite grains, although they do occur in the specimens, are very rare.

Ilmenite generally occurs as discrete grains with diameters up to 0,1 mm. These grains commonly exhibit haematite exsolution lamellae (Fig. 63). No other haematite is present in the specimens and the second observed Curie temperature of approximately 600°C, could be the result of these exsolution lamellae in the ilmenite.

Sulphide grains occur commonly, but are less abundant than the ilmenite grains. Some of the sulphide grains were identified as pyrrhotite.

The opaque mineralogy of sites 75 and 76, differs considerably from that described for sites in group Bmz7AFR. No magnetite grains could be found in either pyroxene or plagioclase crystals and it is noteworthy that the intensity of the NRM of these specimens is two orders of magnitude less than the intensity of NRM of specimens from sites in group Bmz7AFR. Small discrete magnetite grains do occur in these specimens, but are very rare.

A similarity of the opaque minerals in these specimens with respect to specimens from sites in group Bmz7AFR, is the occurrence of ilmenite grains with haematite exsolution lamellae. Although no Curie point could be obtained for these specimens due to the low intensity of magnetization, it can be expected that the haematite lamellae contribute to the remanent magnetization of specimens. Sulphide grains are present in these specimens, some of which have again been identified as pyrrhotite, but the relative abundance is much less than in specimens from other sites.

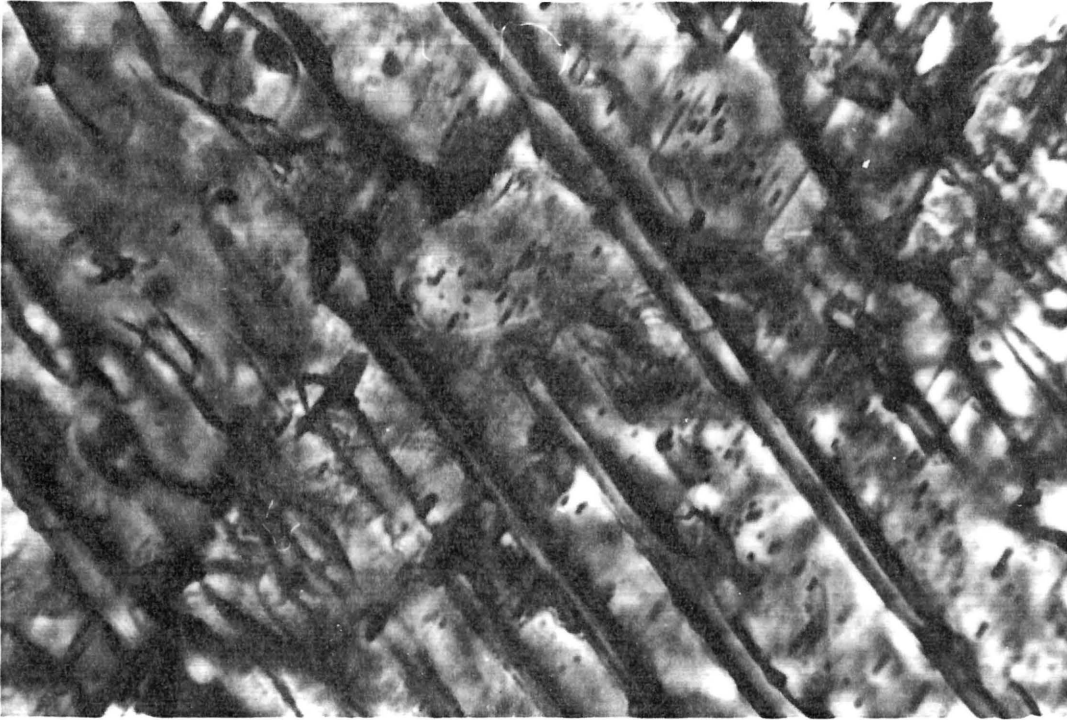


Fig. 61 Magnetite lamellae in a pyroxene crystal, main zone, western Bushveld Complex. Transmitted light, magnification 870X.

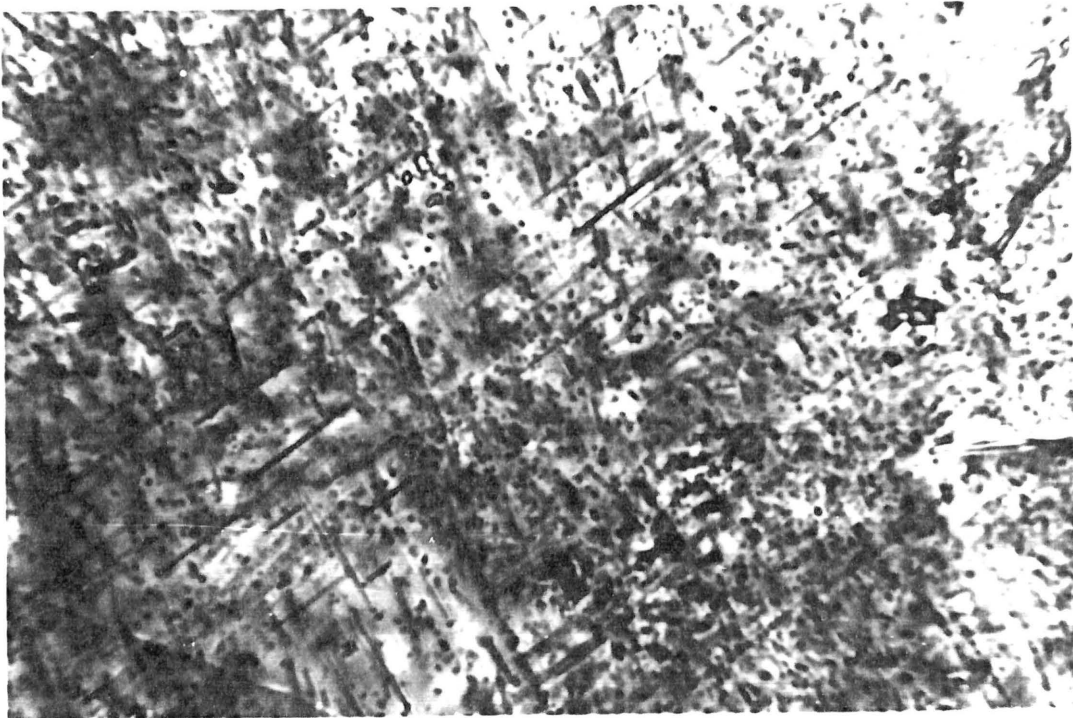


Fig. 62 Magnetite lamellae in a plagioclase crystal, main zone, western Bushveld Complex. Transmitted light, magnification 870X.

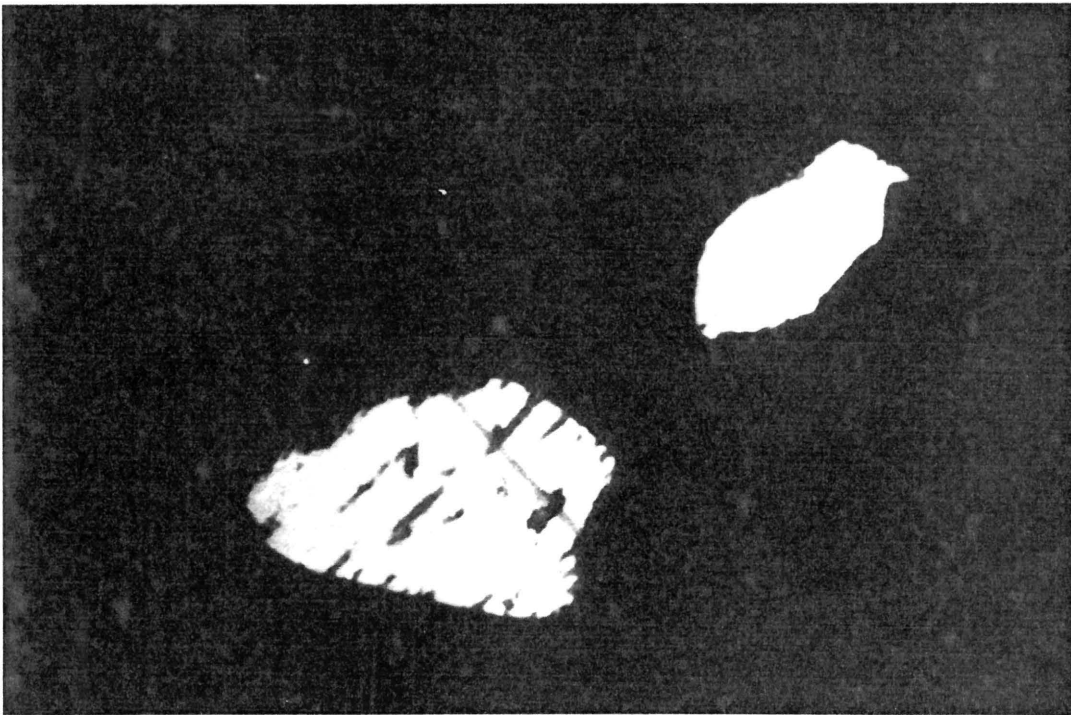


Fig. 63 Ilmenite grains with haematite exsolution lamellae, main zone, western Bushveld Complex. Reflected light, magnification 1800X.

G. Haematite as carrier of the more stable secondary magnetization.

If it were to be assumed that the haematite lamellae are the carriers of the more stable secondary remanent magnetization, it becomes very difficult to explain why the secondary component at each site is apparently different (Section D). According to Haggerty (1976) haematite lamellae in ilmenite reflect oxidation of the magma at high temperatures. McElhinny (1973) estimated the temperature of exsolution to be 900°C, although this also depends on the composition of the ilmenite solid solution. The high exsolution temperature compared to the temperature of acquisition of a TRM at 680° (Curie temperature of haematite, McElhinny, 1973) makes it very unlikely that the haematite could have acquired a different direction of TRM at each site. This is supported by the conclusion that the Curie isotherm of magnetite seems to have moved very rapidly through the main zone in the eastern Bushveld Complex (see Chapter VI, Section B).

There is a remote possibility that a geomagnetic field reversal could have occurred between the acquisition of the two TRM's. A further possibility is that the secondary magnetization directions are the result of a self-reversal of magnetization resulting from a mechanism operating in the haemo-ilmenite grains. Neither of these possibilities can, however, readily explain the apparent difference of the more stable secondary magnetization components between sites.

The haematite can only be the carrier of the secondary magnetization component if one assumes that the dip values and dip directions used to rotate the layering to the horizontal, are in error. To test this possibility dip values and dip directions for sites 56, 57, 65, and 74 were calculated so that the magnetization direction of these sites would, if subjected to a fold test, be within the circle of 95 per cent confidence of the mean direction of group Bmz7AFR. These calculated values, as well as the values measured in the field, are listed in Table XIV.

Table XIV. Measured and calculated dip and dip directions of the igneous layering at four sites in the main zone, western Bushveld Complex assuming a constant direction of secondary magnetization.

Values measured in the field			Values calculated	
Site	Dip	Dip Direction	Dip	Dip Direction
56	25°	N355°	15°	N332°
57	25°	N 05°	17°	N 03°
65	5°	N 25°	13°	N 55°
74	10°	N 40°	10°	N 70°

Although the calculated dip values and dip directions differ from those measured in the field, it can be seen on Figure 1 and on regional maps of the Bushveld Complex (e.g. Hunter, 1975b), that the calculated values are still compatible with the regional dip and strike of the layered sequence at these sites. The calculated values were then used to adjust the stepwise AF demagnetization data of specimens from these four sites. In Figure 64 the resultant vectors at each AF demagnetization step, before and after correction for dip in accordance with the calculated values, are shown for the four specimens listed in Table XIV. The corrected vectors lie roughly on a single remagnetization circle. A remagnetization circle was then fitted with a least squares technique (Halls, 1976) to the corrected magnetization vectors and the part of this circle on the lower hemisphere of the stereographic projection is also shown in Figure 64.

The tendency for the corrected vectors in Figure 64 to lie on a single remagnetization circle, does not prove that the dip values and dip directions measured in the field are faulty, or that the haematite is the carrier of the more stable secondary magnetization component. It does not, however, exclude the possibility that the field measured dip values and dip directions are incorrect, which would further imply that haematite may be the carrier of the secondary magnetization component.

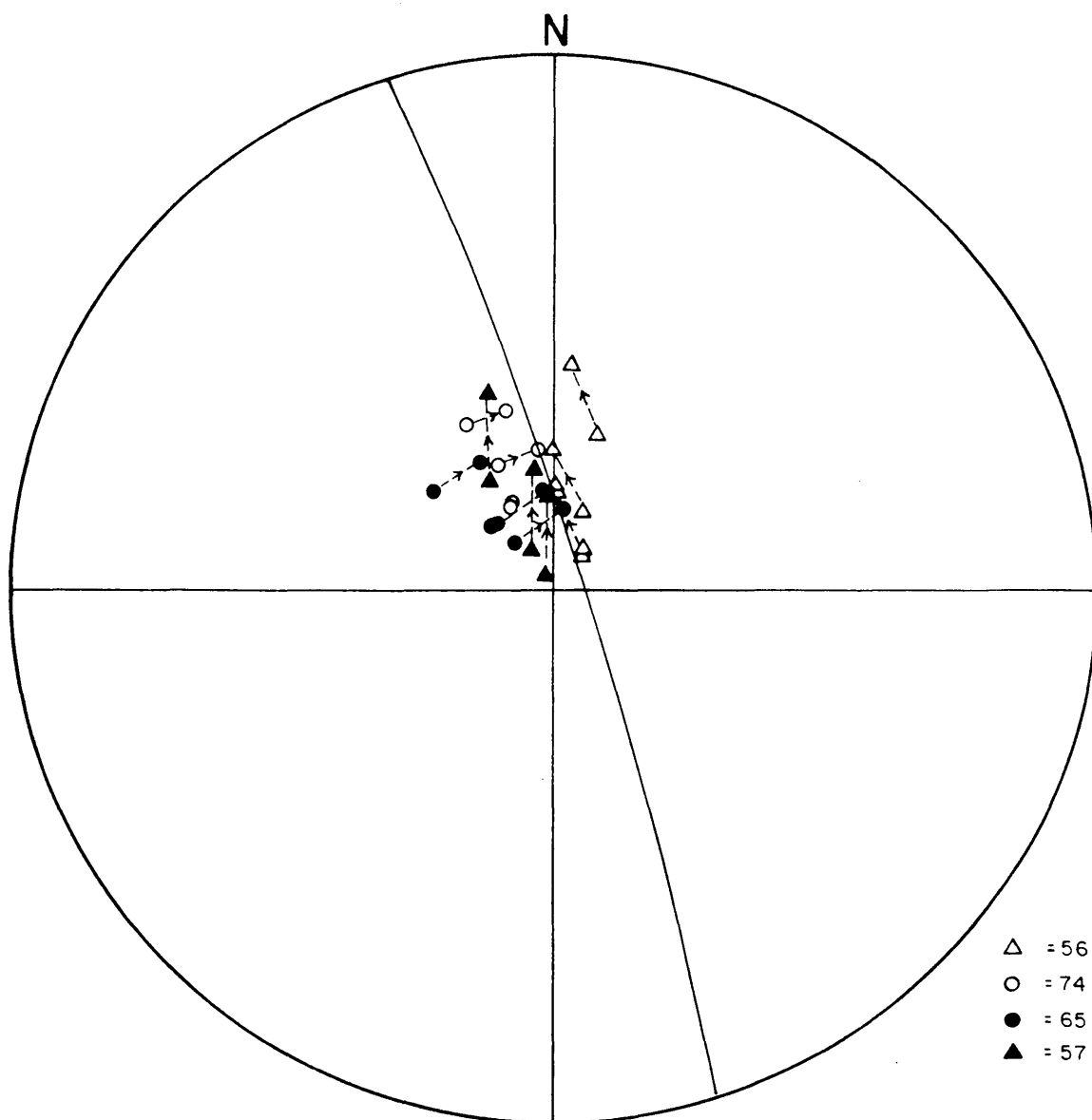


Fig. 64 The directional response of magnetization vectors to AF demagnetization of four specimens, before and after the igneous layering has been rotated to the horizontal. The arrows indicate the direction of movement of the vectors during rotation. The re-magnetization circle shown is the best fit to all the magnetization vectors with the igneous layering in a horizontal position. Only the part of the circle on the lower hemisphere is shown. All symbols represent directions with positive inclinations.

It is of interest to note that, if the circle of remagnetization (Fig. 64) is drawn on both the lower and upper hemispheres the normal magnetization directions of sites 75 and 76 lie in close proximity to this circle of remagnetization (Fig. 65). If the haematite lamellae in the ilmenite of specimens from these two sites are the main carriers of a remanent magnetization (reversed with respect to group Bmz7AFR) acquired more or less during the same time at which all the other sites acquired their magnetization, then one would expect the two magnetization directions of sites 75 and 76 to lie, if not on, then very near to this circle of remagnetization. Furthermore, the magnetization would have had to be acquired through a self-reversal mechanism in the haemo-ilmenite grains, rather than prior to a geomagnetic field reversal, in order to explain the presence of a reversed (with respect to group Bmz7AFR) secondary magnetization component in all the other sites in the main zone.

From the previous arguments, although based on very little evidence, one must concede that it is possible for the haematite exsolution lamellae in the ilmenite grains to be the carriers of a high stability, self-reversed magnetization component in all the specimens from sites in the main zone of the western Bushveld Complex.

H. Summary of results

Fold tests (Graham, 1949) applied to palaeomagnetic directions from the main zone in the western Bushveld Complex, yield results indicating that the main zone possibly acquired its present dip after cooling to temperatures below the Curie points of the respective ferromagnetic components.

The NRM of the main zone comprises a number of magnetization components, but the primary magnetization dominates over the small secondary components to such an extent, that when corrections for these secondary components are applied the mean magnetization direction does not change substantially. This mean magnetization (corrected for the dip of the igneous layering) of the main zone in the western Bushveld Complex is as follows:

Group: Bmz7AFR ; N = 32 ; D = 357,8° ; I = 70,9° ; $\alpha_{95} = 2,8^\circ$; k = 80

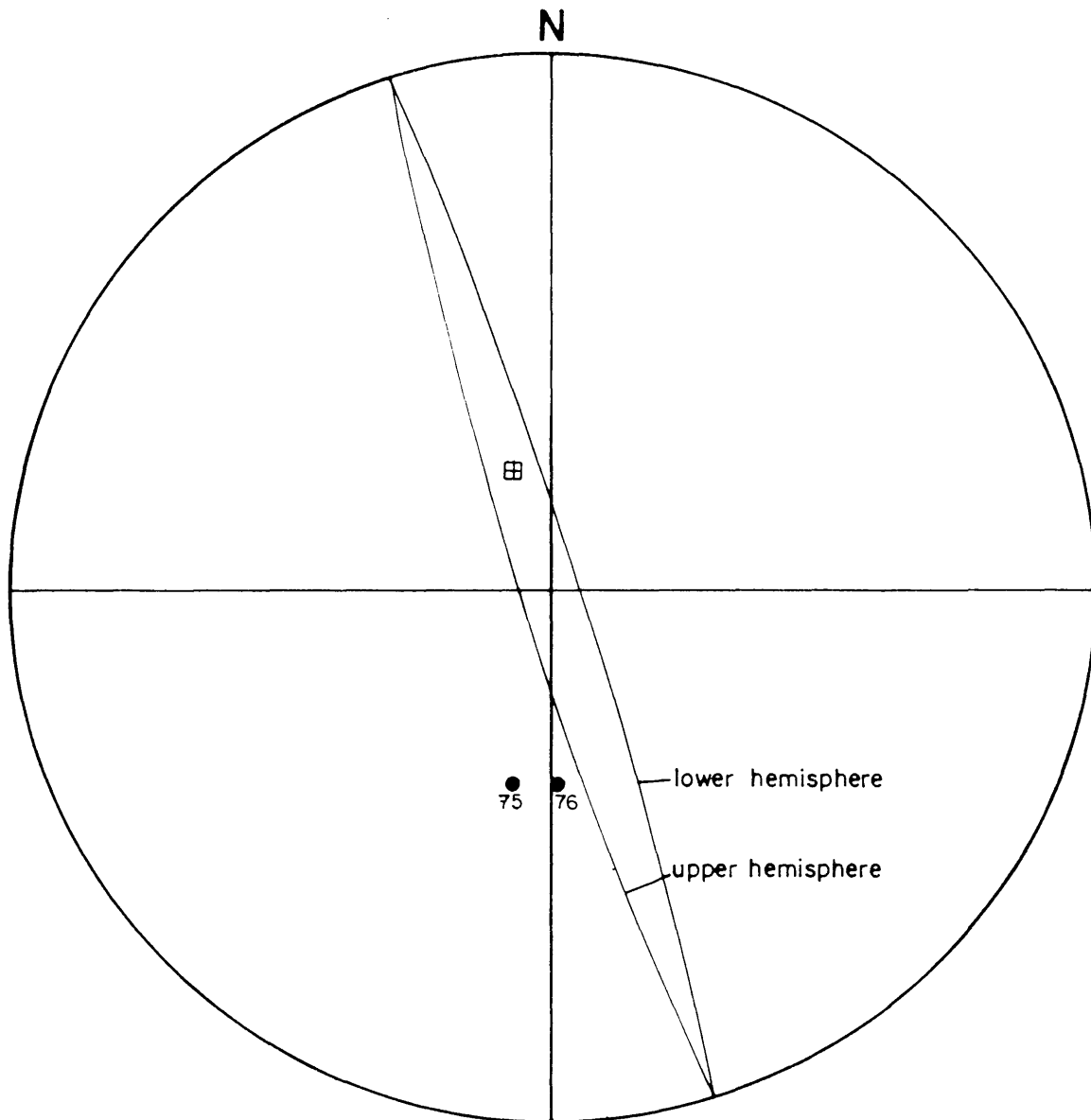


Fig. 65 Magnetization directions of sites 75 and 76 after bulk AF demagnetization. The same circle of remagnetization as in Fig. 64 is shown on both hemispheres of the stereographic projection. Plotting convention as in Fig. 5.

with corresponding palaeomagnetic pole position:

latitude : 9,2°N

longitude : 27,3°E

and polar error (dp,dm) and 4,9° respectively

Magnetization directions from two sites in the lower part of the main zone have a different polarity and are approximately antipodal to the mean direction of group Bmz7AFR. Although these directions have not been incorporated into group Bmz7AFR, one must conclude that the mean magnetization of the main zone in the western Bushveld has a mixed polarity.

The main secondary magnetization component from sites in group Bmz7AFR is more stable than the primary magnetization component and is either due to CRM acquired at different time intervals at each site, or is due to TRM acquired by haematite lamellae present in ilmenite grains. The microscopic evidence and thermal demagnetization data favour the latter origin, which, if correct, will also explain the opposing polarity to group Bmz7AFR, exhibited by two sites in the main zone.

VIII THE PALAEOMAGNETISM OF THE UPPER ZONE

A. Introduction

Nine sampling sites are situated in the upper zone of the layered sequence. Of these, three sites are in quarries, two in road cuttings and the remainder are situated in streambeds. The distribution (Fig. 1) and the relatively few sampling sites, compared with other zones of the layered sequence covered in this study, reflect the general absence of suitable sampling sites in the upper zone.

Consistent magnetization directions were obtained from seven sites. Data from one site had to be rejected due to an error in the orientation of the core samples in the field.

No previous palaeomagnetic work has been done on the upper zone. The study of Gough and Van Niekerk (1959) was confined to the main zone of the layered sequence.

B. Natural remanent magnetization

The average intensity of the NRM of specimens from the upper zone is $6070 \times 10^{-3} \text{ Am}^{-1}$. Although this is lower than that of specimens from the main zone in the eastern Bushveld Complex (Chapter VI, Section B), the range of intensities is remarkably broad and specimens with intensities as high as $41\,000 \times 10^{-3} \text{ Am}^{-1}$ and as low as $800 \times 10^{-3} \text{ Am}^{-1}$ were measured (Fig. 66).

The NRM directions of seven sites were consistent at sample level, but there is no consistency of directions between sites. In Table XV the mean NRM directions of these sites with the relevant statistics for each site are listed, and these NRM directions are stereographically presented in Figure 67.

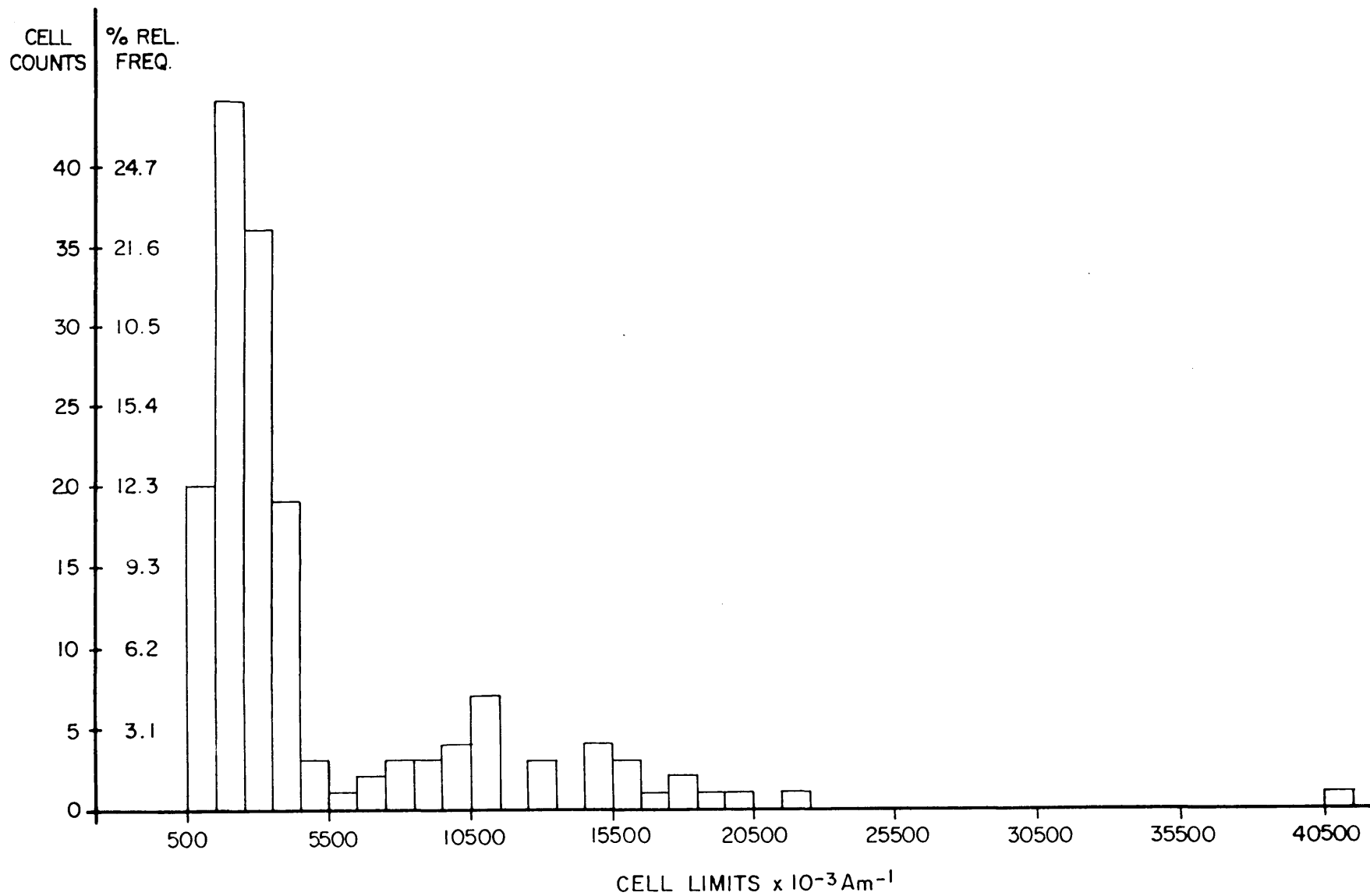


Fig. 66 Histogram plot of NRM intensities of all the specimens from the upper zone of the Bushveld Complex.

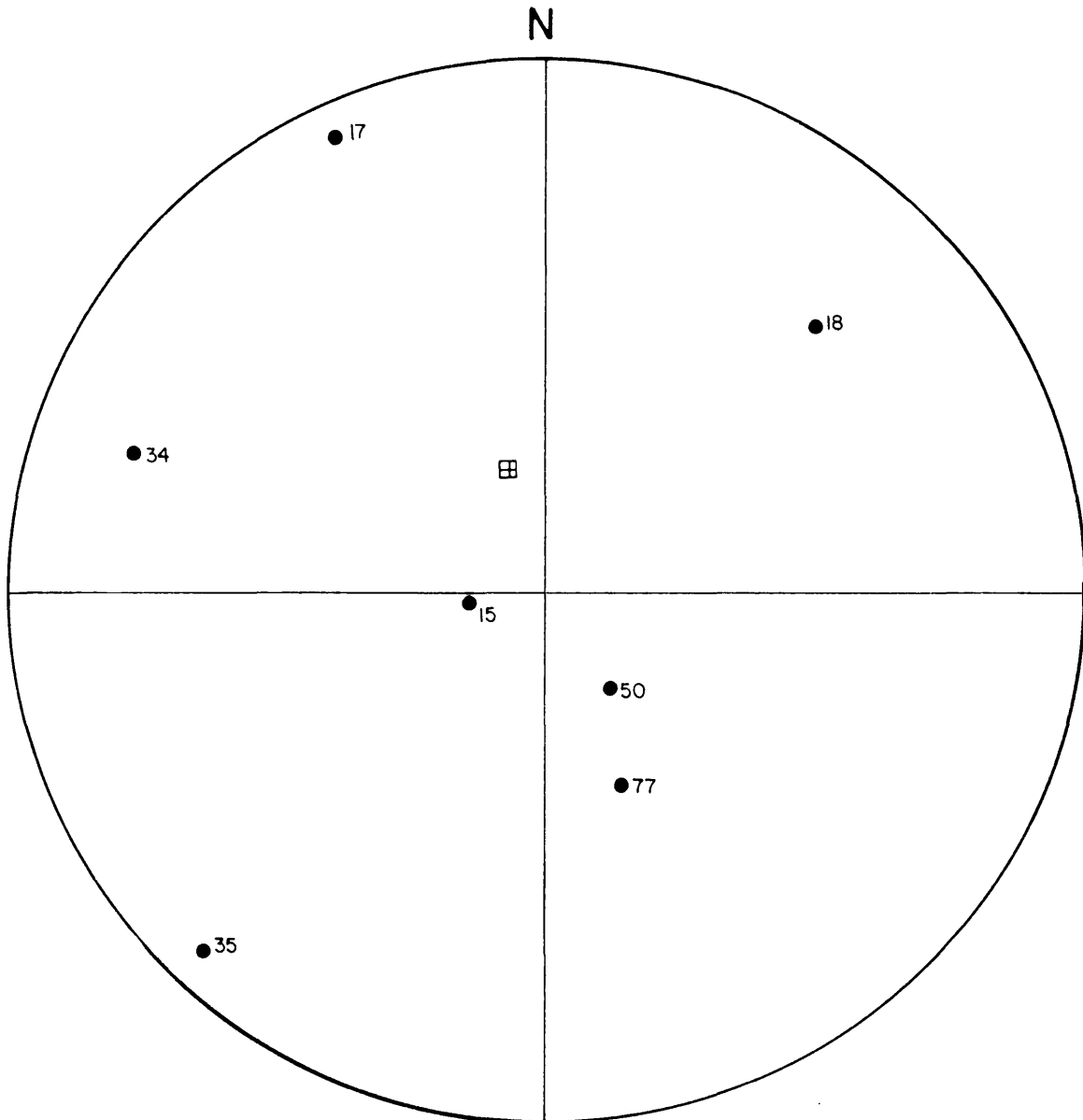


Fig. 67 NRM directions of sites in the upper zone of the layered sequence. Plotting convention as in Fig. 5.

Table XV. Natural remanent magnetization directions of sites in the upper zone.

Site	N*	Declination(D)	Inclination(I)	α_{95}	k
15	4	264,5°	-74,4°	35,0°	7
17	4	335,5°	- 3,4°	11,9°	60
18	4	44,8°	-18,9°	22,9°	17
34	4	289,2°	-11,9°	46,0°	5
35	4	223,2°	- 4,4°	40,8°	10
50	5	145,2°	-65,4°	9,4°	67
77	4	158,6°	-47,5°	22,4°	18

*N is the number of core samples per site

Data from one site (site 16) were rejected, because of a random distribution (95 per cent confidence limit, Watson, 1956) of directions from specimens. The scatter of mean site NRM directions (Fig. 67) is random and cannot be grouped together.

C. Bulk alternating field demagnetization

Site mean magnetization directions obtained after bulk AF demagnetization at an optimum AF value indicated by the Briden SI (Briden, 1972), are listed in Table XVI.

Table XVI. Magnetization directions of sites in the upper zone, after bulk alternating field demagnetization.

Site	Alternating field(mT)	D	I	α_{95}	k
15	40	231,1°	-71,0°	9,1°	101
16	40	194,8°	-52,4°	17,9°	27
17	20	180,5°	-75,1°	23,9°	16
18	40	198,3°	-62,9°	6,1°	224
35	20	196,5°	-57,8°	6,7°	184
50	10	141,5°	-62,8°	7,7°	98
77	50	150,4°	-63,8°	35,0°	13

During stepwise AF demagnetization the change in the magnetization directions from one site (site 34) was random and the site was rejected from further analyses on the grounds of an unstable magnetization. Table XVI further contains one extra site (site 16), which shows a significant grouping of magnetization directions of specimens only after bulk AF demagnetization.

The magnetization directions of sites after bulk AF demagnetization (Fig. 68), show a grouping of directions with the following parameters:

Group: Buz1AF ; N = 7 ; D = 184,3° ; I = -66,0° ; $\alpha_{95} = 11,0^\circ$; k = 31

If a fold test (Graham, 1949) is applied to the magnetization directions obtained by bulk AF demagnetization (corrected data listed in Table XVII) the corrected equivalent of group Buz1AF is formed:

Group: Buz1AFR ; N = 7 ; D = 175,1° ; I = -60,9° ; $\alpha_{95} = 10,6^\circ$; k = 33

Table XVII. Magnetization directions of sites in the upper zone, after bulk alternating field demagnetization, with the igneous layering in a horizontal position.

Site	Dip	Dip direction*	Declination	Inclination
15	18°	N277°	168,8°	-75,8°
16	18°	N293°	174,5°	-46,6°
17	10°	N321°	165,2°	-66,5°
18	10°	N270°	178,2°	-64,4°
35	15°	N220°	179,9°	-70,7°
50	15°	N 06°	155,6°	-50,8°
77	35°	N 57°	197,6°	-46,0°

*Measured from north in a clockwise direction

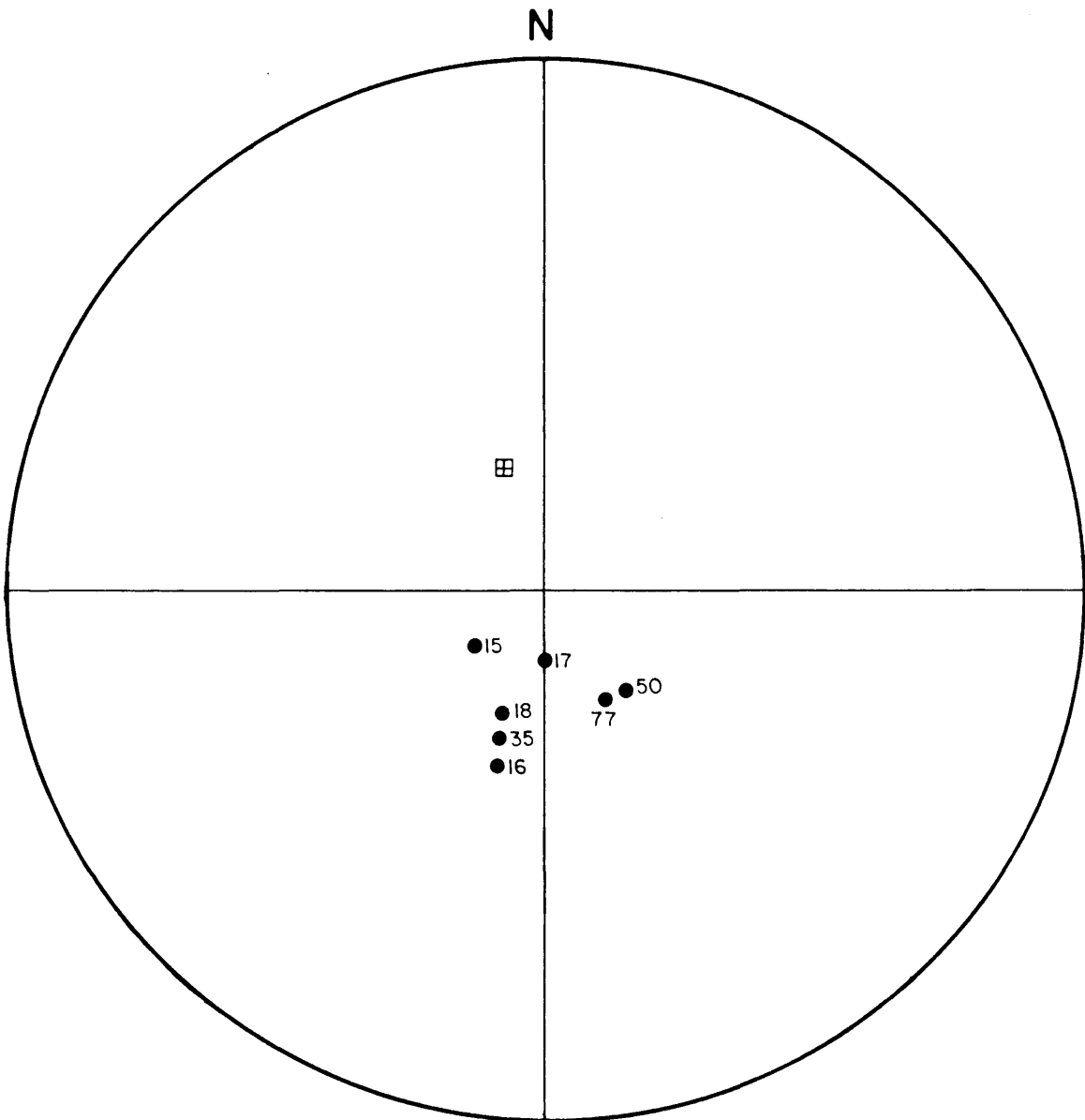


Fig. 68 Magnetization directions of sites in the upper zone after bulk AF demagnetization. Plotting convention as in Fig. 5.

The corrected magnetization directions in Table XVII, are shown in Figure 69. The improvement in k from 31 to 33 after rotation is not significant and this result is at variance with the results obtained from the main and critical zones. Dip directions of the igneous layering at sites used in this test vary considerably and should have led to a significant improvement in k , even though the dip values and dip directions may not be very accurate. Unless the Briden SI (Briden, 1972), has failed completely to locate a primary magnetization component at each site, one has to conclude that the magnetization of the upper zone has been acquired with the igneous layering of the upper zone in its present position.

The circular standard deviation (Δ) of group Buz1AF is $14,5^\circ$ with upper and lower limits of $23,9^\circ$ and $10,9^\circ$ at the 95 per cent confidence limit according to the method of Cox (1969a). The expected value of Δ for a palaeolatitude of 49° is $11,5^\circ$ (Brock, 1971). This indicates that the observed scatter of directions in group Buz1AF, can possibly be due to palaeosecular variation, but it is noteworthy that the value of Δ for group Buz1AF is appreciably higher than the expected value, which could suggest that there may be other factors influencing the observed scatter of directions. The circular standard deviation of group Buz1AFR, is not much different ($\Delta = 14,1^\circ$) and the above also holds true for the scatter of this group.

D. Stepwise alternating field demagnetization of pilot specimens

The directional response of specimens from typical sites to stepwise AF demagnetization, is shown in Figure 70. During stepwise AF demagnetization the magnetization vectors converge rapidly to the mean direction of group Buz1AF. At intermediate AF step values the vectors then move around in the convergence area indicating a stable mid-point, before moving away at high AF values. It is clear from this that the Briden SI (Briden, 1972) succeeded in locating this stable mid-point resulting in the formation of group Buz1AF after bulk demagnetization of specimens.

The intensity response curves to stepwise AF demagnetization of specimens from the upper zone all have a very characteristic shape,

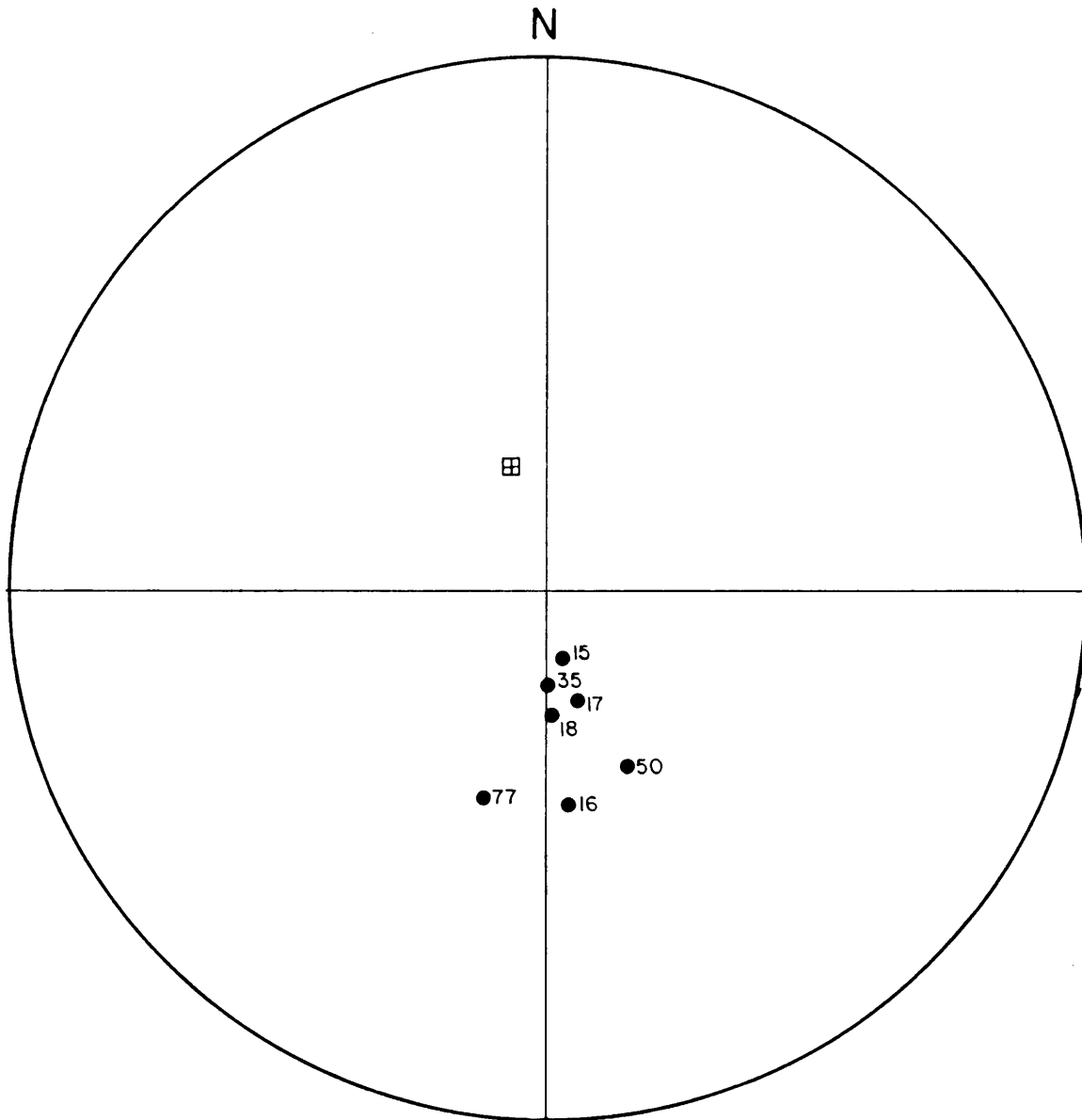


Fig. 69 Magnetization directions of sites in the upper zone after bulk AF demagnetization with the igneous layering in a horizontal position. Plotting convention as in Fig. 5.

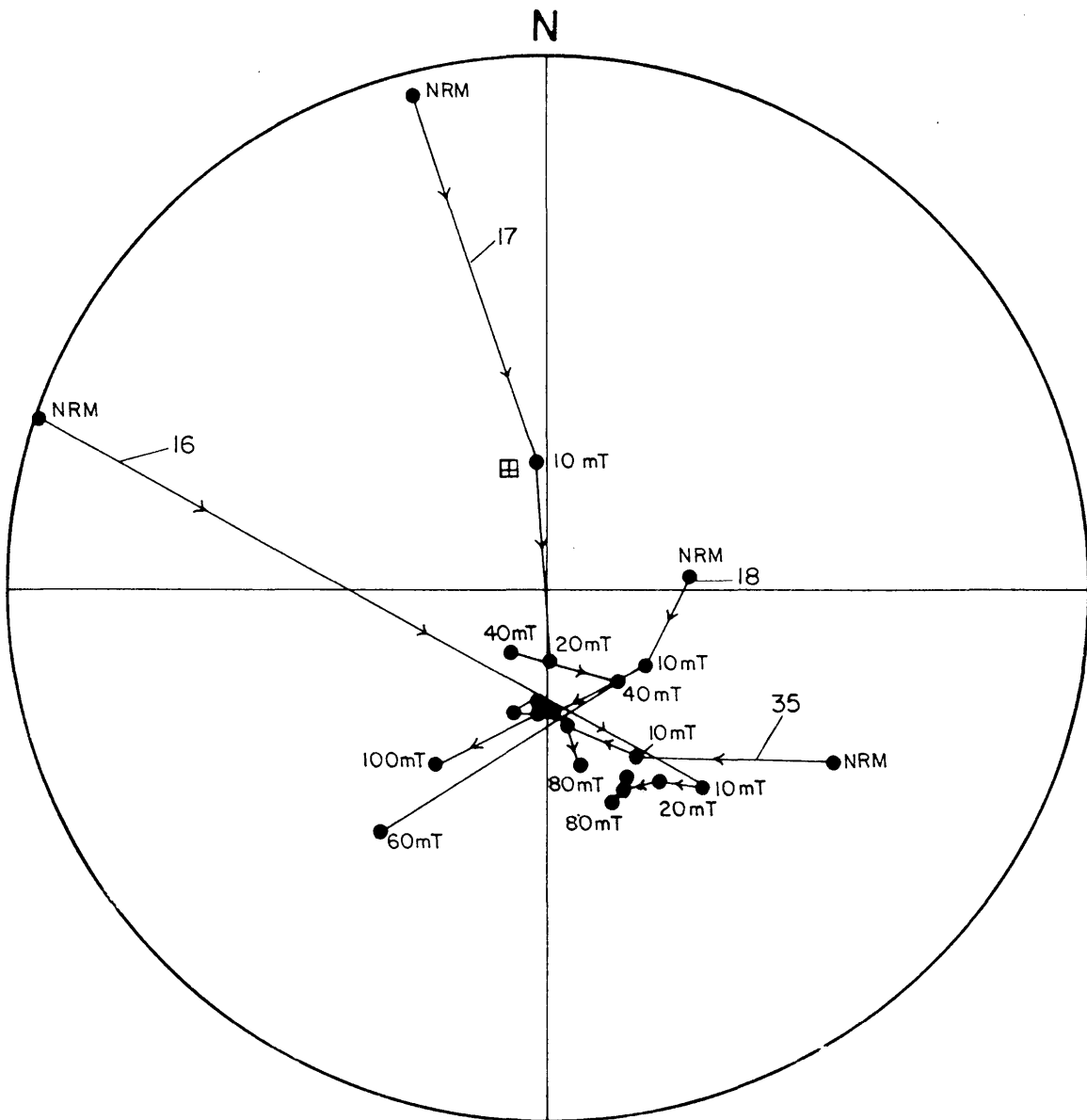


Fig. 70 Directional response of magnetization directions from sites 16, 17, 18 and 35 in the upper zone to stepwise AF demagnetization. Plotting convention as in Fig. 5.

exhibited by no other specimens from the rest of the layered sequence. Such a typical curve, from specimen 17/2D, is shown in Figure 71. The curves all indicate that 80 to 90 per cent of the intensity of the NRM is destroyed in the first 10 mT step during stepwise AF demagnetization. At progressively higher AF values the intensity decreases very slowly and often shows a marginal increase at certain AF steps. This pattern indicates a very "soft", and as seen in Figure 70, unstable magnetization, which dominates the NRM characteristics of these specimens.

According to Dunlop (1981), the shape exhibited by the normalized intensity response curves, indicates that multidomain (MD) particles are the carriers of the remanent magnetization of the specimens. There is a long-argued about hypothesis that unstable components of NRM are preferentially carried by MD grains (Dunlop *et al.*, 1973). If the carriers of magnetization in specimens from the upper zone are in fact MD grains, it is important to establish whether the mean magnetization direction of group Buz1AF contains a magnetization component carried by these grains. To establish this, the Lowrie-Fuller test (Lowrie and Fuller, 1971), as modified by Dunlop *et al.* (1973), was used.

E. Results of Lowrie-Fuller tests

Three specimens of one core sample from site 16 were prepared in the following manner: Specimen 16/3A was demagnetized stepwise in an AF ending at a peak AF-value of 100 mT. This specimen was then given an ARM in an AF of 100 mT with a D.C. magnetic field of 0,04 mT superimposed on it. Specimen 16/3C was demagnetized in an AF of 100 mT and then given a saturation IRM (Dunlop *et al.*, 1973), by placing it in a D.C. magnetic field of 500 mT. The last specimen (16/3B) was heated to 700°C and then left to cool in a magnetic field of 25 000 nT, to acquire a TRM. These specimens with the ARM, IRM and TRM respectively, were then subjected to stepwise AF demagnetization. The normalized intensity response curves to stepwise AF demagnetization of the above specimens are presented in Figure 72. It can be seen that for low AF values the weak field TRM is more stable than the IRM, which is in turn more stable than the NRM. According to Lowrie and Fuller (1971, p. 6346) the stability of TRM increases with decreasing field strength for single domain (SD) carriers, and the saturation IRM is less stable than the

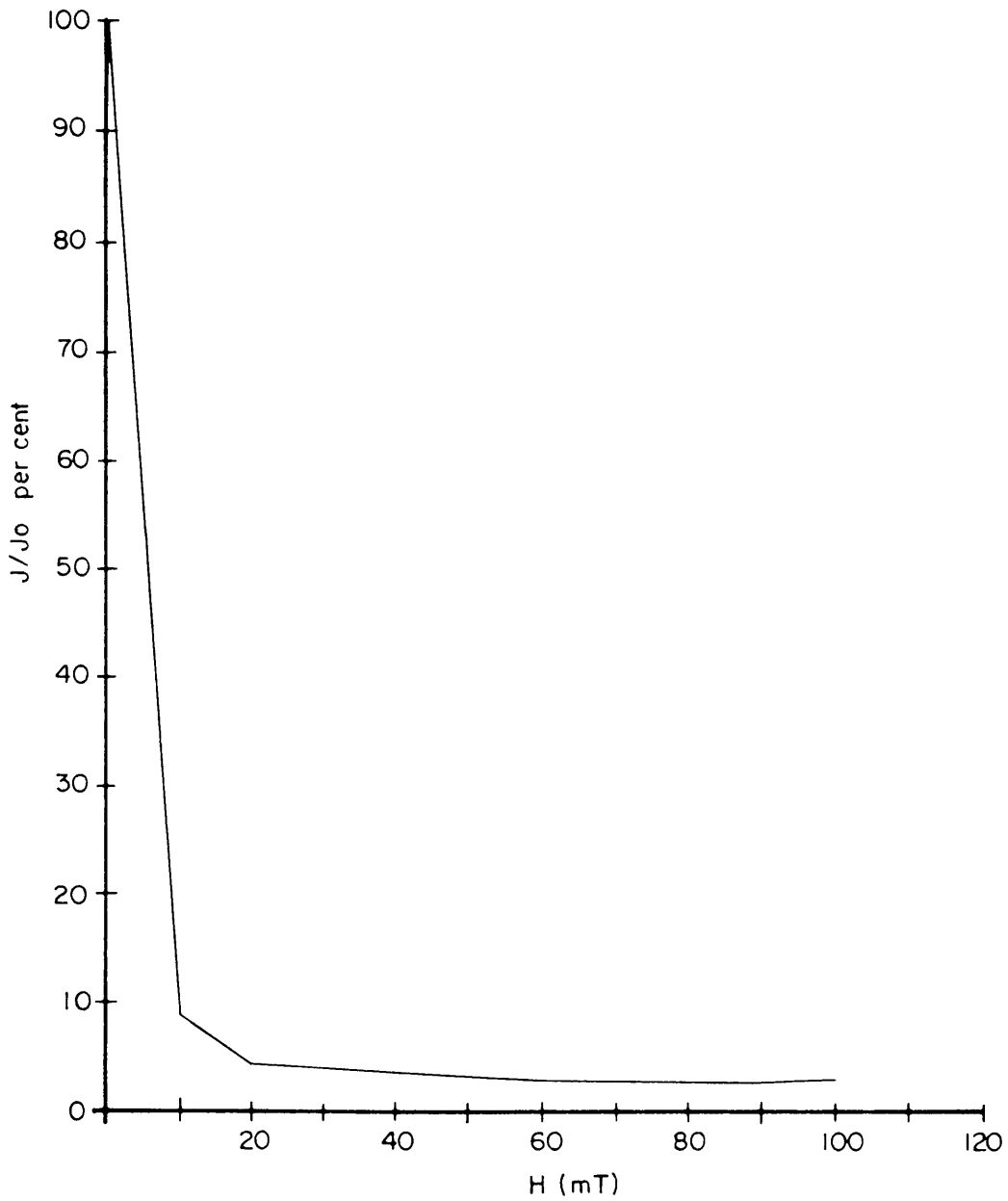


Fig. 71 Typical normalized intensity response curve to AF demagnetization by a specimen from site 17 in the upper zone.

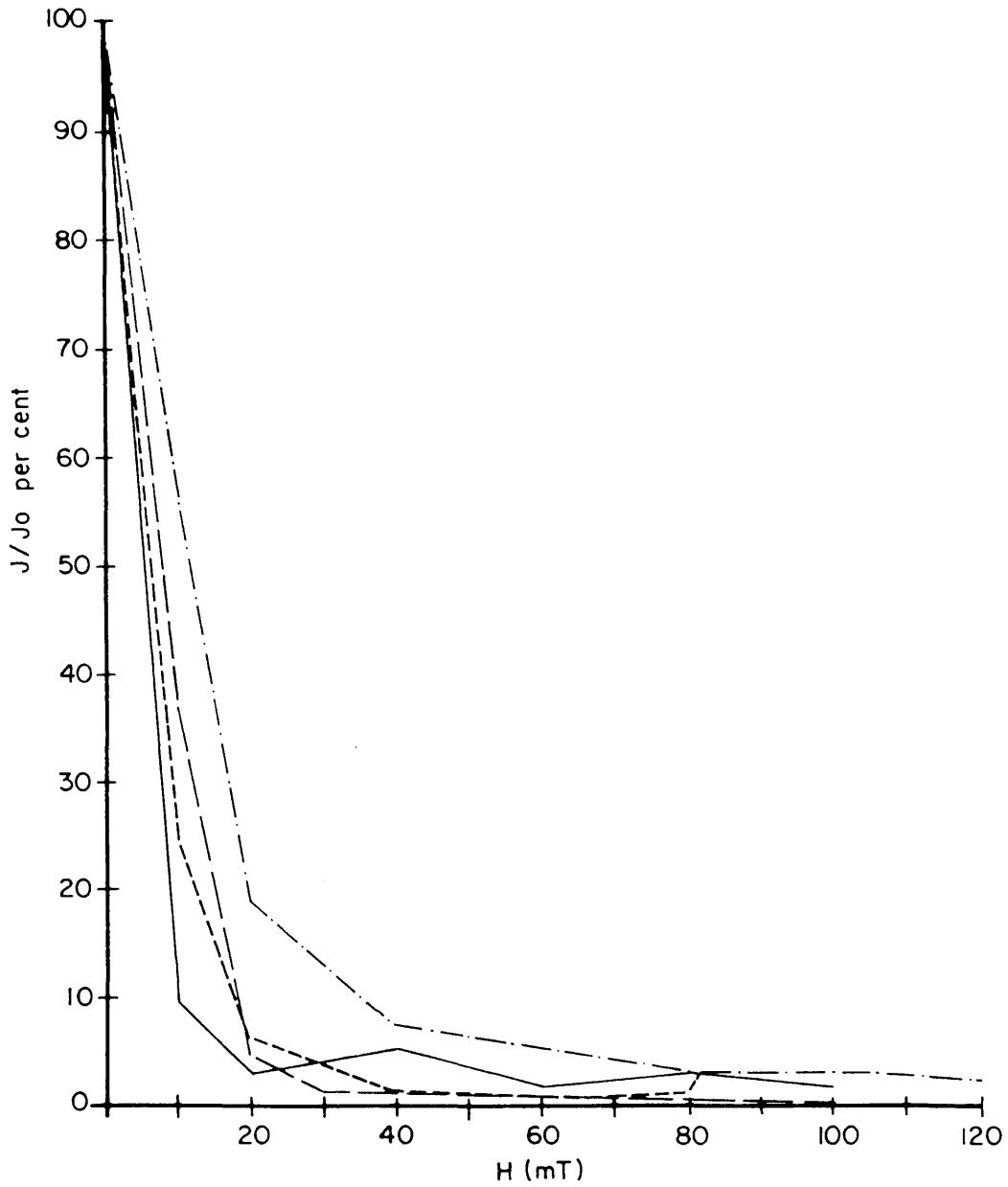


Fig. 72 Normalized intensity response curves of specimens with a NRM (—), a TRM (-·-·), a saturation IRM (---), and an ARM (----) to AF demagnetization. All specimens from one core from site 16.

weak field TRM. For MD carriers, the stability of TRM decreases with decreasing field strength and the IRM is more stable than the weak field TRM.

In Figure 72 the weak field TRM is more stable than the saturation IRM which suggests that the carriers of the magnetization are SD grains. However, the original NRM is less stable than the saturation IRM which, in turn, indicates that MD grains are the carriers (Lowrie and Fuller, 1971, p. 6347). This apparent paradox could, however, be due to chemical changes which occurred during the heating of the one specimen, or to the fact that the newly acquired NRM of these specimens is not solely due to a TRM.

To circumvent this problem the Lowrie-Fuller criteria were then applied according to the method of Dunlop *et al.* (1973) to the saturation IRM and ARM, rather than to TRM. At low AF values (Fig. 72) the saturation IRM is more stable than the ARM. This indicates that MD carriers dominate over that coercivity range. At higher AF values this situation reverses, with the ARM becoming more stable than the saturation IRM suggesting that over the higher part of the coercivity spectrum SD carriers of magnetization dominate.

This test was repeated on specimens from site 15 (Fig. 73). Here the ARM is more stable over the whole coercivity spectrum than the saturation IRM, indicating that SD carriers dominate. At AF values less than 20 mT (Fig. 73), the ARM and saturation IRM response curves differ very little and it is possible that MD carriers play a role in the lower part of the coercivity spectra of these specimens.

This type of behaviour, where MD characteristics are exhibited at low AF values and SD characteristics at high AF values is not unknown. Dunlop *et al.* (1973) found the behaviour in the Glamorgan Gabbro. The results also indicate that the carriers of the magnetization component located by the Briden SI (Briden, 1972), as manifested by group Buz1AF, are SD domain grains, in view of the optimum AF values (Table XVI) used to demagnetize specimens from each site.

The reliability of these results could be questioned on the basis of the observation, that during stepwise AF demagnetization of specimens,

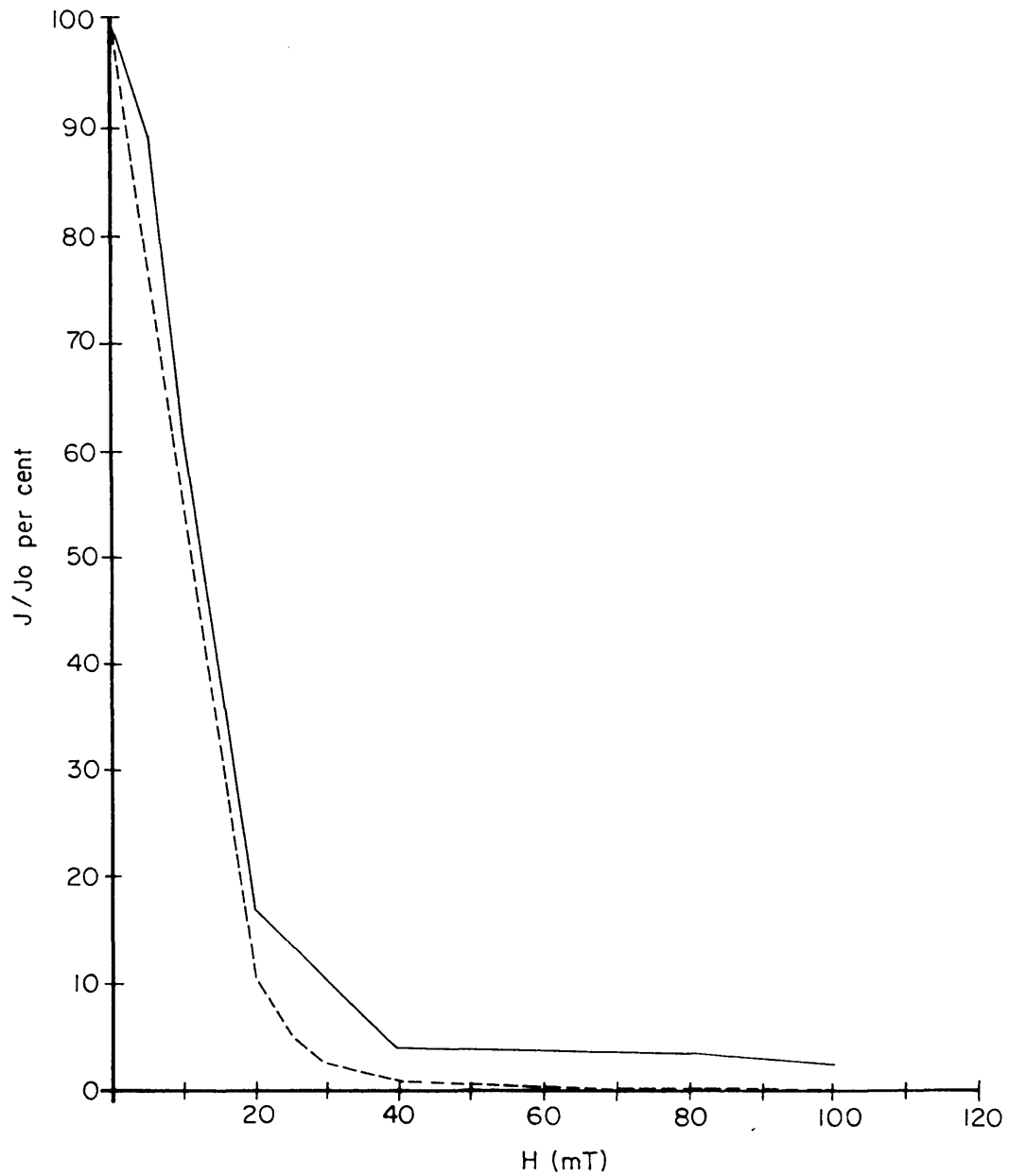


Fig. 73 Normalized intensity response curves of specimens with an ARM (—) and a saturation IRM (----) to AF demagnetization. All specimens from site 15.

the intensities measured at each step were only accurately repeatable at low AF values. At high AF values, intensities tended to fluctuate when repetitive AF demagnetization at a given AF value was done. This fluctuation could also be manifested by the apparent marginal increase of intensities of magnetization observed at certain AF steps during stepwise AF demagnetization of specimens (Fig. 71), and the tendency of magnetization directions to diverge at high AF values (Fig. 70). No data are available on the repeatability of intensities measured during stepwise AF demagnetization of the ARM and IRM of the two specimens 16/3A and 16/3C. These intensities were generally higher at each demagnetization step than those of the NRM, and consequently one can expect the NRM demagnetization response curve to be affected most by the poor repeatability of the intensity measurements. In Figure 74 the average normalized AF demagnetization response curve of the NRM of a specimen from site 16 is shown, with error bars at each AF demagnetization step, indicating the normalized standard deviation from the mean intensity value obtained after repeating the AF demagnetization at that step three times. From this it can be seen that, although the results of the Lowrie-Fuller tests may be influenced by the poor repeatability of the AF demagnetization steps, the form of the curves will not change substantially, even at high AF values.

The incongruous repeatability of the AF demagnetization steps can possibly be explained by the acquisition of a weak ARM by the MD carriers of magnetization of the specimen while subjected to AF demagnetization, or by the acquisition of a VRM during transfer of specimens from the AF demagnetization apparatus to the field free space of the spinner magnetometer. Any of these possibilities will cause the primary magnetization directions located by the Briden SI (Briden, 1972), although carried primarily by SD carriers, to be contaminated to a small extent. This will explain the relatively large circular standard deviation of the magnetization directions in group Buz1AF, as well as the negative results from the fold test applied to this group in Section C.

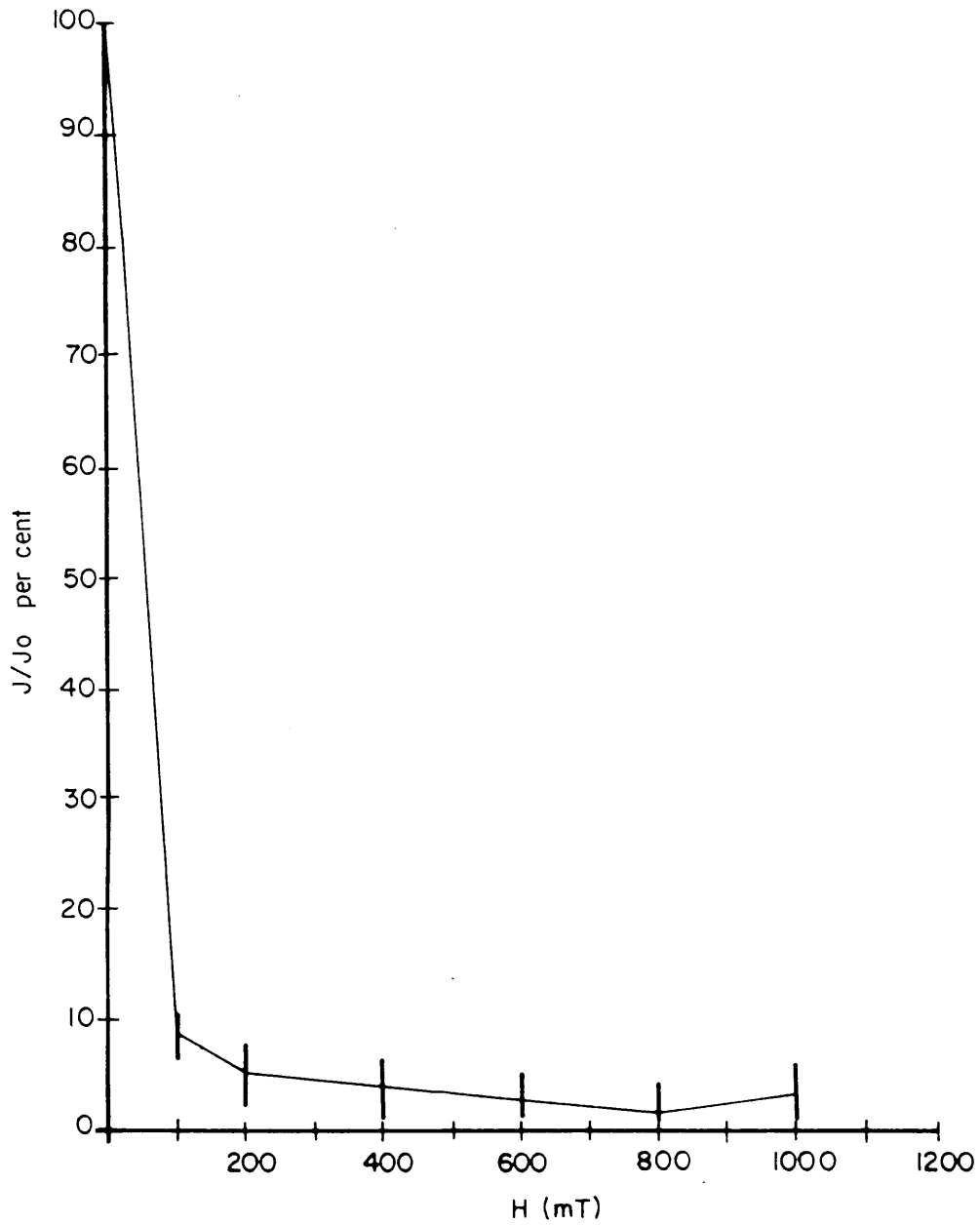


Fig. 74 Normalized average intensity response curve to AF demagnetization. Error bars indicate normalized standard deviation from the average value after three demagnetization cycles and measurements at each step.

F. Thermal demagnetization

The directional response to continuous thermal demagnetization of one specimen from each site in the upper zone is shown in Figure 75. With increasing temperature all the magnetization vectors converge. For five specimens the convergence paths of the vectors describe parts of circles of remagnetization, while in two instances the converging paths are made up of two segments of remagnetization circles (Fig. 75). The magnetization vector of only one specimen, from site 50, remained fairly stable during thermal demagnetization, with very little movement initially and then reaching a stable end point. Magnetization directions of specimens from site 34, which had previously been found to become unstable during AF demagnetization, repeated this behaviour during continuous thermal demagnetization and all data from this site were rejected.

The magnetization vectors shown in Figure 75 are all resultant vectors of two or more magnetization vectors. At very high temperatures, before reaching the Curie point of the specimens, the convergence is a maximum, indicating that most, if not all the secondary magnetization components have been removed by the thermal demagnetization. If these end point vectors (magnetization directions measured just before reaching the Curie point, or in some cases, the last magnetization which could be measured accurately at high temperatures) of the specimens were grouped together, the mean group direction should yield a value the same as or close to the direction of the primary magnetization of the specimens. However, it is clear from Figure 75, that the magnetization direction from site 17 has not fully converged at 500°C, where the last accurate measurement of the magnetization vector was made and consequently, this site will have to be rejected from a group comprising of these end point vectors. The end point vectors are shown in Figure 76 and constitute the following group:

Group: Buz2T ; N = 6 ; D = 182,6° ; I = -62,9° ; α_{95} = 13,7 ; k = 25

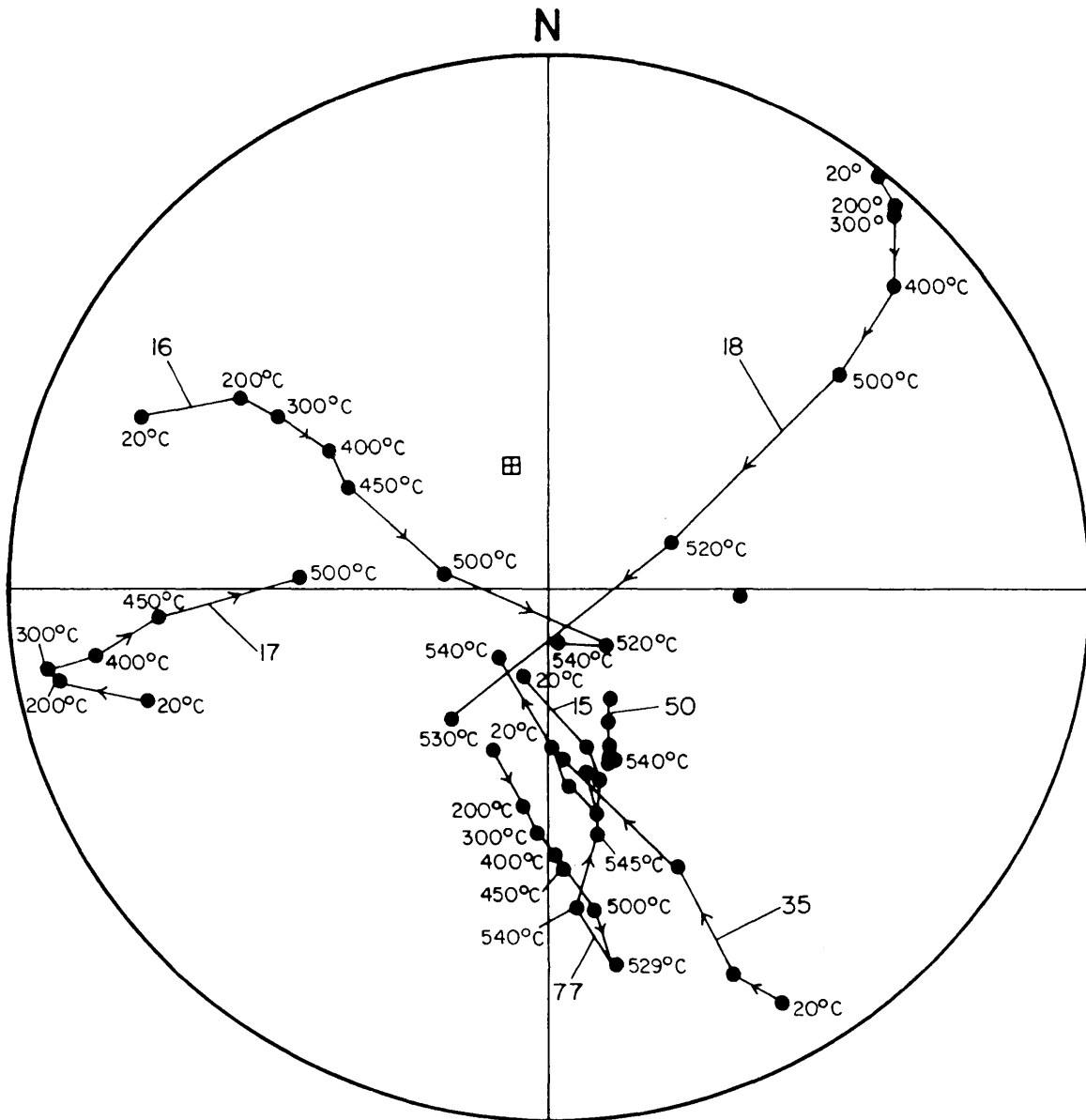


Fig. 75 Directional response of magnetization vectors of specimens from sites in the upper zone to continuous thermal demagnetization. Plotting convention as in Fig. 5.

Group Buz2T does not differ much from group Buz1AF, which was obtained after bulk AF demagnetization; in fact, the respective circles of 95 per cent confidence overlap. This suggests that both the AF demagnetization and the thermal demagnetization succeeded in approximately locating the primary magnetization of the upper zone.

Because the continuous thermal demagnetization of a specimen is completed without removing the specimen from the field free space of the spinner magnetometer, one would expect adverse effects such as the acquisition of an ARM or a VRM by the specimens during demagnetization, to be absent. The magnetization directions of group Buz2T should thus be more suitable for a fold test than those directions obtained from AF demagnetization of specimens. In Table XVIII the end point vectors of Figure 76 are listed after correction for the dip of the igneous layering at each site.

Table XVIII. End point magnetization vectors obtained with thermal demagnetization of specimens from the upper zone, with the igneous layering in a horizontal position.

Site	Declination(D)	Inclination(I)
15	158,1°	-71,9°
16	134,7°	-63,7°
18	202,9°	-61,0°
35	155,2°	-63,7°
50	166,6°	-39,8°
77	194,8°	-30,3°

These vectors are shown in Figure 77 and the corrected equivalent of group Buz2T yields the following values:

Group: Buz2TR ; N = 6 ; D = 172,6° ; I = -57,3° ; $\alpha_{95} = 18^\circ$; k = 15

The value of the estimate k of the precision parameter, has decreased from 25 to 15. This indicates a weaker grouping of directions with the igneous layering in a horizontal position, which suggests that the primary magnetization of the upper zone was acquired with the igneous

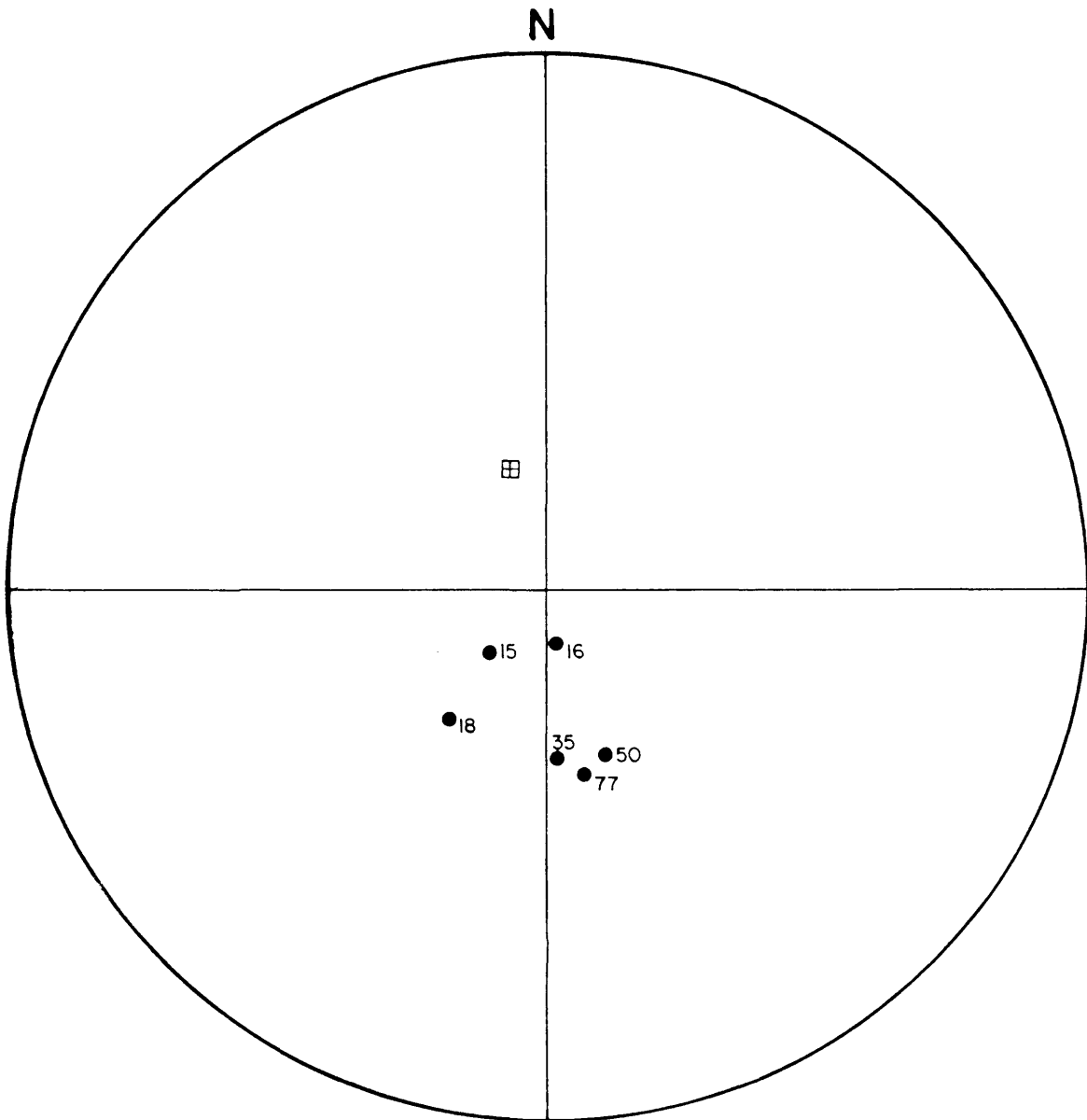


Fig. 76 End point vectors (see text) after continuous thermal demagnetization of specimens from the upper zone. Plotting convention as in Fig. 5.

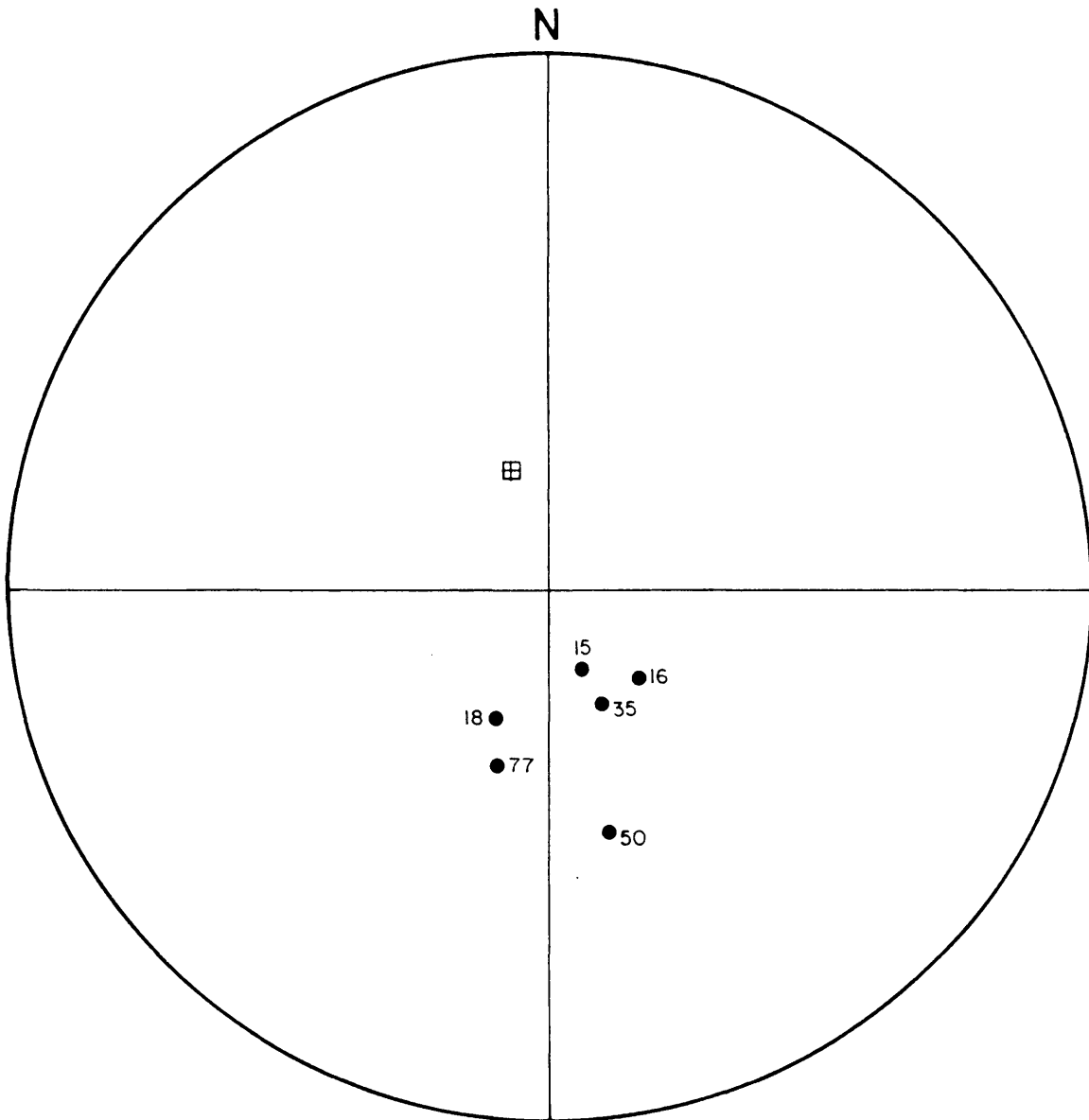


Fig. 77 End point vectors (see text and Fig. 76) corrected for the dip of the igneous layering at each site. Plotting convention as in Fig. 5.

layering in its present attitude. However, the decrease of k is not significant at the 95 per cent confidence limit and the magnetization directions used in the fold test represent one specimen from each site only. Consequently the above result should be treated with caution.

In an attempt to improve the accuracy of the mean magnetization direction given by group Buz2T, circles of remagnetization were fitted to the data of Figure 76 with a least squares technique (Halls, 1976). Where the magnetization vectors from one specimen describe parts of more than one remagnetization circle, only the last converging path was used to fit a circle of remagnetization. These remagnetization circles are shown in Figure 78 with the theoretically calculated intersection point (method of Halls, 1978). This intersection point yields the following direction for the primary magnetization direction: $D = 191,2^\circ$; $I = -85,4^\circ$. This direction is different from the mean directions of groups Buz1AF and Buz2T, and in view of the rather poorly defined intersection point (Fig. 78), can be considered to be the least accurate.

The intensity responses to thermal demagnetization of all the specimens in the upper zone are similar. Two such typical normalized intensity response curves are shown in Figure 79. The shape of these curves suggests a thermally well distributed blocking temperature spectrum, but the average Curie temperature obtained from all the pilot specimens is 547°C , with a standard deviation from the mean value of 7°C . A Curie temperature of 547°C indicates a titanomagnetite with 0,056 mole fraction Fe_2TiO_4 (ulvöspinel), (McElhinny, 1973) in solid solution, as the source of the remanent magnetization.

G. Mineralogy of opaque minerals

Magnetite generally occurs in all the specimens as rather large grains of up to 1 mm in diameter, although a whole range of magnetite particles down to approximately $10\ \mu\text{m}$, are also present. The Curie temperature of the specimens indicates that this is a titanomagnetite with a cell dimension (A_m) of $0,84\ \text{nM}$. This value is identical to the average cell dimensions of titanomagnetite in the upper zone of the

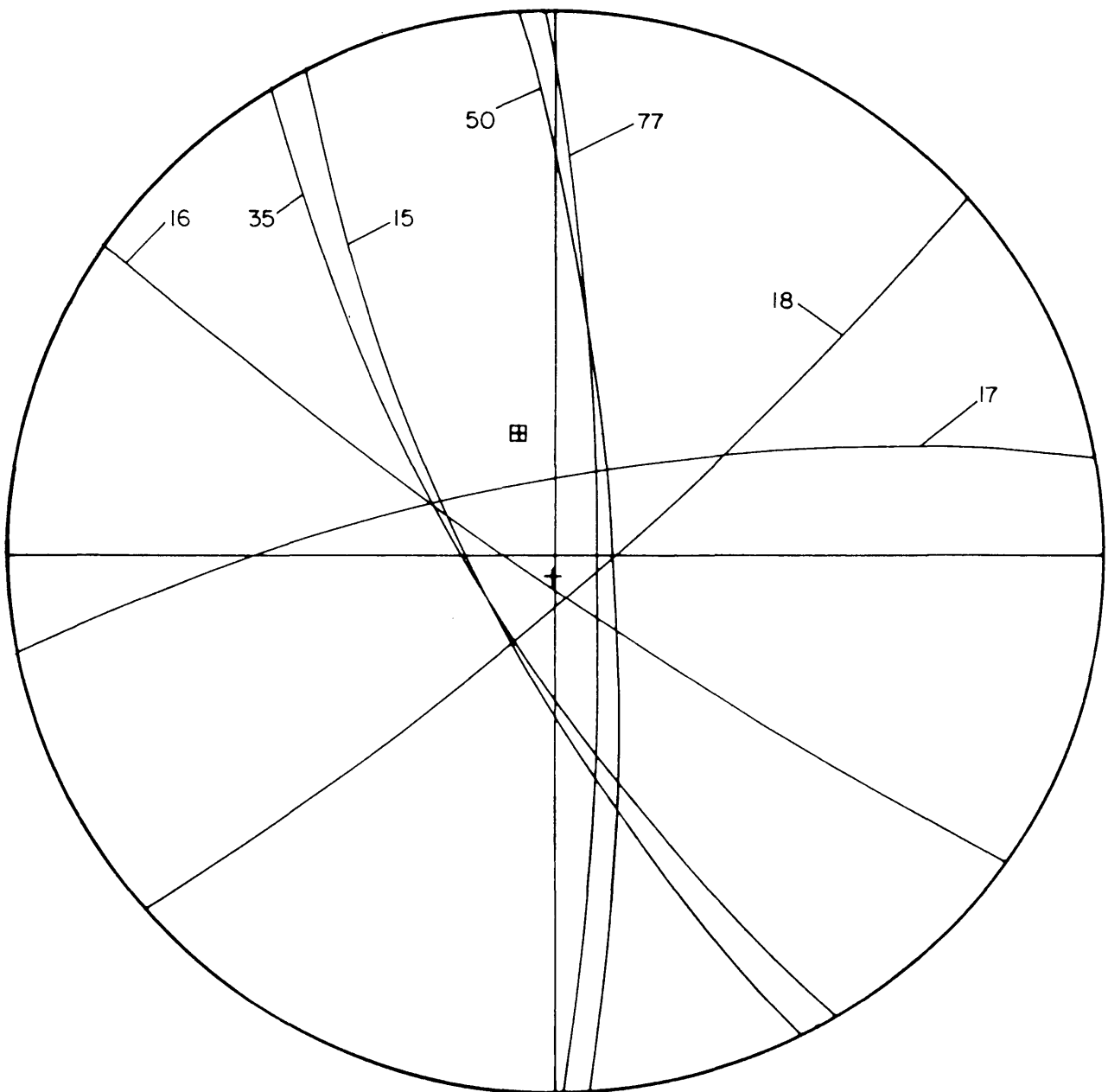


Fig. 78 Remagnetization circles on the upper hemisphere obtained by fitting circles to thermal demagnetization data presented in Fig. 75. Calculated intersection point of remagnetization circles shown by "+".

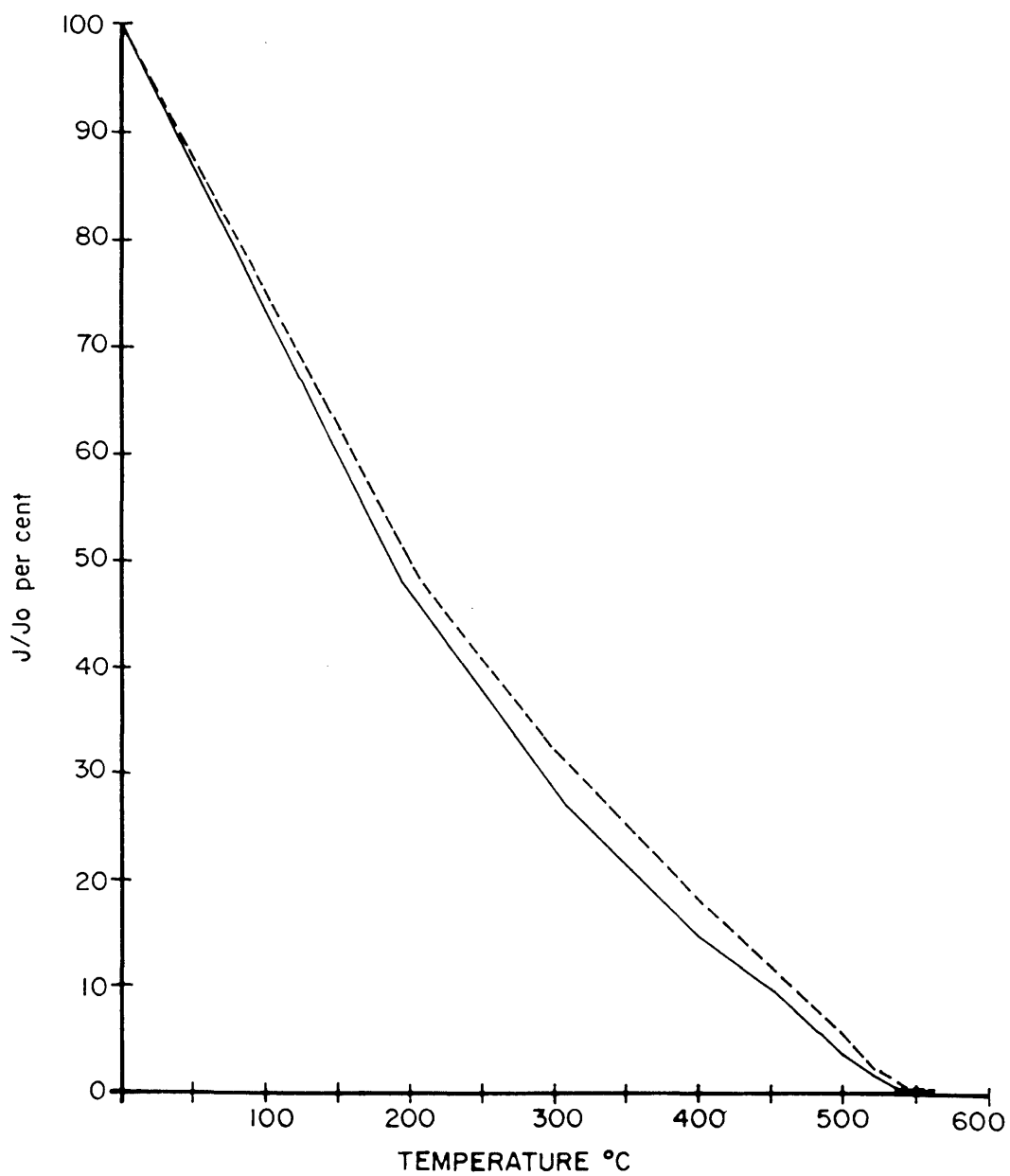


Fig. 79 Normalized intensity response curve to continuous thermal demagnetization of a specimen from site 16.

layered sequence given by Molyneux (1972). Opaque exsolution lamellae in pyroxene and plagioclase crystals are rare, but some were found in specimens from sites 16 and 17, which could possibly be magnetite (see discussion Chapter VI, Section E).

The titanomagnetite consists of magnetite with a cloth-like texture formed by exsolved ulvöspinel. Along the periphery of the titanomagnetite grains, but in some cases also throughout the crystal, the ulvöspinel tends to be oxidized to ilmenite, although well developed coarse lamellae of ilmenite do occur occasionally. Haggerty (1976), classified the degree of magmatic oxidation into seven stages, from C1 the lowest, to C7, the highest, which is characterized by the pseudobrookite-haematite assemblage. According to this classification the titanomagnetite of specimens from sites in the upper zone fall into the C2 and C3 oxidation stages, which are characterized by magnetite-ulvöspinel and a small number of ilmenite exsolution lamellae.

Evidence for low temperature oxidation of the titanomagnetites was found in places by the presence of maghemite at the margins of titanomagnetite grains. However, subsequent XRD investigation of separated titanomagnetite grains failed to confirm the presence of maghemite, which could be due to the relative scarceness of the mineral in the specimens. The XRD-data confirmed the cell dimension of 0,84 nm obtained from the average Curie temperature, for the magnetite.

The large size of the titanomagnetite grains is consistent with the MD characteristics of the AF demagnetization data at low AF values. Titanomagnetite grains of only 10 μm will, however, still be MD grains (Soffel, 1971) and although smaller titanomagnetite grains could be present in the specimens, it becomes very difficult to support the evidence for SD carriers on the basis of the observed opaque minerals apart from the two sites where opaque lamellae, conceivably magnetite, have been observed in pyroxene and plagioclase crystals.

Apart from occurring as exsolution lamellae in the titanomagnetite grains, ilmenite also exists as large discrete grains in the specimens.

The average cell parameters (Arh) of the coarse ilmenite grains in the upper zone of the layered sequence is 0,553nm (Molyneux, 1972, p. 865), which indicates a mole fraction of 80 per cent FeTiO_3 (McElhinny, 1973). From chemical analyses by Molyneux (1972, p. 870) the ilmenite contains, on average, less than four molecular per cent Fe_2O_3 , about 80 per cent FeTiO_3 and about 16 per cent MgTiO_3 . No haematite exsolution lamellae were observed in the ilmenite and with the previously quoted cell parameter which should result in a Curie temperature of approximately 0°C for the ilmenite, the ilmenite in the specimens in all probability does not contribute significantly to the remanent magnetization

H. Geomagnetic field reversal or self-reversal?

The mean magnetization direction of the upper zone (group Buz1AF) is normal. It is, however, reversed with respect to the magnetization direction of the main zone in the western Bushveld (group Bmz7AF) and the magnetization direction of subzone B of the main zone in the eastern Bushveld (group Bmz3AF) (Fig. 80). This difference in magnetic polarities can either represent a geomagnetic field reversal or a self-reversal of magnetization. Although occurrences of magnetic self-reversals can be considered rare (Merril, 1975; Tarling, 1971), with evidence overwhelmingly in favour of geomagnetic field reversals (Cox, 1969b), it is always pertinent to consider the possibility of self-reversal.

In an attempt to reproduce a self-reversal of magnetization in specimens from the upper zone, six randomly selected specimens were heated to 650°C in presence of nitrogen gas and then left to cool in the Earth's magnetic field. The TRM's acquired by the specimens were in all instances parallel to the magnetic field in which the specimens cooled down. Further AF and thermal demagnetization of the specimens yielded no corroborative information for a possible self-reversal, or even partial self-reversal of magnetization. The evidence although overwhelmingly against self-reversal cannot, however, be considered as absolute proof that a self-reversal did not take place, because the chances of reproducing a self-reversal of magnetization of specimens will depend on the degree to which experiments conducted in the laboratory conform to conditions in nature.

Specimens from the upper zone and subzone C of the main zone, immediately below the upper zone in the eastern Bushveld have the same magnetic

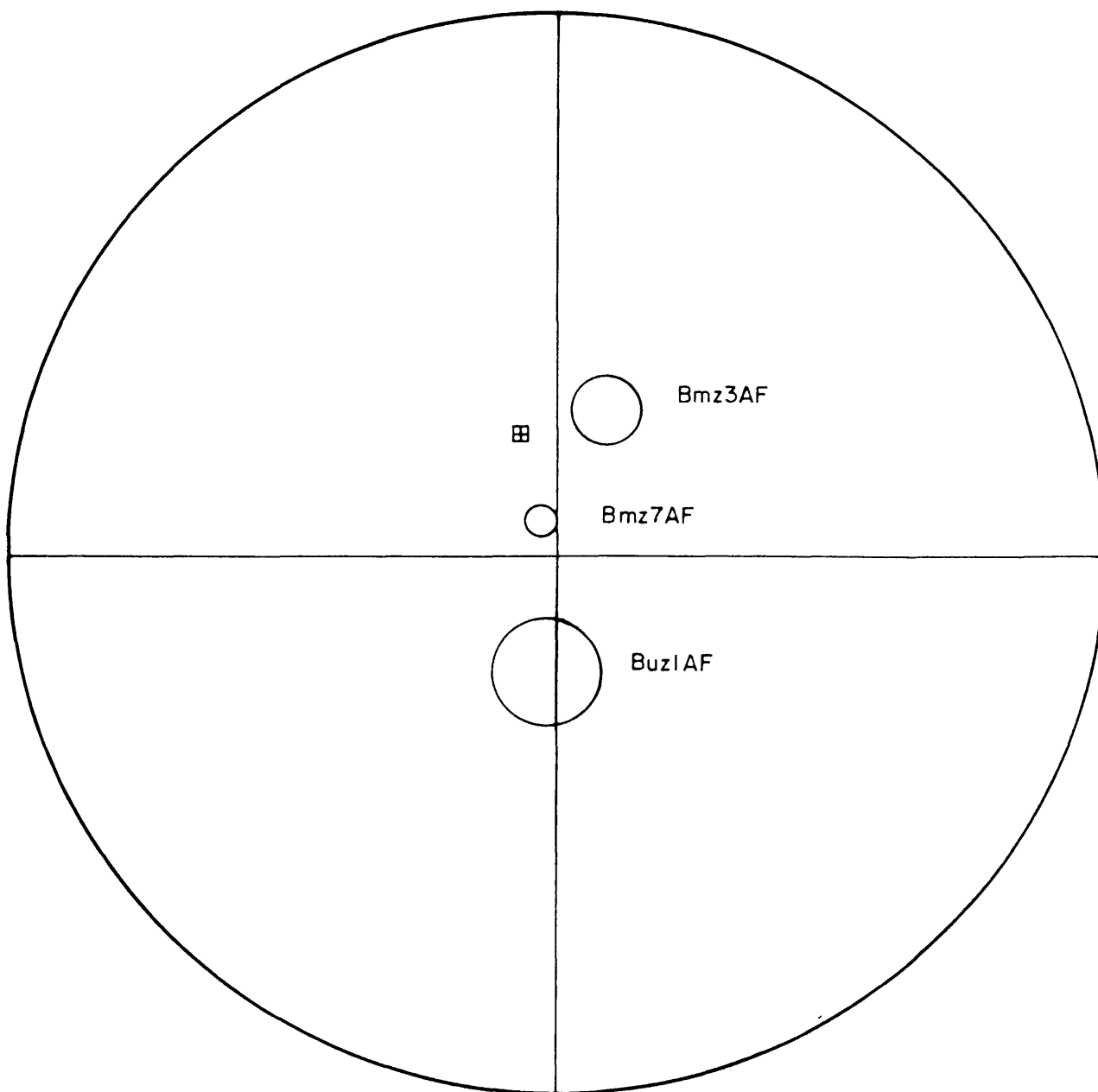


Fig. 80 Mean magnetization directions and circles of 95 per cent confidence for groups Bmz3AF, Bmz7AF and Buz1AF.

polarity (Chapter VI, Section I). If the magnetization direction of the upper zone is the result of a self-reversal, one must assume the same for subzone C of the main zone. The opaque mineralogy of the two zones are dissimilar and consequently any self-reversals of magnetization would have to have been the result of different mechanisms in each zone. Although this is not impossible, such a situation is unlikely in view of the general scarceness of self-reversals of magnetization.

According to Morgan and Briden (1981, p. 164), a geomagnetic field reversal occurred at about 1950 m.y. ago. The effect of such a reversal of the geomagnetic field with an approximate age not much different from that of the layered sequence, may be manifested in the palaeomagnetic polarity of the layered sequence and can very well be the cause of the change in magnetic polarity towards the top of the layered sequence.

I. Summary of results

No evidence could be found that the upper zone of the layered sequence had acquired its remanent magnetization with the igneous layering in a horizontal position. This is in contrast to the main and critical zones, which, from data presented in previous chapters, apparently had acquired their magnetization with the igneous layering in a horizontal position.

Application of AF demagnetization techniques yielded a mean primary magnetization direction for the upper zone. This direction was confirmed with results from thermal demagnetization of specimens and has the following parameters:

Group: Buz1AF ; N = 7 ; D = 184,3° ; I = -66,0° ; $\alpha_{95} = 11^\circ$; k = 31

with corresponding (north) pole position:

latitude : 16,1°S

longitude : 148,5°W

and polar error (dp, dm) : 14,7° and 13,0° respectively

The magnetic polarity of the upper zone is different from that of the main zone in the western Bushveld Complex and of subzone B of the main zone in the eastern Bushveld Complex. No evidence could be found that this difference is the result of a self-reversal of magnetization.

IX DISCUSSION OF PALAEOMAGNETIC RESULTS

A. Palaeomagnetic subdivision of the layered sequence

The palaeomagnetic polarity pattern is a striking feature of the palaeomagnetism of the mafic layered sequence of the Bushveld Complex. Although a resemblance exists there is no close relation between either the zonal or lithostratigraphic subdivision and the observed polarity pattern which is basically a chronostratigraphic subdivision. This apparent unconformal relationship may be pertinent to the evolution of the layered sequence, but it also lends itself to a clear palaeomagnetic subdivision of the sequence.

Whether any change in polarity is due to a reversal of the geomagnetic field, or due to a self-reversal of remanent magnetization, is not important in the context of a proposed subdivision. This is because any subdivision of a rock sequence based on a magnetic polarity pattern need not be concerned with the genesis of the existing and observed palaeomagnetic pattern *per se*.

The magnetic polarity pattern of the layered sequence in the western and eastern Bushveld in terms of either a normal magnetization direction (defined here as a magnetization direction in the same sense as the present-day magnetic field in southern Africa) or a reversed magnetization direction is shown in Figure 81. In Figures 82 and 83 the pattern is superimposed on the simplified lithostratigraphic columns representing the layered sequence in the western and eastern Bushveld Complex respectively. The positions of the boundaries between polarity zones shown in Figures 82 and 83, can only be regarded as approximate at this stage. Many more sampling sites will be necessary to locate the exact positions. This is especially true for the lower part of the critical zone, the lower zone, the marginal zone and to a lesser extent the top of the upper zone.

The layered sequence can be subdivided into three magnetic polarity zones, namely A, B and C, (MPzA, MPzB and MPzC), as shown in Figures 82 and 83.

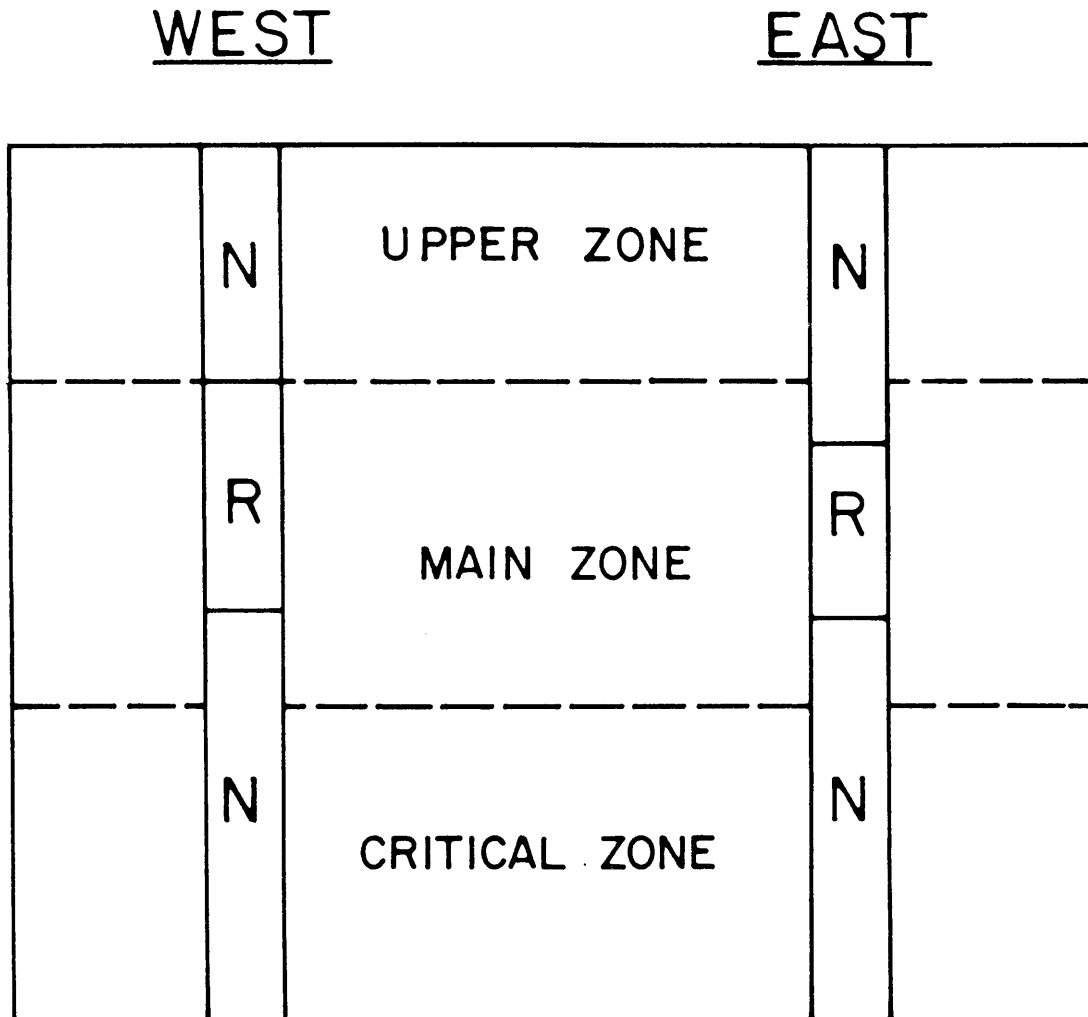


Fig. 81 The zonal subdivision of the mafic layered sequence showing the magnetic polarity pattern observed in the western and eastern Bushveld Complex (N=normal magnetization defined here as a magnetization with the same sense of inclination as the present-day magnetic field in southern Africa, R=reversed magnetization).

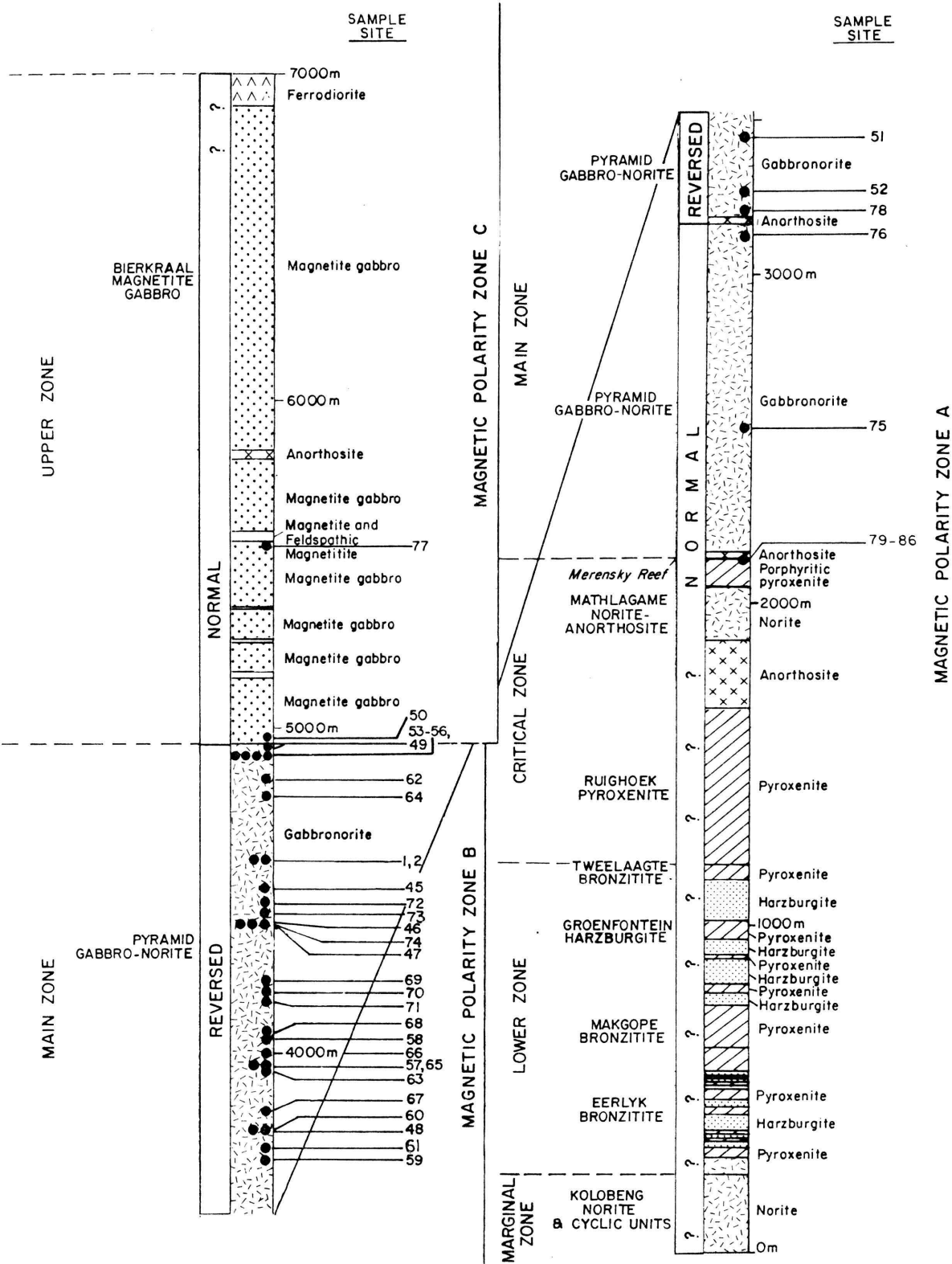


Fig. 82 A simplified lithostratigraphic column of the layered sequence in the western Bushveld Complex showing the magnetic polarity zones.

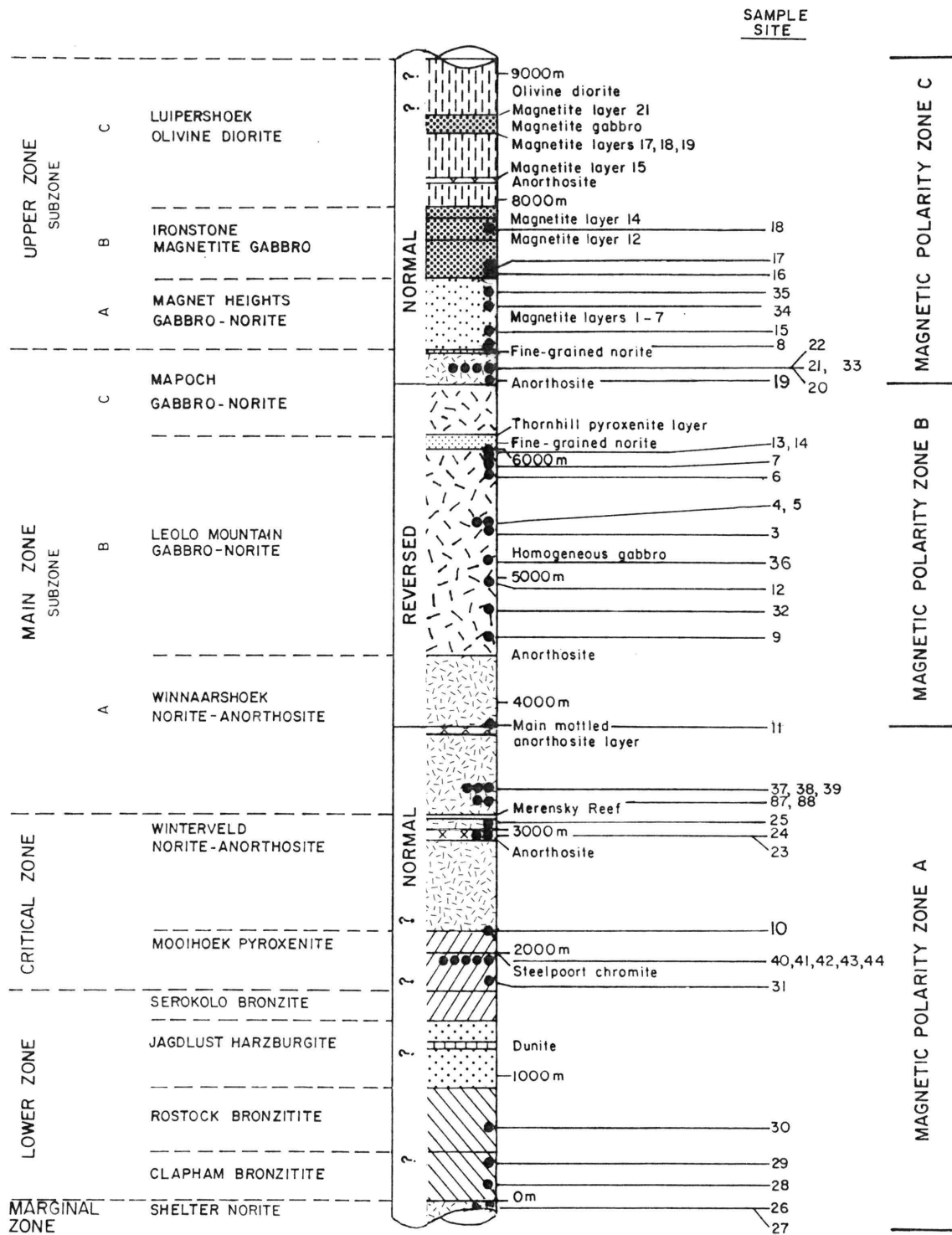


Fig. 83 A simplified lithostratigraphic column of the layered sequence in the eastern Bushveld Complex, showing the magnetic polarity zones.

B. Palaeomagnetic pole positions of the layered sequence

The apparent polar wander (APW) path for African cratons for the interval ca. 2300 m.y. - 1900 m.y. as interpreted by McElhinny and McWilliams (1977), is shown in Figure 84. The palaeomagnetic pole position of the layered sequence on this APW path, based on the data of Gough and Van Niekerk (1959) corresponds with an age of ca. 1950 m.y. In view of the rapid apparent polar wander for the interval 2100 m.y. - 1900 m.y., it is clear that the average age of 2095 ± 24 m.y. for the layered sequence determined by Hamilton (1977), is irreconcilable with the palaeomagnetic data.

In Figure 85 a smaller segment of the APW path for the interval ca. 2070 - 1700 m.y. is shown, compiled from paleomagnetic directions originating from the southern part of Africa. Here again, an age of 1950 m.y., fits well with the position of the Gough - Van Niekerk Bushveld pole, but not an age of 2095 m.y. The position of the Phalaborwa 1 pole (Morgan and Briden, 1981) poses a similar problem. With an age of 2067 m.y. (Holmes and Cahen, 1957), one would expect from Figure 84 to find the Phalaborwa pole position much more to the south on the APW path for Africa. Despite these discrepancies, the APW path for the interval 2070 m.y. - 1700 m.y. is well defined by several palaeomagnetic pole positions, but one must conclude that the absolute ages of pole positions on the APW path are questionable.

The APW path in Figure 85 further displays a magnetic polarity change, with poles to the east of the 20 degree meridian predominantly corresponding to N-seeking magnetization directions and those poles to the west of the 20 degree meridian corresponding generally to S-seeking magnetization. This polarity transition on this part of the APW path for Africa was first pointed out by Morgan and Briden (1981).

The positions of the two poles for the main zone in the eastern and the western Bushveld (Fig. 86), do not differ substantially from the pole position previously determined by Gough and Van Niekerk (1959) for the main zone thus the data from this study generally confirm the work of Gough and Van Niekerk. One important new aspect, however, is the polarity of pole

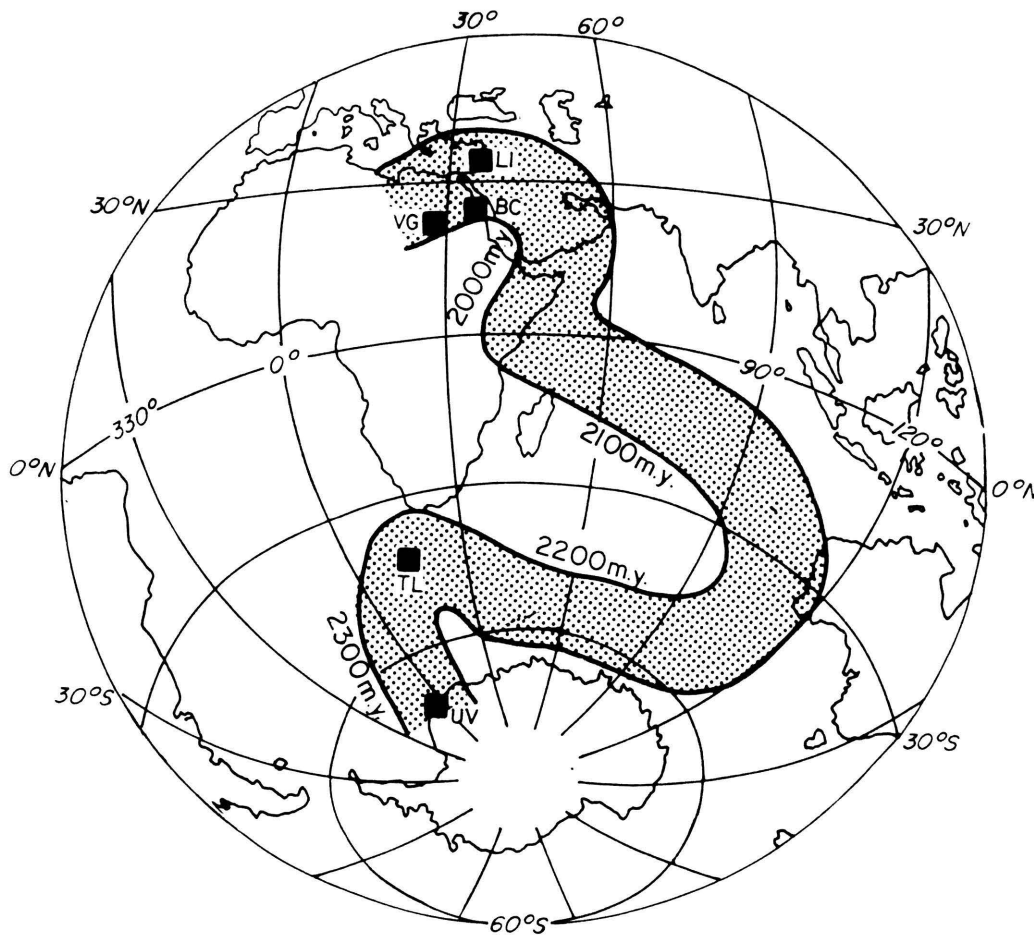


Fig. 84 Apparent polar wander path for African cratons, 2300–1900 m.y. Only pole positions originating from southern Africa are shown: UV=Upper Ventersdorp (2300 m.y.), TL=Abel Erasmus Basalt (2250 m.y.), BC=Bushveld Complex (1950 m.y.), (Gough and Van Niekerk, 1959), LI=Losberg Intrusion (1950 m.y.), VG=Vredefort granophyre (1970 m.y.). All the poles used to define the APW path, including those shown here and ages are listed in Piper (1976, p.435). Redrawn from McElhinny and McWilliams (1977).

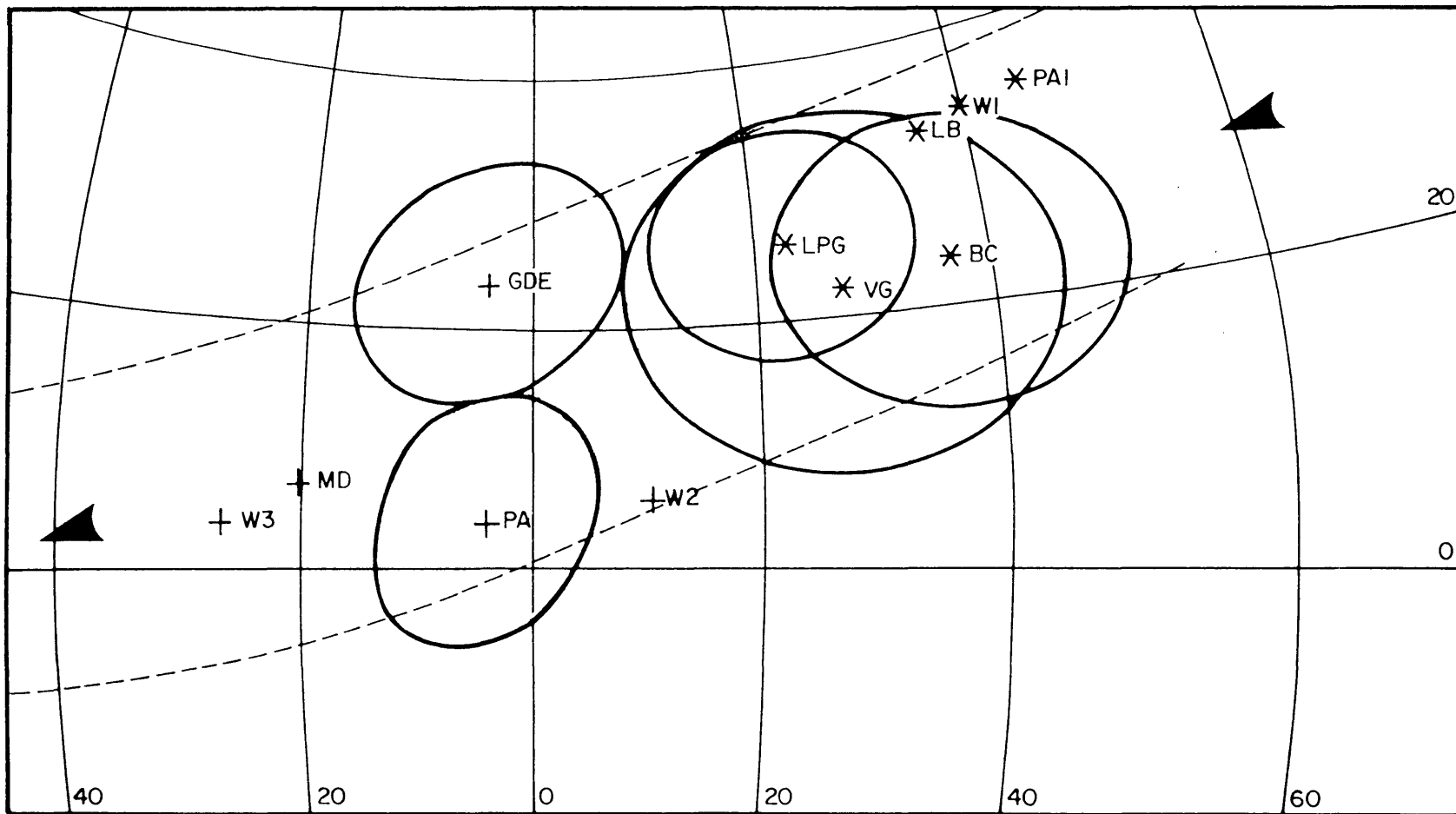


Fig. 85 APW path for Africa with selected pole positions shown for Southern Africa ca. 2070 m.y.-1700 m.y. PA1 (2067 m.y.) = Phalaborwa pyroxenite (Morgan and Briden, 1981); W1 - W3 = Waterberg sediments (stratigraphically arranged poles E, D and C in McElhinny, 1968); VG (1970 m.y.) = Vredefort Granophyre (Hargraves, 1970); LPG (2000 m.y.) = Limpopo gneisses (Morgan and Briden, 1981); BC (1950 m.y.) = Bushveld Complex (Gough and Van Niekerk, 1959); LB (1950 m.y.) = Losberg Gabbro Hargraves (1970); GDE (1935 m.y.) = Great Dyke extensions into Limpopo belt (Jones *et al.*, 1975); PA = Phalaborwa syenite and dolerites (Morgan and Briden, 1981); MD (1850-1910 m.y.) = Mashonaland dolerites, (McElhinny and Opdyke, 1964). All rock ages from Morgan and Briden (1981). * = N-seeking magnetizations; + = S-seeking magnetizations.

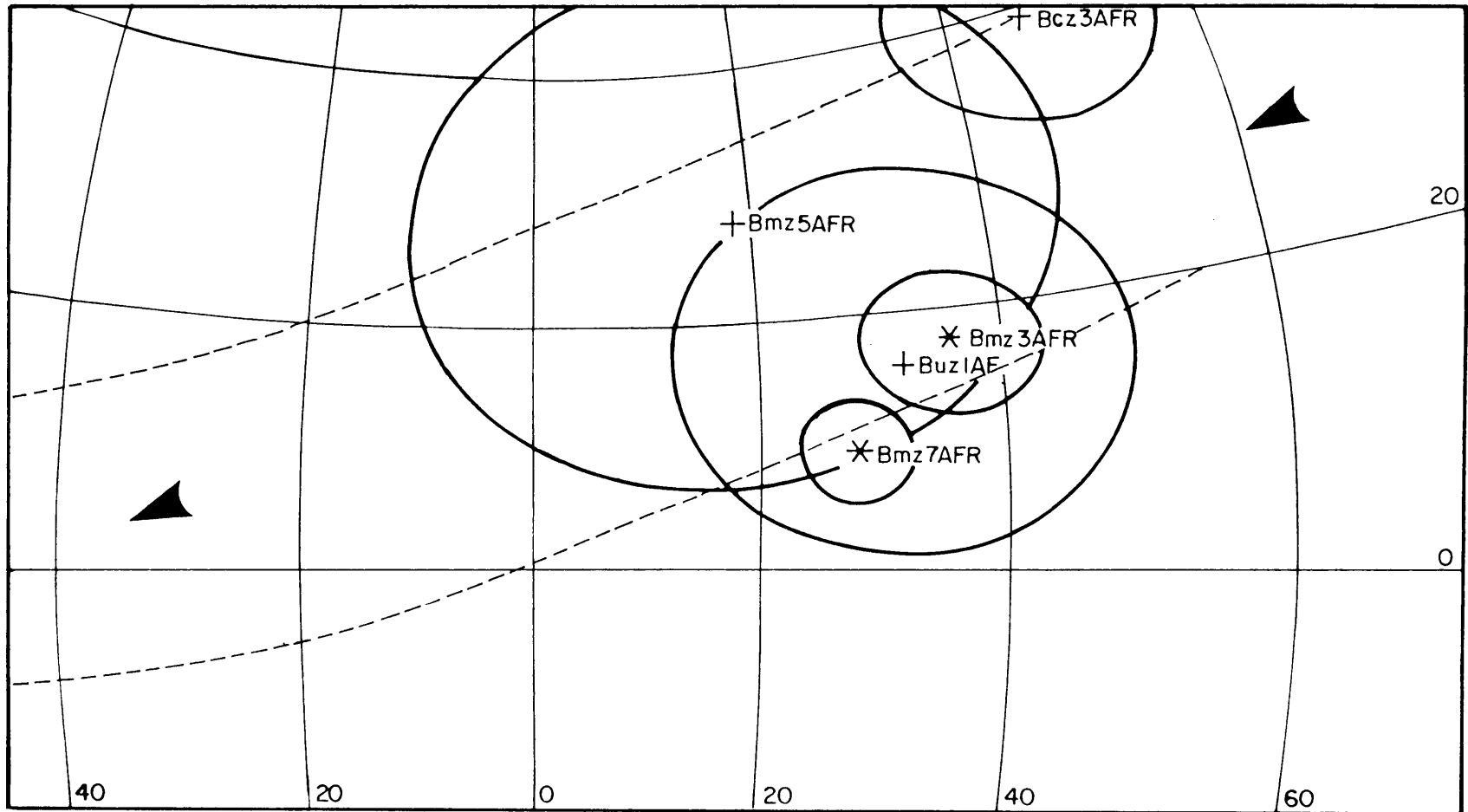


Fig. 26 APW path for Africa with pole positions from this study. Bcz3AFR=critical zone; Bmz3AFR=main zone, eastern Bushveld Complex; Bmz5AFR=subzone C of main zone, eastern Bushveld Complex; Bmz7AFR=main zone western Bushveld Complex; Buz1AF=upper zone.

* = N-seeking magnetizations; + = S-seeking magnetizations.

Ovals of 95 per cent confidence shown. Stereographic projection.

Bmz5AFR, which has a different polarity and lies slightly to the north west of poles Bmz3AFR and Bmz7AFR (Fig. 86). Pole Bmz5AFR (normal) represents subzone C of the main zone in the eastern Bushveld and its position on the APW path as well as its polarity suggests that this part of the main zone is younger than the rest of the main zone. In view of the polarity transition observed on this part of the APW path by Morgan and Briden (1981), the change of polarity of Bmz5AFR with respect to poles Bmz3AFR and Bmz7AFR, is probably due to a geomagnetic field reversal. The position of pole Buz1AF, (upper zone, Fig. 86), does not confirm its younger age, but with rather large ovals of 95 per cent confidence around the mean pole positions of poles Buz1AF and Bmz5AFR, the change in polarity still corresponds to the observed overall polarity change observed on the APW path.

Pole Bcz3AFR (critical zone), which represents a majority of south seeking magnetization directions, is positioned on a part of the APW path dominated by north seeking magnetization directions. This supports the previous conclusion (Chapter V, Sections G and H) that the observed mean magnetization direction of the critical zone is possibly due to a self-reversal of magnetization. From the APW path it is also evident that the formation of the critical zone preceded that of the main and upper zones of the layered sequence (Fig. 86).

To present an overall view of the palaeomagnetic poles of the layered sequence, magnetization directions of the various zones must be combined in terms of the magnetic polarity division of the layered sequence (Figs. 82 and 83). The following groups and corresponding pole positions are then obtained.

Magnetic polarity zone A:

Group: MPzA ; N = 9 ; D = 191,5° ; I = -44,5° ; $\alpha_{95} = 8,7^\circ$; k = 35

with (north) pole position latitude : 37,1°S
 longitude : 138,5°W
 polar error (dp, dm) : 6,9°, 10,9° respectively

Magnetic polarity zone B:

Group: MPzB ; N = 45 ; D = 2,2° ; I = 69,2° ; $\alpha_{95} = 2,5^\circ$; k = 75

with (north) pole position ; latitude : 11,6°N
 longitude : 29,9°E
 polar error (dp, dm) : 3,6°, 4,3° respectively

Magnetic polarity zone C:

Group: MPzC ; N = 10 ; D = 178,4° ; I = -63,1° ; $\alpha_{95} = 9,0^\circ$; k = 30

with (north) pole positions : latitude : 19,8°S
 longitude : 152,7°W
 polar error (dp, dm) : 11,1°, 14,1° respectively

The pole positions of the magnetic polarity zones A, B and C are shown in Figure 87 together with the APW path from Figure 85. The regrouping of the magnetization directions to produce palaeomagnetic poles MPZA, MPZB and MPZC, changes the pole distribution of the layered sequence on the APW path only marginally, and conclusions drawn from pole positions derived from magnetization directions arranged according to the stratigraphic zonal division of the layered sequence, remain valid.

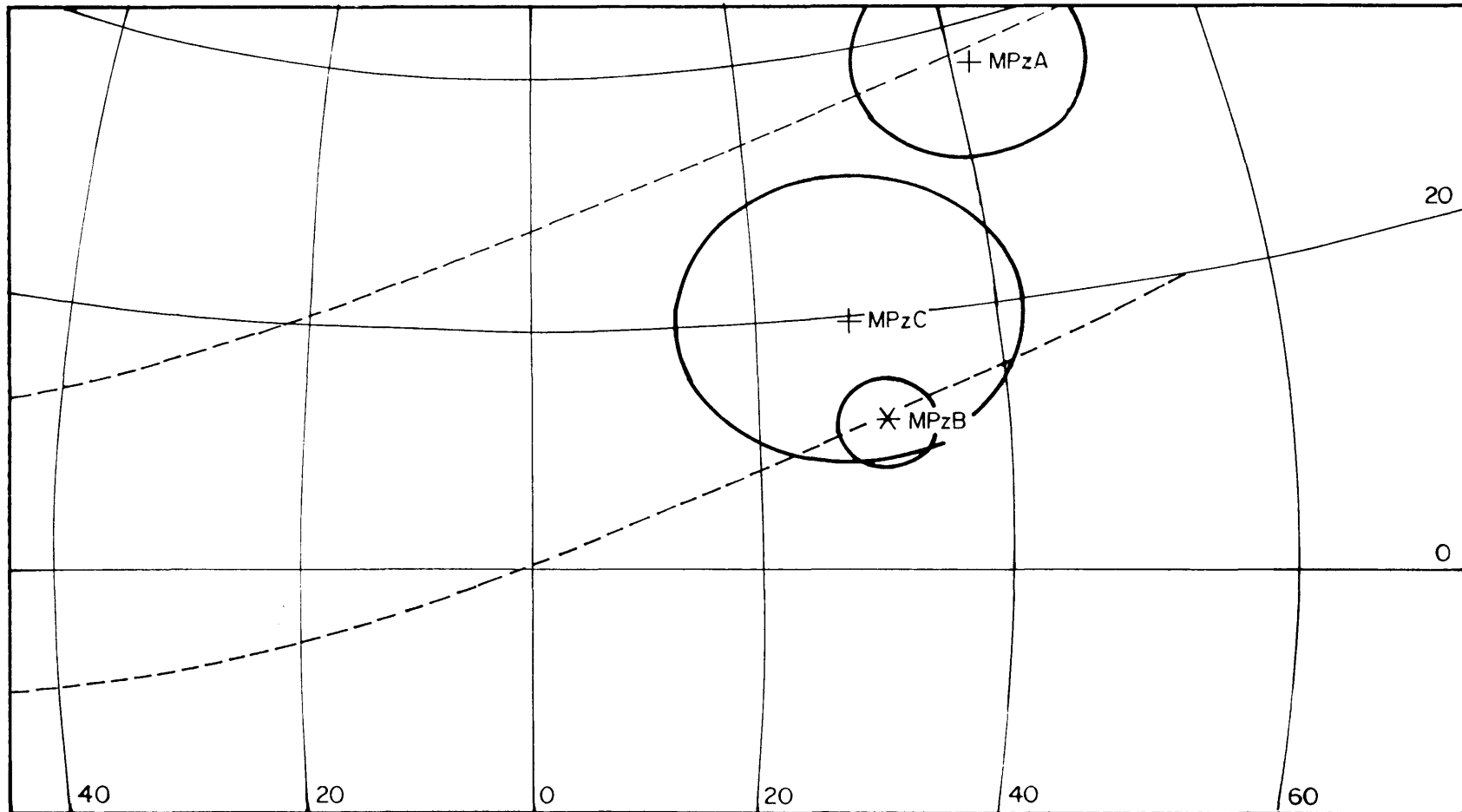


Fig. 87 APW path for Africa with pole positions corresponding to the magnetic polarity zones of the layered sequence. MPzA, MPzB and MPzC = magnetic polarity zones A, B and C respectively. See Figs. 82 and 83. Ovals of 95 per cent confidence shown. Plotting convention as in Fig. 86. Stereographic projection.

X TECTONIC IMPLICATIONS

The genesis of a layered igneous sequence normally comprises elements such as the loci of emplacement, age relations, the origin of rock types present, the origin of layering, the tectonic history of the sequence and lastly the origin of mineralization, if present. Of these elements, the age relations and the tectonic history are most amenable to elucidation by palaeomagnetic studies. Instances where palaeomagnetic data enabled workers to solve complex tectonic histories are numerous, one recent example being that of Sudbury (Morris, 1980, 1981).

With the exception of that part of the layered sequence to the north of the Pilanesberg Complex (Fig.1), the palaeomagnetic results of this study do not indicate a complex tectonic history for the layered sequence of the Bushveld Complex. However, the palaeomagnetic data impose certain constraints on any hypothesis or models which strive to explain the genesis and subsequent tectonic history of the layered sequence and adjacent geological units. These constraints are:

- 1) The emplacement of the critical zone was part of the first phase in the intrusion of the layered sequence and occurred slightly before or contemporaneously with the formation of the Phalaborwa Complex and the onset of the deposition of the Waterberg Group sediments (Figs 85 and 86).
- 2) The second and third phases involve the formation of the main and upper zones which took place virtually simultaneously (Fig. 86).
- 3) According to Coertze *et al.* (1977) deposition of early Waterberg sediments in the central Transvaal was contemporaneous with late Bushveld magmatic activity, represented by the emplacement of the Bushveld granite. The palaeomagnetic pole positions shown in figures 85, 86 and 87 imply an even earlier onset of the Waterberg sedimentation cycle, with older Waterberg sediments the same age as the mafic rocks of the Bushveld Complex.
- 4) The igneous layering of the main and possibly also the critical zones was initially horizontal. The present dip was acquired only after these zones had cooled to a temperature below their respective Curie temperatures. This does not necessarily hold true for the

critical and main zones to the north of the Pilanesberg Complex, as insufficient suitable samples were available for investigation of this area.

- 5) If the dip directions of the main and critical zones, which at certain localities point away from the centre of the Bushveld Complex, are the result of dome-like features in the centre of the Complex then obviously, these features post-date the main and critical zones. Furthermore, these features cannot be components of events which led to the emplacement of the layered sequence.
- 6) The results indicate that the upper zone had acquired its remanent magnetization with the igneous layering of this zone in its present orientation. This implies that the central subsidence of the whole Bushveld basin took place during or immediately after solidification of the upper zone and that subsidence could have been in response to the influx of rather voluminous quantities of magma at the level of the Thornhill pyroxenite layer (Fig. 83), (Von Gruenewaldt, 1973 and Marais, 1977).

ACKNOWLEDGEMENTS

Numerous companies institutions and persons made this study possible by providing material aid and granting permission to visit a number of mines and quarries. The author would like to express his gratitude to all those involved, but in particular to the following persons or institutions:

- 1) The University of Pretoria for a research grant which made this study possible.
- 2) The Chief Director of the Geological Survey of South Africa for permission to use the palaeomagnetic laboratory of the Geological Survey.
- 3) My research assistant for the last phase of the project, Miss Maxi Lubbe; also Mr Manfred Hauger of the Geological Survey and Mrs M.E. de Kock.
- 4) The Institute for Geological Research on the Bushveld Complex for additional financial support.
- 5) Many colleagues and friends, especially Proff Hargraves, Dunlop and Dr Halls for their interest and stimulating discussions and suggestions.
- 6) My promoters Prof G von Gruenewaldt and Dr J S V van Zijl who deserve a special word of thanks for their guidance and helpful suggestions.

Lastly, I would like to express my sincerest gratitude to my wife for her patience and encouragement.

REFERENCES

- ALMOND, M., CLEGG, J.A. and JAEGER, J.C., 1956. Remanent magnetism of some dolerites, basalts and volcanic tuffs from Tasmania. *Phil. Mag.*, v. 1, 771-782.
- BANERJEE, S.K., 1972. Iron-titanium-chromite a possible new carrier of remanent magnetization in lunar rocks. *Proc. Third Lun. Sc. Con.*, (Suppl. 3, *Geochim. et Cosmochim. Acta*), v. 3, 2337-2342.
- BHIMASANKARAM, V.L.S., 1964. Partial self-reversal pyrrhotite. *Nat.*, v. 202, 478-479 (Lond.)
- BRANDT, J.W., 1946. Corundum indicator, basic rocks and associated pegmatites in northern Transvaal. *Trans. geol. Soc. S. Afr.*, v. 49, 51-103.
- BRIDEN, J.C., 1972. A stability index of remanent magnetization. *J. Geophys. Res.*, v. 77, 1401-1404.
- BRINK, A.B.A., 1979. *Engineering geology of Southern Africa*. Building Publications, Pretoria, 319pp.
- BROCK, A., 1971. An experimental study of palaeosecular variation. *Geophys. J.R. Astr. Soc.*, v. 24, 303-317.
- CAMERON, E.N., 1970. Composition of certain coexisting phases in the eastern Bushveld Complex. *Geol. Soc. S. Afr., Spec. Publ.* 1, 46-58.
- COERTZE, F.J., 1974. The geology of the basic portion of the western Bushveld Igneous Complex. *Mem. geol. Surv. S. Afr.*, 66, 148pp.
- , JANSEN, H. and WALRAVEN, F., 1977. The transition from the Transvaal Sequence to the Waterberg Group. *Trans. geol. Soc. S. Afr.*, v. 80, 145-156.

- COUSINS, C.A., 1959. The structure of the mafic portion of the Bushveld Igneous Complex. *Trans. geol. Soc. S. Afr.*, v. 62, 179-189.
- COX, A., 1969a. Confidence limits for the precision parameter K. *Geophys. J.R. Astr. Soc.*, v. 18, 545-549.
- , 1969b. Geomagnetic reversals. *Science*, v. 163, 237-244.
- CREER, K.M. and SANVER, M., 1967. The use of the sun compass, 11-16. In: Collinson, D.W., Creer, K.M. and Runcorn, S.K. (ed). *Methods in Palaeomagnetism*. Developments in solid Earth Geophysics, 3, Elsevier Publishing Company, Amsterdam.
- DALY, R.A., 1929. Bushveld Igneous Complex of the Transvaal. *Bull. geol. Soc. Amer.*, v. 39, 703-768.
- DAVIES, R.D., ALLSOPP, H.L., ERLANK, A.J. and MANTON, W.I., 1970. Sr-isotope studies on various layered mafic intrusions in southern Africa. *Geol. Soc. S. Afr., Spec. Publ. 1*, 576-593.
- DOELL, R.R. and COX, A., 1967. Analysis of alternating field demagnetization equipment, 241-253. In: Collinson, D.W., Creer, K.M. and Runcorn, S.K. (ed). *Methods in Palaeomagnetism*. Developments in solid Earth geophysics, 3, Elsevier Publishing Company, Amsterdam.
- DUNLOP, D.W., 1981. The rock magnetism of fine particles. *Phys. Earth Plan. Int.*, v. 26, 1-26.
- , HANES, J.A. and BUCHAN, K.L., 1973. Indices of multi-domain magnetic behaviour in basic igneous rocks : alternating field demagnetization, hysteresis and oxide petrology. *J. Geophys. Res.*, v. 78, 1387-1393.

- EVANS, M.E., McELHINNY, M.W. and GIFFORD, A.C., 1968. Single domain magnetite and high coercivities in a gabbroic intrusion. *Earth Plan. Sc. Lett.*, v. 4, 142-146.
- EVERITT, C.W.F., 1962. Self-reversal in a shale containing pyrrhotite. *Phil. Mag.*, v. 7, 831-842.
- FISHER, R., 1953. Dispersion on a sphere. *Proc. R. Soc. Lond.*, A217, 295-305.
- FLEET, E.M., BILCOX, G.A. and BARNETT, R.L., 1980. Oriented magnetite inclusions in pyroxenes from the Grenville province. *Can. Min.*, v. 18, 89-99.
- GEOLOGICAL SURVEY OF SOUTH AFRICA, 1973. 1:50 000 Geological Series: Maps 2527DA, 2527DB, 2528CA. Government Printer, Pretoria.
- GOUGH, D.I., 1956. A study of the palaeomagnetism of the Pilanesberg dykes. *Mon. Not. R. Astr. Soc. Geophys. Suppl.*, 7, 196-213.
- , 1967. Notes on rock sampling for palaeomagnetic research, 3-7. In: Collinson, D.W., Creer, K.M. and Runcorn, S.K. (eds). *Methods in Palaeomagnetism*. Developments in solid Earth geophysics, 3, Elsevier Publishing Company, Amsterdam.
- and VAN NIEKERK, C.B., 1959. A study of the palaeomagnetism of the Bushveld gabbro. *Phil. Mag.*, v. 4, 126-136.
- GRAHAM, J.W., 1949. The stability and significance of magnetism in sedimentary rocks. *J. Geophys. Res.*, v. 54, 131-167.
- GRAHAM, K.W.T. and HALES, A.L., 1957. Palaeomagnetic measurements on Karoo dolerites. *Phil. Mag. Suppl. Adv. Phys.*, v. 6, 149-167.

- GROENEVELD, D., 1970. The structural features and the petrography of the Bushveld Complex in the vicinity of Stoffberg, eastern Transvaal. *Geol. Soc. S. Afr., Spec. Publ. 1*, 36-46.
- HAGGERTY, S.E., 1976. Opaque mineral oxides in terrestrial igneous rocks. Hg101-Hg300. In: Rumble, D. (ed). *Oxide Minerals*. Min. Soc. Am., Short Course Notes.
- HALL, A.L., 1932. The Bushveld Igneous Complex of the central Transvaal. *Mem. Geol. Surv. S. Afr., v. 28*, 554pp.
- HALLS, H.C., 1976. A least-squares method to find a remanence direction from converging remagnetization circles. *Geophys. J.R. Astr. Soc., v. 45*, 297-304.
- , 1978. The use of converging remagnetization circles in palaeomagnetism. *Phys. Earth Plan. Int., v. 16*, 1-11.
- , 1979. Separation of multicomponent NRM : combined difference and resultant magnetization vectors. *Earth Plan. Sc. Lett., v. 43*, 303-308.
- HAMILTON, W., 1970. Bushveld Complex - product of impacts. *Geol. Soc. S. Afr., Spec. Publ. 1*, 367-374.
- HAMILTON, P.J., 1977. Sr-isotope and trace element studies of the Great Dyke and Bushveld mafic phase and their relation to early Proterozoic magma genesis in southern Africa. *J. Petrol., v. 18*, 24-52.
- HARGRAVES, R.B., 1970. Palaeomagnetic evidence relevant to the origin of the Vredefort ring. *J. Geol., v. 78*, 253-263.
- and YOUNG, W.M., 1969. Source of stable remanent magnetism in Lambertville diabase. *Am. J. Sc., v. 267*, 1167-1177.
- HATTINGH, P.J., 1980. The structure of the Bushveld Complex in the Groblersdal-Lydenburg-Belfast area of the eastern Transvaal as interpreted from a regional gravity survey. *Trans. geol. Soc. S. Afr., v. 83*, 125-133.

- HOFFMAN, K.A. and DAY, R., 1978. Separation of multicomponent NRM : a general method. *Earth Plan. Sc. Lett.*, v. 40, 433-438.
- HOLMES, A. and COHEN, L., 1957. Geochronologie, Africaine 1965. *Mem. Acad. r. Sc. colon., n Ser. T-S, Fasc. 1*, 169pp.
- HUNTER, D.R., 1975a. The regional setting of the Bushveld Complex (An adjunct to the Provisional Tectonic Map of the Bushveld Complex). *Econ. geol. res. Unit., Univ. of the Witwatersrand*, 18pp.
- , 1975b. Provisional Tectonic Map of the Bushveld Complex. *Econ. geol. res. Unit., Univ. of the Witwatersrand*.
- , 1976. Some enigmas of the Bushveld Complex. *Econ. Geol.*, v. 71, 229-248.
- and HAMILTON, P.J., 1978. The Bushveld Complex, 107-173. In: Tarling, D.H. (ed). *Evolution of the Earth's Crust*. Academic Press, London.
- IRVING, E., 1964. *Palaeomagnetism and its application to geological and geophysical problems*. John Wiley and Sons, New York, 399pp.
- JONES, D.L., ROBERTSON, I.D.M. and McFADDEN, P.L., 1975. A palaeomagnetic study of Precambrian dyke swarms associated with the Great Dyke of Rhodesia. *Trans. geol. Soc. S. Afr.*, v. 78, 57-65.
- LOMBAARD, B.V., 1934. On the differentiation and relationship of the rocks of the Bushveld Igneous Complex. *Trans. geol. Soc. S. Afr.*, v. 33, 179-189.
- LOWRIE, W. and FULLER, M., 1971. On the alternating field demagnetization characteristics of multidomain thermoremanent magnetization of magnetite. *J. Geophys. Res.*, v. 76, 6339-6349.

- MARAIS, C.L.M., 1977. *An investigation of the pyroxenite marker and the associated rocks in the main zone of the eastern Bushveld Complex*. MSc thesis (unpublished), Univ. of Pretoria, 87pp.
- McELHINNY, M.W., 1964a. An improved method for demagnetising rocks in alternating magnetic fields. *Geophys. J.R. Astr. Soc.*, v. 10, 369-374.
- , 1964b. Statistical significance of the fold test in palaeomagnetism. *Geophys. J.R. Astr. Soc.*, v. 8, 338-340.
- , 1967. Statistics of a spherical distribution, 313-321. In: Collinson, D.W., Creer, K.M. and Runcorn, S.K. (ed). *Methods in palaeomagnetism*. Developments in solid Earth geophysics, 3, Elsevier Publishing Company, Amsterdam.
- , 1968. Palaeomagnetic directions and pole positions. *IX Geophys. J.R. Astr. Soc.*, v. 16, 207-224.
- , 1973. *Palaeomagnetism and plate tectonics*. Cambridge Univ. Press, 358pp.
- and OPDYKE, N.D., 1964. The palaeomagnetism of the Precambrian dolerites of eastern southern Rhodesia an example of geologic correlation by rock magnetism. *J. Geophys. Res.*, v. 69, 2465-2475.
- and McWILLIAMS, M.O., 1977. Precambrian geodynamics - a palaeomagnetic view. *Tectonophysics*, v. 40, 137-159.
- MERRIL, R.T., 1975. Magnetic effects associated with chemical changes in igneous rocks. *Geophys. Surveys*, v. 2, 277-311.
- MOLYNEUX, T.G., 1970. The geology of the area in the vicinity of Magnet Heights, eastern Transvaal, with special reference to the magnetic iron ore. *Geol. Soc. S. Afr., Spec. Publ. 1*, 228-241.

- , 1972. X-ray data and chemical analysis of some titanomagnetites and ilmenite samples from the Bushveld Complex, South Africa. *Min. Mag.*, v. 38, 863-871.
- MORGAN, G.E. and BRIDEN, J.C., 1981. Aspects of Precambrian palaeomagnetism, with new data from the Limpopo mobile belt and Kaapvaal craton in Southern Africa. *Phys. Earth Plan. Int.*, v. 24, 142-168.
- MORRIS, W.A., 1980. Tectonic and metamorphic history of the Sudbury norite : the evidence from palaeomagnetism. *Econ. Geol.*, v. 75, 260-277.
- , 1981. Intrusive and tectonic history of the Sudbury micropegmatite : the evidence from palaeomagnetism. *Econ. Geol.*, v. 76, 791-804.
- NAGATA, T., 1953. *Rock-magnetism*. Maruzen Company, Tokyo, 225pp.
- NICOLAYSEN, L.O., DE VILLIERS, J.W.L., BURGER, A.J. and STRELOW, F.W.E., 1958. New measurements relating to the absolute age of the Transvaal System and of the Bushveld Complex. *Trans. geol. Soc. S. Afr.*, v. 61, 137-163.
- OPDYKE, N.D., 1972. Palaeomagnetism of deep-sea cores. *Rev. Geophys.*, v. 10, 213-249.
- PATTON, B.J. and FITCH, J.L., 1962. Anhysteretic remanent magnetization in small steady fields. *J. Geophys. Res.*, v. 67, 307-311.
- PIPER, J.D.A., 1976. Palaeomagnetic evidence for a Proterozoic super continent. *Phil. Trans. R. Astr. Soc. Lond.*, A280, 469-490.
- ROBERTSON, W.A., 1963. The palaeomagnetism of some Mesozoic intrusives and tuffs from eastern Australia. *J. Geophys. Res.*, v. 68, 2299-2312.

- RUNCORN, S.K., 1967. Statistical discussion of rock samples, 329-339.
In: Collinson, D.W., Creer, K.M. and Runcorn, S.K. (ed). Methods in palaeomagnetism. Developments in solid Earth geophysics, 3, Elsevier Publishing Company, Amsterdam.
- SCHARLAU, T.A., 1972. *Petrographische und petrologische Untersuchungen in der Haupt-Zone des östlichen Bushveld - Komplexes, Distriet Groblersdal /Transvaal.* Dissertation, Johann Wolfgang Goethe Universität zu Frankfurt am Main.
- SCHMIDTBAUER, E., 1971. Magnetization and lattice parameters of Ti substituted Re-Cr spinels. *J. Phys. Chem. Solids, v. 32, 71-76.*
- SCHREINER, G.D.L., 1958. Comparison of the $^{87}\text{Rb}/^{87}\text{Sr}$ ages of the red granites of the Bushveld Complex from measurements on the total rock and separated mineral fractions.
Proc. R. Soc. Lond., A245, 112-117.
- SCHWARZ, E.J., COLEMAN, L.C. and CATTROLL, H.M., 1979.
 Palaeomagnetic results from the Skaergaard Intrusion, east Greenland. *Earth Plan. Sc. Lett., v. 42, 437-443.*
- SCHWELLNUS, J.S.J., ENGELBRECHT, L.N.J., COERTZE, F.J., RUSSEL, H.D., MALHERBE, S.J., VAN ROOYEN, D.P. and COOKE, R., 1962.
 The geology of the Olifants River area, Transvaal.
Explan. Sheets 2429B (Chuniespoort) and 2430A (Wolkberg), Geol. Surv. S. Afr., 87pp.
- SHARPE, M.R., 1980. Evolution of the Bushveld magma chambers.
Inst. geol. Res. Bushveld Complex, Univ. of Pretoria, Res. Rep. 30, 57pp.
- , 1982. The floor contact of the eastern Bushveld Complex : field relations and petrography. *Inst. geol. Res. Bushveld Complex, Univ. of Pretoria, Res. Rep. 36, 43pp.*
- SHARPE, M.R. and BAHAT, D., 1981. The Great Dyke - a possible expression of combined hydrofracturing and Hertzian fracture.
Inst. geol. Res. Bushveld Complex, Univ. of Pretoria, Res. Rep. 26, 13pp.

- and SNYMAN, J.A., 1978. A model for the emplacement of the eastern compartment of the Bushveld Complex. *Inst. geol. Res. Bushveld Complex, Univ. of Pretoria, Res. Rep. 11*, 33pp.
- SMIT, P.J., HALES, A.L. and GOUGH, D.I., 1962. The gravity survey of the Republic of South Africa. *Geol. Surv. S. Afr., Hb. 3*, 462pp.
- SOFFEL, H.C., 1971. The single-domain (multidomain) transition in intermediate titanomagnetites. *J. Geophys.*, v. 37, 451-470.
- SOUTH AFRICAN COMMITTEE FOR STRATIGRAPHY, 1980. Stratigraphy of South Africa, Part 1 : Lithostratigraphy of the Republic of South Africa, South West Africa/Namibia and the Republic of Bophuthatswana, Transkei and Venda. *Geol. Surv. S. Afr. Hb. 8*, 690pp.
- TARLING, D.H., 1971. *Principles and applications of palaeomagnetism*. Chapman and Hall, London, 164pp.
- TRUTER, F.C., 1955. Modern concepts of the Bushveld Igneous Complex. *Compte Rendu, C.C.T.A., South Regional Committee, Salisbury*, 77-92.
- VAN BILJON, S., 1949. Transformation of the Pretoria Series in the Bushveld Complex. *Trans. geol. Soc. S. Afr.*, v. 52, 1-172.
- VERMAAK, C.F. and HENDRIKS, L.P., 1976. A review of the mineralogy of the Merensky Reef, with specific reference to new data on precious metal mineralogy. *Econ. Geol.*, v. 71, 1244-1269.
- VON GRUENEWALDT, G., 1973. The main and upper zones of the Bushveld Complex in the Roossenekal area, eastern Transvaal. *Trans. geol. Soc. S. Afr.*, v. 76, 207-227.
- , 1979. A review of some recent concepts of the Bushveld Complex, with particular reference to sulfide mineralization. *Can. Mineral.*, v. 17, 233-256.

- VOUTETAKIS, S.K., 1970. I anastrofos monimos magntisis ton khromiton notiou Vourinou Kozanis. *Inst. Geol. Ereunon Hypedaphous, Geol. Geophys. Metetai*, v. 15, 121pp.
- WAGER, L.A. and BROWN, G.M., 1968. *Layered Igneous Rocks*. Oliver and Boyd, Edinburgh and London, 588pp.
- WATSON, G.S.A., 1956. A test for randomness of directions. *Mon. Not. R. Astr. Soc. Geophys. Suppl.*, v. 7, 153-159.
- WILLEMSE, J., 1964. A brief outline of the geology of the Bushveld Igneous Complex, 91-128. In: Haughton, S.H. (ed). *The geology of some ore deposits in southern Africa, II*. Geol. Soc. S. Afr., Johannesburg.
- , 1969. The geology of the Bushveld Complex, the largest repository of magmatic ore deposits in the world. *Econ. Geol. Monogr.* 4, 1-22.
- and VILJOEN, E.A., 1970. The fate of the argillaceous material in the gabbroic magma of the Bushveld Complex. *Geol. Soc. S. Afr., Spec. Publ.* 1, 336-366.